Report Prepared by:
Francisco J. Presuel-Moreno
With
Hariharan Balasubramanian
Bongjoon Seo
Brian Weber

Final Report

Concrete Pipe – Electrochemical Cell, Phase II
BDV27-977-03

Submitted to
Florida Department of Transportation Research Center
605 Suwannee Street
Tallahassee, Florida 32399

Submitted by
Francisco Presuel-Moreno
Principal Investigator
Department of Ocean and Mechanical Engineering
Center for Marine Materials
Florida Atlantic University
SeaTech
101 North Beach Road
Dania Beach, Florida 33004

August 2016

Disclaimer

The opinions, findings, and conclusions expressed in this publication are those of the authors and not necessarily those of the State of Florida Department of Transportation.

SI* (MODERN METRIC) CONVERSION FACTORS

APPROXIMATE CONVERSIONS TO SI UNITS

Symbol	When You Know	Multiply By	To Find	Symbol
		LENGTH		
in	inches	25.4	millimeters	mm
ft	feet	0.305	meters	m
yd	yards	0.914	meters	m
mi	miles	1.61	kilometers	km
		AREA		
in^2	square inches	645.2	square millimeters	mm^2
ft^2	square feet	0.093	square meters	m^2
yd^2	square yard	0.836	square meters	m^2
ac	acres	0.405	hectares	ha
mi^2	square miles	2.59	square kilometers	km^2
		VOLUME		
fl oz	fluid ounces	29.57	milliliters	mL
gal	gallons	3.785	liters	L
ft^3	cubic feet	0.028	cubic meters	m^3
yd^3	cubic yards	0.765	cubic meters	m^3
	NOTE: volumes greater than 1000 L shall be shown in m^3			
		MASS		
oz	ounces	28.35	grams	g
lb	pounds	0.454	kilograms	kg
T	short tons (2000 lb)	0.907	megagrams (or "metric ton")	Mg (or "t")
		TEMPERATURE (exact degrees)		
^oF	Fahrenheit	5 (F-32)/9 or (F-32)/1.8	Celsius	^oC
		ILLUMINATION		
fc	foot-candles	10.76	lux	lx
fl	foot-Lamberts	3.426	candela/m^2	cd/m^2
		FORCE and PRESSURE or STRESS		
lbf	poundforce	4.45	newtons	N
lbf/in^2	poundforce per square inch	6.89	kilopascals	kPa

APPROXIMATE CONVERSIONS FROM SI UNITS

Symbol	When You Know	Multiply By	To Find	Symbol
		LENGTH		
mm	millimeters	0.039	inches	in
m	meters	3.28	feet	ft
m	meters	1.09	yards	yd
km	kilometers	0.621	miles	mi
		AREA		
mm^2	square millimeters	0.0016	square inches	in^2
m^2	square meters	10.764	square feet	ft^2
m^2	square meters	1.195	square yards	yd^2
ha	hectares	2.47	acres	ac
km^2	square kilometers	0.386	square miles	mi^2
		VOLUME		
mL	milliliters	0.034	fluid ounces	fl oz
L	liters	0.264	gallons	gal
m^3	cubic meters	35.314	cubic feet	ft^3
m^3	cubic meters	1.307	cubic yards	yd^3
		MASS		
g	grams	0.035	ounces	oz
kg	kilograms	2.202	pounds	lb
Mg (or "t")	megagrams (or "metric ton")	1.103	short tons (2000 lb)	T
		TEMPERATURE (exact degrees)		
^oC	Celsius	1.8C+32	Fahrenheit	^oF
		ILLUMINATION		
lx	lux	0.0929	foot-candles	fc
cd/m^2	candela/m^2	0.2919	foot-Lamberts	fl
		FORCE and PRESSURE or STRESS		
N	newtons	0.225	poundforce	lbf
kPa	kilopascals	0.145	poundforce per square inch	lbf/in^2

*SI is the symbol for the International System of Units. Appropriate rounding should be made to comply with Section 4 of ASTM E380.
(Revised March 2003)

1. Report No.	2. Government Accession No.	3. Recipient's Catalog No.
4. Title and Subtitle Concrete Pipe - Electrochemical Cell, Phase II		5. Report Date August 2016 6. Performing Organization Code FAU-OE-CMM-08-3
7. Author(s) Francisco J. Presuel-Moreno, Hariharan Balasubramanian, Bongjoon Seo, Brian Webber		8. Performing Organization Report No. BDV27-977-03
9. Performing Organization Name and Address Center for Marine Materials Florida Atlantic University – SeaTech 101 North Beach Road Dania Beach, Florida 33004		10. Work Unit No. (TRAIS) 11. Contract or Grant No. BDV27-977-03
12. Sponsoring Agency Name and Address Florida Department of Transportation 605 Suwannee Street, MS 30 Tallahassee, FL 32399		13. Type of Report and Period Covered Final Report March 18, 2014 – August 26, 2016 14. Sponsoring Agency Code
15. Supplementary Notes		

16. Abstract

The research was conducted to better understand the corrosion propagation stage on dry-cast reinforced concrete pipes (RCP) while exposed to high moisture conditions and chlorides. The research had both a field component and laboratory components. Two types of dry-cast reinforced concrete pipes were used in this investigation for the laboratory component. Ring specimens and segmented arch section specimens were instrumented. All specimens were subjected to accelerated chloride transport via an electric field. Corrosion of the steel wire mesh initiated after a few days to a few months rather than several years. The specimens were then transferred to high moisture environments (immersed in water, high humidity, and/or covered with wet sand) during the corrosion propagation stage. The corrosion activity was monitored using linear polarization resistance and electrochemical impedance spectroscopy measurements. The corrected polarization resistance (Rc) was calculated by subtracting the solution resistance from the apparent polarization resistance measured. The Rc values measured over time were used to obtain the calculated mass loss (using an integration method). Most specimens were forensically analyzed and the measured mass loss compared to the calculated mass loss. Field visits were also part of the project. Segments were obtained from sites on which the RCP had been removed. These segments were taken to the lab and forensically analyzed. Corrosion potentials were measured along selected longitudinal wires. After concrete removal, steel wire mesh showed corrosion on segments obtained from three of the visited sites. A second set of visited sites corresponded to sites in which the RCP continues to be in service while being exposed to an aggressive environment. Evidence was found that steel corrosion was ongoing – either visual (cracks or corrosion product bleed) or via corrosion potential measurements – at several of these sites that were exposed to wet and dry cycles.

17. Key Word	18. Distribution Statement
Reinforced Concrete Pipe, Corrosion Initiation, Corrosion Propagation, Forensic Examination	

19. Security Classif. (of this report)	20. Security Classif. (of this page)	21. No. of Pages	22. Price
Unclassified	Unclassified	190	

Form DOT F 1700.7 (8-72) Reproduction of completed page authorized

Acknowledgments

The authors are indebted to the FDOT State Materials Office (SMO) for assisting in conducting several tests at SMO for this study, in particular, Mr. Mario Paredes, Mr. Ivan Lasa, Mr. Ronald Simmons, Mr. Ghulam Mujtaba, and several SMO Technicians (Dennis Baldi, Teresa Risher, Cody Owen). The assistance of several students who worked as graduate/undergraduate research assistants at FAU-SeaTech marine materials and corrosion lab is also acknowledged. The authors also acknowledge Rinker Materials Concrete Pipe Division/CEMEX for testing one-foot-long ring specimens for 3EB testing.

Executive Summary

Dry-cast reinforced concrete pipes (RCP) are frequently used as drainage pipes by several state departments of transportation (DOTs) across the United States. Corrosion has been found on culverts at locations close to the ocean where RCPs experience wet/dry cycles of chloride-rich solution. However, modest or no corrosion of RCPs has been observed on RCPs placed in soils and exposed at sites with known high chloride concentration and high moisture content. It is frequently assumed that this good performance is due to oxygen concentration limitations at the reinforcement. Another factor contributing to this observation is that on those dry-cast RCPs in which corrosion had initiated, the high porosity of dry-cast RCPs allows the corrosion products to move through the pore structure without causing cracks or spalls. This report presents results of an investigation carried out to better understand and characterize ongoing corrosion on RCPs exposed to relevant conditions (concrete in a high moisture content state and/or exposed to low oxygen concentration at the steel). Three methods were developed to accelerate chloride transport so as to initiate corrosion within a short period of time (a few days to a few months instead of a several years). This was followed by monitoring the propagation stage (via linear polarization, electrochemical impedance, and potential) of the corroding steel on specimens while exposed to high moisture environments. The calculated mass was obtained from these measurements. Several specimens were forensically analyzed. The steel wire mesh was chemically cleaned. The measured mass loss (with respect to the mass before cleaning) was obtained. The surface condition after cleaning was documented. It was found that not all specimens experience the same amount of corrosion. Some had significant cross-section loss, but did not produce cracks. The area that corroded ranged 0.2 cm^2 to 14 cm^2. The corrosion products penetrated into the concrete on the specimens with larger corroding areas and significant cross-section loss. In some cases, the penetration was on the order of two to three centimeters.

A subset of specimens was subjected to a galvanostatic pulse (constant applied current) during the propagation stage so as to accelerate the corrosion of the steel reinforcement. A current that ranged from 0.5 to 2.5 $\mu A/cm^2$ was applied (assuming that all the area under the reservoir was corroding). The galvanostatic pulse was applied from 200 to 400 days; some specimens were forensically analyzed within this period of time. The remaining specimens continued to be exposed to high moisture but were no longer subjected to the galvanostatic pulse. Forensic analysis was conducted on most of the remaining specimens.

A third set of samples correspond to ring specimens (i.e., approximately 10 to 12 inches wide) that were instrumented and subjected to chloride transport to initiate corrosion (as the specimens described above). The electrochemical properties were monitored during the corrosion propagation while exposed to high moisture. These specimens were exposed outdoors. Four ring specimens were forensically analyzed after 400 days in high moisture exposure. The remaining six specimens continued to be monitored, and three edge bearing (3EB) tests were conducted in the fall of 2015. Selected sections were forensically analyzed.

Field visits were also part of the project. Segments of RCP removed from field sites were obtained and taken to the lab for forensic testing. Corrosion potentials were measured along selected longitudinal wires. Steel wire mesh, after concrete removal, showed corrosion for three of these sites. A second set of visited sites corresponded to sites in which the pipe continues to be in service while exposed to an aggressive environment. Evidence was found that steel corrosion was ongoing (either visual or via corrosion potential measurements) at several of these sites.

The research results presented above confirm that under certain circumstances, corrosion propagation can take place to the extent that either there is no longer reinforcement and with no cracks visible. This appears to take place for situations in which the concrete is kept under high moisture conditions. This was found in lab observations (e.g., Specimen F1 and Specimen F2), and ring specimens (FS2 and FS3). It was later confirmed via forensic examination from segments obtained from one of the field sites visited.

However, if the concrete is exposed to wet/dry cycles, cracks develop. Such situations were confirmed via field observations on pipes that continue to be in service. Some of these pipes have been 45 to 60 years in service, at Madeira Beach and Dunedin. Similar observations were seen at a couple of sites visited in the Panama City Beach area. Thus, duration of exposure and wet/dry cycle exposure appear to be important parameters that lead to cracks after corrosion has propagated for several years.

Table of Contents

Disclaimer ii
Technical Report Documentation Page iv
Acknowledgments v
Executive Summary vi
List of Figures xiii
List of Tables xix
Chapter 1 - Introduction 1
Chapter 2 - Experimental 6
2.1 Materials and Samples 6
2.2 Testing of Dry-Cast Concrete Porosity, Rapid Chloride Migration Test, and Resistivity 8
2.3 Methods Used to Accelerate Chloride Transport 8
2.3.1 Potentiostatic Method 9
2.3.2 Galvanostatic Method 9
2.3.3 Migration Cell 11
2.4 Potential Measurements Prior to Corrosion Initiation 11
2.5 Environmental Exposures during Natural Corrosion Propagation Stage 12
2.5.1 High Humidity 13
2.5.2 Specimens Covered with Saturated Sand 14
2.5.3 Immersed in Water 15
2.5.4 Vertical Specimens Immersed in Water 15
2.6 Electrochemical Measurements during Natural Corrosion Propagation 16
2.7 Environmental Exposure Sequence after Corrosion Initiated 16
2.8 Specimens Selected for Accelerated Corrosion (During the Corrosion Propagation Stage) 20
2.8.1 Periodic Anodic Polarization via Constant Current Application 22
2.8.2 Environmental Exposures during the Corrosion Propagation Stage 23
2.9 Ring Specimens Experimental Description 25
2.9.1 Accelerated Chloride Transport for Corrosion Initiation 26

2.9.2 Experimental Setup and Electrochemical Measurements during Natural Corrosion Propagation Stage Period 28
2.10 Forensic Analysis 34
2.10.1 Autopsy of Ring Specimens 34
2.10.2 Autopsy and Gravimetric Analysis of Selected Lab Specimens 36
2.11 Calculated Mass Loss Using Integrated Charge and Faraday's Law 39
Chapter 3 – Results 40
3.1 Concrete Cover 40
3.2 Porosity, Resistivity, and Dnssm 41
3.3 Depolarization Prior to Corrosion Initiation 43
3.4 Time to Corrosion Initiation 45
3.5 Corrosion Propagation Stage Monitoring 48
3.5.1 Laboratory Specimens (Rs, Rc, Ecorr) 48
3.5.2 Corrosion Propagation on Specimens for Which Corrosion Was Accelerated 58
3.5.3 Corrosion Propagation on Ring Specimens 73
3.5.4 Potential, Rc, and Rs on Segmented Specimens Obtained from Terminated Ring Specimens 76
3.6 Calculated Mass Loss 79
3.7 Discussion 81
3.7.1 Change in Chloride Concentration 82
3.7.2 Change in Anode Area 83
3.7.3 Change in Cathode Area 83
Chapter 4 – Forensic Examinations: Lab Specimens 84
4.1 Concrete Removal 84
4.1.1 Specimen F0 84
4.1.2 Specimen F1 85
4.1.3 Specimen F2 87
4.1.4 Specimen F3 87
4.1.5 Specimen F11 89
4.1.6 Specimen F12 90

4.1.7 Specimen F21 90
4.1.8 Specimen F22 91
4.1.9 Specimen F41 92
4.1.10 Specimen C0 92
4.1.11 Specimen C1 92
4.1.12 Specimen C5 93
4.1.13 Specimen C7 94
4.1.14 Specimen C8 96
4.1.15 Specimens C12 and C22 97
4.1.16 Specimen C24 98
4.1.17 Specimens C16 98
4.1.18 Specimen C43 99
4.1.19 Specimen F7 100
4.1.20 Specimens F18 103
4.1.21 Specimen F20 103
4.1.22 Specimen F23 106
4.1.23 Specimen C4 107
4.1.24 Specimen C6 109
4.2 Pictures of Specimens after Chemical Cleaning the Steel Wire Mesh 111
4.2.1 Specimen F0 111
4.2.2 Specimen F1 112
4.2.3 Specimen F2 112
4.2.4 Specimen F3 113
4.2.5 Specimen F4 113
4.2.6 Specimen F6 114
4.2.7 Specimens F9, F12, and F21 115
4.2.8 Specimen F22 116
4.2.9 Specimen C0 116
4.2.10 Specimen C2 117

4.2.11 Specimen C7 117
4.2.12 Specimen C8 118
4.2.13 Specimen C9 118
4.2.14 Specimen C16 119
4.2.15 Specimens C12 and Specimen C22 119
4.2.16 Specimen C24 120
4.2.17 Specimen F7 121
4.2.18 Specimen F20 and Specimen F19 121
4.2.19 Specimen F23 122
4.2.20 Specimen C4 122
4.2.21 Specimen C6 123
4.3 Calculated and Measured Mass Loss 124
Chapter 5 – Field Visits 129
5.1 Sites Where RCPs Have Been Removed 129
5.2 Visited Sites with Pipe Not Removed 131
5.2.1 Madeira Beach Area (April 2016). Two sites were visited. 131
5.2.2 Dunedin (April 2016). Two sites were visited. 131
5.2.3 Panama City Beach area (May 2016) 132
5.3 Typical Measurements 132
5.3.1 Miami Beach (Alton Road) 133
5.3.2 Dania Beach, at Dania Beach Marina 134
5.3.3 Titusville Airport (pipes inspected at Apopka) 136
5.3.4 Indian Rock Beach, FL 137
5.3.5 Tallahassee 138
5.3.6 US19- SR52 (Hudson, FL) 139
5.3.7 Panama City 141
5.4 Measurements on Pipes That Continue to Be in Service. 143
5.4.1 Madeira Beach 143
5.4.2 Dunedin 144

5.4.3 Panama City Beach Area 147
5.5 Forensic Examination 150
5.5.1 Dania Beach Marina 150
5.5.2 Indian Rock (Close to Largo Florida) 151
5.5.3 Alton Road – Small Diameter Pipe 153
5.5.4 Apopka (Titusville Airport RCP) 153
5.5.5 Tallahassee 154
5.5.6 US19 SR52 156
5.6 3EB Testing on Ring Specimens 157
5.6.1 Non-corroded Segment 158
5.6.2 C Group Specimens 159
5.6.3 F Group Specimens 162
Chapter 6 – Conclusions 167
References 169

List of Figures

Figure 1 – Angles at which each ring specimen was segmented. 7
Figure 2 – (a) Horizontal specimens with one reservoir, (b) Vertical specimens with 2 reservoirs. 8
Figure 3 – Typical ponding setup installed on specimens (horizontal setup). 10
Figure 4 – Migration cell setup (vertical setup). 11
Figure 5 – Specimens exposed to high humidity environment. 13
Figure 6 – Specimens covered with saturated sand. 14
Figure 7 – Specimens immersed in water. 15
Figure 8 – Type C specimens exposure schedule during propagation stage. 19
Figure 9 – Type F specimens exposure schedule during propagation stage. 20
Figure 10 – Current application during corrosion propagation stage. 21
Figure 11 – Galvanostatic method during corrosion propagation stage. 21
Figure 12 – Schematic diagram of the accelerated corrosion test set-up. 22
Figure 13 – Schematic illustration of depolarization potential vs. time after disconnection. 23
Figure 14 – Specimens in laboratory environment. 23
Figure 15 – High humidity environmental chamber. 24
Figure 16 – Specimens submerged in saturated sand. 25
Figure 17 – Reservoirs on vertically oriented specimen (left) and horizontally oriented (right). 26
Figure 18 – Galvanostatic method for accelerated chloride transportation. 27
Figure 19 – Migration cell method in high humidity container. 28
Figure 20 – (a) Specimens partially immersed in water; and (b) Potential measurement of partially water-immersed specimen. 29
Figure 21 – LPR & EIS measurement (left) and potential measurement (right) of water-immersed specimens. 30
Figure 22 – Specimen FS2 and FS3 partially buried in sand in container. 31
Figure 23 – CS specimen fully covered by wet saturated sand. 32
Figure 24 – Specimen FS1, CS1, and CS2 in container 2. 33
Figure 25 – Specimen CH1 in high humidity container. 34
Figure 26 – Location where initial cuts took place. 34
Figure 27 – Specimen termination and autopsy process. 35
Figure 28 – Removal of the solution reservoir. 37
Figure 29 – Indenting along the longitudinal and transverse steel wires using a thin chisel. 37
Figure 30 – Concrete indented along the longitudinal and transverse steel wires. 38
Figure 31 – Larger chisel hit with a sledge hammer to break concrete away from the steel. 38
Figure 32 – Concrete cover distribution (Groups Fp and Cp). L-Longitudinal, C-Circumferential directions. 40

Figure 33 – Concrete cover distribution (Groups Fg and Cg). L-Longitudinal, C-Circumferential directions. 40
Figure 34 – Concrete cover distribution (Groups Fm and Cm). L-Longitudinal, C-Circumferential directions. 41
Figure 35 – Concrete cover distribution summary. L-Longitudinal, C-Circumferential directions. 41
Figure 36 – Chloride migration coefficient vs. resistivity. 43
Figure 37 – Typical depolarization tests conducted on specimen C2 (Cp group). 43
Figure 38 – Potential, Rs and Rc values measured on F6 specimen. 49
Figure 39 – F2 specimen: a) potential vs. time b) Rc and Rs vs. time. 50
Figure 40 – C23 specimen: a) potential vs. time b) Rc and Rs vs. time. 51
Figure 41 – Potential, Rs, and Rc values measured on F1 specimen. 51
Figure 42 – Potential, Rs, and Rc values measured on C1 specimen. 52
Figure 43 – C3 specimen: a) potential vs. time b) Rc and Rs vs. time. 53
Figure 44 – F10 specimen: a) potential vs. time b) Rc and Rs vs. time. 54
Figure 45 – F21 specimen: a) potential vs. time b) Rc and Rs vs. time. 55
Figure 46 – C8 specimen: a) potential vs. time b) Rc and Rs vs. time. 55
Figure 47 – Cathodic potentiodynamic scans performed on F13. 57
Figure 48 – Cathodic potentiodynamic scans performed on C18. 58
Figure 49 – On- and off-potential vs. time for specimen F7. 60
Figure 50 – On- and off-potential vs. time for specimen F20. 60
Figure 51 – On and off-potential vs. time for specimen F23. 62
Figure 52 – On- and off-potential vs. time for specimen C4. 63
Figure 53 – Potential vs. time after corrosion initiation for specimen C6. 64
Figure 54 – Plot of Rc_LPR, Rc_EIS, and Rs vs. time for specimen F7. 65
Figure 55 – Nyquist plot of specimen F7. 65
Figure 56 – Plot of Rc_LPR, Rc_EIS, and Rs vs. time for specimen F20. 66
Figure 57 – Nyquist plot of specimen F20. 67
Figure 58 – Plot of Rc_LPR, Rc_EIS, and Rs vs. time for specimen F23. 68
Figure 59 – Nyquist plot of specimen F23. 68
Figure 60 – Plot of Rc_LPR, Rc_EIS, and Rs vs. time for specimen C4. 69
Figure 61 – Nyquist plot for specimen C4. 70
Figure 62 – Plot of Rc_LPR, Rc_EIS, and Rs vs. time for specimen C6. 71
Figure 63 – Nyquist plot of specimen C6. 71
Figure 64 – Potential, Rs, and Rc values measured on specimen C10. 72
Figure 65 – Potential, Rs, and Rc values measured on specimen F16. 72
Figure 66 – Potential, Rs, and Rc values measured on specimen F17. 73
Figure 67 – Potential, Rs, and Rc values measured on specimen F18. 73

Figure 68 – Potential and Rc values for specimen CS2. 74
Figure 69 – Potential and Rc values vs. time for specimen FS2. 74
Figure 70 – Potential and Rc values for specimen FS3. 75
Figure 71 – Potential and Rc values for specimen FI1. 75
Figure 72 – Potential and Rc values for specimen CI2. 76
Figure 73 – Potential and Rc values for specimen CH1. 76
Figure 74 – Potential, Rs, and Rc values for specimens C40 and C45. 77
Figure 75 – Potential, Rs, and Rc values for specimens F40 and F45. 78
Figure 76 – Evans diagram: (a) change in Cl^- concentration and/or O_2, (b) change in areas. 82
Figure 77 – Forensic examination of specimen F0. 85
Figure 78 – Corrosion penetration into the concrete for specimen F0. 85
Figure 79 – Removal of concrete on specimen F1. 86
Figure 80 – Section of steel wire with greater cross-section loss of specimen F1. 86
Figure 81 – Removal of concrete on specimen F2. 87
Figure 82 – Red and black/green rust observed upon opening specimen F3. 88
Figure 83 – Black/green rust observed outside the ponding along the transverse reinforcement for specimen F3. 88
Figure 84 – Autopsy result of specimen F3 – full steel wire mesh. 89
Figure 85 – Autopsy result of specimen F3. Left: location 1. Right: location 2. 89
Figure 86 – Specimen F11 while concrete was being removed. 90
Figure 87 – Steel wire removed from specimen F12. 90
Figure 88 – Concrete removal on specimen F21. 91
Figure 89 – Steel wire removed from specimen F21. 91
Figure 90 – Steel wire removed from specimen F22. 91
Figure 91 – Specimens F41 prior to and after concrete removal. 92
Figure 92 – Steel wire after removing concrete for specimen C0. 92
Figure 93 – Specimen C1 while removing concrete. 93
Figure 94 – Steel wire mesh removed from specimen C1. 93
Figure 95 – Steel wire while concrete is removed on specimen C5. 94
Figure 96 – Steel wire after removing concrete for specimen C5. 94
Figure 97 – Dark black/green rust stains on the bottom of specimen C7. 95
Figure 98 – Corrosion observed under the ponding on specimen C7. 95
Figure 99 – Autopsy result for specimen C7 – whole steel wire mesh. 96
Figure 100 – Autopsy result for specimen C7 (location 1). 96
Figure 101 – Steel wire after removing concrete for specimen C8. 97
Figure 102 – Steel wire mesh for specimen C12. 97
Figure 103 – Steel wire areas showing the most corrosion (specimen C22). 98
Figure 104 – Steel wire area showing significant corrosion from specimen C24. 98

Figure 105 – Corrosion extent on steel while removing concrete specimen C16. 99
Figure 106 – Steel wire removed from specimen C16. 99
Figure 107 – Partially exposed steel wire on specimen C43. 100
Figure 108 – Rust stains observed near the ponding on specimen F7 before opening. 101
Figure 109 – (1) Black/green rust observed upon cracking open specimen F7. 101
Figure 110 – (2) Black/green rust observed upon cracking open specimen F7. 102
Figure 111 – Autopsy result of specimen F7 – whole steel wire mesh. 102
Figure 112 – Autopsy result of specimen F7. Left: location 1. Right: location 2. 103
Figure 113 – Surface condition and exposed steel wire from specimen F18. 103
Figure 114 – Rust stain observed under the ponding on specimen F20 before opening. 104
Figure 115 – Black/green rust observed upon cracking specimen F7 open. 105
Figure 116 – Autopsy result of specimen F20. 105
Figure 117 – Autopsy result of specimen F20. Left: location 1. Right: location 2. 106
Figure 118 – Red rust observed upon cracking specimen F23 open. 106
Figure 119 – Autopsy result of specimen F23. 107
Figure 120 – Autopsy result of specimen F23. Left: location 1. Right: location 2. 107
Figure 121 – Exposed steel reinforcement ends corroding on specimen C4. 108
Figure 122 – Red and black/green rust observed on specimen C4 after opening. 108
Figure 123 – Autopsy result of specimen C4. 109
Figure 124 – Autopsy result of specimen C4. Left: location 1. Right: location 2. 109
Figure 125 – Red rust observed under the ponding upon opening specimen C6. 110
Figure 126 – Black/green rust observed upon opening the end of specimen C6. 110
Figure 127 – Autopsy results of specimen C6 – whole steel wire mesh. 111
Figure 128 – Autopsy result for specimen C6. Left: location 1. Right: location 2. 111
Figure 129 – Close-up of corroding sites for specimen F0 (along the ponding reinforcement), top and back side. 112
Figure 130 – Close up of steel corroding sites after cleaning on specimen F1. 112
Figure 131 – Close-up of corroding sites for specimen F2. 113
Figure 132 – Autopsy result of specimen F3. Left: after opening. Right: close-ups. 113
Figure 133 – Steel wire mesh after cleaning for specimen F4. 114
Figure 134 – Steel wire mesh for specimen F6 after cleaning. 114
Figure 135 – Steel wire mesh of specimen F9 after cleaning. 115
Figure 136 – Steel wire mesh specimen F12 after cleaning. 115
Figure 137 – Steel wire mesh specimen F21 after cleaning. 116
Figure 138 – Steel wire mesh specimen F22 after cleaning. 116
Figure 139 – Steel wire mesh specimen C0 after cleaning. 117
Figure 140 – Steel wire mesh specimen C2 after cleaning. 117
Figure 141 – Autopsy result for specimen C7 – Left: full wire mesh. Right: close-up. 118

Figure 142 – Steel wire mesh after cleaning for specimen C8. 118
Figure 143 – Steel wire mesh specimen C9 after cleaning. 119
Figure 144 – Close-up after cleaning steel wire of specimen C16. 119
Figure 145 – Steel wires after cleaning for specimen C22 and specimen C12. 120
Figure 146 – Close-up after cleaning steel wire for specimen C24. 120
Figure 147 – Specimen F7: Left: shortly after opening. Right: locations under the ponding. .. 121
Figure 148 – Autopsy result of specimen F20. Left: all reinforcement 1. Right: corroding sites. 121
Figure 149 – Autopsy result of Specimen F19: Left: all reinforcement, Right: corroding sites.. 122
Figure 150 – Autopsy result of specimen F23. Left: all steel wire. Right: corroding sites. 122
Figure 151 – Autopsy result of specimen C4. Left: after opening. Right: close-up after cleaning. 123
Figure 152 – Autopsy result of specimen C6. Left: after opening. Right: close-ups of corroding sites. 123
Figure 153 – Two of the pipes removed at Dania Beach Marina. 130
Figure 154 – Reinforced concrete pipe removed from Miami Beach (Alton Road). 133
Figure 155 – Potential profile along longitudinal. 134
Figure 156 – Chloride profile for Miami Beach specimen. 134
Figure 157 – Potential profiles measured along longitudinal wires (Dania Beach Marina). 135
Figure 158 – Chloride profile from RCP at Dania Beach Marina. 136
Figure 159 – Potential profiles measured on pipes taken from the Titusville Airport. 137
Figure 160 – Potential maps along the longitudinal reinforcements on samples at Indian Rock Beach. 138
Figure 161 – Potential values along the longitudinal reinforcements on RCP (Tallahassee). 139
Figure 162 – Reinforcement potential along longitudinal wires (Elliptical 1). 140
Figure 163 – Reinforcing wire potential along the top longitudinal wire (Elliptical 2). 140
Figure 164 – Reinforcing wire potential along three longitudinal wires, on a round RCP. 141
Figure 165 – Potential values along longitudinal wires on pipe #1 north of Hathaway Bridge. 142
Figure 166 – Potential values along longitudinal wires on pipe #2 north of Hathaway Bridge. 142
Figure 167 – Pictures of pipes found in Madeira Beach, FL (Left – SR-666, right –127th Ave). .. 143
Figure 168 – Potential values along longitudinal wires measured on pipe at 127th Ave. Madeira Beach, FL. 144
Figure 169 – RCP located at San Jose Park (Dunedin, FL). 145
Figure 170 – Potential values along longitudinal wires at St. Jose Park pipe (Dunedin FL). 145
Figure 171 –RCP found at Tilden Street (Dunedin, FL). 146
Figure 172 – Potential values along longitudinal wires at Tilden St. pipe (Dunedin, FL). 146
Figure 173 – RCP found at location close to Sugar Sands Inn. 147
Figure 174 – Potential values measured along longitudinal wires on RCP at Sugar Sand site... 147

Figure 175 – Potential values measured along longitudinal wires on RCP close to 17942 148
Figure 176 – Potential values measured along longitudinal wires on RCP close to 16690 Front Beach Road Site. 149
Figure 177 – Pipe tested for 3EB. 150
Figure 178 – Reinforcement exposed from a small segment obtained from Dania Beach Marina site. 151
Figure 179 – Reinforcement exposed from a small segment obtained from Dania Beach Marina site. 151
Figure 180 – After breaking the segment in two pieces. Significant cross-section loss observed on wire. 152
Figure 181 – Section with no solid steel wire 152
Figure 182 – Steel wire mesh removed from a different concrete segment from the same pipe 152
Figure 183 – Removed concrete revealed that only surface rust was observed. 153
Figure 184 – Cross-section shortly after wet cut. No signs of corrosion are visible. 154
Figure 185 – Corrosion extent observed on the wire mesh from segment obtained at Tallahassee site. 155
Figure 186 – Wire mesh after removing concrete on several segments. 156
Figure 187 – Rinker's specimen tested in November 2014. 158
Figure 188 – CHH specimen prior to 3EB load test and on the right after starting to remove the concrete. 159
Figure 189 – Pictures were taken after removing and while removing the concrete. 160
Figure 190 – Steel wire mesh after removing concrete on two pieces from CI2 specimen. 160
Figure 191 – Close-ups of sites showing corrosion for steel wire from CI2 specimen. 161
Figure 192 – Steel wire mesh after removing concrete on a segment for CS2 specimen. 161
Figure 193 – Close-ups pics for sites showing corrosion of the steel wire from CS2 specimen. 162
Figure 194 – Steel wire while removing the concrete on segment 1 of FI1 specimen. 162
Figure 195 – Steel wire after removing concrete on segment 2 of FI1 specimen. 163
Figure 196 – Specimen FS3 after 3EB load test. Note the various rust spots. 163
Figure 197 – Steel wire upon removing the concrete on a segment (Specimen FS3). 164
Figure 198 – Specimen FS2 prior to 3EB load test. Note the various rust spots. 164
Figure 199 – Partial concrete removal after 3EB test (FS2). 165
Figure 200 – Penetration into the concrete from the corrosion products (FS2). 165
Figure 201 – Partial and full concrete removal exposing steel wire mesh (FS2). 165
Figure 202 – Close-ups of selected sites where significant cross-section took place (FS2). 166

List of Tables

Table 1 – Mixture proportion of products. 6
Table 2 – Specimen name and grouped per method. 10
Table 3 – Environmental exposure during corrosion propagation stage for type F specimens... 17
Table 4 – Environmental exposure during corrosion propagation stage for type C specimens. . 18
Table 5 – Specimen ID based on type of concrete and environmental exposures. 25
Table 6 – Mean and standard deviation on cumulative concrete cover distribution. 41
Table 7 – Porosity of Concrete. 42
Table 8 – Label ID of F test specimens and time to corrosion initiation. 44
Table 9 – Label ID of C test specimens and time to corrosion initiation. 44
Table 10 – Re-polarization of specimens. 46
Table 11 – Cover, resistivity, solution resistance, applied potential and estimated electric field. 47
Table 12 – Specimen's ID, minimum concrete cover, time since corrosion initiation. 59
Table 13 – Calculated mass loss on specimens exposed on the vertical direction. 79
Table 14 – Calculated mass on specimens expose in the horizontal orientation. 80
Table 15 – Calculated mass on specimens subjected to accelerated corrosion. 80
Table 16 – Calculated mass on ring specimens. 81
Table 17 – Calculated mass on specimens 40s group 81
Table 18 – Comparison of calculated mass and measured mass loss (horizontal specimens). . 125
Table 19 – Comparison of calculated mass and measured mass loss (vertical specimens). 126
Table 20 – Calculated and measured mass loss. 127
Table 21 – Measurements performed on collected soils. 132
Table 22 – Chlorides and resistivity measured on solution (Sites visited 2016). 133
Table 23 – Results of 3EB load tests on ring specimens. 157

Chapter 1 - Introduction

Dry-cast reinforced concrete pipe (RCP) is a frequently used drainage pipe. Its durability and service life in aggressive environments is of great concern. Exposure to chlorides from marine environments can result in the premature corrosion of reinforcing steel and the resulting failure of such structures. Several departments of transportation, including Florida's, have developed models to estimate the service life of various types of drainage pipes, including dry-cast RCPs.

Florida Department of Transportation's (FDOT) existing model for reinforced concrete pipes is based on the assumption that the durability of reinforced concrete pipes in the Florida environment is controlled by the corrosion initiation of the steel. The equation in the model was first developed by Cerlanek[1] and later updated based on research by Sagüés et al.[2] The equation in the model is a function of the environmental sulfate content, environmental chloride content, pH of the soil and/or water, cement content, cover thickness, and total percentage of mix water. The correlations in the model are based on empirical field and lab observations. For a reinforced concrete structure, the service life ends when the cracks occur in concrete due to the corrosion of reinforcing steel and/or they can't carry the structural load. A field survey on a total of eight reinforced concrete pipes in Florida[2] revealed that only one pipe of those visited had degraded significantly. The appearance of one other pipe was in fair condition while the remaining RCPs were generally in very good condition. Four or these pipes were re-visited as part of this project; three of the pipes were found to be in poor condition. Field performance of reinforced concrete pipe in chloride environments has also been reviewed and studied by the California Department of Transportation (CalTrans)[3]. The results from the CalTrans study showed that only one of the visited pipes in California experienced corrosion-induced damage. A similar investigation has been also conducted in Australia, where reinforced concrete pipes were exposed in the tidal zone of a marine environment[4]. The authors concluded that the corrosion initiation of steel was evident in many pipes, but none of the buried pipe cases had corrosion advanced to the extent of causing cracking or spalling of the concrete.

As indicated above, the current FDOT service life prediction model for reinforced concrete pipes uses an equation that includes parameters such as the water-to-cement ratio (w/c), pipe diameter, cement content, ppm of chloride (in soil/solution), soil pH, and other parameters, but the model does not consider several other parameters. The current model estimates the expected service life based on time to corrosion initiation. It is important to mention that the time to initiation might be shorter than that predicted by the current equation due to the high porosity and high chloride diffusivity coefficient of dry-cast RCPs and due to the fact that regions with smaller than target concrete cover have been found[2]. FDOT-sponsored research has shown that the concrete porosity of dry cast reinforced concrete pipes can be high[2]; tests performed in this project confirm it. Moreover, two reports[2,5] and our ongoing research found concrete covers that vary over a large range. However, there is no widespread need for replacing dry-cast RCPs due to corrosion problems. Therefore, time to corrosion initiation might not be the only period that needs to be considered when estimating the dry-cast RCPs' service

life. Oxygen concentration surrounding the dry-cast RCPs and concrete degree of saturation (i.e., moisture content) in the installed condition are two of the parameters currently not included in the model equation (in part because these factors can vary seasonally and over time and are difficult to measure onsite). These two parameters might be relevant during the corrosion propagation stage. Situations under stagnant air could affect corrosion propagation differently from when an in-flux of fresh air is present (e.g., close to the culvert mouth). Seawater vs. brackish water could react with the concrete surface differently (e.g., marine growth could form in contact with seawater and/or brackish water).

Concrete with high porosity typically results in concrete with high diffusivity[2] and the results presented here suggest that this is indeed the case. Under these conditions, the time to corrosion initiation can be compromised (be shorter than predicted by the current model), particularly in the regions where the concrete cover is small. Under these circumstances, what might determine the time to critical corrosion damage (useful life based on corrosion) is the duration of the corrosion propagation stage. Traditional methods assign 5 to 10 years for the propagation stage. However, as it has been mentioned above there are limited, if any, cracked or spalled RCPs that have been reported due to corrosion of the reinforcement. The limited number of reported failures might be in part explained because it is difficult to inspect the pipe surface condition.

During the propagation stage, corrosion products can build up at the corroding steel. After some time the accumulated volume of these products become constrained and can produce significant tensile stress onto the concrete. These stresses can eventually lead to cracks of the reinforced concrete structure. This is typically found for atmospherically exposed concrete and the section at the splash zone. However, the small-diameter steel stirrup and high porosity of RCP might allow the corrosion products to move through the pore structure under high moisture conditions and not produce cracks or produce only small cracks. Moreover, when the concrete is quite saturated it has been observed that the corrosion products flow more easily into the available concrete pores structure[6]. Furthermore, it also has been reported that under saturated concrete, the corrosion rate of the reinforcing steel is also slower than when wetting/drying cycles are taking place. It is frequently assumed that this is due to oxygen concentration limitations.

Factors affecting the corrosion propagation period include: porosity, cover, degree of saturation, availability of water, availability of oxygen, resistivity (the last three parameters both in the concrete and at the surrounding soil), corrosion rates, and environment. The corrosion rate of steel in concrete can be limited by the concrete resistivity which is controlled by w/c, moisture content, and the presence of admixtures such as fly ash. Fly ash usually reduces the porosity with time as hydration and the pozzolanic reaction progresses. Some researchers claim that the corrosion rate is highest when the relative humidity (RH) ranges from 70% to 95%, i.e., under conditions where plenty of oxygen is available and for a given intrinsic resistivity[7-11]. It has been reported that the corrosion rate would decrease when the environmental humidity increase from 95% to 100%[12], but it is not clear at what RH value the transition occurs. It is widely understood that the corrosion rate of the submerged or fully

saturated reinforced concrete is low compared to atmospherically exposed reinforced concrete. Previous studies have confirmed that the corrosion rate is reduced in such conditions due to the supply of insufficient oxygen at the steel depth[13-18]. More recently, Hussain, et al., investigated the coupled effect of oxygen and moisture on the corrosion of reinforcing steel in concrete[19,20]. The results reported by Hussain revealed that the diffusion of oxygen is a vital limiting factor for corrosion of the steel reinforcement only when the reinforced concrete structure is either submerged or in a high RH environment with a thick concrete cover and low w/c ratio. There is no agreement as to at what relative humidity (hence concrete moisture content) - the oxygen reduction reaction would slow down. For example, Hunkeler[12] suggest that this takes place at humidities > 95%, Hussain[19,20] and Raupach[15,16] suggest that even at 97% RH: O_2 transport takes place allowing the oxygen reduction reaction to take place at the reinforcement at a rate enough to support corrosion. For dry-cast reinforced concrete pipes in marine environments, it is therefore apparent that considerable development is still required in order to obtain an updated service life model that better reflects dry-cast RCP composition and exposure conditions.

To investigate the propagation stage, it would be desirable to shorten the time to corrosion initiation via an accelerated method. Trejo[21,22], Castellote and Andrade[23,24], among others, have proposed methods to determine the chloride threshold on freshly prepared specimens (usually mortar) that apply an electric field. Because of this, an accelerated transport of chlorides occurs. Migration tests (e.g., Rapid chloride permeability, Nordtest Build-492[25] named here rapid migration test (RMT)) have also been developed to obtain chloride permeability into concrete after a short period of time. These methods influenced the design of the three approaches implemented here, and were applied to dry-cast RCP instrumented segments. The results of applying these different approaches show that the time to corrosion initiation varied from a couple of days to several months. It also demonstrated that the time range was not just as a function of the applied method, but also the type of concrete, moisture content and concrete cover.

Many studies of corrosion of the reinforcing steel in concrete have been performed to identify time to corrosion initiation. Experiments are usually stopped shortly after corrosion initiation has occurred[22,23,26-29]. When investigating corrosion of the reinforcing steel that produces cracks due to accumulation of corrosion products, the specimens are typically cast with chlorides and a large current applied to minimize the duration of the test[6,30-32]. A few investigations have been carried out in which the applied current was smaller (within the larger observed field values i.e., < 100 $\mu A/cm^2$), but with the specimens cast with chlorides[6,30-32]. The effect of the anode length/cover has recently been investigated by Sagüés and collaborators[6,32]. However, when corrosion of the reinforcing steel takes place naturally (lab or field) due to chlorides, localized corrosion is typically observed, i.e., the length of the anode is usually small and initially starts at one side of the steel wire.

Laboratory size specimens were obtained from dry-cast reinforcing pipes. Each specimen was instrumented to monitor the steel embedded in the concrete. Three methods were used to accelerate the chloride transport. This allowed the reinforcing steel of specimens to initiate

corrosion after the driven chlorides exceeded the critical threshold concentration. Accelerated chloride transport was achieved by applying an electric field which was then suspended once corrosion initiated. Upon corrosion initiation of the reinforcement, the specimens were exposed to high moisture conditions during the propagation stage, and a selected number of specimens were subjected to modest accelerated corrosion via anodic polarization - using a galvanostatic pulse. After corrosion initiated, some of the specimens were exposed to lab humidity and temperature for several weeks to a few months before transferring them to a high moisture environment. Additionally, two other sets of specimens were prepared and monitored. One set consisted of ring specimens (i.e., pipe slices) that are approximately 10 to 12 inches wide; The second set consisted of lab sized specimens that were prepared after terminating selected full ring specimens.

Periodically, linear polarization resistance, electrochemical impedance spectroscopy, and corrosion potentials were measured. The polarization resistance (Rc = measured apparent polarization resistance minus the solution resistance) values were used to compute the corrosion current. The average current from pairs of consecutive measurements was then used to calculate the charge over a given period of time. The total charge per sample was calculated by adding the charge for each of these periods. It was assumed that most of this charge is due to corrosion of the reinforcement. Then, using Faraday Law, the mass loss was calculated. The calculated mass loss values might deviate some from the actual mass loss, but these calculated mass loss values were used to decide which specimens were to be forensically analyzed first. Most lab specimens were forensically analyzed and the steel wire mesh was chemically cleaned to remove corrosion products. The measured mass loss was calculated with respect to the mass of the steel wire mesh before cleaning it. The calculated mass loss values vs. measured mass loss values are discussed.

As indicated above on selected specimens, a current was applied of a magnitude equivalent to 0.5 $\mu A/cm^2$ via a galvanostat (this current was later increased in some specimens to one and/or 2.5 $\mu A/cm^2$). This applied current modestly accelerates the corrosion process. The applied current density assumed that half of the steel area under the reservoir was undergoing corrosion. However, if the corroding area was smaller, for example $1/20^{th}$ of the total surface area, then the corroding site would have experienced an applied current density of 5 to 25 $\mu A/cm^2$. The current was applied cyclically: typically current-on for 11 days, and then disconnected for 3 days. The specimens during the accelerated corrosion period were stored in high humidity, and after several cycles, selected ones were covered with saturated sand while others remained under the high humidity exposure. During the disconnected periods, electrochemical measurements such as corrosion potential, linear polarization resistance, and electrochemical impedance spectroscopy were performed; the latter two tests at least two days after removal of the applied current. Selected specimens were terminated and gravimetric weight loss measured. These weight loss values were compared to the mass loss calculated by using Faradays Law from the measured Rc values.

Field visits were also part of the project. Segments were obtained from sites on which the RCP had been removed. These segments were taken to the lab and forensically analyzed. Corrosion

potential were measured along selected longitudinal wires. Steel wire mesh after concrete removal showed corrosion for three of these sites. A second set of visited sites corresponded to sites in which the pipe continues to be in service while exposed to aggressive environment. Evidence was found that steel corrosion was on-going (either visual or via corrosion potential measurements) at several of these sites.

The research results presented above confirm that under certain circumstances corrosion propagation can take to the extent that either there is no longer reinforcement and not cause cracks. This appears to take place for situations in which the concrete is kept under high moisture conditions. This was found on lab observations (e.g., Specimen F1 and Specimen F2), ring specimens (FS2 and FS3).It was later confirmed via forensic examination of samples obtained from the field.

Chapter 2 - Experimental

2.1 Materials and Samples

In the present investigation stock dry-cast RCP (from this point forward, dry-cast RCPs are named RCPs) sections were segmented to prepare instrumented samples. RCP sections of 61 cm (24 inches) in diameter and 153 cm (60 inches) long were supplied by FDOT. The RCP sections conform to ASTM C76[33]. These RCP sections were stored outdoors for more than 3 years at FDOT's State Materials Office prior to delivery to FAU. Two different types of dry-cast RCPs were supplied by FDOT. One type of RCP contained fly ash and is named here samples type F. The second type contained only ordinary Portland cement as the cementitious material. This second type of dry-cast RCP is referred in here as samples type C. Table 1 shows the composition provided by the producers for both pipe types. The pipe sections were cut with a heavy duty hand held concrete wet-saw equipped with a diamond blade designed to cut concrete. The RCP was marked before cutting. The RCP segments were first cut into slices (rings) 28 cm wide. A total of twenty slices of RCP rings were obtained from the two type F RCP segments and the two type C RCP segments. Five type F RCP rings and five type C RCP rings remained in a ring shape. The other ten (5 type F and 5 type C) rings were sectioned at 30°, 45° and 60° angles as shown in Figure 1. The reason for segmenting the test pieces at different angles is to end up with 1, 2 and 3 longitudinal reinforcement bars for the test specimens. Both full ring specimens and test specimens were instrumented.

Table 1 – Mixture proportion of products.

Mix Design 4000 PSI			
Materials Type	Materials		Unit
	Type F	Type C	Lb/yd^3
Cement	391	590	Lb/yd^3
Fly Ash	103	0	Lb/yd^3
Sand	1689	1895	Lb/yd^3
Stone	1773	1300	Lb/yd^3
Water	16	29	Gal/yd^3
Admixture	0	0	Oz

The various test specimen sizes produced different cathode to anode ratios, as for each specimen only a portion of one of the longitudinal bars and a small fraction of transverse wires (below the longitudinal wire) were subjected to chloride solution (see explanation below). Each specimen was labeled and grouped as the type of concrete and a number corresponding from where the segment came relative to the cut (labeled clockwise); i.e., the base segment from the type F dry-cast RCP is labeled F0. A sequential numbering was used when moving to the other segmented rings. The exposed steel reinforcement bars of each specimen were checked for electrical continuity with respect to the other longitudinal and transverse (spiral) wires. This was verified by using a multi-meter on the Ω (ohm) setting then placing one needle probe on a

steel reinforcement bar and touching the rest of the reinforcement ends with the other needle. All of the reinforcements were found to be continuous on all specimens.

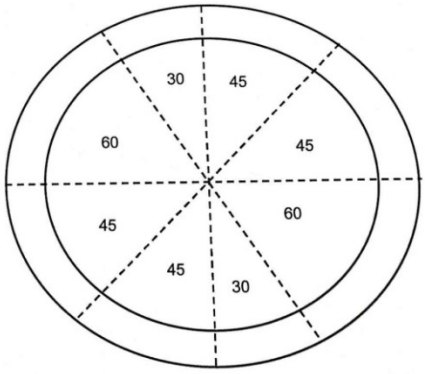

Figure 1 – Angles at which each ring specimen was segmented.

Most test specimens were converted into electrochemical cells. On each specimen one of the exposed steel wires was selected to establish an electrical connection. This was accomplished by threading a #2 or #4 machine stainless steel screw onto the center of the selected reinforcement. This was achieved by locating the center of the selected steel stirrup with a proper indentation by punch mark and then drilling a one cm deep hole into that reinforcement. Threads were created from carefully turning a plug tap then finishing it off with a bottoming tap to ensure the screw secured properly. Two nuts were placed on the screw with two washers on each side so an electrical wire could be secured in contact with the reinforcement. This connection was used to monitor the corrosion potential and for some set-ups to polarize the reinforcement as part of the accelerated transport methods described below. The other exposed wire cross-sections were covered with marine grade sealant. All specimens were then placed in laboratory environment (at 21^{o}C and RH 72-75%), unless otherwise noted.

Reservoirs were installed on the specimens in horizontal or vertical orientations (with respect to the orientation of the longitudinal reinforcement of the specimens). On specimens with the reservoir exposed in the horizontal orientation, the reservoir was made-up of Plexiglas and was held together by a waterproof UV-resistant marine sealant. The nominal cross-section area for the horizontal reservoir was 6.35 cm x 15.2 cm. The reservoir was glued on the inner curvature of the specimen right above the selected reinforcement, where the electrical installation was made, as shown in Figure 2a. The bottom edge of the reservoir's horizontal section was also cut in a concave shape so that it matched with the inner curvature profile of the specimens. The height of the reservoir was 5 cm. In specimens with the reservoir in the vertical direction, two elliptical plastic containers were first cut to the shape of the inner and outer diameter of the pipe. The containers were then glued using marine grade silicon, and left to cure for one day as shown in Figure 2b. Each container reservoir has an area of 6.35 cm x 17.8 cm and the reservoirs were filled with the solution up to 12.7 cm height.

Figure 2 – (a) Horizontal specimens with one reservoir, (b) Vertical specimens with 2 reservoirs.

The concrete cover over each exposed steel wire on each specimen was measured and tallied to obtain concrete cover cumulative distribution. These covers were measured from the internal diameter to the top of the exposed steel wire. They were measured by using a caliper and the results were recorded. These measurements were performed prior to attaching the solution reservoir or making the electrical connection.

2.2 Testing of Dry-Cast Concrete Porosity, Rapid Chloride Migration Test, and Resistivity

To further characterize the characteristic of both types of dry-cast RCPs, two segments from each RCP type were selected to obtain concrete cores for a modified (i.e., smaller diameter core) Rapid Migration Test[25] and surface resistivity using a probe spacing of 2 cm. Both tests were performed once the cores were water saturated. These cores were obtained using a wet-coring device with a nominal 5.7 cm diameter drill bit that produced 5 cm diameter cores. Additional cuts were done on a second pipe segment per sample type to obtain rectangular prismatic specimens for porosity tests. This latter test was done in accordance with ASTM C642[34], except that the concrete was dried at 55°C instead of 105°C.

2.3 Methods Used to Accelerate Chloride Transport

Three approaches were used to shorten the time to corrosion initiation of the steel wire embedded in dry-cast reinforced concrete pipe instrumented specimens. The concrete contained no chlorides to start with and each of the approaches described below accelerated the chloride transport via electro-migration. Two of the approaches were used directly on the embedded steel wire as one of the electrodes with a second electrode placed in the installed solution reservoir. For the third method, two solution reservoirs were installed and stainless steel mesh electrodes were immersed in each reservoir. These approaches are named: potentiostatic, galvanostatic, and migration methods. The samples were exposed to lab humidity and temperature (except if indicated otherwise). A list of specimens and approaches employed are included in Table 2. The letter next to the concrete type indicates the method used to accelerate chloride transport: p-potentiostatic, g-galvanostatic, m-electro-migration.

2.3.1 Potentiostatic Method

A ponding set-up made of Plexiglas was glued with marine epoxy. Nominal dimensions of the cross-section were 6.35cm x 15.24cm. The reservoir was installed on the inner radius section of the RCP. The nominal surface area of the steel wires under the ponding is given below. An activated titanium mesh was placed in the solution reservoir. For this experiment, a 15% NaCl solution (by mass) was used. A saturated calomel reference electrode (SCE) was inserted through a lid covering the solution reservoir, and was connected to the reference electrode terminal of the potentiostat. The activated titanium mesh was connected to the counter electrode terminal of the potentiostat. A 100-Ω resistor was connected across counter and working terminals of the potentiostat to measure the current flowing at any given time. The reinforcing steel contact (via the tapered screw) was connected to the working electrode terminal of the potentiostat. Once the connections were made, the potentiostat was then turned on. A potentiostat was needed per each dry-cast RCP specimen. The potentiostat was set to a potential hold of +2 Vsce for Group Fp specimens and +3 Vsce for Group Cp specimens. This potential difference was set between the reference electrode and the reinforcing steel. The actual applied potential between the counter and the steel was also measured. Figure 3 shows the ponding set-up; the longitudinal steel wires are in the horizontal direction.

2.3.2 Galvanostatic Method

The solution reservoir used in this test was similar to that described for the potentiostatic approach. A constant current was applied; therefore, there was no need to have a reference electrode in the solution all the time. Constant current was delivered via 6 multi-channel galvanostat (one specimen per channel). Initially, a current of 1.5 mA was applied to each specimen. The positive terminal of one of the channels was connected to the reinforcement terminal post on the specimen and the corresponding negative terminal in the multi-channel box galvanostat was connected to the counter electrode activated titanium mesh. Group Fg specimens (See Table 2) and Group Cg specimens (see Table 2) were polarized using the galvanostat method of constant current value of 1.5 mA. The solution reservoir was filled with 3,400 ppm of chloride ions (~120 g of NaCl to 20 L) for specimens Fg(4) and Cg(6). The lower chloride concentration was used as the 3,400 ppm are within the range observed in Florida soils. The chloride concentration was 10,150 ppm for specimens part of group 2nd-Fg(9). (See Table 2.)

Table 2 – Specimen name and grouped per method.

Group (number of specimens)	Specimen ID
Fp(4)	F0
	F1
	F2
	F3
Fg(4)	F4
	F5
	F6
	F7*
2nd-Fg(9)	F12
	F16*
	F17*
	F18*
	F19*
	F20*
	F21
	F22
	F23*
Fm(6)	F8
	F9
	F10
	F11
	F13
	F15

Group (number of specimens)	Specimen ID
Cp(6)	C0
	C1
	C2
	C3
	C4*
	C5
Cg(6)	C6*
	C7
	C8
	C9
	C10*
	C11
Cm(7)	C12
	C13
	C14
	C15
	C16
	C17
	C18
Cm-HH(5)	C21
	C23
	C24
	C25
	C26
Crack Not Polarized	C22

Note:* indicates that specimen was selected for accelerating corrosion during the corrosion propagation.

Figure 3 – Typical ponding setup installed on specimens (horizontal setup).

2.3.3 Migration Cell

Solution reservoirs were installed on both sides of the selected longitudinal steel wires. In this case, the longitudinal wires are in the vertical direction. Typical setup is shown in Figure 4. Two elliptical plastic containers are cut to the shape of the inner and outer diameter of the pipe. The containers are then glued using marine-grade silicon and allowed to cure for one day. The chloride solution was filled in the container glued to the inside curvature of the specimen (typically smaller cover). The container glued to the outside curvature of the specimen was filled with $Ca(OH)_2$ solution (two grams/Liter). The solution volume added at each side was approximately 200 ml, and a re-fill took place when necessary. The electrodes for this approach were made of stainless steel meshes cut to fit inside each container. The negative side of a power supply was connected to the stainless steel mesh placed inside the chloride solution, and the positive was connected to the mesh placed inside the calcium hydroxide solution.

Figure 4 – Migration cell setup (vertical setup).

The chloride solution concentration was 10,150 ppm (the salt used was NaCl). The increase in chloride concentration with respect to the galvanostatic approach was two-fold: (1) to try to reduce time to initiation on dry-cast RCP specimens tested using this approach, and (2) to have another values for surface concentration, Cs, representative of a higher concentration also observed in Florida soils. The applied voltages between the stainless steel electrodes were 30 volt and 15 volt for Group Fm specimens and Group Cm specimens, respectively. For this setup, there was no direct connection to the reinforcing steel while applying the electric field. A number of the vertical specimens were placed in a high humidity environment for a week prior to applying the electric field. The moisture of the concrete was increased and likely produced a lower concrete resistivity. Specimens C21, C23, C24, C25, and C26 were the specimens subjected to this conditioning, and remained in the high humidity chamber while the electric field was applied.

2.4 Potential Measurements Prior to Corrosion Initiation

The applied potential (regardless of method used) produced an electric field that promoted the chlorides to be transported mainly by electromigration. The total applied potential ($V_{applied}$) was

measured periodically on all systems while the electric field was applied. The voltage-drop across the resistor ($V_{resistor}$) was periodically measured for specimens subjected to the potentiostatic and galvanostatic approaches. They were used to monitor the amount of current flowing between the activated titanium mesh and steel reinforcement. The measured potential was converted to current by using Ohm's Law, V=IR.

The applied potential was removed once a week. Following removal of the applied potential, a procedure similar to a depolarization test was performed periodically on all specimens to identify the time to corrosion initiation, via the corrosion potential. The potential difference between the reference electrode and the working electrode (steel) was measured shortly after disconnecting the corresponding system, and after some time (see below). For example, for the case of the migration set-up, the potential vs. a saturated calomel reference electrode was measured upon turning off the power supply, i.e., a few seconds after turning off the electric field. The $V1_{off}$, was recorded about 5-10 seconds after disconnection. Three more measurements of the steel potential were done 10, 30 and 60 minutes later ($V2_{off}$, $V3_{off}$ and $V4_{off}$) with the system off. Additional V_{off} potential measurements were performed if the steel potential shifted to more negative values with a significant potential decay, and remained disconnected up to 24 hours. If the potential was more negative than -180 mVsce, the specimen was left disconnected and the potential monitored once a day for the next few days. Similar depolarization tests were conducted for specimens subjected to the potentiostatic or galvanostatic approaches. For the migration and galvanostat approaches the reference electrode was momentarily immersed in the solution; whereas for the potentiostatic approach, the reference electrode remained immersed in the solution all the time during both polarization and depolarization.

2.5 Environmental Exposures during Natural Corrosion Propagation Stage

The three methods used to accelerate chloride transport allowed corrosion of the steel to initiate within a reasonable amount of time (typically less than 6 months). To study the steel corrosion propagation, the specimens were exposed to various laboratory environmental conditions ranging from specimens exposed to laboratory humidity, high humidity, partially immersed in water and partially covered with simulated saturated soil (water saturated sand). The latter three set-ups were implemented to try to replicate high concrete moisture content and lower O_2 concentrations at the reinforcement surface. Under most of these scenarios, the corroding and non-corroding reinforcing steel would be surrounded by highly moist concrete, which reduces the oxygen transport and typically limits oxygen transport (mass control develops), particularly on specimens immersed in water. As corrosion progresses (corrosion propagation stage), it was unknown whether due to oxygen limitations the cathodic reaction would slow down the corrosion rate, or if a macrocell would develop that allowed the corrosion to continue at the same/higher rate (i.e., a larger area provide cathodic current to keep the anode demand).

All samples were eventually transferred to a high humidity environmental exposure. While preparing the different high humidity environment set-ups, the corrosion-activated samples

were kept in the laboratory conditions (i.e., lab humidity and temperature) for periods that ranged from a few weeks to several months. Some samples were exposed in sequence to various exposure conditions before being moved to the present exposure condition. Different high humidity exposure conditions were prepared so as to replicate field conditions during the corrosion propagation stage. The environments will be described first and then bar-plots are used to describe if a specimen was exposed to more than one of these environments and for how long. A number of specimens were selected to be subjected to galvanostatic pulse during the corrosion propagation. Both the environmental exposure and procedure used on these specimens are described in a different section.

2.5.1 High Humidity

A high density polyethylene 91.4 x 91.4 x30.48h cm container was used as a high humidity chamber. Hollow plastic cylinders 5 cm in height and 10.1 cm diameter were placed at the bottom of the container. A plastic mesh was placed on top of these cylinders. The high humidity condition was achieved by filling with water to a height of 3.8 cm. Specimens C1, C3, C11, F1 and F5 were placed on this chamber. The picture on the left in Figure 5 shows the container and the samples. Each specimen was installed with its individual reference electrode. Wires of sufficient length were prepared and installed for each specimen to reach outside the box. Electrochemical measurements described below were performed once a week or once every other week (eventually the frequency changed to once a month or every other month). Water was sprayed manually inside the box twice a week. A hole of 1.25 cm diameter was drilled on top cover of the box and fitted with a coupling. A humidity sensor probe was inserted periodically to check the relative humidity inside the box by momentarily removing the plastic couple. The box cover was clamped down using six C clamps. After the initial set of measurements were processed (a couple of weeks) the measured relative humidity was ~90%. It was decided to install weathering strips on the box top to improve the seal. The relative humidity after this set-up modification was approximately 95%. However, no decay in the corrosion rate was observed after five months of exposure in this environment. The specimens were then exposed covered with simulated soil condition as explained below (the same container was used). A few specimens were placed on plastic containers that held one or two specimens (F2, F3, F6, C9 and C7) exposed to high humidity. Specimens F0 was exposed to lab humidity 880 days and then transfer to a high humidity chamber for 140 days.

Figure 5 – Specimens exposed to high humidity environment.

Additionally, a fiberglass tank was also set-up as a high humidity chamber for specimens placed in the vertical position (Figure 5, picture on the right). The chamber bottom was laid with the same type of plastic cylinders (5 cm high) and a plastic grid was placed on top of these plastic cylinders. The bottom of the chamber was filled with water to approximately 3.8 cm in height. The chamber was covered with half-inch thick Plexiglas plates. Weather tight strips were used to achieve 95-98% RH at room temperature (~21 °C) inside this chamber.

Figure 6 – Specimens covered with saturated sand.

2.5.2 Specimens Covered with Saturated Sand

Horizontal samples that were subjected to the high humidity environment (HDPE described above) were later covered with water saturated sand in the same container. The container was momentarily emptied and the bottom two inches filled with the saturated sand. The samples were then transferred back into the HDPE container. The sand was spread evenly over the specimens and support wedges were placed as needed. The space around the samples (C1, C3, C11, F5, F1) and below the curved profile was also filled with the sand, but leaving the electrical connection area uncovered (See Figure 6b). Sand covered the top of the specimens except for the reservoir area. During the initial measurements, it was observed that the sand on the surface dried after a few days. The sand was periodically sprayed with tap water to keep the high moisture.

A HDPE container of 91.4 x 91.4 x 45.7h cm was used to accommodate nine samples oriented vertically (C13, C21, C16, C25, C24, F8, F9, F11, and F13), as can be seen in Figure 6a. The bottom of the container was first filled with two inches of sand. The samples were then placed in two rows on the evenly-spread sand. The spaces around the samples were filled with the saturated sand up to the upper edge of the reservoir. Most of the upper parts of the samples were covered with saturated sand, leaving uncovered only the area above the reservoirs. During the initial exposure period (~ 2 weeks), it was observed that the sand surface dried. Water was added to the sand by gently pouring additional water using a small beaker. Later the addition of water was stopped, since the sand remained saturated. The container had a cover that was momentarily removed when performing the electrochemical tests described below. Water was periodically sprayed.

A third group had the samples covered with sand up to one-third of the specimen height. A semi-transparent plastic container of 38.1x61x30.5 inches in size was used for this set-up. The container bottom was filled evenly with saturated sand to a height of one inch. Three specimens of type C (C22, C23, and C16) were chosen from those already exposed in the high humidity fiber glass chamber. See Figure 6c. The plastic container was placed inside the fiber glass high humidity chamber. After approximately 900 days additional wet sand was added to the container.

2.5.3 Immersed in Water

The electrical connection post was immersed in water due to its location on the horizontally-oriented specimens selected to be immersed in water. Hence, an isolation chamber was installed around the electrical post connecting the reinforcement on each selected specimen to prevent direct contact with water, such that monitoring measurements could be performed. The isolation chamber was a reinforced fiber glass trapezoidal shape enclosure (or an L shape plastic section). The bottom of the isolation chamber was sealed by an acrylic plate using a UV resistance epoxy marine sealant. The top was left open for access during measurements. A hole of 8mm was made on the flat side of the isolation chamber to accommodate the electrical post. The isolation chamber was then glued to the specimen. The glue was allowed to cure for at least 24 hours. The isolation chamber was checked for leaks and if none were present, then the specimen was immersed in water. Under this arrangement, most of the specimen was immersed in water but not completely. See Figure 7a.

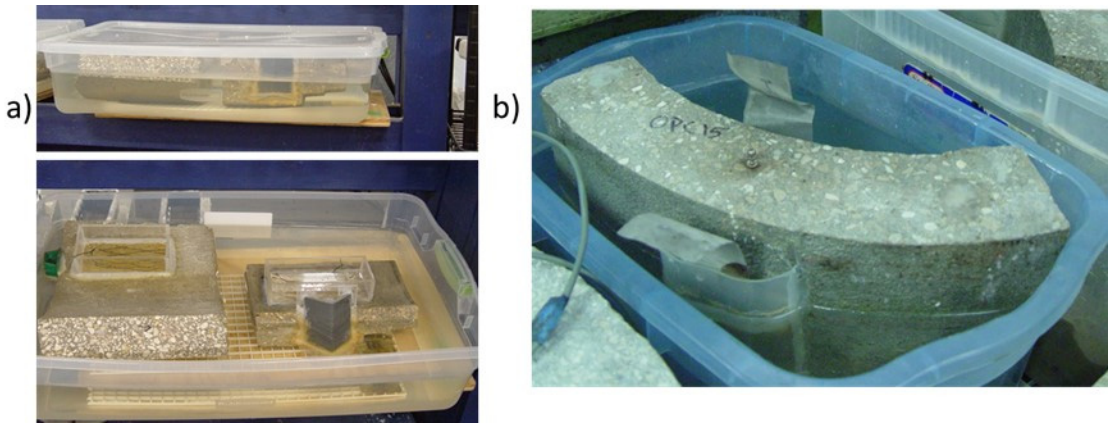

Figure 7 – Specimens immersed in water.

2.5.4 Vertical Specimens Immersed in Water

Two plastic containers of dimensions 66x43.2x38.1h cm and 60.9x30.5x30.5h cm were placed inside the high humidity fiber glass chamber. One type C (C18) and two type F (F10, F15) specimens were placed inside the larger container. C15 specimen was placed in the smaller container (See Figure 7b). The containers were filled with water until the top edge of the reservoirs was reached.

2.6 Electrochemical Measurements during Natural Corrosion Propagation

Half-cell potential measurements (of the reinforcement steel on each specimen) were carried out using a high impedance voltmeter (> one MOhm). Initially, the potential measurements were made once a week (or every two weeks) during the corrosion propagation stage exposure. Later, the potential measurements were performed once a month and eventually once every other month. The solution resistance Rs was measured via electrochemical impedance spectroscopy (EIS) tests. The impedance magnitude measured at a frequency of approximately 60 Hz was assumed to be the Rs of the system. During the months that followed corrosion initiation, the linear polarization measurements were performed every other week during the corrosion propagation stage to monitor corrosion rate of the steel. Later the measurements were performed once a month or once every other month. The measured value is named herein "Rp_meas" and includes the solution resistance of the system. The corrected polarization resistance Rc (i.e., after subtracting Rs) was calculated. The linear polarization test was performed from 10 mV below OCP to OCP at a scan rate of 0.1 mV/sec. An area of one cm was assumed during the test, but the corroding area was not known. The surface area under the reservoir for each specimen was calculated. Since chlorides were transported from one side only, once corrosion initiated the corrosion site might be smaller than steel surface under the reservoir.

2.7 Environmental Exposure Sequence after Corrosion Initiated

Tables 3 and 4 show a detailed description of each specimen's exposure sequence (i.e., the duration in each exposure condition) during the corrosion propagation stage. In several instances, a specimen was exposed to more than one exposure environment during the propagation stage. Also, some specimens remained under laboratory RH conditions from several weeks to several months after corrosion initiation prior to transfer to a high moisture environment.

Table 3 – Environmental exposure during corrosion propagation stage for type F specimens.

Dry-Cast Pipe Type	Group (number of specimens)	Specimen ID	Amount of Time in Days as of 5/15/16			
			LAB RH	High Humidity	Covered with Sand	Immersed in Water
F	Fp(4)	F0_T	880	140	X	X
		F1_T	181	147	787	X
		F2_T	71	1551	X	X
		F3_T	267	525	X	X
	Fg(4)	F4_T	246	X	1247	X
		F5	98	147	1317	X
		F6_T	179	1298	X	X
		F7*_T	532	175	X	X
	2^{nd}-Fg(9)	F12	182	X	X	1180
		F16*_T	322	189	523	X
		F17*_T	322	189	523	X
		F18*_T	322	712	X	X
		F19*_T	322	320	X	X
		F20*_T	322	182	138	X
		F21	133	X	X	1134
		F22	176	X	X	1143
		F23*_T	224	320	X	X
	Fm(6)	F8	134	X	1303	X
		F9_T	144	X	1205	X
		F10	32	136	X	1221
		F11_T	58	X	991	X
		F13	134	X	1303	X
		F15	90	136	X	1221

Note: Nominal steel area under the reservoir was 54 cm^2 for F0 to F3; all other specimens were 46 cm^2

Table 4 – Environmental exposure during corrosion propagation stage for type C specimens.

Dry-Cast Pipe Type	Group (number of specimens)	Specimen ID	Amount of Time in Days as of 5/15/2016			
			LAB RH	High Humidity	Buried in Sand	Immersed in Water
C	Cp(6)	C0	377	X	X	1227
		C1_T	24	147	787	X
		C2_T	302	X	1266	X
		C3	28	147	1317	X
		C4*_T	335	182	138	X
		C5_T	328	X	X	1079
	Cg(6)	C6*_T	335	175	191	X
		C7_T	176	529	X	X
		C8	83	X	110	1192
		C9_T	54	1216	X	X
		C10*	156	203	829	X
		C11	49	147	1310	X
	Cm(7)	C12**_T	X	48	1267	X
		C13	X	X	1303	X
		C14	**X**	**X**	**X**	**X**
		C15	45	136	X	1221
		C16_T	X	182	987	X
		C17	X	1254	X	X
		C18	38	136	X	1221
	Cm-HH(5)	C21	X	46	1305	X
		C23**	X	36	1313	X
		C24_T	X	46	987	X
		C25	X	46	984	X
		C26	X	1354	X	X
	Crack Not Polarized#	C22_T	X	X	1267	X

Note: Nominal steel area under the reservoir was 66 cm^2 for specimens C0 to C11; all other specimens were 46 cm^2

Figures 8 and 9 show how long each specimen was exposed, and also indicates if the specimen was exposed to more than one of the environmental conditions. The length of each bar indicates exposure duration. C and F group specimens are displayed on Figure 8 and Figure 9, respectively. The _T marking on the specimen name indicates if a specimen was terminated for forensic analysis. An asterisk on the sample name indicates that that specimen was selected for accelerated corrosion via a galvanostatic pulse (see section that follows for details) during the corrosion propagation stage.

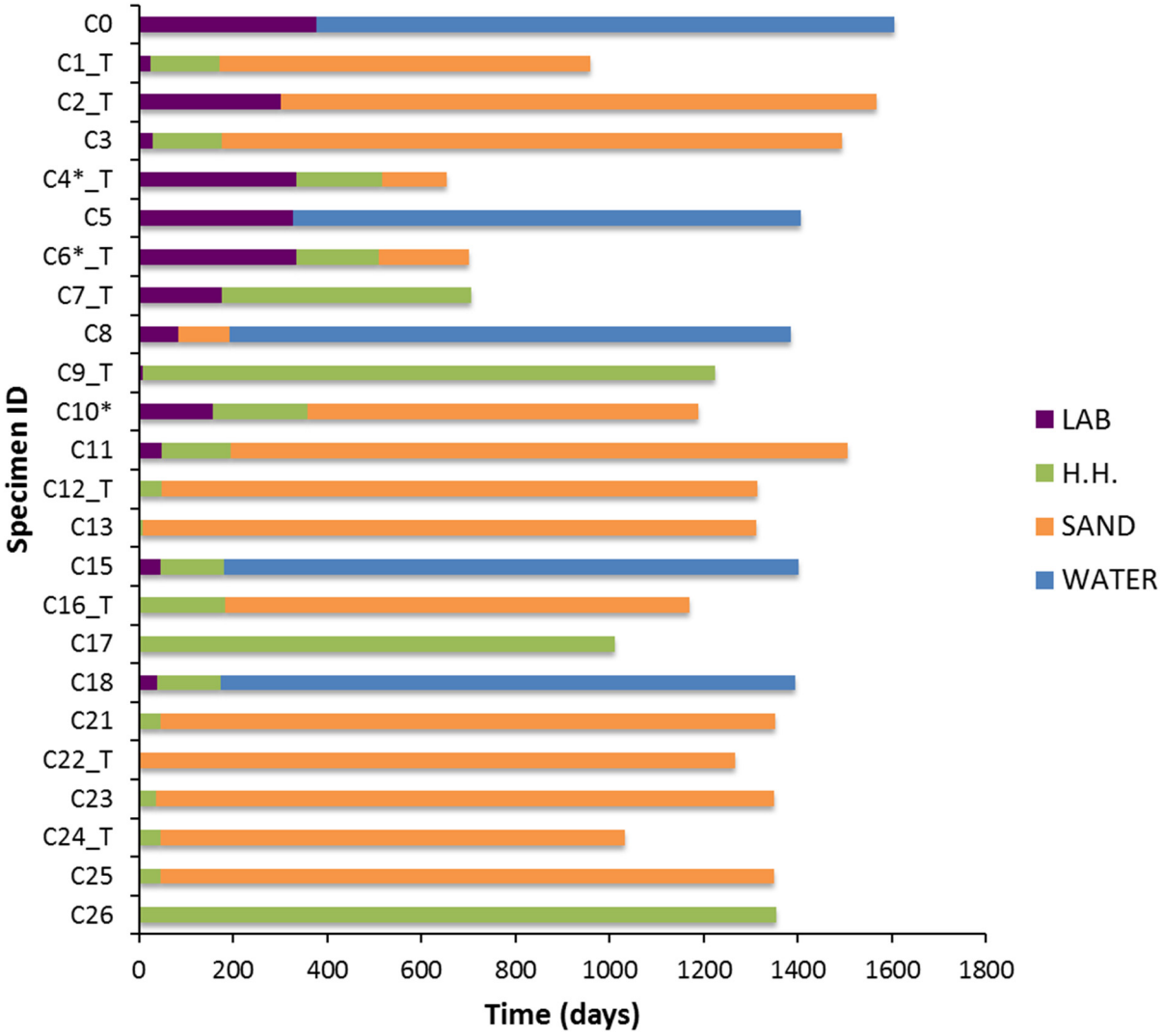

Figure 8 – Type C specimens exposure schedule during propagation stage.

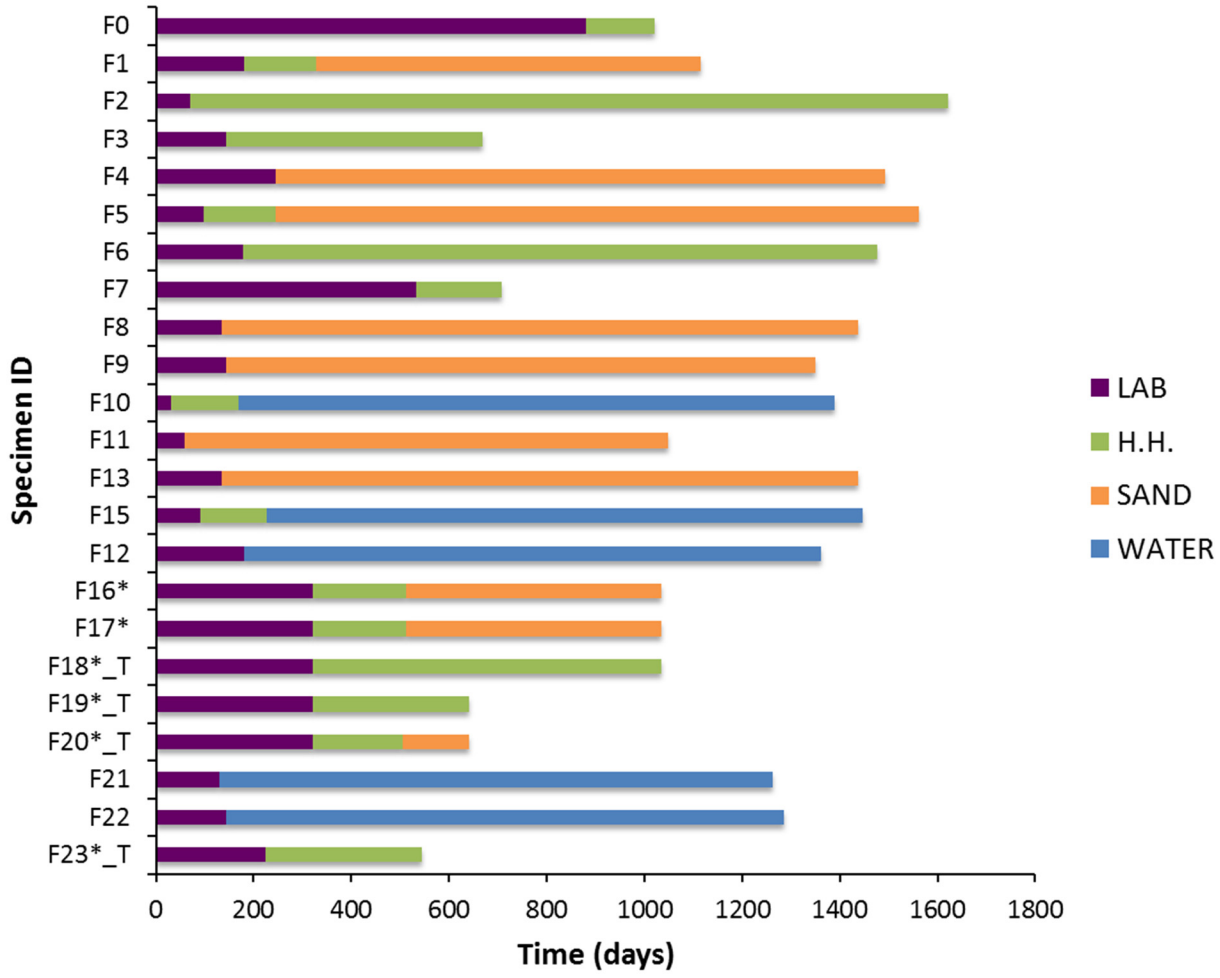

Figure 9 – Type F specimens exposure schedule during propagation stage.

2.8 Specimens Selected for Accelerated Corrosion (During the Corrosion Propagation Stage)

After corrosion of the reinforcing steel wire had initiated, some specimens were selected for application of galvanostatic pulse(s) so as to moderately accelerate the corrosion of the steel wire. The specimens that were later subjected to accelerated corrosion by applying a small current during the propagation stage are: F7, F16, F17, F18, F19, F20, F23, C4, C6 and C10. The selected specimens were transferred to a high humidity environment. For the initial seven days the specimens were not polarized. At this point, the foregoing specimens were anodically polarized via a six multichannel galvanostat. The set-up was the same as during corrosion initiation, but the current was significantly smaller. Initially, the current applied was set at 25 µA (assumed to be a current density of 0.5 µA /cm^2 if half of the steel surface below the reservoir was corroding), for all specimens. The applied current was later increased for select specimens (F7, F20, C4 and C6) after 56 days to 50 µA. After 112 days, these specimens'

applied currents were increased to 125 µA; whereas, for the remaining specimens, the applied current was increased to 50 µA. The applied current, in addition to the natural corrosion rate, is intended to modestly accelerate the corrosion so as to simulate higher corrosion rates that could be experienced in the field at later times. The current application versus time can be seen in Figure 10. Every two weeks, the specimens were disconnected to perform depolarization tests (potential readings were taken after 0 (<10 seconds), 5, 15, 30, and 240 minutes after disconnection). Linear polarization resistance (LPR), and electrochemical impedance spectroscopy (EIS) measurements were typically performed three days after removing the current. Thus, the current was applied for 11 days on and 3 days off and re-applied after completing the electrochemical measurements. A picture of the galvanostatic method during the corrosion propagation stage can be seen in Figure 11.

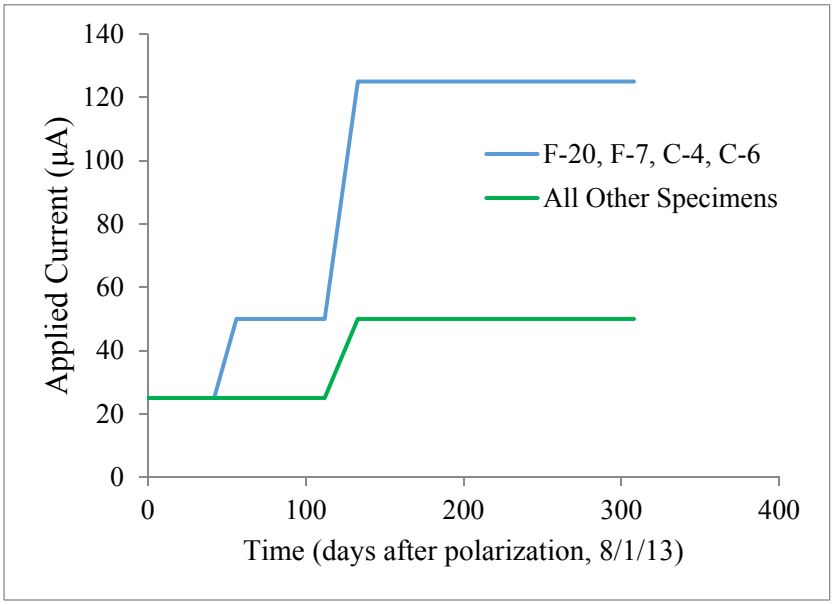

Figure 10 – Current application during corrosion propagation stage.

Figure 11 – Galvanostatic method during corrosion propagation stage.

2.8.1 Periodic Anodic Polarization via Constant Current Application

For this research, it was decided to apply a current calculated by multiplying a factor of 0.5, 1 and 2.5 times the estimated area under the ponding, i.e., 25 µA, 50 µA and 125 µA. These current values assume that the top half of the steel area under the reservoir was undergoing corrosion. The target current densities thus were 0.5, 1 and 2.5 µA/cm^2. However, the applied current density likely was higher if the actual corroding area was small. The polarization was configured in a way so the steel reinforcement was polarized anodically, i.e., the steel's potential is shifted to a more positive value. A schematic representation of the accelerated corrosion set-up can be seen in Figure 12. Anodic polarization can rapidly give the judgment about the system whether the steel is in passive condition or in active condition. The polarization performs two tasks: increasing the anodic reaction rate (this is the primary task) and, to a smaller extent, chloride migration toward the steel reinforcement (due to the small applied electric field). Note that these processes are dependent upon the magnitude of current applied. The galvanostatic pulse (the above-mentioned current magnitudes) was applied cyclically: typically 11 days on and then disconnected for 3 days. During the disconnected days, the steel depolarized (similar to what occurs during a cathodic depolarization), in this case, toward more negative values, to a new natural corrosion potential.

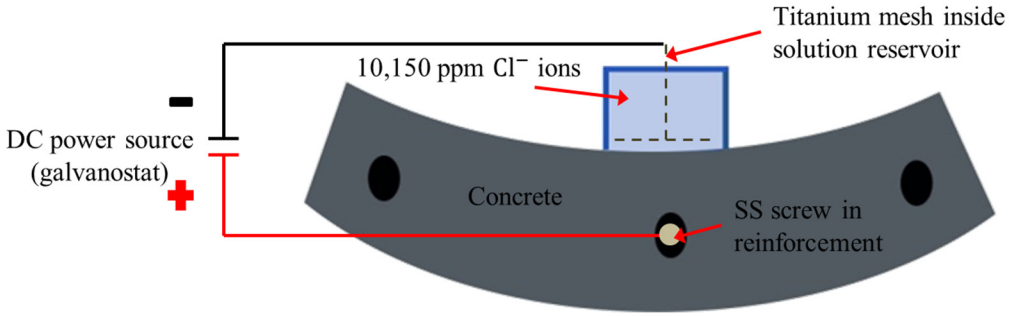

Figure 12 – Schematic diagram of the accelerated corrosion test set-up.

A method similar to that used during cathodic depolarization test was used to assess the magnitude of the depolarization as it applied to the corrosion state of the steel reinforcement. Figure 13 illustrates a plot of potential change with time during a current interruption for a specimen polarized anodically. Due to the voltage drop seen at point A, the potential change with time subsequent to current interruption was initially rapid. Error can occur in the identification of the actual instant-off potential. Normally, a time period of 4 hours is allowed to establish the new Φ_{corr} of the metal, but for high moisture conditions, this could take longer. For the specimens subjected to this galvanostatic pulse, the specimens were left disconnected for at least 24 hours (most of the time, 48 hours) before performing LPR and EIS tests.

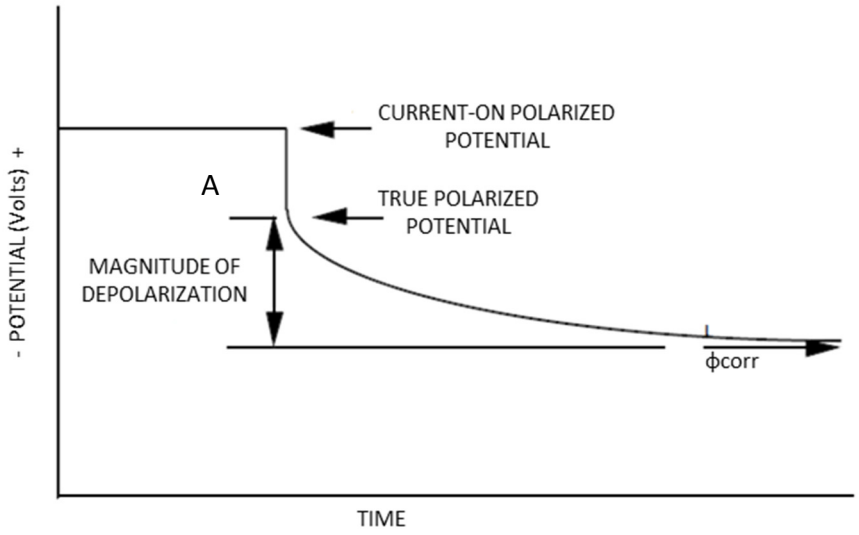

Figure 13 – Schematic illustration of depolarization potential vs. time after disconnection.

2.8.2 Environmental Exposures during the Corrosion Propagation Stage

Upon corrosion initiation the specimens remained exposed to laboratory temperature and humidity, with the solution reservoir filled with chloride containing solution (~3500 or 10150 ppm). After suspension of the current that caused corrosion initiation of the steel reinforcement, specimen F7 remained exposed in a laboratory environment for 526 days, F23 remained exposed to lab environment for 236, whereas all other type F specimens were exposed to the lab environment for ~322 days. C specimens remained in a laboratory environment for at least 450 days. During that time, corrosion propagation occurred under laboratory humidity and temperature. A picture of some of the specimens in the laboratory environment can be seen in Figure 14.

Figure 14 – Specimens in laboratory environment.

During the accelerated corrosion period, the solution was changed to 10,000 Cl^- ppm, and the RCP samples were subjected to a high humidity environment; after 168 days, selected specimens were covered with saturated sand. The other specimens continued to be exposed to high humidity. Additional details of these exposure set-ups are provided below. These environmental exposure conditions were intended to replicate what is experienced in the field in locations with high moisture that allow the concrete to saturate around the steel reinforcement.

2.8.2.1 High Humidity Container

The high humidity condition was achieved by filling the bottom of a transparent plastic container with water up to 0.25 inches. A plastic grid mesh was placed underneath the specimen to avoid water contact with the bottom of the specimen. Additional water was sprayed on top of the specimens two times per week while momentarily removing the container's top cover. The high humidity chamber can be seen in Figure 15. Later, the samples were moistened once a week and eventually once every other week.

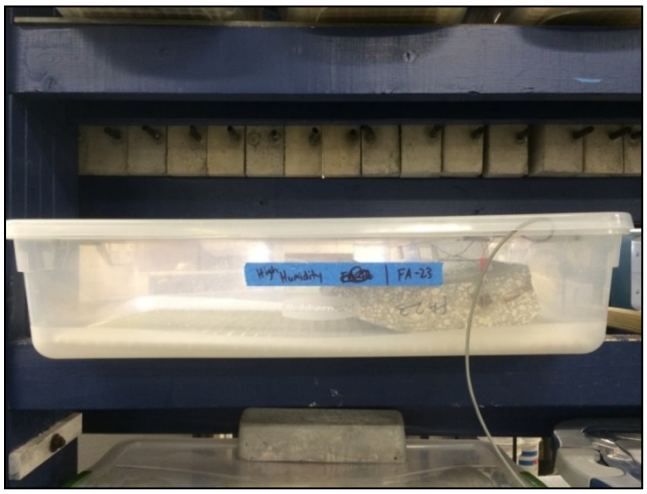

Figure 15 – High humidity environmental chamber.

2.8.2.2 Specimens Covered with Saturated Sand

The sand used was the type commonly used in playgrounds. Before covering the specimens with sand, the sand was saturated with tap water. Two specimens of each type were moved from the high humidity plastic container to a similar plastic container and covered with saturated sand in the horizontal direction. The bottom of the container was filled with the saturated sand up to one inch to ensure the entire specimen was surrounded by the wet sand. Plumber's putty was used to seal the connection from the environment and the exposed reinforcement with the connection post. The specimens were sprayed initially twice per week to maintain saturation, and later on more sporadically. A picture of this set-up can be seen in Figure 16.

Figure 16 – Specimens submerged in saturated sand.

2.9 Ring Specimens Experimental Description

Each ring specimen was named based on the type of concrete and experimental environmental exposure during the corrosion propagation stage. The name of each RCP ring began with C or F, depending upon the sample type. A second letter: I, S or H was added after either C or F. This second letter was added based on the experimental exposure during the corrosion propagation stage (described below). The letter I stands for samples immersed in water, S refers to samples that were fully or partially covered with wet saturated sand (simulating wet soil conditions), and H indicates samples under high humidity exposure condition. Finally, to complete the sample name ID, a consecutive number was assigned to the samples in the group that have the same materials type and environmental conditions. Table 5 shows the specimens' IDs. Some samples were terminated for forensic analysis after approximately one year (two covered in sand and two immersed in water and identified with an asterisk).The other two ring samples that were immersed for about a year were then exposed and covered with sand (FI1, CI2). Four (two per specimen type: FS2, FS3, CS2, CI2) ring specimens were later selected for additional chloride transport via a modified migration approach that affected a larger section of the pipe. This was followed by moderate corrosion accelerated via a potential hold (additional details are given below).

Table 5 – Specimen ID based on type of concrete and environmental exposures.

Concrete Type	Immersed Water	Saturated Sand	High Humidity
C type	CI1*	CS1*	CH1
	CI2	CS2	
F type	FI1	FS1*	
	FI2*	FS2	
		FS3	

On each ring specimen, one of the exposed steel wires was selected to set-up an electrical connection. The center of the determined steel wire was marked and a (approximately) 1 cm deep hole was drilled, then tapped for inserting a #2 or #4 machine stainless steel screw. Two

nuts and washers were installed on the screw to ensure stability and conductivity of the reinforcing steel for future electrical measurements. This procedure is quite similar to that used for the smaller specimens.

Figure 17 – Reservoirs on vertically oriented specimen (left) and horizontally oriented (right).

Two different types of reservoirs were installed based on the orientation of specimens as seen in Figure 17. For the specimens with the reservoirs in the horizontal orientation as shown in the right picture of Figure 17, a reservoir made of Plexiglas was fabricated with dimensions of 2.5" x 6", which is the nominal cross-section of the area for the sample reservoir. The fabricated Plexiglas was attached with waterproof UV resistant marine sealant on the surface of the inner curvature, just above the steel wire with the tapped screw. The bottom edge of the Plexiglas was cut in the same profile of the inner curvature, so that the reservoir would securely fit on the concave-curve surface. The height of the reservoir was 2 inches and solution filled the reservoir up to 1.5 inches in height. For reservoir construction in vertically-oriented specimens, seen in the left picture of Figure 17, two elliptical plastic containers were cut to fit the inner curvature profile and outer curvature profile of D-RCP ring, respectively. The fabricated elliptical plastic containers were attached to the surface of the inner curvature and the outer curvature with marine grade silicon. The surface area of the reservoir was 2.5" x 7" and solution was typically filled up to 5" in height.

2.9.1 Accelerated Chloride Transport for Corrosion Initiation

Two methods for accelerating the chloride transport were used. This was done to shorten the time to corrosion initiation of the steel reinforcement in the D-RCP ring specimens. A galvanostat method and a migration cell method were used in order to accelerate the chloride transport from the solution into the concrete toward the reinforcing steel.

2.9.1.1 Galvanostat Method

Seven RCP ring specimens (CI1, CI2, FI1, FI2, FS1, FS2, and FS3) were set-up outdoors in a semi-sheltered exposure condition. A galvanostat was used (however, not all of them concurrently). A six multi-channel galvanostat was used. Each channel applied a current of 1 mA to each D-RCP ring specimen, with the current mainly going to the reinforcement underneath the reservoir. The positive terminal of the galvanostat channels was connected to the instrumented

reinforcing steel wire of the RCP. An electric connection was made between the negative terminal of the galvanostat channel and a titanium mix metal oxide mesh placed in the chloride solution reservoir. The Ti_{MMO} mesh acted as the counter electrode. The concentration of chloride ions in the solution in the reservoir was 10,150 ppm (340 g NaCl per 20L of water). Initially, a 15% sodium chloride solution was used for sample CI2, FF1, and FF2 for two weeks; after that period of time, the solution was changed to a solution with 10,150 ppm of chloride ions. The chloride transport occurred mainly via migration as a result of the electric field produced by the potential difference between electrodes resulting from the applied current. During the galvanostatic process, applied current was removed periodically and then measurements of off potential, V_{off} were carried out. As soon as the galvanostat was disconnected, the first off potential measurement was taken, usually within 5 to 10 seconds. After 10 minutes, 30 minutes, and 60 minutes, additional measurements of off potential were carried out. If more measurements were deemed necessary, additional measurements were taken after 2 hours, 4 hours, and 24 hours. Declaration of active steel state of a specimen was based on the threshold off potential voltage being more negative than -250mVsce. After 24 hours of disconnection, if the off potential,V_{off}, was close to or more negative than -250 mVsce, the specimen was considered to have reached the active state. However, if V_{off} after 24 hours did not meet this requirement, the galvanostat was reconnected and current was applied again until the specimens reached -250mVsce. However, for the samples that initially used 15% of sodium chloride solution (CI2, FS1, and FS2), the potential value used to declare the steel reinforcement active was set as -150mVsce or more negative values. Figure 18 shows a schematic of the set-up.

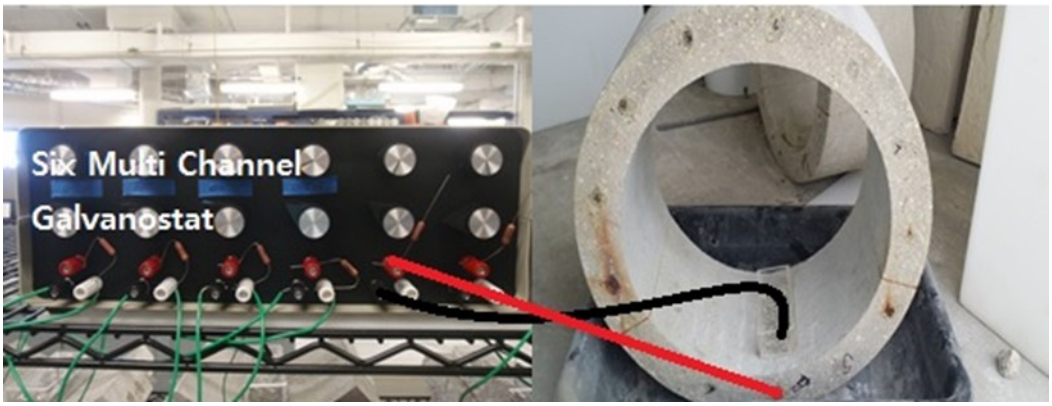

Figure 18 – Galvanostatic method for accelerated chloride transportation.

2.9.1.2 Electro-Migration Cell

The migration cell method accelerated the transport of chloride ions on three specimens (CH1, CS1, and CS2). The solution reservoir installed at the outer curvature was filled with calcium hydroxide solution and the solution reservoir installed at the inner curvature was filled with a solution containing 10,150 ppm of chloride ions. The amount of solution filled at both reservoirs was about 200 ml. Stainless steel meshes were placed on both reservoirs to act as electrodes. Before starting the migration test, the three D-RCP ring specimens containing solutions were exposed to laboratory temperature and humidity for two weeks. Then the

specimens were moved to a high humidity chamber that provided relative high humidity of between 95% and 98% RH. The specimens were exposed to the high humidity environment for three days before starting the migration test. Since the high humidity chamber had to be covered in order to keep the humidity level, power source wires were connected through the wall of the chamber.

The positive terminal from the power source was connected to a mesh immersed in a calcium hydroxide solution and the negative terminal of the power source was connected to the mesh in the chloride solution reservoir. A power supply was set to 15 volts potential difference between the stainless steel electrodes so as to accelerate the chloride transport via migration due to the applied electric field. About once a week during the electric field application, the high humidity chamber was momentarily open and the power supply was shut down in order to check the off potential values of the reinforcement of each specimen. Measurements were taken every week and off potentials were measured right after powering off the power supply. During depolarization of the specimens, additional measurements of off potentials were conducted after 5, 15, and 30 minutes after power shutdown. Once the off potential after 24 hours of power shutdown reached -250mVsce or more negative, the specimen was considered as active. Figure 19 shows the three ring specimens subjected to electro-migration while in high humidity exposure.

Figure 19 – Migration cell method in high humidity container.

2.9.2 Experimental Setup and Electrochemical Measurements during Natural Corrosion Propagation Stage Period

Various environments were prepared for studying the corrosion of RCP ring specimens during the propagation stage. In this study, the primary focus of the investigation was to understand some of the factors that affect the corrosion rate of the reinforcing steel in RCP during the

propagation stage, i.e., how the availability of oxygen and moisture influenced the corrosion rate of the reinforcement embedded in RCP ring specimens. Three simulated environments were investigated which controlled the oxygen level and moisture content to different degrees. The specimens were immersed in water, exposed to high humidity, and (partially or fully) covered with saturated sand. With these exposure environments, different sections of the RCP ring specimens would become water saturated to various degrees, resulting in lower oxygen concentration around the corroding reinforcing steel and the non-corroding surrounding steel.

2.9.2.1 RCP Ring Specimens Fully or Partially Immersed in Water

For the RCP ring specimens exposed immersed in water were placed in large HDPE containers. Four HDPE containers were placed outdoors (in the semi-sheltered area where the accelerated chloride transport experiments took place). The dimension of the three HDPE containers for specimens FI1, FI2, and CI2 was 26 x 20 x 25 inches and the fourth HDPE container for specimen CI1 was 26 x 20 x 30 inches. Since these specimens were immersed in water, the chloride solution was removed from the solution reservoir before these RCP rings were relocated in the HDPE containers. Each specimen was carefully moved into each plastic container. Then each sample was rotated such that the concrete covering the reinforcement with the electric post was located at the most high (12 o'clock). Tap water was used as the solution on each container, and initially each container was filled up to about two inches below the exposed reinforcing steel with the electric post (i.e., specimens were partially immersed in water, as seen in Figure 20). After the water was poured, the RCP ring specimens were rotated about 90 degree in order to immerse the reinforcing steel with the post in water (i.e., the longitudinal steel strand undergoing corrosion). The longitudinal wire with the connection was brought back to the 12 O'clock when electrochemical measurements were to be made.

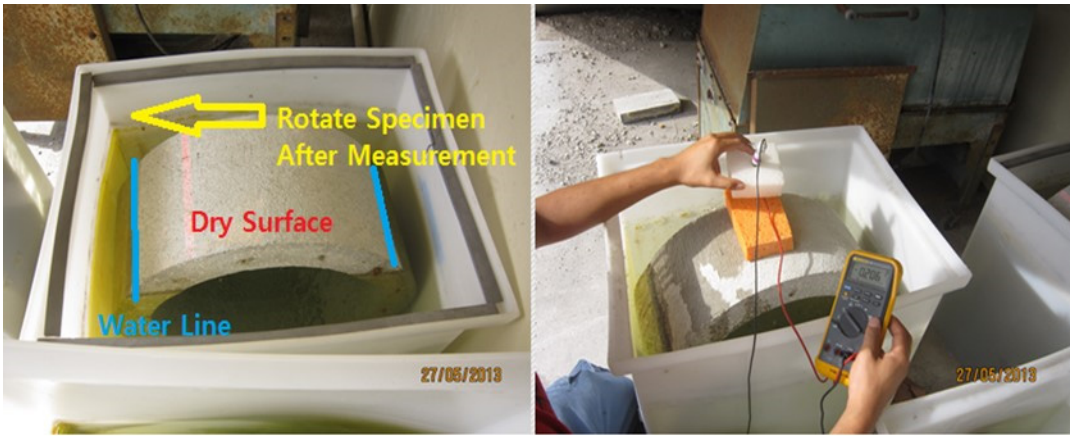

Figure 20 – (a) Specimens partially immersed in water; and (b) Potential measurement of partially water-immersed specimen.

The initial open circuit potential measurement for FI1, CI1 and CI2 was taken 9 days after immersion, and for FI2, the first measurement was taken after 7 days. During the first three months immersed in water, only open circuit potential was measured (about once every other week) by placing a saturated calomel reference electrode on the outer surface of D-RCP just above the instrumented reinforcing steel. In order to measure the open circuit potential, the D-

RCP ring specimens were rotated to expose the reinforcing steel with the electric post to air. The electric post was carefully dried with a paper towel and connected to the positive terminal of a high impedance voltage meter. The reference electrode (saturated calomel electrode) was connected to the negative terminal of the voltage meter. After 3 months passed, the method of open circuit potential measurement was changed. Instead of placing the reference electrode on the D-RCP ring surface above the reinforcing steel with the post, the reference electrode was placed at the inner curvature of the concrete pipe below the reinforcing steel with the connection, as seen in Figure 21. Additionally, a rectangular sponge was folded into half and a Ti_{MMO} mesh counter electrode was inserted in the folded sponge. The sponge was secured with a plastic set-up, so that the counter electrode could be fixed for the measurement, which enabled EIS and LPR measurements to be performed on each sample. From this point forward the following measurements were performed periodically: open circuit potential, electrochemical impedance, and linear polarization measurements. These measurements were carried out once every two weeks (and later on, more sporadically). The tap water was typically replaced once a month.

Figure 21 – LPR & EIS measurement (left) and potential measurement (right) of water-immersed specimens.

Figure 21 shows how the LPR test and EIS test were made for water immersed specimens. The tests were conducted with a potentiostat, Gamry Reference 600, (left picture). A picture of how the open circuit potential measurement was made is also shown in Figure 20, while FI and CI specimens were mostly or fully immersed in water. After day 225 in this exposure, the specimens were completely immersed in tap water. The water level was momentarily lowered when performing open circuit potential, LPR, and EIS tests. When electrochemical measurements were taken, the water was drained with a water pump to a level about 2 inches below the steel reinforcement with the post (but the inside reservoir region was still filled with water). As indicated above, the counter electrode mesh was placed underneath a square sponge that was positioned inside the solution reservoir (located at the inner curvature of the RCP ring specimen and with the sponge fully immersed in water), and the activated titanium mesh had a strand that was long enough to make the electrical connection above water. The reference electrode had to be fixed under water with a designed device as seen in the right

picture of Figure 21; it was placed on top of the sponge. The electric post connection to the steel reinforcement was dried carefully, and EIS and LPR tests were conducted immediately after the water was drained so that the measurements were conducted under wet concrete conditions, which minimized the amount of oxygen that could penetrate in the drying concrete. After these tests, the tank was refilled with water until the next set of measurements.

2.9.2.2 RCP Ring Specimens Fully or Partially Covered by Wet Sand

Five RCP ring specimens, CS1, CS2, FS1, FS2, and FS3, were relocated under simulated water-saturated soil for a portion of the corrosion propagation stage period. A HDPE container with dimensions of 29 x 30 x 18 inches was used. This container was called sand container 1, and was prepared to accommodate specimens FS2 and FS3. The FS specimens were not fully covered with sand. For the D-RCP ring specimens, CS1, CS2, and FS1, a plastic container of 47 x 43 x 29 inches, named sand container 2, was prepared. These two containers were placed outdoors. Since specimens FS1, FS2, and FS3 contained solution reservoirs installed horizontally and these specimens were partially buried in wet saturated soil, an isolation chamber was required to prevent the solution reservoir from filling with wet saturated sand. Plexiglas plates were cut and attached to the front and back side of these RCP ring specimens, with waterproof UV-resistant marine sealant. This design allowed the RCP specimen to be fully covered up to 15 inches in height for both the front and back sides. Specimens CS1 and CS2 that had the solution reservoir vertically installed were fully buried in wet soil (sand). The sand was obtained from a local quarry and was stored in one of the containers. The sand was thoroughly washed with several rinses to lower the chloride concentration. As can be seen in Figure 22 and Figure 23, FS specimens were not fully covered with the wet sand as each ring was partially covered. On the other hand, CS specimens were mostly wet as most of the specimens were covered by wet sand, excluding the reservoirs and electric post connection areas.

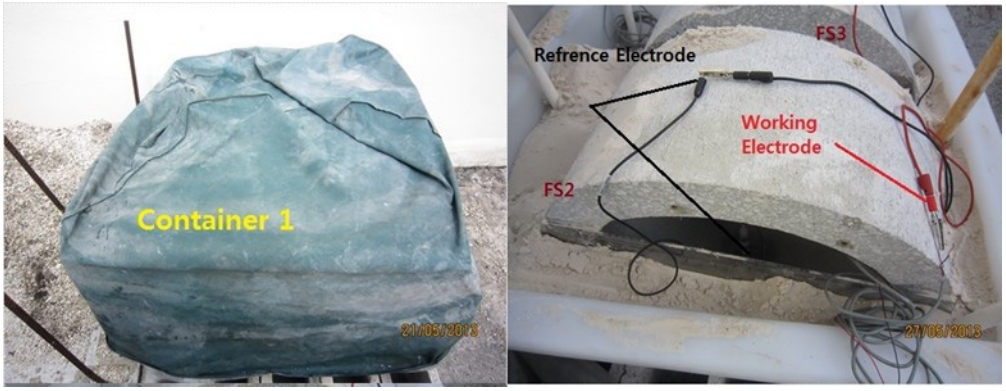

Figure 22 – Specimen FS2 and FS3 partially buried in sand in container.

Figure 23 – CS specimen fully covered by wet saturated sand.

Samples from the F group stayed at the semi-sheltered area about 300 days after corrosion initiated and then the FS specimens were moved to containers 1 and 2. The C group samples were stored at a high humidity chamber for 270 days after corrosion initiated, and CS specimens were then transferred to container 2. A layer 2 inches deep of wet saturated sand was placed at the bottom of each container. The and FS3 specimens were carefully placed horizontally in the sand container 1 and rotated to adjust the orientation of the reinforcing steel with the electric post, so that this was located near the bottom of the container. The FS1 specimen was also moved into sand in container 2, and followed a similar approach. The CS1 and CS2 specimens were set up in a sand container 2 by laying them vertically. Chloride solution filled all reservoirs. Counter electrode meshes were placed in the reservoirs. Once in the containers, extra wiring was installed on FS samples to perform electrochemical measurements. The wiring was made by using general Cu cable 22 AWG that contained one red wire and one black wire. One of the red wire ends was installed with an alligator clip which was then connected to the reinforcing steel electric post. The electric post connected with red wire was sealed carefully with waterproof sealant plumber's putty in order to protect the electric post from any moisture sources. The black wire was installed with an alligator clip that was connected to the counter electrode mesh placed in the reservoir. Both wires were long enough to extend outside the box to perform the EIS and LPR measurements. This set-up took place before the specimens were covered by wet sand. The outer portion of FS specimens were covered with wet sand as seen in Figure 19 (front). The CS specimens were placed vertically in sand container 2 and were mostly buried, leaving only the electrical connection and solution reservoir exposed. Sand container 1 was semi-sealed with the container covered and wrapped with an additional vinyl cover to reduce evaporation. The high moisture in the sand was maintained every week by adding tap water to the sand. Measurements of open circuit potential were initially taken every week. Linear polarization and solution resistance (via EIS) measurements were carried out every two weeks.

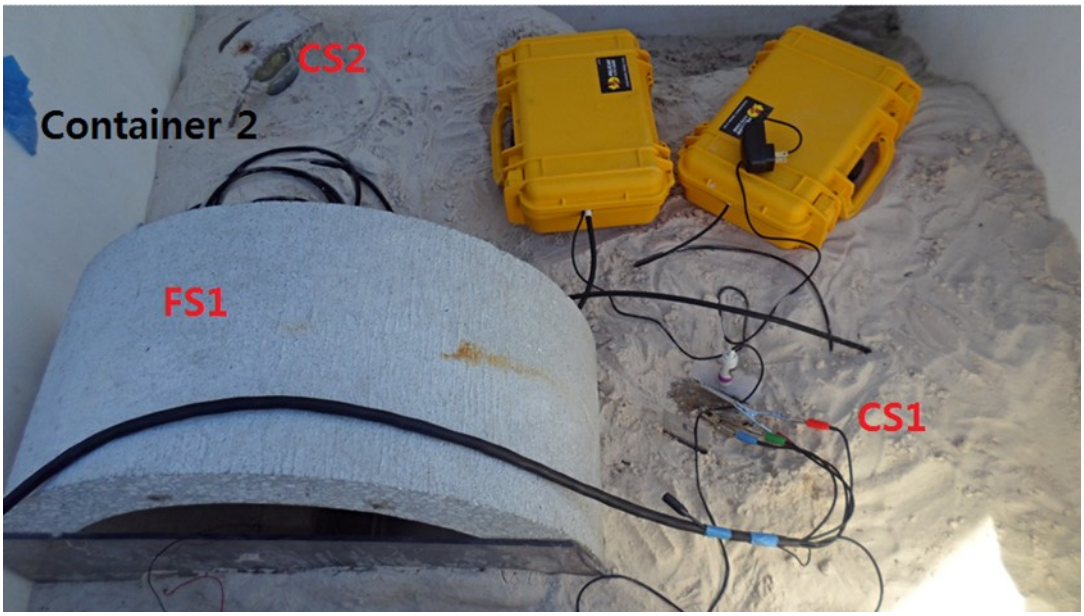

Figure 24 – Specimen FS1, CS1, and CS2 in container 2.

2.9.2.3 RCP Ring Specimen Exposed to High Humidity

Specimen CH1 remained in the high humidity environment condition for the duration of the propagation study. A 36x36x18 inch container was prepared as a high humid chamber. Two inch high and 4 inch diameter PVC cylinder slices were laid on the bottom of the high humid chamber and plastic mesh was placed on top of the PVC cylinders. In order to maintain the high humidity in the chamber, tap water was used to fill up to 1.5 inches of height. Weathering strips were applied on the top surface of the chamber to seal the box. The observed relative humidity value was close to 95%. Both the initiation and the propagation stage of specimen CH1 took place in the high humidity container (See Figure 25). After the reinforcing steel activated, the open circuit potential was measured every two weeks and linear polarization and solution resistance measurements were carried out every two weeks for the next few months.

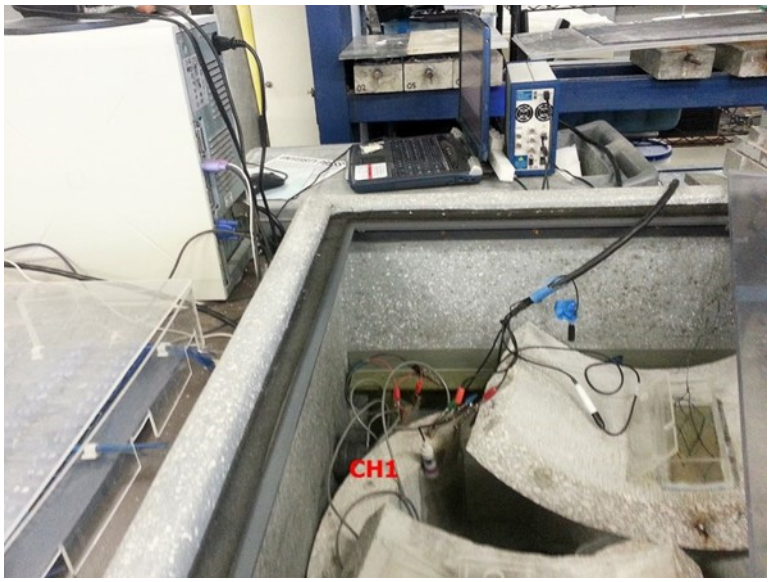

Figure 25 – Specimen CH1 in high humidity container.

2.10 Forensic Analysis

2.10.1 Autopsy of Ring Specimens

Two specimens for each simulated environment (covered with water saturated sand and water immersion) were selected for autopsy after 400 days of the above-described exposures. Figure 26 shows one of the selected specimens prior to the initial cuts. These autopsies allowed us to visually observe the areas undergoing corrosion (See Figure 27). Specimens CS1, FS1, CI1, and FI2 specimens were chosen for forensic analysis. A section that included the solution reservoir was cut from the ring. The steel wire mesh was exposed and observed according the following procedure:

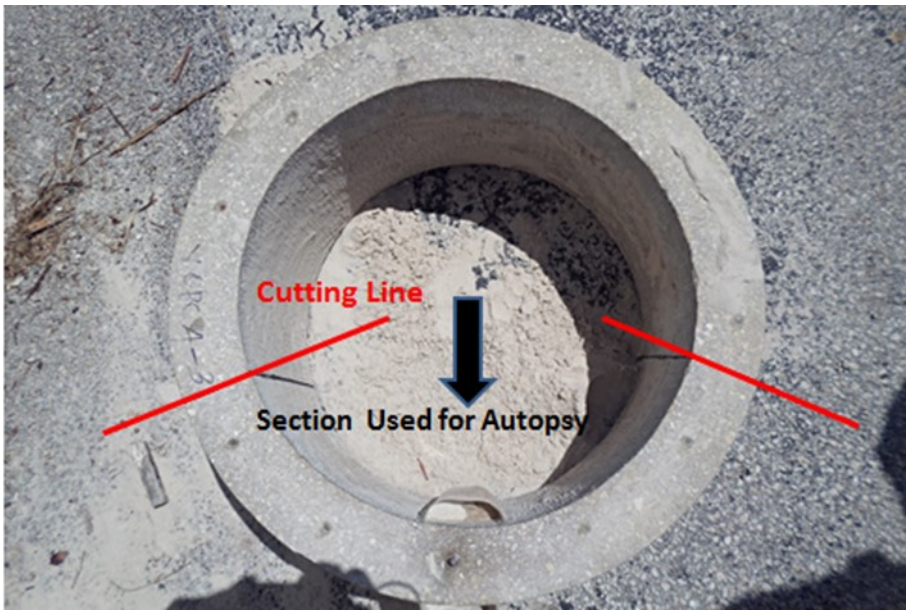

Figure 26 – Location where initial cuts took place.

Figure 27 – Specimen termination and autopsy process.

Each selected ring specimen was removed from the testing environment. The specimen was marked and the attached solution reservoir was removed. The RCP ring specimen was cut into four pieces with a wet saw. The concrete was removed only for the piece where the solution reservoir was located as seen on the picture on the left in Figure 27. The other three pieces were used to create new lab specimens.

On the piece selected to expose the steel wire, the location of the steel wire was projected and traced on the concrete surface. See picture on the left of Figure 27. These markings allowed us to identify the reinforcements in the longitudinal and transverse directions. Along the drawn lines, a chisel was used to indent the concrete. Then, a larger-sized heavy duty splitting chisel was placed on the indented lines and hit with a sledge hammer until the concrete segments were completely detached from the steel mesh. See the Figure 27 picture on the right. The exposed steel wire mesh was transported into the lab and visual inspections were conducted. Photographs were taken to document the corrosion areas. Deliverable 2.b describes the documented results for the forensic analysis. A similar procedure was performed on the remaining specimens once these were subjected to forensic analysis.

The remaining sections of the pipe ring were used to create additional arch specimens. Three additional specimens were obtained per terminated sample. The C specimens were named C40 to C45, and those from F ring specimens were named F40 to F45. The solution reservoir and electrical contact were set up on each specimen similar to what was described above. The longitudinal wires were on the horizontal orientation. All samples were exposed to high humidity exposure starting late summer 2014. Selected specimens (C40, C41, C42, C45, F40, F42 and F43) were subjected to a galvanostatic pulse (500 μA) for about 100 days, and then continued to be exposed in high humidity. The applied current was periodically removed, similar to what was described above for the galvanostatic pulse. Two days after removing the applied current, the LPR and EIS were measured. The specimens not subjected to applied current pulse were also monitored for LPR and EIS. The LPR and EIS tests continued to be monitored on all 40's group specimens for an additional 550 days. Two specimens (C43 and F41) were forensically analyzed after 440 days.

The two remaining ring samples that had been exposed immersed in water were also brought into the laboratory for electrochemical characterization and then they were moved back outdoors and placed in the containers with wet sand. The remaining six ring specimens continued to be monitored. Five specimens were exposed outdoors covered with wet sand, and one was exposed in high humidity environment indoors. Four specimens (two per specimen type) covered with wet sand were selected during the summer of 2015 for additional chloride transport (samples were moved into the lab) followed by modest current application so as to accelerate corrosion. A Plexiglas plate was glued to isolate the inner section of the pipe (a chloride solution was placed inside this reservoir). A method similar to the electromigration approach was used; however, in this case, the size of each Ti_{MMO} mesh was large so as to conform with the outer and inner diameter of the pipe. Close to two-thirds of the pipe were immersed. The two selected F specimens were subjected to this procedure first (FS2 and FS3). The specimens were then taken back outdoors and covered with sand. The two selected C type ring specimens (CS2 and CI2) were then brought into the lab and subjected to accelerated chloride transport procedure. These four specimens and the other two remaining ring specimens (FI1 and CH1) were transported to Rinker Materials Concrete Pipe for 3BE testing during November 2015. In addition to the six ring specimens at FAU, three other ring specimens were provided by Rinker and were also tested, after the 3EB tests selected sections were cut and brought back to FAU for forensic analysis.

2.10.2 Autopsy and Gravimetric Analysis of Selected Lab Specimens

Some arch specimens were selected for forensic analysis at various times while the remaining specimens continued to be monitored. Autopsies were carried out on selected specimens. The steel reinforcement of these specimens was exposed and evaluated according to the following procedure:

1. Testing/exposure was terminated, the solution in the reservoir was removed, and then the plastic solution reservoir was removed with a box cutter as seen in Figure 28. The concrete surface was inspected for cracks.

Figure 28 – Removal of the solution reservoir.

2. A smaller chisel was used to indent the concrete along the reinforcement in the longitudinal and transverse directions (shown in Figure 29 and Figure 30) to ensure the concrete split in sections and so that the steel could be removed. A larger wood splitting chisel held by a vise was then placed in the indent and slowly hit by a sledge hammer until segments broke free of the steel wire as shown in Figure 31.

Figure 29 – Indenting along the longitudinal and transverse steel wires using a thin chisel.

Figure 30 – Concrete indented along the longitudinal and transverse steel wires.

Figure 31 – Larger chisel hit with a sledge hammer to break concrete away from the steel.

3. Pictures of the steel wire mesh and reinforcement trace (i.e., concrete surrounding steel) were immediately taken upon exposure.

4. The reinforcement's dimensions were recorded, i.e., longitudinal and transverse length, and diameter.

The following two steps were performed on most steel wires selected for autopsy.

5. The steel was cleaned and prepared for weight loss measurement according to ASTM G1 - 03[35]. The weight loss measured (with respect with initial mass) was compared to a theoretical

calculation (obtained from the calculated charge over time). Forensically-examined steel wire sections from ring specimens were not subjected to this step, nor were a number of the specimens subjected to natural corrosion propagation.

6. Pictures were taken before and after cleaning the reinforcement to capture the most severe corrosion areas. The surface area showing corrosion was estimated using a visual approach and using thin paper to record corroding areas. Representative pictures for selected specimens are presented in the results section.

2.11 Calculated Mass Loss Using Integrated Charge and Faraday's Law

The total charge was calculated for specimens (i.e., all types of specimens) that had Rc values calculated from measurements obtained over time. A cumulative numerical approach was used. The total charge within a period of time can be calculated by integration. The average corrosion current within a period of time was calculated from two Rc values, and assumed to be a representative value between two given measuring times. The corresponding cumulative charge for each specimen was calculated by taking the area under the curve, i.e., the average corrosion current was multiplied by the time interval between each measurement. The apparent mass loss was obtained by applying Faraday's law. For specimens subjected to galvanostatic pulse, an additional mass value was calculated that included the charge that resulted from the applied current (assuming 100% efficiency) and was added to the integrated charge.

Chapter 3 – Results

3.1 Concrete Cover

The cover of each arch pipe segment was measured and recorded. Figure 32, Figure 33 and Figure 34 show the cumulative cover distribution measured on type F and type C specimens (grouped by set, i.e., polarization approach and orientation). Figure 35 contains the overall cumulative distribution for all specimens grouped per specimen type and direction. It is identified that the concrete covers of type C specimens in both longitudinal and circumferential direction are generally deeper than the type F specimens. The thickness of concrete cover for both types of pipes is summarized in Table 6. Recall that these values were measured from the pipes' inner-curvature.

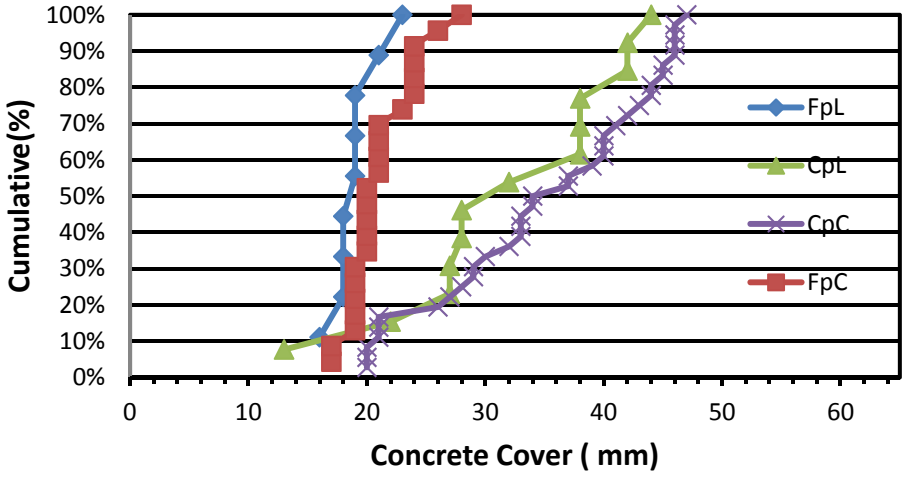

Figure 32 – Concrete cover distribution (Groups Fp and Cp). L-Longitudinal, C-Circumferential directions.

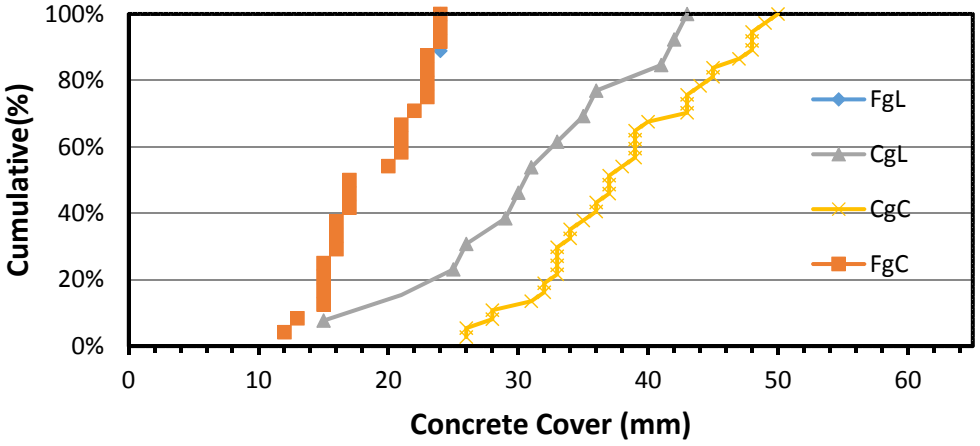

Figure 33 – Concrete cover distribution (Groups Fg and Cg). L-Longitudinal, C-Circumferential directions.

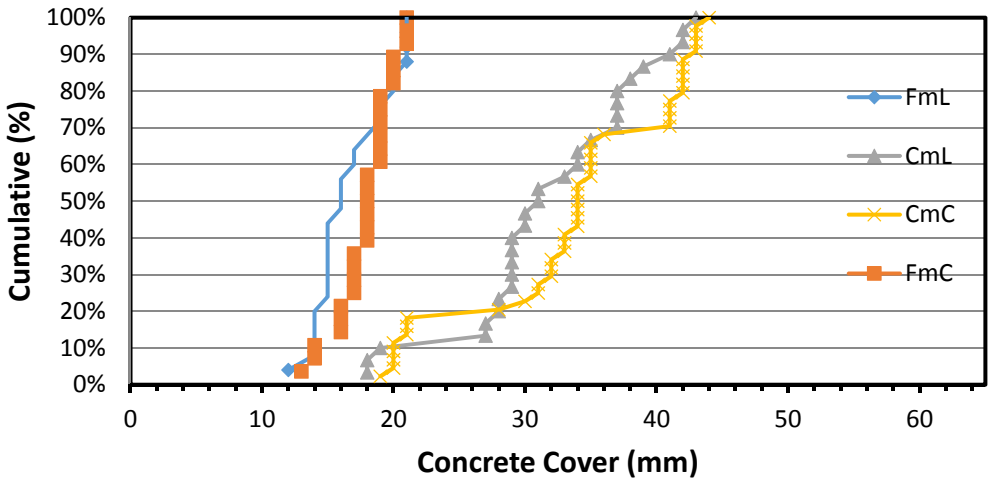

Figure 34 – Concrete cover distribution (Groups Fm and Cm). L-Longitudinal, C-Circumferential directions.

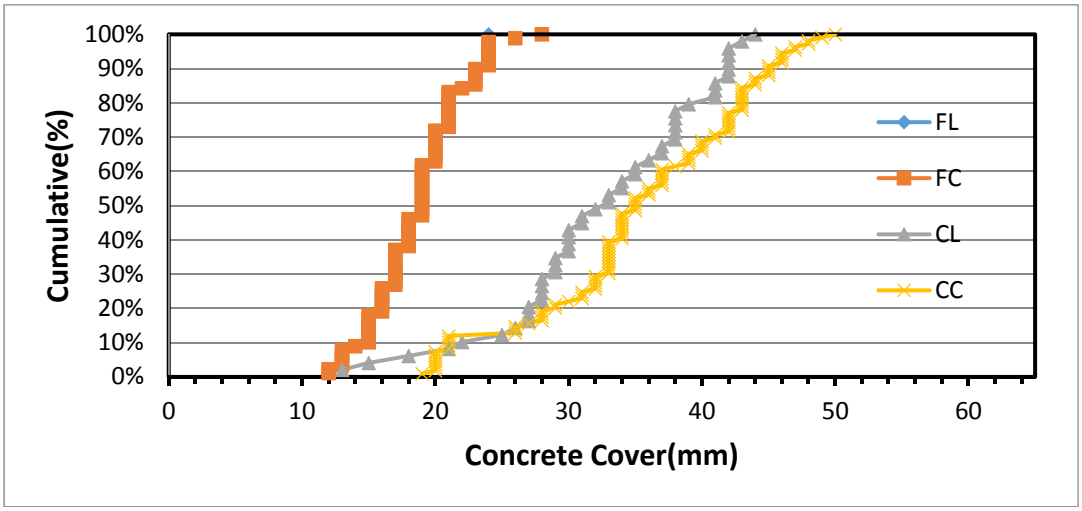

Figure 35 – Concrete cover distribution summary. L-Longitudinal, C-Circumferential directions.

Table 6 – Mean and standard deviation on cumulative concrete cover distribution.

Pipe Type	Items	Mean (mm)	STD (mm)
F	Longitudinal (F_L)	17.78	2.93
	Circumferential (Fc)	19.31	3.2
C	Longitudinal (C_L)	31.91	7.549
	Circumferential (Cc)	33.065	10.71

3.2 Porosity, Resistivity, and Dnssm

The porosity of each tested piece from type F and type C is listed in Table 7. The results listed in Table 7 illustrate that the porosities of type F pipes (average of 9.1%) are generally lower than those of type C pipes (10.4%) by about 1%. These porosity values would likely produce adsorption values within the acceptance range for both RCP types. The chloride migration

coefficient and resistivity measured on saturated concrete specimens are shown in Figure 36. From Figure 36, one can observe that the chloride migration coefficient (Dnssm) of each type F (with fly ash) specimen is generally less than that of each type C specimen while the resistivity of the F specimens is higher than that of the C specimens. The use of fly ash and its corresponding pozzolanic reaction in dry-cast RCPs of type F resulted in a reduced porosity (compared to its initial porosity) and likely produced a more tortuous path, which in turn, resulted in a somewhat improved resistance to chloride penetration. Additionally, it can be observed from Figure 8 that for type C cores the Dnssm (6×10^{-12} m^2/s) of inner concrete (where the inside curvature was exposed to the chloride solution) is lower than the Dnssm (10×10^{-12} m^2/s) measured on cores with the outer side exposed to chlorides (where the outside curvature was directly exposed to chloride solution). This would agree with the visual observation that the outer portion was more porous. The Dnssm values measured on type F cores were generally similar and independently of which surface (inner or outer) was directly in contact with the chlorides. The Dnssm values measured on F cores, ranged between 3.3 and 3.75 $\times10^{-12}$ m^2/s. Overall, the Dnssm values measured are comparable to those observed on wet-cast concretes with similar resistivity. As part of a different project, porosity, Dnssm, and resistivity values were measured on concrete cylinders. The measured values of Dnssm and resistivity were $10.2x10^{-12}$ m^2/s and 7 kΩ-cm respectively, for a concrete with only Portland cement and w/cm of 0.38 and porosity of 5.4% porosity by volume[36]. Similarly, for samples tested as part of a different project, concrete cylinders with a porosity of 9.7% registered a (average of 4 values) Dnssm of $4.1x10^{-12}$ m^2/s and a resistivity of 29.3 kΩ-cm, whereas a cylinder with a porosity of 8.6% registered a Dnssm of $3.3x10^{-12}$ m^2/s and a resistivity of 29.1 kΩ-cm[37]. These values are comparable to those shown on Figure 36 for F type concrete.

Table 7 – Porosity of concrete.

Pipe Type	Specimen	Porosity (%)	Average Porosity (%)
F	Fs1	9.41	9.135
	Fs2	8.90	
	Fs3	8.96	
	Fs4	9.16	
	Fs5	9.24	
C	Cs1	9.12	10.385
	Cs2	9.19	
	Cs3	9.63	
	Cs4	12.21	
	Cs5	11.78	

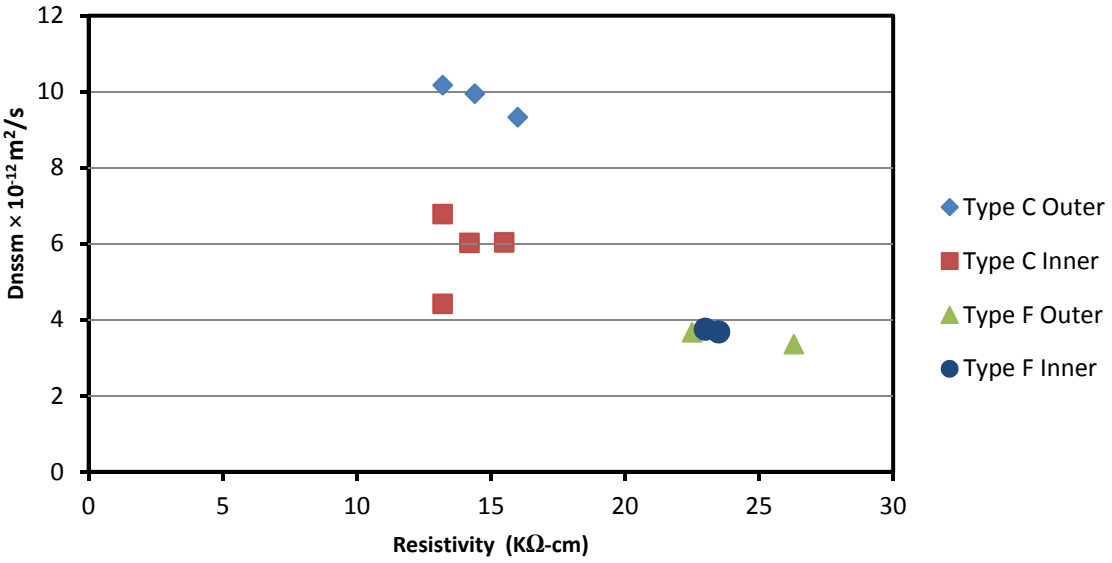

Figure 36 – Chloride migration coefficient vs. resistivity.

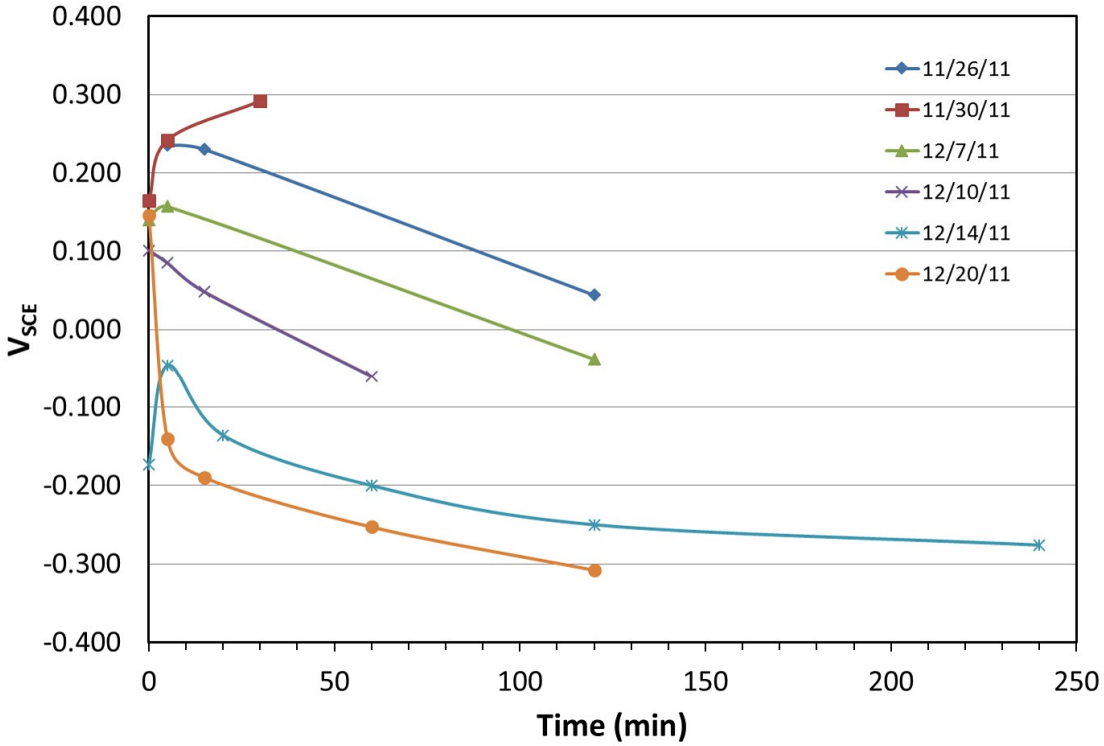

Figure 37 – Typical depolarization tests conducted on specimen C2 (Cp group).

3.3 Depolarization Prior to Corrosion Initiation

Figure 37 shows depolarization tests performed on the C2 specimen on different days. This approach was used to determine when corrosion had initiated. Once corrosion of the steel initiated, the measured potential quickly transitioned to a stable negative, say -300 mVsce, and

drifted very slowly. The specimen was left disconnected for 24 hours to verify that the steel wire remained active. A target value of -200 mVsce was usually used. Based on the potential rate change after the first few measurements following disconnection, readings were performed only up to 30 minutes and then the system was re-energized if the steel potential was more positive than -100 mVsce. Briefly, the electric field (any of the used methods) was periodically interrupted and the off potential monitored up to one day. If the potential was more negative than -250 mVsce, the specimen was declared active. Once this occurred accelerated chloride transport was interrupted.

Table 8 – Label ID of F test specimens and time to corrosion initiation.

Pipe Type	Group	Specimen ID	Cover Depth (cm)	Days to Corrosion Initiation	24 hours off Potential Vsce (mV)	Method
F	Fp	F0	1.75	3	-566	Potentiostat
		F1	1.86	7	-540	
		F2	2.06	3	-600	
		F3	2.05	4	-520	
	Fga	F4	1.8	2	-302	Galvanostat
		F5	2.1	10	-280	
		F6	1.9	9	-270	
		F7	1.65	7	-372	
	Fgb	F12	2	5	-427	
		F16	1.5	5	-441	
		F17	1.4	5	-544	
		F18	1.7	5	-413	
		F19	1.9	4	-476	
		F20	1.6	5	-572	
		F21	1.4	5	-491	
		F22	2.2	17	-336	
		F23	2.3	37	-473	
	Fm	F8	2.0	13	-417	Migration Cell
		F9	1.6	44	-289	
		F10	1.4	72	-295	
		F11	1.5	13	-280	
		F13	2.7	78	-368	
		F15	2.2	27	-414	

Note: Fp potentiostat group, Fg galvanostat group, Fm migration group

Table 9 – Label ID of C test specimens and time to corrosion initiation.

Pipe Type	Group	Specimen ID	Cover Depth (cm)	Days to Corrosion Initiation	24 hours off Potential Vsce (mV)		Method
C	Cp	C0	3.80	91	-263		Potentiostat
		C1	3.02	28	-215	-150, Yes	
		C2	2.78	22	-308		
		C3	2.87	30	-205		
		C4	3.80	77	-273		
		C5	4.33	68	-193	-110, Yes	
	Cg	C6	3.30	105	-250		Galvanostat
		C7	2.00	11	-250	-150, Yes	
		C8	4.30	163	-330		
		C9	3.50	163	-330		
		C10	2.50	60	-250		
		C11	4.20	58	-265		
	Cm	C12	3.80	89	-188		Migration Cell
		C13	3.10	55	-293		
		C14	3.30	7	-279		
		C16	3.90	84	-285	-105, Yes	
		C17	1.60	27	-290	-160, Yes	
		C18	4.20	79	-333		
	Cm2	C21	2.9	7	-384		
		C23	2.9	7	-394		
		C24	4.3	7	-379		
		C25	3.7	7	-364		
		C26	3.7	7	-392		
	Crack	C22	2.5	7			

Note: Cp potentiostat group, Cg galvanostat group, Cm migration group

3.4 Time to Corrosion Initiation

Table 8 (F Specimens) and Table 9 (C Specimens) show selected results: cover, time to corrosion, and the steel potential 24 hours after disconnection when the specimen was declared active. The specimens were subjected to the different methods used for accelerating chloride transport; the column (second column from the left indicates group) farthest to the right indicates which method was used on each specimen. The results in Table 8 show that corrosion initiated within 10 days on the instrumented type F specimens (group Fp and groups Fga, Fgb) where the potentiostatic method and the galvanostatic method was employed to accelerate chloride transport. Two exceptions were observed for specimens F22 and F23 where it took up to 37 days, but these two specimens had slightly thicker covers. One factor that might have contributed to the activation within a few days is that the cover in these samples ranged

from 1.8 to 2.1 cm. The magnitude of the electric field applied, nobler potential at the embedded steel, higher resistivity and that the solution mostly remain under the ponded area (downward direction due to gravity) are additional factors. Specimens in group Fm (migration set-up) required a longer time for corrosion to initiate. One argument is that those electrically connected to the reinforcement (Fp and Fg) were polarized to more noble potential values and hence the chloride threshold was lowered; whereas, if polarization of the reinforcement took place on the Fm group of specimens, this was due to stray-current currents (more modest polarization) and might not reduce the chloride threshold as much. Another factor is that the solution going into the concrete might not be contained within the volume under the ponded area (gravity might allow transport of solution and ions downwards and sideways), which might have contributed also to the longer period of time before corrosion initiation on the Fm specimens. The time to corrosion initiation on these groups of specimens ranged between 13 and 78 days.

The results in Table 9 also show that corrosion initiation on three groups (Cp, Cg, Cm and Cm2) of specimens took longer when compared to specimens from F groups. There were a few specimens where the time to initiation was shorter than 30 days. All six specimens from group Cp have become active (time to initiation ranged from 22-91 days) and the concrete cover ranged between 2.7 and 4.3 cm. For group Cg specimens, the time to corrosion initiation ranged from 11 days to 105 days for most specimens. On specimens C8 and C9, 163 days passed before corrosion initiation was detected. In general, it took a similar number of days before corrosion initiated on group Cm samples. Two exceptions were observed: C14 needed 7 days and C17 needed 27 days. Other samples required between 55 and 90 days. For specimens that were placed in high humidity prior to applying the migration method (concrete with increased moisture content), the time to corrosion initiation was 7 days (C21, C23, C24, C25 and C26).

Table 10 – Re-polarization of specimens.

Group	Specimen	Potential before re-polarization	Days before re-polarization	Days to corrosion second time
C_p	C1	-150	110	20
	C5	-110	57	32
C_g	C7	-150	50	30
C_m	C16	-105	3 & High humidity	7
	C17	-160	3 & High humidity	7

Sometime after activation the potential measured on a few specimens shifted toward more positive potential values (more positive than -160mVsce), suggesting that these specimens might have re-passivated or that the non-corroding areas polarized the average potential to these more noble values. It was decided to re-polarize these specimens. These new tests were carried out either under previous conditions or moved to a high humidity environment and then re-polarized. The measured potential after the potential shift to less negative values, as

well as the conditions and how long it took for corrosion to initiate again are shown in Table 10. One possible reason could be that some of the chloride drifted away from the steel wire (once the electric field was removed) due to concentration gradient with a lower concentration present in some of the surrounding concrete. This could have caused a concentration lower than the chloride threshold at the surface. Another contributor to the potential shift is that the non-corroding steel might have polarized the active steel toward more positive potentials. However, in general, either no potential shift or very modest drift was observed on all other specimens upon corrosion initiation (over the next few days). The specimens that experienced this ennoblement were repolarized. The chloride solution contained 10,150 ppm while additional chloride transport took place. The solution was renewed at regular intervals until the specimen became active again.

Table 11 – Cover, resistivity, solution resistance, applied potential, and estimated electric field.

Group	Specimen ID	Concrete Cover (cm)	ρ (kΩ-cm)	Rs (kΩ)	Days to Initiation	Applied Potential (V)	Electric Field (N/C)
Fp	F0	1.75	22.69	0.28	3	3.1	177.1
	F1	1.86		0.3	7	3.4	182.8
	F2	2.06		0.2	3	3.2	155.3
	F3	2.05		0.38	4	3.2	156.1
Fg	F4	1.8		0.65	2	2.75	152.8
	F5	2.1		0.92	10	4.33	206.2
	F6	1.9		1.12	9	3.63	191.1
	F7	1.65		0.68	7	2.14	125.9
Fm	F8	2			25	5, 12, 15	76.9, 184, 230
	F9	1.6			27	15	230.8
	F10	1.4			72	15	230.8
	F11	1.5			13	15	230.8
	F12	2.7			78	15	230.8
Cp	C0	3.8	13.65	2.02	91	5.8	152.6
	C1	3.02		0.98	28	3.2	114.3
	C2	2.78		0.77	22	4.2	155.6
	C3	2.87		1.01	30	3.4	121.4
	C4	3.8		2.04	77	6.69	176.1
	C5	4.33			68	4.2	166.7
Cg	C6	3.3		1.79	105	3.3	150
	C7	2		1.48	11	2	280
	C8	4.3		1.57	163	4.3	100
	C9	3.5		1.43	163	3.5	120
	C10	2.5		0.88	60	2.5	128
	C11	4.2		1.61	58	4.2	107.1
Cm	C12	3.8			89	10, 12, 30	142, 171.4, 428.6
	C13	3.1			55	30	428.6
	C14	3.3			7	30	428.6
	C16	3.9			84	30	428.6
	C17	1.7			27	30	428.6
	C18	4.2			79	30	428.6

It is clear from above that both: testing approach and concrete cover played key roles to determine how long it took before corrosion initiated. Table 11 presents values of concrete resistivity for each concrete type. It also presents the solution resistance values measured at 56 Hz (i.e., impedance magnitude) using electrochemical impedance spectroscopy tests shortly after corrosion initiated, the applied potential and the estimated electric field observed for each specimen. The electric field was estimated by dividing the applied potential by the

distance separating the electrodes. For Fp, Fg, Cp and Cg specimens, the distance equaled the cover depth, whereas for Fm and Cm specimens, the distances of 6.5 cm and 7 cm, respectively, were given by the thickness of the corresponding RCP type. For example, on Cm specimens, the potential applied between the two stainless meshes is 30 volts, hence the calculated electric field driving the chloride ions transport for these specimens is 428.6 N/C, which is a higher value than the electric field applied on Fm specimens of 230 N/C (applied potential is 15 V and distance is 6.5 cm). Under natural chloride transport; it is usually expected that specimens from type F would show a longer time to corrosion initiation[2].

All three approaches used to accelerate chloride transport shortened the time to corrosion initiation of the reinforcing steel, i.e., the three methods were successful in initiating corrosion of the reinforcing steel after a short period of time (from a few days to a few months). In the following sections the monitoring results during the corrosion propagation stage (for some specimens up to 1400 days) will be presented and a brief discussion presented of what appears to currently be taking place during the corrosion propagation stage. At various times, selected specimens were forensically examined, i.e., the concrete covering the steel wire reinforcement was removed.

3.5 Corrosion Propagation Stage Monitoring

3.5.1 Laboratory Specimens (Rs, Rc, Ecorr)

This section presents typical plots of potential vs. time and plots of Rs, Rc vs. time for specimens subjected to the various high moisture exposure environments during the corrosion propagation stage. The exposure environment is also indicated. The potentials in the lab were measured against a saturated calomel electrode.

Figure 38 shows on the left plot the reinforcement potential evolution, and on the right, the Rs and Rc evolution with time for specimen F6 during the propagation period. The steel potential was approx. -0.4 V upon placing it in the high humidity, then it drifted to values as positive as -0.3 V (the environmental chamber stopped working for some time), and upon increasing the moisture in the high humidity chamber, the reinforcement potential shifted back to -0.4 V. The steel potential continued to drift toward more negative values and around day 1200 it reached a value of -0.475 V, then drifted once more to more noble values. The last reading, close to day 1500, the steel potential was -0.55 V. The Rc values ranged between 0.2 and 0.8 kΩ, with the most recent values being about 0.2 kΩ. The last two Rc values measured were less than 0.1 kΩ. For this specimen, the Rs decreased as time passed with some oscillations on the Rs value. The Rs ranged between 0.9 kΩ and 0.6 kΩ.

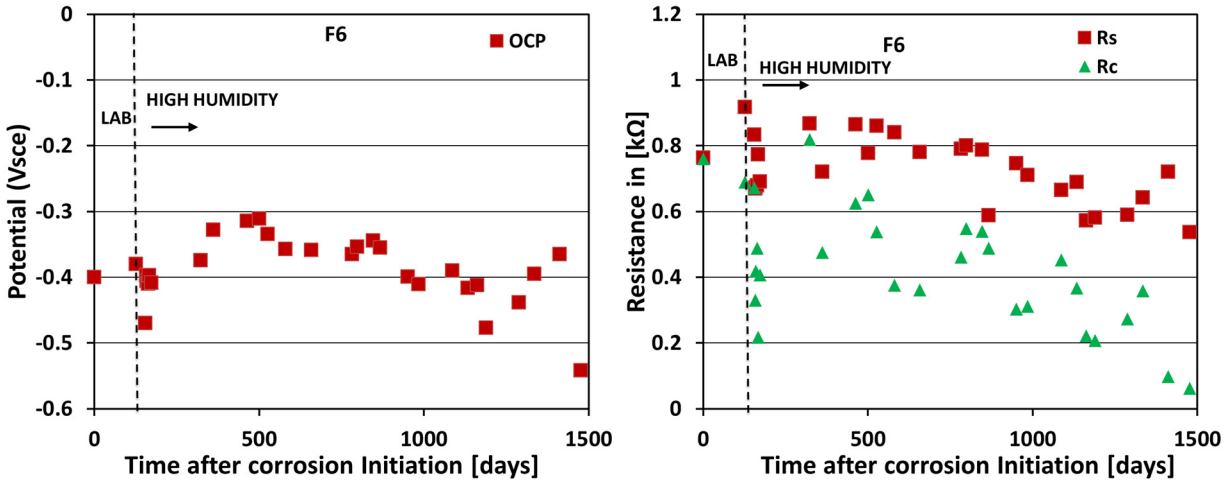

Figure 38 – Potential, Rs and Rc values measured on F6 specimen.

Figure 38 shows on the left plot the reinforcement potential evolution, and on the right, the Rs and Rc evolution with time for specimen F2 during the propagation period. Specimen F2 was kept in the laboratory environment after corrosion initiated for about 70 days and then the specimen was transferred to high humidity exposure. The potential measured after corrosion initiated was -570 mV. A large chloride concentration is believed to be present at the reinforcement as the initial solution used was 15% NaCl. The potential of the reinforcement remained around this value during the laboratory exposure period and also during the prolonged high humidity exposure. The plot on the right of Figure 39 presents the Rs, Rc evolution vs. time after corrosion had initiated. The Rc value remained almost the same throughout the exposure periods, and the magnitude of Rc was small, which likely suggests that the steel wire is corroding. It has been reported by Sagués and others that when the magnitudes of Rs and Rpapp (apparent measured value) are comparable there might be a large error when trying to determine the corrosion rate. On this specimen, the Rs value shifted from 200 ohms to 800 ohms by day 1500. The moisture remained high inside the high humidity chamber. One possible explanation is that the corrosion products produce a pore structure that created an additional resistance. This specimen was forensically examined. Before the forensic analysis, specimen F2 was exposed to room humidity for a week and the potential drifted to a more positive value; the corresponding Rc value also increased.

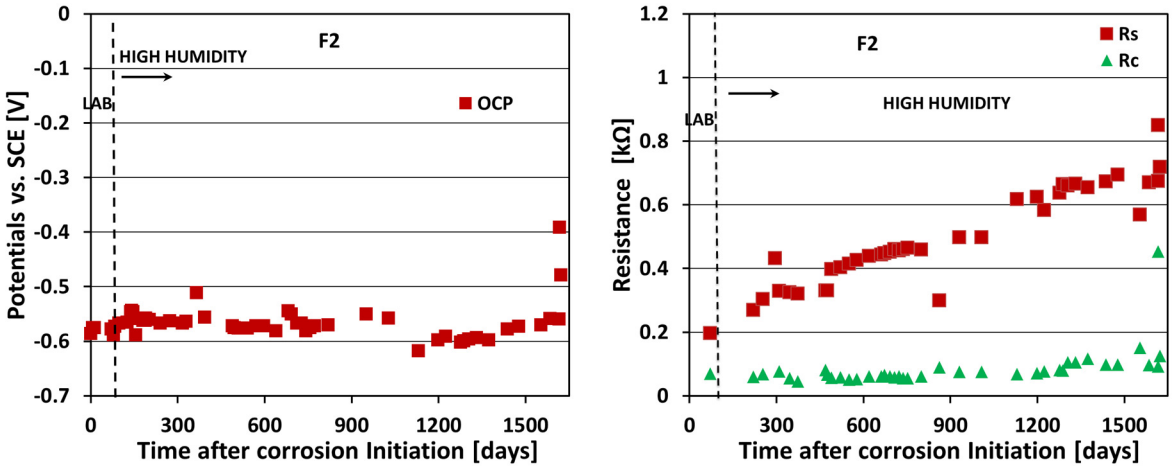

Figure 39 – F2 specimen: a) potential vs. time b) Rc and Rs vs. time.

The plot on the left in Figure 40 presents the reinforcement potential evolution measured for reinforcement embedded in specimen C23. This specimen was exposed to a high humidity condition, while the accelerated chloride transport took place, i.e., Cm-HH group. After corrosion had initiated, the specimen remained under the same environment for 25 days, then it was transferred to an exposure in which the specimen was covered by sand up to 1/3rd of the specimen's height. The specimen remained in the high humidity environment. The potential one day after corrosion initiated was -394 mV. The potential measured during the high humidity exposure remained close to the value measured after the corrosion initiated. While the specimen was partially covered with sand, the reinforcement potential gradually drifted toward more negative values, and by day 380, the potential of the reinforcement had reached a value of -442 mV. The potential started to drift toward more positive values and reach a value of -400 by day 700; this was followed by a downward shift to -500 mV. By day 1200, the specimen was moved to be fully covered on day 1300, and by the last potential reading, the steel potential was -600 mV. The plot on the right of Figure 40 presents the trends for Rs, and Rc obtained on specimen C23 vs. time. The corrosion rate is likely high as the average Rc value was 0.15 KΩ while partially covered with sand.

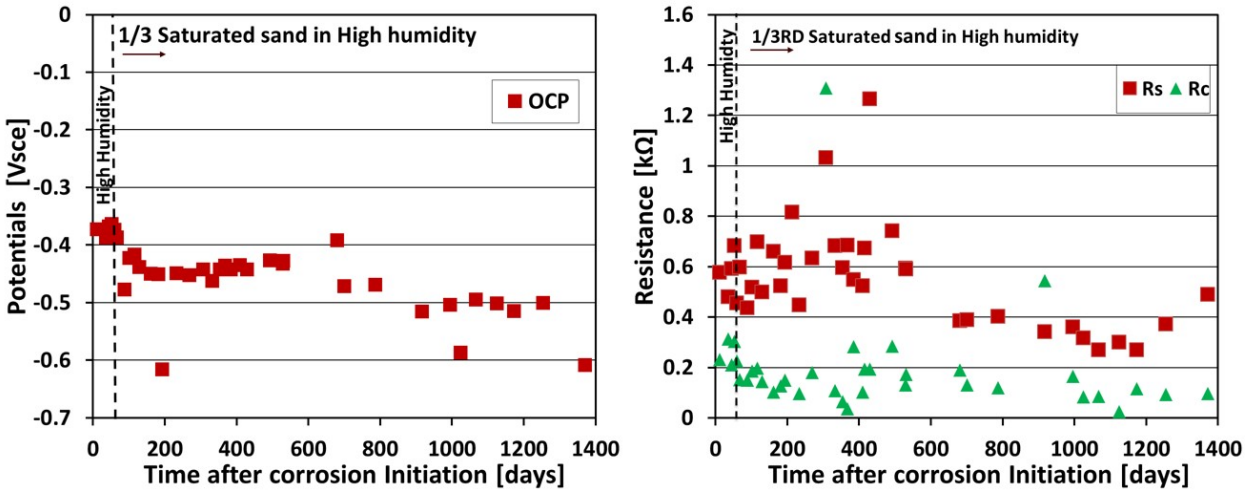

Figure 40 – C23 specimen: a) potential vs. time b) Rc and Rs vs. time.

Specimens F1 and C1 have been terminated. Figure 41 shows on the left a plot of the reinforcement potential evolution, and on the right, the Rs and Rc measured values on specimen F1. The reinforcement potential - once corrosion initiated - was more negative than -0.5 V. Initially, the value was close to -0.6 V; while exposed in lab conditions, it drifted to -0.5 V. Upon placing the specimen in a high humidity environment, the reinforcement potential moved to slightly more negative values, and when covered with saturated sand, the reinforcement potential reached values as negative as -0.63 V, plateaued for some time, and after day 600, slowly drifted to more positive values. The potential was -0.59 V before terminating this specimen. Regarding the Rs evolution with time, it went from a value of 0.21 kΩ to a value of 0.6 kΩ. The Rc values were always less than 0.2 kΩ and toward the end of the exposure, the Rc value appeared to slightly increase, suggesting a modest reduction in the corrosion rate. The Rc and Rs values are in kΩ because a unit area (1 cm^2) was assumed when the test was run. The reported Rc values are not area-corrected. The area of the reinforcement under the reservoir is about the same for all samples with the same orientation.

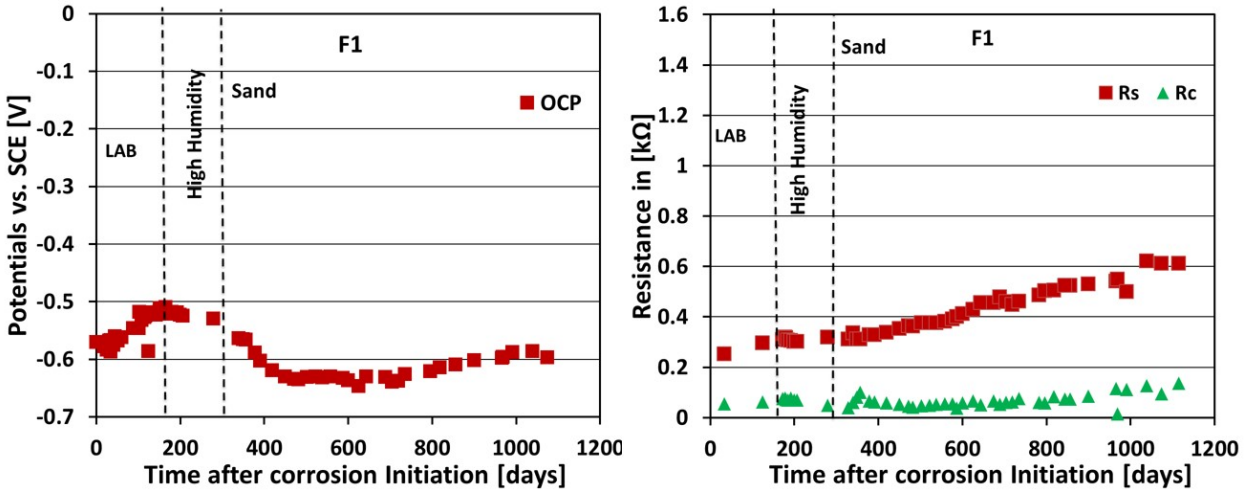

Figure 41 – Potential, Rs, and Rc values measured on F1 specimen.

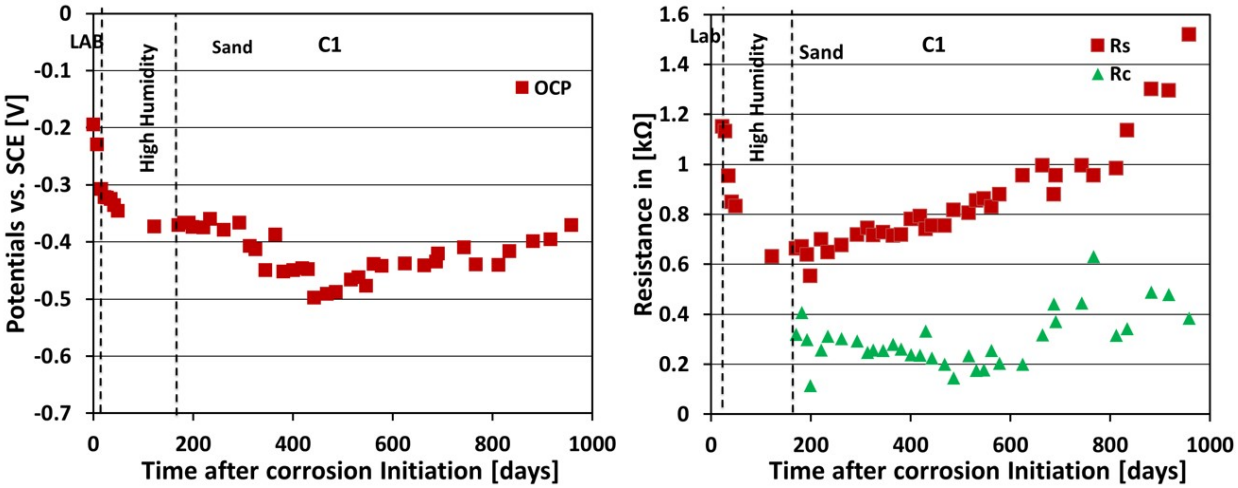

Figure 42 – Potential, Rs, and Rc values measured on C1 specimen.

Figure 42 shows on the left a plot of the reinforcement potential evolution and, on the right, the Rs and Rc values measured on specimen C1. The potential, once corrosion initiated, was close to -0.2 V; while exposed in lab conditions, it drifted to -0.23 V. Upon placing it in high moisture, the potential shifted to more negative values and reached a value of -0.38 V. The specimen was then placed in a container covered with saturated sand; the reinforcement potential then drifted further to more negative potential values and reached a potential value of -0.5 V by day 400. The reinforcement potential values then started to drift toward more positive values, but plateaued for some time (200 days) at a potential value of -0.43 V and, after day 600, slowly drifted to more positive values. The potential was -0.38 Vsce before terminating this specimen. Regarding the Rs evolution with time, it went from a value of 0.6 kΩ to a value of 1.6 kΩ by day 950. Most Rc values were between 0.2 and 0.4 kΩ. The Rc values initially decreased and then, after day 600, showed an slight increase in magnitude, suggesting that a modest reduction in the corrosion rate might have taken place.

Figure 43 shows on the left a plot of the potential evolution measured during three different exposures for the reinforcing steel of specimen C3. The potentiostatic method was used to accelerate the chloride transport in specimen C3. Corrosion initiation was declared after 30 days, in this case, when the reinforcement potential had reached a value of -205 mVsce. The specimen was then exposed to the laboratory environment for 29 days and then transferred to the high humidity exposure for 147 days; the specimen was then covered with saturated sand. The potential of the reinforcement during the laboratory exposure quickly shifted to a more negative value of -342 mV and remained close to this value during the lab humidity exposure. Once the specimen was transferred to the high humidity exposure, the potential of the reinforcement decreased from -342 mV to -402 mV by day 176. Then the specimen was transferred to an exposure that fully covered the specimen with saturated sand. The potential of the reinforcements showed a gradual and moderate decrease in value to -426 mV by day 298 of exposure. After day 320, the reinforcement potential gradually increased, and by day 406 of exposure, the potential of the reinforcing steel had reached a value of -320 mVsce. Afterward,

the potential oscillated, and by day 495, it had returned to -400 mVsce. The potential remained around -400 mVsce till day 1200, and slowly increased to -380 mVsce by day 1500.

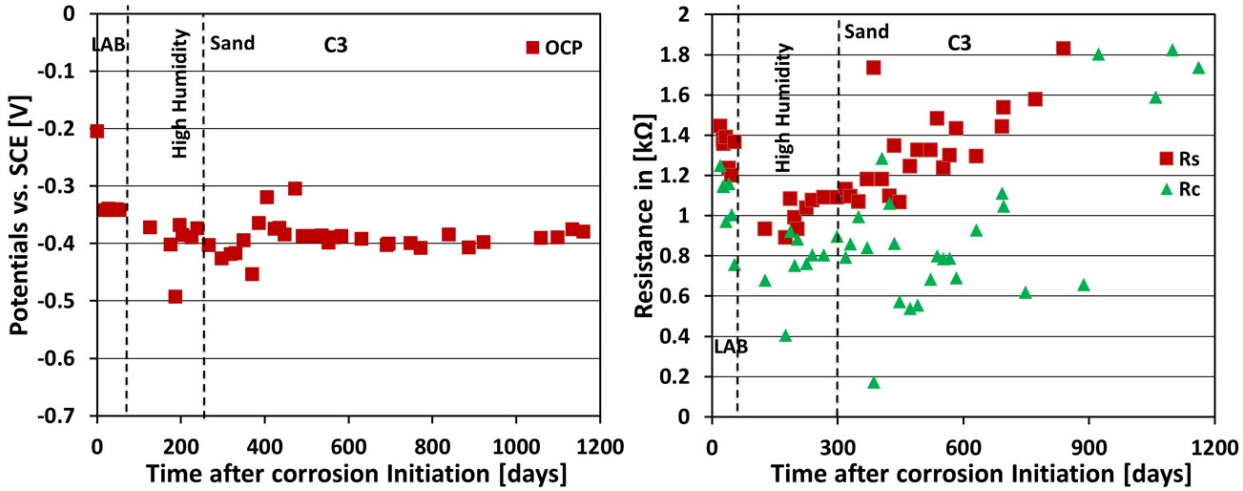

Figure 43 – C3 specimen: a) potential vs. time b) Rc and Rs vs. time.

The plot on the right of Figure 43 shows that the Rc values decreased from 1.25 kΩ to 0.97 kΩ by day 33 under lab RH exposure. Then the Rc value decreased further to 0.41 kΩ by day 176, while exposed to high humidity. When the specimen was exposed covered with saturated sand, the Rc value ranged between 0.5 and 1.2 kΩ (till day 900). Toward the end of the reported period, it increased to a value of 2 kΩ, with the last reading being a little over 3 kΩ. The Rs on this specimen experienced a monotonic increase from day 176 to day 1500, from 1 kΩ to 2.6 kΩ.

Figure 44 presents on the left a plot of the potential evolution measured during three different exposures for the reinforcing steel of specimen F10. After corrosion had initiated, this specimen was exposed to the laboratory environment for 32 days and then transferred to a high humidity environment for 136 days; it was then immersed in water. Figure 9a shows that the potentials of the reinforcement, during the laboratory exposure condition, gradually increased from -435 mV to -345 mV by day 32. While in the high humidity exposure, the reinforcement potential momentarily increased from -345 mV to -280 mVsce and shifted to -309 mV by day 168. In the immersed water condition, the reinforcement potential decreased to -534 mV by day 222 and remained around this value for 30 days. This was followed by a modest increase in potential to a value of -493 mV by day 309, and remained at this level subsequently till day 600. The steel potential then drifted toward more positive values and eventually reached a value of -0.35 by day 1400. Figure 44 – plot on the right – presents the observed trend for Rs and Rc on specimen F10. It shows that the Rc measured value (while exposed to high humidity conditions) decreased from 0.435 kΩ to 0.225 kΩ by day 168. The specimen was then immersed in water and the Rc value slowly decreased to a value of 0.099 kΩ by day 236, followed by a gradual modest increase to 0.4 kΩ by day 490. The Rc value then oscillated between 0.05 kΩ and 0.6 kΩ, with the last Rc values being 0.3 kΩ.

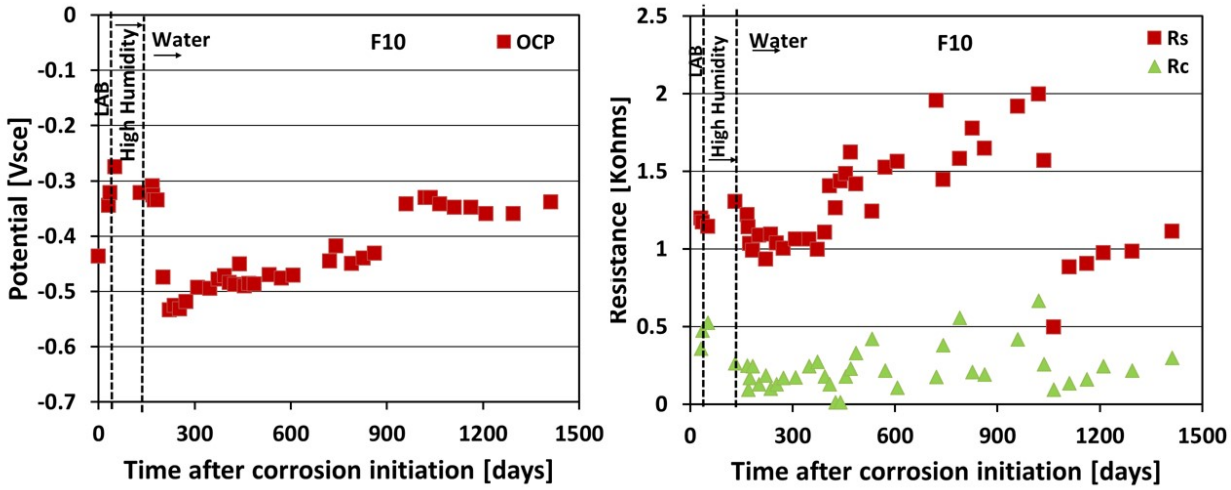

Figure 44 – F10 specimen: a) potential vs. time b) Rc and Rs vs. time.

The plot on the left in Figure 45 presents the potential evolution measured during three different exposures for the reinforcing steel of specimen F21. Specimen F21 was subjected to the galvanostatic method for accelerated chloride transportation. The reinforcement potential, upon corrosion initiation, was -491 mV. After corrosion initiated, the specimen was exposed to laboratory conditions for 120 days and then immersed in water for more than 100 days. During the laboratory exposure, the potential values showed a moderate increase to -461 mV, but while immersed in water, the potential values decreased to a more negative value of -633 mV by day 168, and then was followed by a gradual increase in potential to a value of-546 mV by day 266 of exposure, and remained there until day 390. The plot on the right in Figure 45 shows that the Rc value remains almost unchanged while exposed to laboratory atmosphere. While immersed in water, the Rc value initially decreased from 0.493 kΩ to 0.245 kΩ by day 127 and gradually reached a lower value of 0.177 kΩ by day 168. Then the Rc value showed a modest gradual increase and reached a value of 0.24 kΩ by day 400. While immersed in water, the average Rc value was 0.2 kΩ.

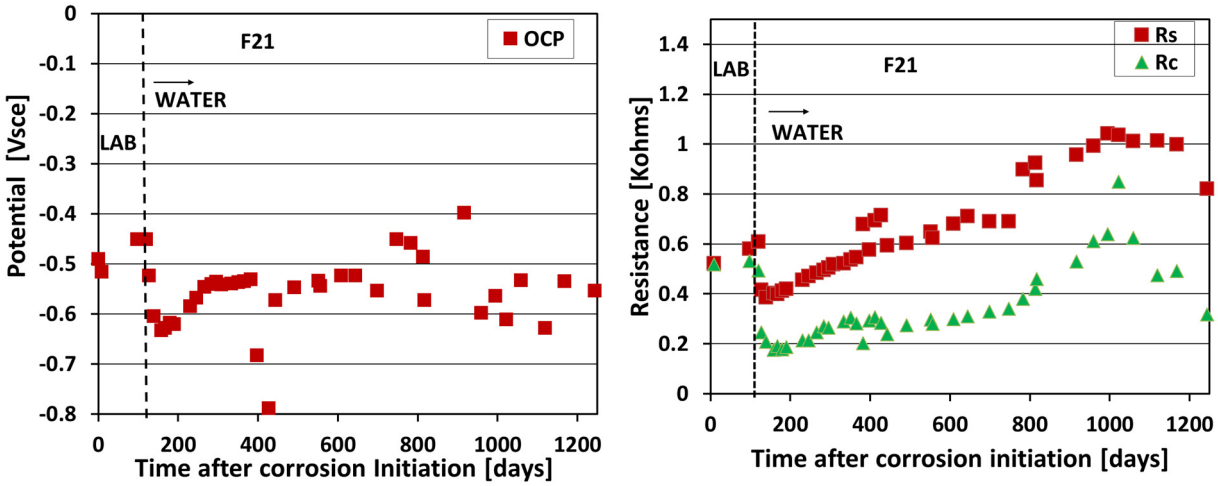

Figure 45 – F21 specimen: a) potential vs. time b) Rc and Rs vs. time.

The potential evolution measured during three different exposures for the reinforcing steel of specimen C8 is shown in Figure 46 (plot on the left). C8 was subjected to the galvanostatic method for accelerated chloride transportation. The specimen started corroding after 163 days, and the corresponding potential was -330 mV. After corrosion had initiated, the specimen was exposed to laboratory conditions for 83 days and then it was placed in the fully buried sand condition for 110 days. C8 was then immersed in water. The potential gradually increase to -240 mV by day 83 while in laboratory conditions. Then, while covered with sand, the potential decreased gradually and reached a similar value (-338 mV) to the potential value measured upon corrosion initiation by day 193. While fully immersed in water, the potential values decreased further: to -538 mV by day 239. This was followed by a gradual shift to nobler values reaching a potential value of -481 mV by day 315.

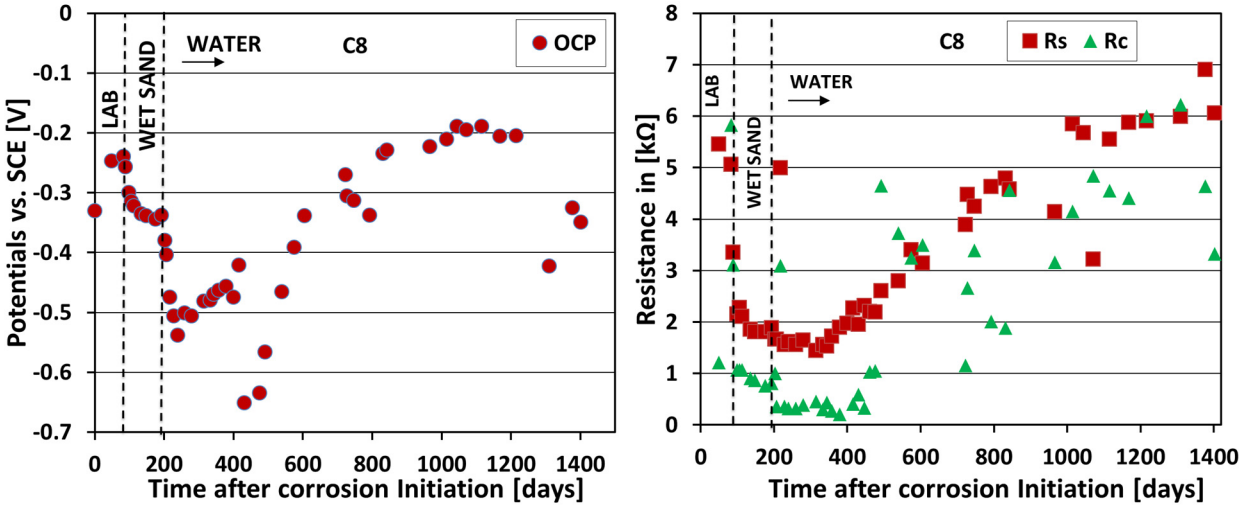

Figure 46 – C8 specimen: a) potential vs. time b) Rc and Rs vs. time.

The evolution of the Rs and Rc values in the C8 specimen against time in days is shown in Figure 46 (plot on the right). The plot shows that the Rc value increased from1.2 kΩ to 3.063 kΩ by day

83 of laboratory exposure. While covered with saturated sand exposure, the Rc value decreased from 3.063 kΩ to 0.762 kΩ by day 99. When immersed in water, it gradually decreased to an even lower value from 0.762 kΩ to 0.2 kΩ by day 400. The average Rc value, while immersed in water condition was 0.3 kΩ.

3.5.1.1 Cathodic Polarization

The following two plots present cathodic potential scans performed on the selected specimens during the propagation stage exposure.The horizontal axis shows the current density in log scale corrected for the assumed surface area. The vertical axis represents the potentials in volts measured with respect to SCE. The legend in the plots shows the date when the scans were performed.

Figure 47 shows three potentiostatic scans performed on three different days on specimen F13 while exposed to saturated sand environment (corrosion propagation experiments). The right most curve was the earliest cathodic polarization scan performed on the F13 specimen; the open circuit potential of the steel was -550mV, and the current density, measured at -800m Vsce, was 7.35×10^{-6} A/cm^2. During the second potentiostatic scan (middle cure) it was observed that the potential of the specimen was now -580mVsce. There was a small reduction in the current density (6.0×10^{-6}A/cm^2) observed at a potential of -800 mV. In the latest scan performed after a long exposure, there was no change in the open circuit potential; only a small reduction in the current density measured was observed (i.e., at -800 mV the current density was 5.0×10^{-6} A/cm^2). The three polarization scans suggest that at open circuit potential the cathodic reaction was under mix control, i.e., both activation potentials and mass transfer control. The recorded current density measured at -600 mV had gradually decreased by an order of magnitude from January to July. Hence, although the cathodic reaction was not under mass transport only, it significantly influences the cathodic output per unit area. It was possible that the area where the cathodic reaction that took place increases with time, partially due to larger throwing power, and also, as corrosion progresses, it increases the surface area. This change was not reflected in the curves shown below; thus, the corresponding current densities for latter scans might be smaller than that reported in here.

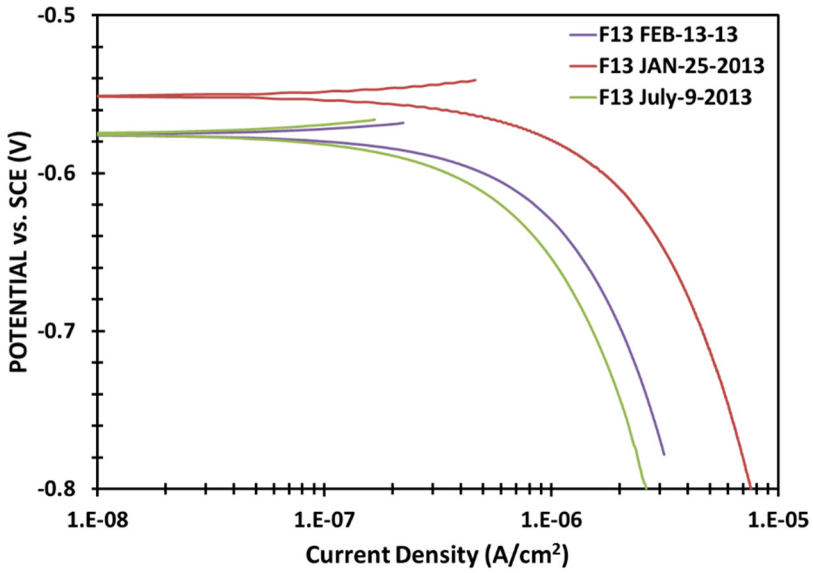

Figure 47 – Cathodic potentiodynamic scans performed on F13.

Figure 48 presents the three potentiodynamic scans performed on specimen C18 after immersed in water. The scan performed in January suggests that the open circuit potenial was-440 mV and the current density was 5.7×10^{-6} A/cm^{2}for -700 mVsce. From the cathodic polarization scan performed after a long exposure, it can be observed that the open circuit potential decreased to -520mV. At a potential of -800 mV, the current density was 8×10^{-6} A/cm^2. This current density was an indication of the limiting current density, as indicated above. It could be possible that the area correction was off and the limiting current density could be lower. When comparing the current density from both curves at a potential of -660 mV, there was a modest reduction (log scale) in the measured current density to about 1/3rd.

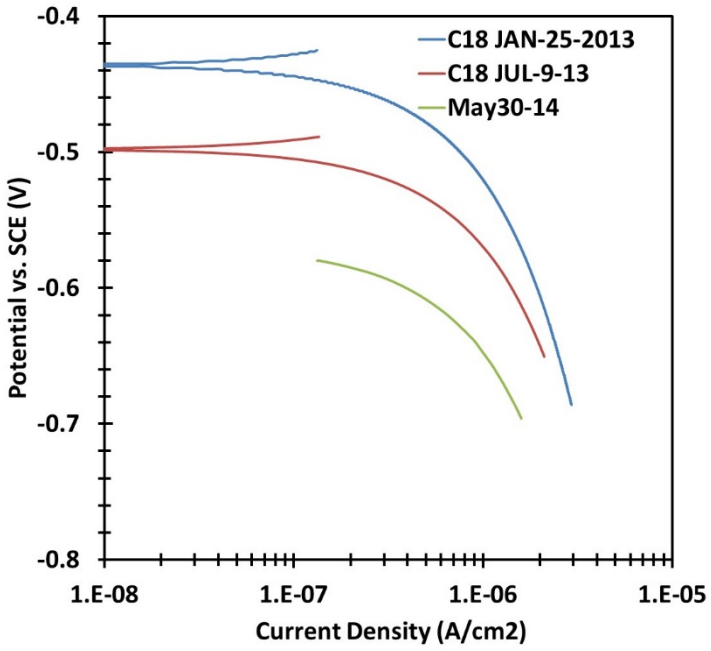

Figure 48 – Cathodic potentiodynamic scans performed on C18.

3.5.2 Corrosion Propagation on Specimens for Which Corrosion Was Accelerated

Table 12 presents the minimum concrete cover, the number of days since initiation to the day the specimen was terminated (or as of 5/15/16, if the specimen was not terminated), and the date when specimen was terminated. Table 12 also lists the exposure time in days in the different environments for each specimen once corrosion had initiated. Note that the exposures listed are in sequential order from left to right, i.e., first exposure was laboratory humidity, then high humidity and last, for some specimens, covered with saturated sand. During the laboratory environment exposure, the specimens were not polarized. Recall that seven days after being transferred from laboratory environment to high humidity environment, these specimens were polarized. Selected specimens were covered with saturated sand after 168 days in HH and continued to be polarized. The current cycle application for each specimen is not included herein due to space constraints (but can be found in an appendix - section 8.2 from a recent thesis[38]). The current was applied for 330 days (including the days when applied current was momentarily removed) from the first galvanostatic pulse.

3.5.2.1 Potential Evolution during the Propagation Stage

Selected plots of the steel on- and off-potential evolution vs. time are shown in this section. For most specimens, natural corrosion propagation at lab humidity occurred for at least 300 days, which is the data plotted to the left of the dotted line in each. The plots in this section show the potential values in mV vs. sce; whereas, for other sections, the potential values are reported in Volts. To the right of the dotted line, in the Figures in this section, are the potentials values measured during the accelerated corrosion propagation (shaded region). The steel on-potential values are those measured just before disconnecting and steel-off values are the potential values measured 2-3 days after disconnecting the specimens. This approach

allowed us to quantify the recovery (depolarization) and stabilization of the steel potential after each electric field application. During the accelerated corrosion propagation phase, the steel reinforcement was anodically polarized. This caused the potential of the steel to move to a more positive value (while the current was being applied). While the small current was applied an electric field was generated that likely allowed the transport via migration and in parallel allowed diffusion of a small additional amount of chlorides. Note that the magnitude of the current application is color coded in the Figures. No current was applied on specimens F16, F17, F18 and C10 after August/2014 but continued to be monitored; the F specimens were later forensically analyzed.

Table 12 – Specimens' ID, minimum concrete cover, and time since corrosion initiation.

Specimen ID	Minimum Concrete Cover (mm)	Days since corrosion initiated	Lab RH (70%)	High Humidity (95%)	Covered with wet sand
F7_T	16.5	707	526	175	
F16_T	15	1349+	322	190	837
F17_T	14	1349+	322	169	858
F18_T	17	1027	322	705	
F19_T	19	642	322	320	
F20_T	16	642	322	168	152
F23_T	23	544	236	308	
C4_T	38	847	465	168	152
C6_T	33	604	428	176	
C10+*	25	1184+	465	189	530

+* indicates specimens not yet terminated (as of 5/16/16)

Figure 49 displays the on- and off-potential evolution versus time of the reinforcement for specimen F7. Note that for the time period between 659-689 days, the current was not applied. The specimen was repolarized for 2 weeks before being terminated. Initially, the off-potential was ~-500 mV_{sce} after corrosion initiated. The off-potential increased over time and was in the range of ~-305 mV_{sce} to ~-320 mV_{sce} before applying the current. After exposure in the high humidity container and the initial application of 25 µA cycle, the off-potential of the reinforcement became more negative to ~-480 mV_{sce}; whereas, the steel on-potential was slightly more positive, ranging between ~-405 mV_{sce} to ~-440 mV_{sce}. After a few cycles (49 days of current application), the current was increased to 50 µA where the off-potentials decreased to around ~-500 mV_{sce}. The on-potentials initially were ~-480 mV_{sce} 7 days after increasing the current to 50 µA, and then increased slightly to ~-450 mV_{sce} by day 91 of the current application. After 105 days, the current application was increased to 125 µA. The off-potentials increased to values between -436 mV_{sce} to -449 $mV_{sce,}$ whereas, the on-potentials increased significantly to ~-300 mV_{sce}. Although the current was suspended for ~30 days after 130 days of current being applied (between day 659-689), the off-potentials remained the same. When the applied current was increased, the potential separation between the on- and off-potential steel

values increased. Specimen F7 was terminated on day 701 after corrosion initiated with the last 175 days under current application.

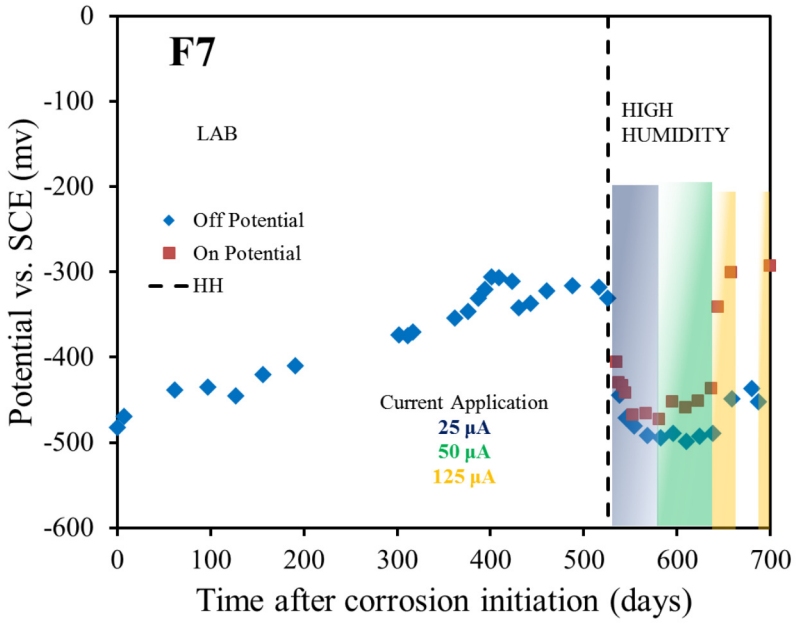

Figure 49 – On- and off-potential vs. time for specimen F7.

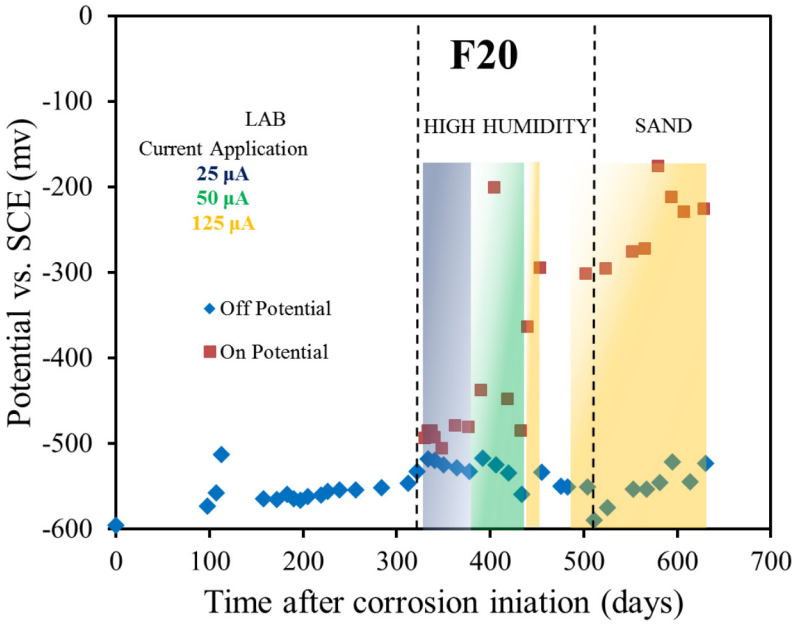

Figure 50 – On- and off-potential vs. time for specimen F20.

Figure 50 displays the on- and off-potential evolution versus time of the reinforcement for specimen F20. Note that for the time period between 455-483 days, the current was not applied. After corrosion initiated, the potential was ~-600 mV_{sce} and had increased to ~-540 mV_{sce} before being placed in high humidity and polarized. After the sample was in the high

humidity container and the initial current application of 25 µA for two weeks, the off-potential of reinforcement was ~-545 $mV_{sce,}$ whereas, the on-potential saw a slight increase to -484 mV_{sce}. After 56 days of current application, the current was increased to 50 µA. During this time, the off-potentials slowly decreased to ~-575 mV_{sce} and the on-potentials increased to ~-450 mV_{sce}. After 112 days, the current was increased to 125 µA and the off-potential measured was comparable to values after the first two weeks with a current application of 25 µA. The on-potentials measured drastically increased to values between -365 mV_{sce} to ~-294 mV_{sce}. The specimen was disconnected for four weeks where the off-potentials remained stable. Shortly after repolarizing the reinforcement on day 450, the sample was covered with saturated sand where it remained under 125 µA current application. While covered with saturated sand, the off-potential ranged between -600 and -530 mV_{sce}. The on-potentials gradually increased to values that ranged between -175 mV_{sce} to -228 mV_{sce}. Similar to what was observed for specimen F7, when the current application was increased, the potential separation between the on- and off-potentials increased. Specimen F20 was terminated on day 642 with the last 321 days under current application.

Figure 51 displays the on- and off-potential evolution versus time of the reinforcement for specimen F23. Note that for the time period between 357-385 days, the current was not applied. After corrosion initiated, the potential measured was -201 mVsce and decreased to -233 mVsce before applying the galvanostatic pulse. After spraying water on the sample in the high humidity container and the initial electric field application of 25 µA for two weeks, the off-potential of the reinforcement became more negative to -283 mVsce before the current was increased. The on-potential increased dramatically to values between -38 mVsce to +659 mVsce and then decreased to values that ranged between -60 mVsce to +98 mVsce. Upon increasing the applied current to 50 µA, the on-potential increased dramatically to +934 mVsce and off-potential slightly increased to -214 mVsce. The off-potential initially increased to -178 mVsce, then gradually decreased to -222 mVsce before being terminated. The specimen was terminated after 544 days after corrosion initiated with the last 327 days under accelerated corrosion. The separation between the on- and off-potentials increased when the current was increased similar to what was observed on specimens F7 and F20; however, the separation was much larger. The off-potentials were also more positive than specimens F7 and F20, indicating that corrosion may be taking place at a lower rate (and possibly over a smaller area).

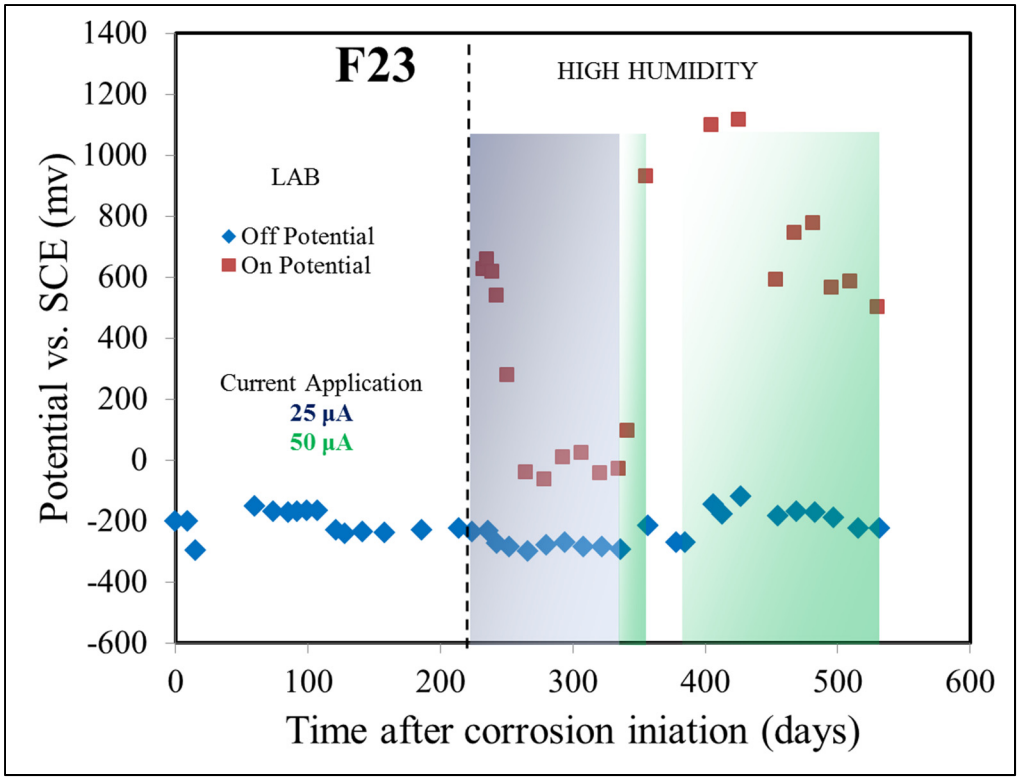

Figure 51 – On and off-potential vs. time for specimen F23.

Figure 52 displays the on- and off-potential evolution versus time of the reinforcement for specimen C4. Note that for the time period between 468-496 days, the current was not applied. After corrosion initiated, the potential measured -180 mVsce. The potential increased to -89 mVsce after 133 days of natural corrosion propagation and then decreased to -269 mVsce before applying the electric field. After spraying water on the sample in the high humidity container and the initial current application of 25 µA for two weeks, the off-potential of the reinforcement became more negative measuring -374 mVsce and slightly decreased to -379 mVsce before increasing the magnitude of the applied current. The on-potential measured -219 mVsce and became more negative to -317 mVsce before increasing the current. After 56 days of current application, the current was increased to 50 µA. During this time, the off-potentials slowly decreased to -391 mVsce, and the on-potentials increased to -308 mVsce before increasing the current further. After 112 days, the current was increased to 125 µA. The off-potentials decreased to -409 mVsce before the specimen was covered with saturated sand. The on-potentials measured drastically increased to values between -191 mVsce to +5 mVsce. The specimen was disconnected for four weeks while the off-potentials remained stable, whereas the on-potential, upon polarization, recovered to -126 mVsce. Shortly after covering the specimen with saturated sand, the sample's reinforcement was repolarized via the 125 µA current application. While covered with saturated sand, the off-potentials remained stable for the next ~80 days around -415 mVsce and then finally decreased to a potential of -433 mVsce before forensic analysis took place. The on-potentials gradually increased to values from -49 mVsce to +250 mVsce before being terminated from day 510 to day 655. Similar to the F specimens, when the current application was increased, the potential separation between the

on- and off-potentials increased. Specimen C4 was terminated on day 655 with the last 320 days under current application.

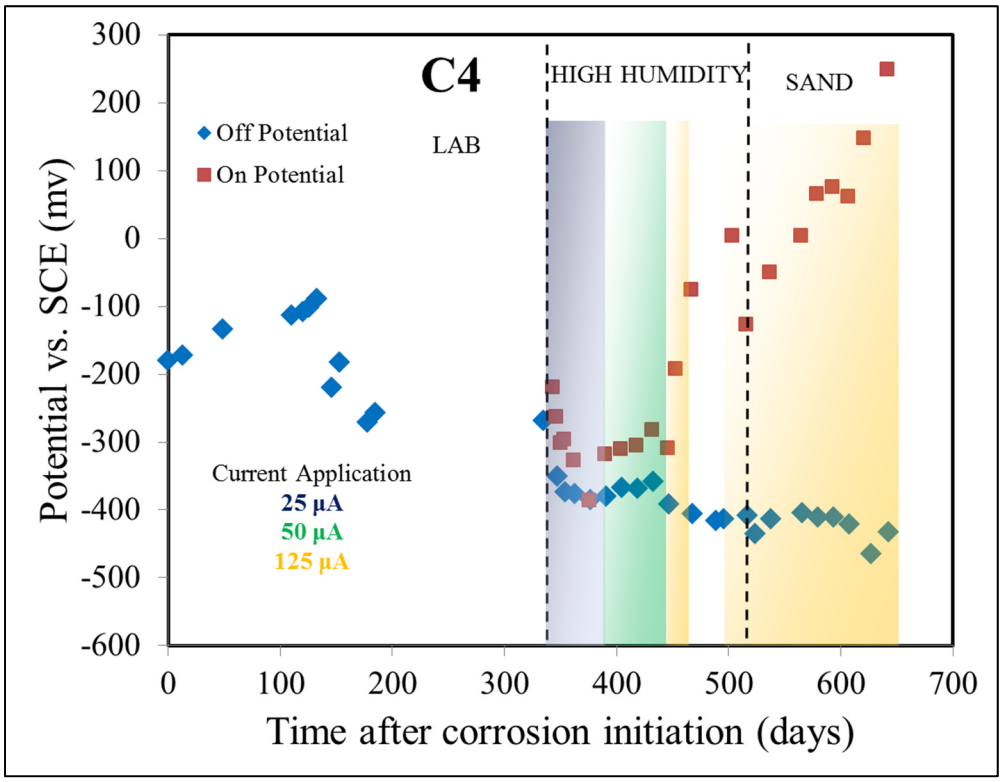

Figure 52 – On- and off-potential vs. time for specimen C4.

Figure 53 displays the on- and off-potential evolution versus time of the reinforcement for specimen C6. Note that for the time period between 468-496 days, the current was not applied. The specimen was repolarized the final 2 weeks before being terminated. Similar to what was observed on specimen F7, the potentials - shortly after corrosion initiation for C6 - initially increased over time to values between -220 mVsce to -150 mVsce. After ~200 days following corrosion initiation, the off-potential drastically decreased to -300 mVsce, then recovered to a value (-200 mVsce) comparable ~100 days after corrosion initiation before applying the electric field. After spraying water on the sample in the high humidity container and the initial electric field application of 25 µA for two weeks, the off-potential of the reinforcement became more negative, to -343 mVsce, whereas, the on-potential was slightly more positive - around -223 mVsce to -300 mVsce. After 56 days of current application, the current was increased to 50 µA, where the off-potentials measured were comparable to values measured at 25 µA. The on-potentials decreased slightly after the current was increased from 25 µA to 50 µA to values between -320 mVsce to -340 mVsce. After 105 days, the current was increased to 125 µA. The off-potentials slightly decreased to -400 mVsce and remained there until the specimen was terminated. The on-potentials drastically increased to around -100 mVsce and measured +274 mVsce before being terminated the following week. Similar to specimen F7, when the current application was increased to 125 µA, the potential separation

between the on- and off-potentials increased. The on-potential moved to more noble values. Specimen C6 was terminated on day 510 with the last 176 days under current application.

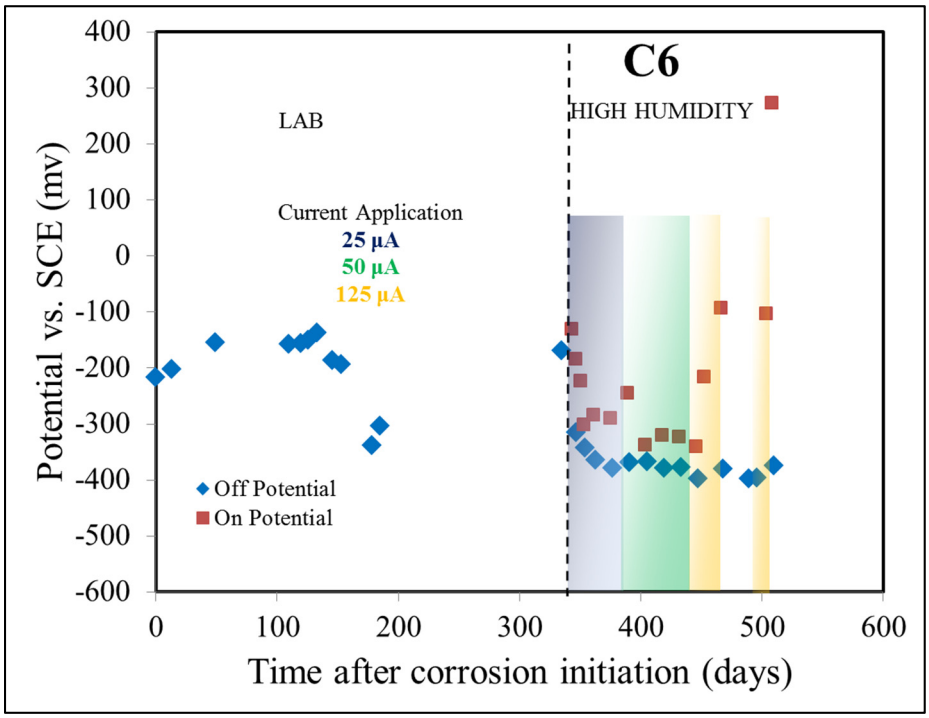

Figure 53 – Potential vs. time after corrosion initiation for specimen C6.

3.5.2.2 Rs, Rc_EIS, Rc_LPR, Nyquist

Typical plots of solution resistance (Rs), polarization resistance of the steel reinforcement (Rc) vs. time and Nyquist plots of impedance results after current application (but disconnected for 3 days before performing LPR or EIS) are shown in this section. Rc is the charge transfer (polarization resistance) value after removing the Rs from Rp_app calculated after the LPR measurement. Note that Z' is the real part and Z'' is the imaginary part of the impedance measured. For each impedance measurement, the lowest frequency measured is in parenthesis next to the day in each plot's legend.

The Rs, Rc_LPR and Rc_EIS values can be seen in Figure 54 for specimen F7. After being placed in high humidity and polarized but measured while disconnected, the LPR Rc (Rc_LPR) values of specimen F7 decreased slightly and remained constant around ~0.10 kΩ after 56 days of current application. The Rs also decreased slightly after the first two measurements before stabilizing around ~0.40 kΩ. After 56 days of galvanostatic pulse, the current was increased to 50 µA, where the Rc_LPR values remained between 0.10 kΩ - 0.12 kΩ. After the current was increased to 50 µA, the frequency for the EIS test ranged from 300 Hz - 0.001 Hz. The Rc values obtained from impedance (Rc_EIS) after the current was increased to 50 µA were larger than that of LPR on the order of 0.25 kΩ - 0.45 kΩ using a CPE model. The Rs values were comparable during the 25 µA current application at ~0.40 kΩ. After 112 days of current application, the current was increased to 125 µA. The Rc_LPR values increased slightly to ~0.15

kΩ before being terminated. The Rs values increased slightly to ~0.50 kΩ before being terminated. The Rc_EIS values remained stable around ~0.4 kΩ - 0.5 kΩ before the specimen was terminated. A final Rc_LPR and Rc_EIS value of ~0.15 kΩ and ~0.5 kΩ suggests that the steel was actively corroding. Looking at the Nyquist plot of specimen F7 in Figure 55, a shift in Rs as time passed (applied current magnitude increased also) suggesting that corrosion products may have formed, accumulated and entered the concrete's pore structure. Also, the Nyquist results do not completely represent a CPE response (perfect depressed semi-circle); it was beyond the scope of this project to identify a more adequate equivalent circuit. The F7 specimen was terminated 510 days after corrosion initiation.

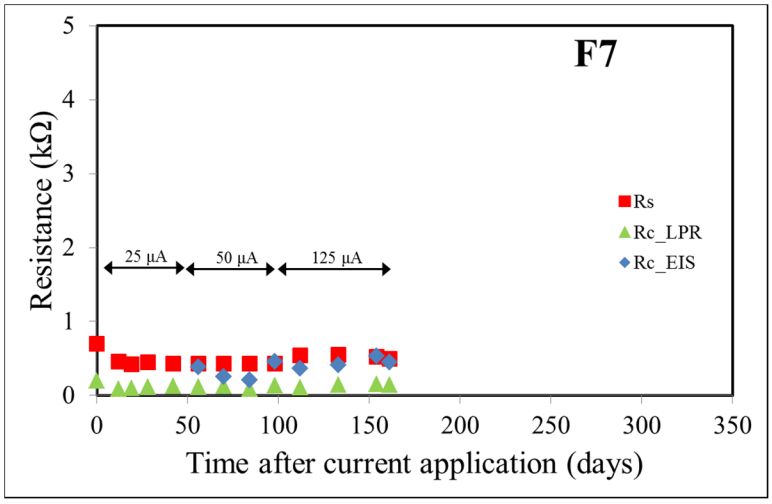

Figure 54 – Plot of Rc_LPR, Rc_EIS, and Rs vs. time for specimen F7.

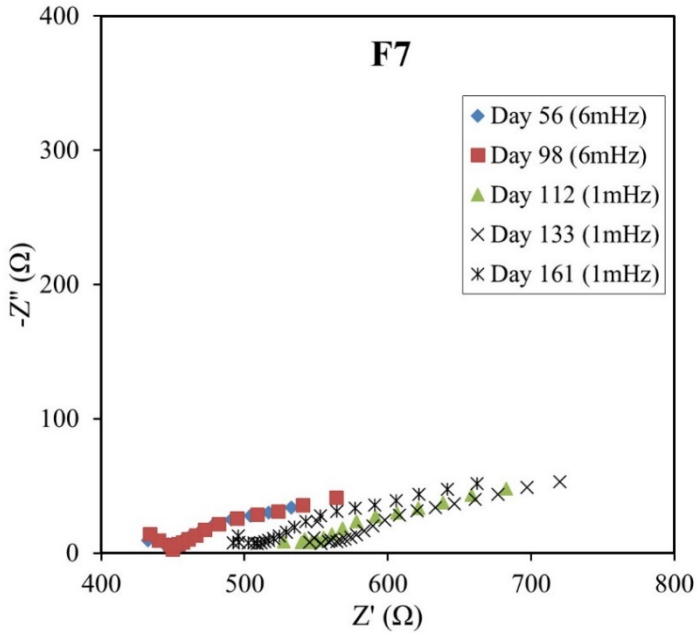

Figure 55 – Nyquist plot of specimen F7.

The Rs, Rc_LPR and Rc_EIS values can be seen in Figure 56 for specimen F20. After being placed in high humidity and polarized but measured while disconnected, the LPR Rc (Rc_LPR) values of specimen F20 ranged from 0.31 kΩ to 0.37 kΩ after 56 days, whereas the Rs values initially measured 0.27 kΩ and then increased slightly to 0.41 kΩ before increasing the current to 50 µA. After 56 days, the current was increased to 50 µA where the Rc_LPR values were constantly ~0.37 kΩ, but decreased to 0.29 kΩ before increasing the current to 125 µA. After the current was increased to 50 µA, the frequency for the EIS test ranged from 300 Hz - 0.001 Hz. The Rc values obtained from impedance (Rc_EIS) after the current was increased to 50 µA were larger than that of LPR. The Rc_EIS values initially measured 0.56 kΩ and then increased to 0.76 kΩ. The Rc_EIS values were obtained using a CPE model. The Rs values were comparable during the 25 µA current application around ~0.40 kΩ before increasing the current to 125 µA. After 112 days, the applied current was increased to 125 µA. The Rc_LPR values increased slowly from 0.29 kΩ to 0.45 kΩ before terminating the specimen. The Rs values increased similar to the Rc_LPR values from ~0.40 kΩ to 0.60 kΩ before terminating the specimen. The Rc_EIS values significantly increased from 0.76 kΩ to 1.67 kΩ before terminating the specimen. These Rc values indicate that the steel was actively corroding. The large increase in Rc_EIS values was believed to have been due to a bad fit using a CPE model. Similar to specimen F7 as the time and current increased, the shape of the Nyquist plots at lower frequencies tended to display an even more depressed semicircle and might require additional elements in the equivalent circuit model for a better fit. (This was also beyond the scope of this project.) A possible component to be added is a transmission line, sometimes used to simulate corrosion products that have filled into the concrete pores. The Nyquist plot can be seen in Figure 57. Also notice the shift in the Rs to the right (higher values) indicating that the Rs now include the resistance of the corrosion products that may have entered the concrete's pore structure. Specimen F20 was terminated 642 days after corrosion initiation.

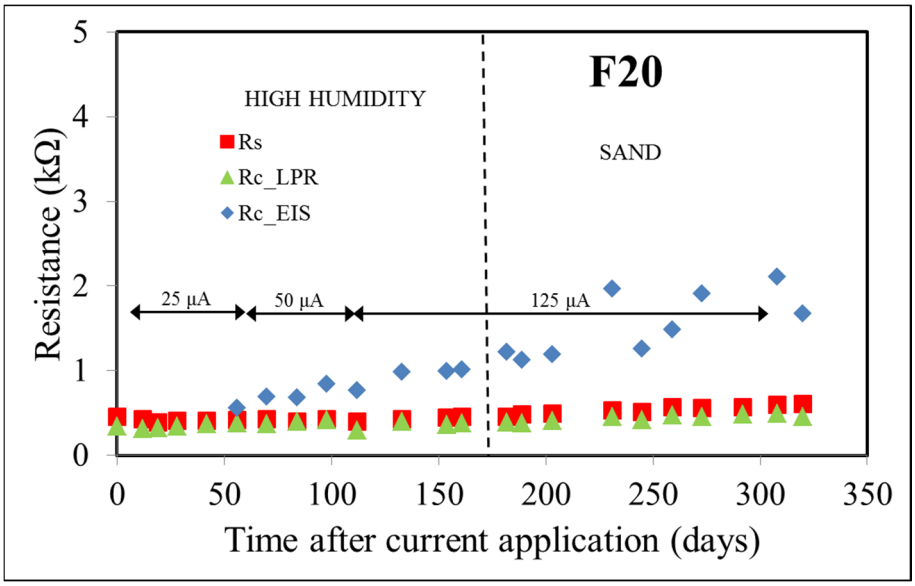

Figure 56 – Plot of Rc_LPR, Rc_EIS, and Rs vs. time for specimen F20.

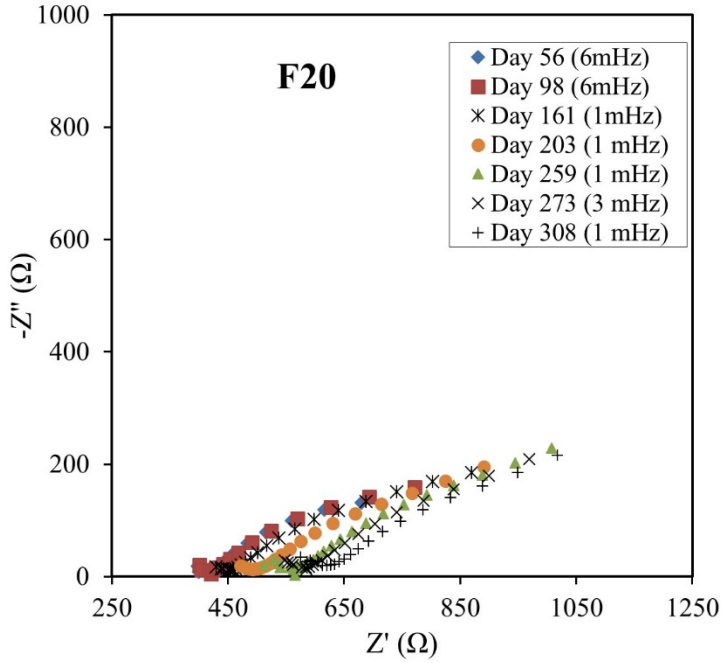

Figure 57 – Nyquist plot of specimen F20.

The Rs, Rc_LPR and Rc_EIS values can be seen in Figure 58 for specimen F23. After being placed in high humidity and polarized but measured while disconnected, the LPR Rc (Rc_LPR) values of specimen F23 initially decreased from 2.38 kΩ to 2.05 kΩ after 112 days before increasing the current to 50 µA. Initially, the Rs values measured 3.13 kΩ and decreased to 2.05 kΩ after 112 days with an applied current of 25 µA. After 56 days, the frequency range for the EIS test ranged from 300 Hz - 0.01 Hz. The CPE model did not provide a good fit for the impedance data past day 161 of current application. The Nyquist plot shown in Figure 59 shows that the impedance measured does not appear to be a depressed semi-circle. After 112 days, the current was increased to 50 µA. The Rc_EIS values were greater than 4 kΩ, especially after the current was increased to 50 µA. Surprisingly, the Rc_LPR values increased from 2.05 kΩ to 3.19 kΩ after 245 days of current application, then decreased to 2.22 kΩ before being terminated. The Rs values increased significantly on days 203, 273, and 308 after the current was increased to 50 µA from 2.05 kΩ to more than 5 kΩ before being terminated. The increase in Rc_LPR and Rs values after the current was increased to 50 µA indicate that the corrosion products might have penetrated the pore structure adding an additional resistance. It is possible that as the current was increased to 50 µA, a small actively corroding area became saturated with current and then displaced the extra applied current to the larger non-corroding area, thus causing part of those areas to activate. This can be verified by the corrosion potentials that were measured being ~-200 mVsce and the autopsy in the forensic analysis chapter. The specimen was terminated 544 days after corrosion initiation.

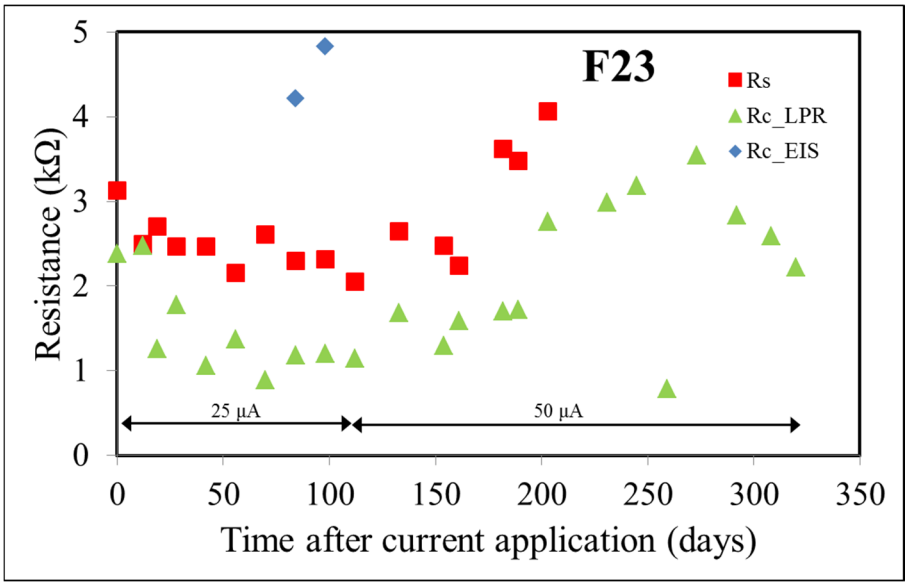

Figure 58 – Plot of Rc_LPR, Rc_EIS, and Rs vs. time for specimen F23.

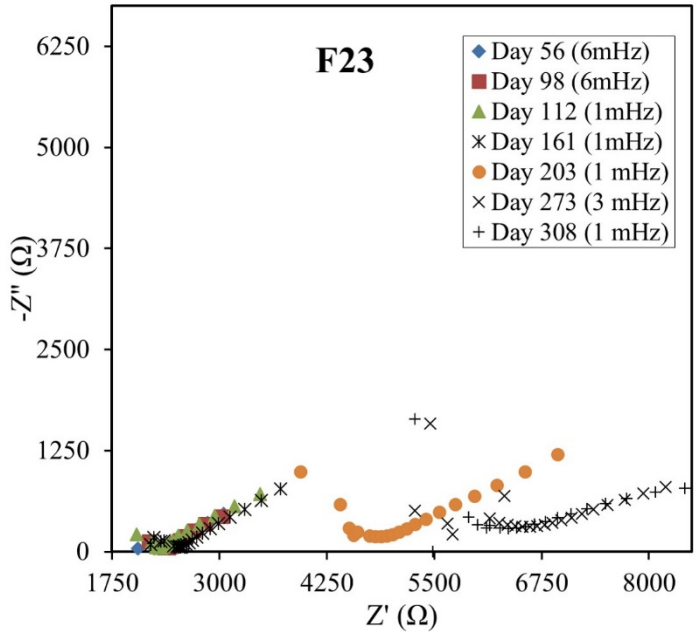

Figure 59 – Nyquist plot of specimen F23.

The Rs, Rc_LPR and Rc_EIS values can be seen in Figure 60 for specimen C4. After being placed in high humidity and polarized, but measured while disconnected, the LPR Rc (Rc_LPR) values of specimen C4 initially were ~1.80 kΩ and decreased to 0.48 kΩ after 56 days of 25 µA current application. Initially, the Rs was 2.70 kΩ and decreased to 0.75 kΩ before increasing the current. After 56 days of current application, the current was increased to 50 µA. The Rc_LPR values remained constant during this time between 0.48 kΩ and 0.42 kΩ. The Rs values also remained constant between 0.76 kΩ to 0.72 kΩ. After 56 days of current application, the frequency measured for the EIS test ranged from 300 Hz - 0.01 Hz. A simple CPE model did not provide a good fit for the impedance data. The Nyquist plot shown in Figure 61 shows a high

frequency tail (left side of data) that made it difficult to accurately fit. The Rc_EIS values initially were as high as 4.9 kΩ and significantly decreased to ~1.80 kΩ before increasing the current to 125 µA. After 112 days of current application, the current was increased to 125 µA. The Rc_LPR and Rs values remained constant for the next ~40 days before covering the specimen with saturated sand. The Rc_LPR values ranged from 0.45 kΩ to 0.39 kΩ. The impedance data fit to a CPE model slightly better when the current was increased to 125 µA, but still did not completely represent a CPE situation. The values decreased from ~1.50 kΩ to ~1.20 kΩ over the ~40 days span. After 165 days of current application, the specimen was covered with saturated sand and repolarized to 125 µA. The Rc_LPR and Rs values initially remained constant around ~0.32 kΩ and ~0.66 kΩ and then linearly increased to final values of 0.91 kΩ for the Rc_LPR and 1.33 kΩ for the Rs, before being terminated 655 days after corrosion initiation. The Rc_EIS values were not valid. As you can see in Figure 61, there existed a high frequency tail that made it difficult to model to a CPE. The Rc_LPR, Rc_EIS, and Rs values were all larger for C4 compared to the type F specimens except for specimen F23.

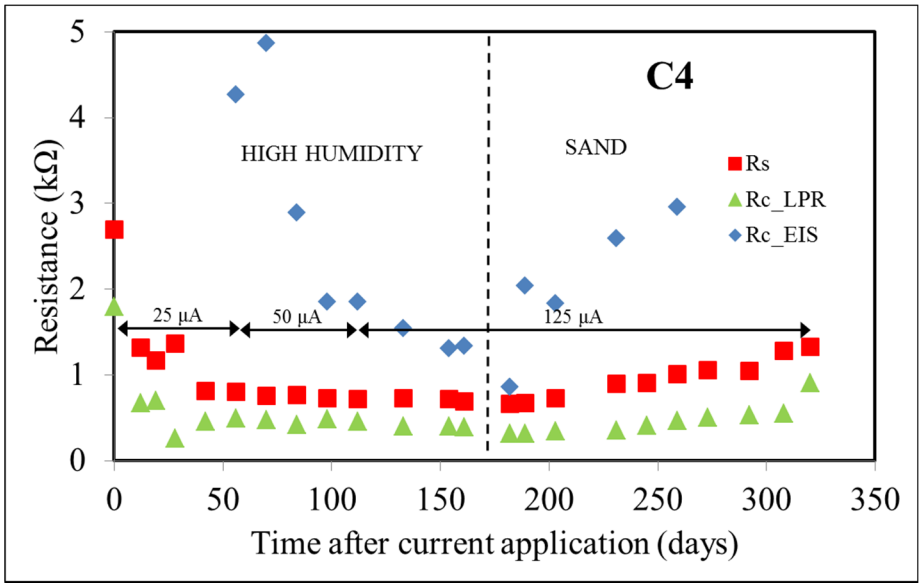

Figure 60 – Plot of Rc_LPR, Rc_EIS, and Rs vs. time for specimen C4.

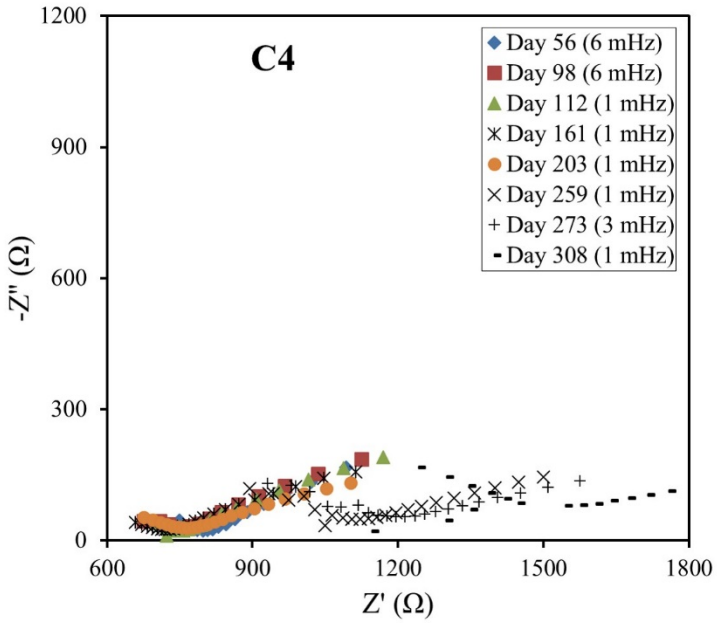

Figure 61 – Nyquist plot for specimen C4.

The Rs, Rc_LPR and Rc_EIS values can be seen in Figure 62 and the Nyquist plot in Figure 63 for specimen C6. After being placed in high humidity and polarized, but measured while disconnected, the LPR Rc (Rc_LPR) values of specimen C6 decreased from 1.50 kΩ to 0.50 kΩ after 56 days of applying a 25 µA current. The Rs values initially measured 4.54 kΩ, then significantly reduced to 1.43 kΩ after 56 days of applying a 25 µA current. After 56 days, the current was increased to 50 µA. The Rc_LPR values remained almost constant around 0.48 kΩ and reduced to 0.45 kΩ before increasing the current to 125 µA. The Rs values remained almost constant around 1.43 kΩ after 14 days of applying a 50 µA current and then recovered to 1.60 kΩ before increasing the current to 125 µA. After the current was increased to 50 µA, the frequency for the EIS test ranged from 300 Hz - 0.01 Hz. Similar to specimen C4, the Rc values obtained from impedance (Rc_EIS) after the current was increased to 50 µA did not provide a good fit to a simple EC with a CPE model. The Rc_EIS values for a CPE model initially measured 16.85 kΩ, decreasing to 3.07 kΩ before increasing the current. After 112 days of current application, the current was increased to 125 µA. The Rc_LPR values increased steadily from 0.45 kΩ to 1.10 kΩ before terminating the specimen. Similarly, the Rs values increased from 1.60 kΩ to 1.97 kΩ before terminating the specimen. Again the impedance data did not provide a good fit to a CPE model to acquire a Rc_EIS value. The Rc_EIS values for a CPE model decreased from 3.07 kΩ to 0.77 kΩ before being terminated. Similar to all of the type F specimens, the Rs values tended to increase as the current increased, but with a greater magnitude. The Rc_LPR values were larger than the type F specimens except for specimen F23. The specimen was terminated 510 days after corrosion initiation.

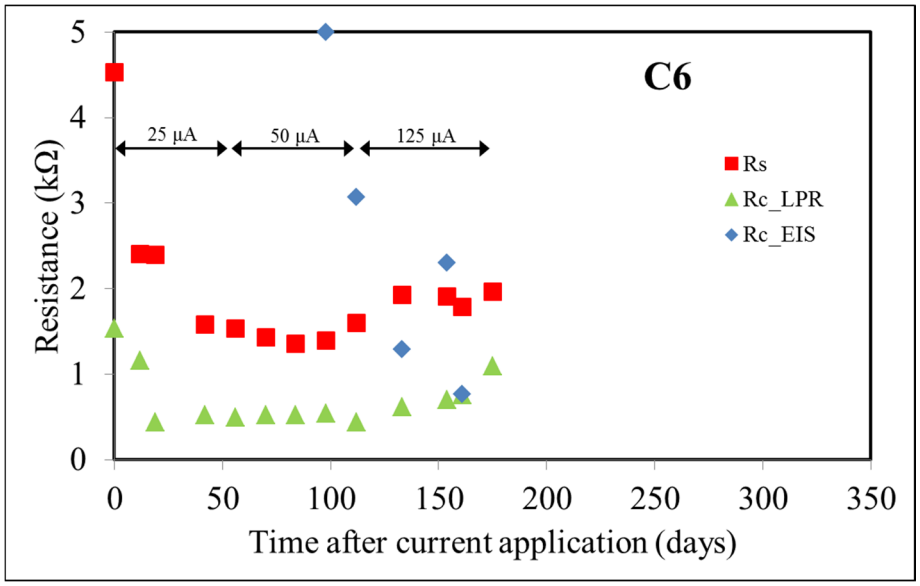

Figure 62 – Plot of Rc_LPR, Rc_EIS, and Rs vs. time for specimen C6.

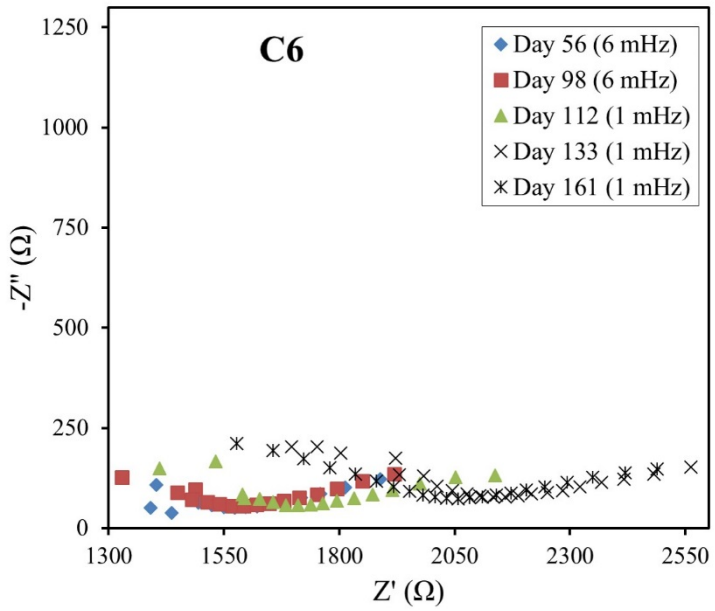

Figure 63 – Nyquist plot of specimen C6.

One specimen remained for this group of samples (C10), and specimens F16, F17 (July 2016), and F18 (summer 2015) were forensically analyzed recently. Updated plots for C10, F16, F17 and F18 specimens are shown below. On these plots only the off-potential is shown, and no color to the right of the shaded areas indicates that current was no longer applied. Figure 64 shows the potential, Rc (from LPR tests Rp_app minus Rs), and Rs evolution corresponding to specimen C10. The moisture content was not maintained as high past day 900; the potential and Rc values were affected by this moisture change. Figure 65 shows the potential, Rc, and Rs evolution measured on specimen F16. Specimen F16 was place in the same container as specimen C10, and was also affected by the lower moisture past day 900, but to a lesser

degree. Figure 66 and Figure 67 show similar plots for specimen F17 and specimen F18, respectively. The potential values in Figures 64, 65, 66 and 67 are given in mV. The color-shaded areas indicate the amount and duration of current applied on the potential plots shown on the left (potential vs. time). The Rc and Rs vs. time plots shown here start when the specimens were transferred to a high humidity environment for current application. The potential values measured on specimen F17 were somewhat more negative than those recorded for specimen F18. The steel potential on specimen F16 increased to values as positive as -200 mVsce past day 950, and the Rs increased from one kΩ to four kΩ. However, upon increasing the moisture content, the steel potential on F16 shifted to -500 mVsce, and the Rs and Rc shifter to values smaller than one kΩ and two kΩ, respectively.

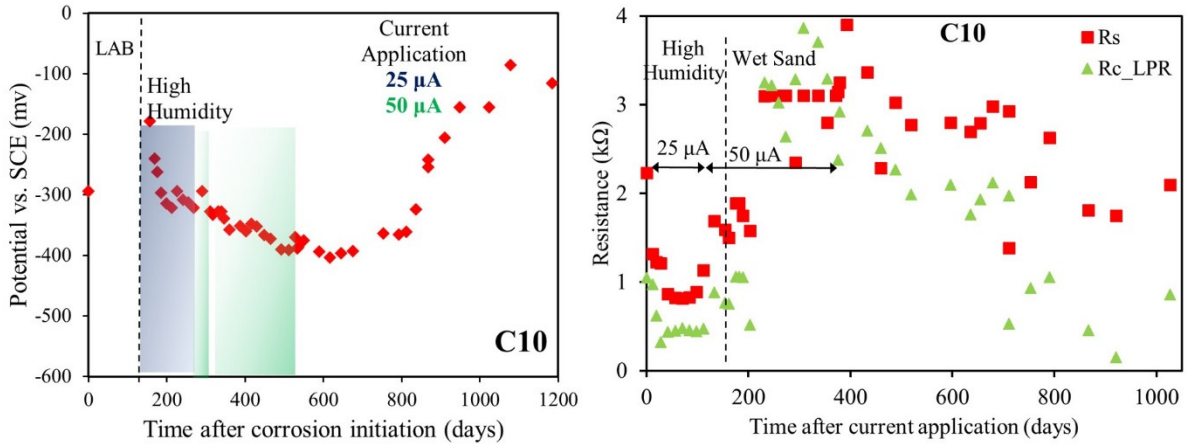

Figure 64 – Potential, Rs, and Rc values measured on specimen C10.

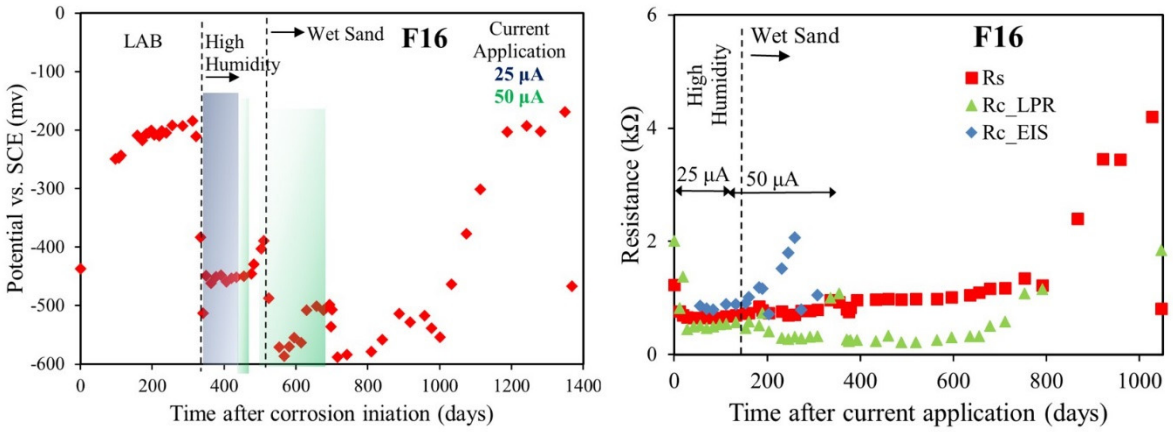

Figure 65 – Potential, Rs, and Rc values measured on specimen F16.

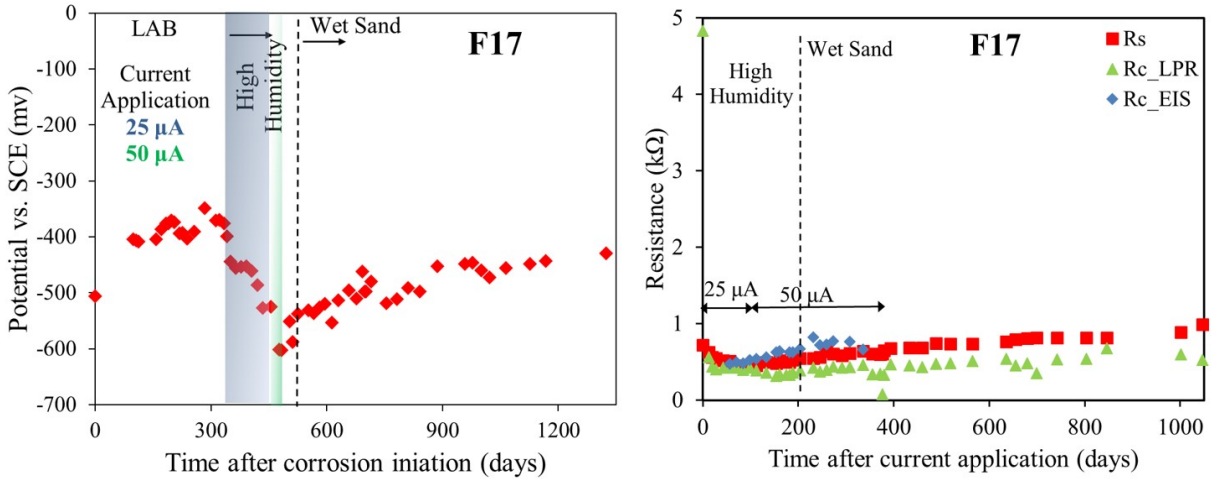

Figure 66 – Potential, Rs, and Rc values measured on specimen F17.

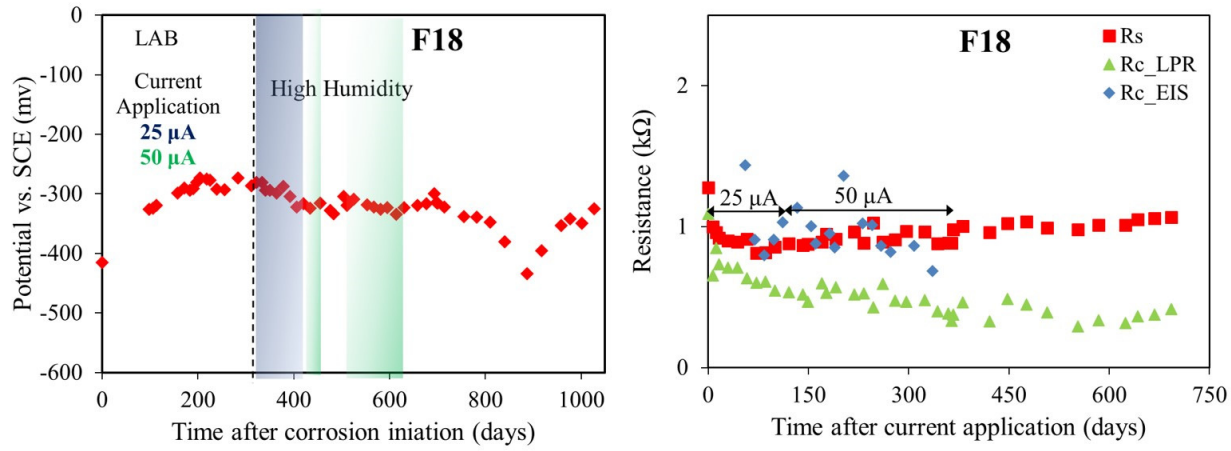

Figure 67 – Potential, Rs, and Rc values measured on specimen F18.

3.5.3 Corrosion Propagation on Ring Specimens

A recent thesis describes the potential evolution and Rc evolution of the ring samples that were terminated around 400 days' exposure in high moisture conditions. (B. Seo[39] M.S. thesis describes the results for these specimens). The following sections describe the potential evolution and Rc evolution for the 6-ring specimens that were recently 3EB tested.

3.5.3.1 Covered with Sand

Figure 68 shows two plots: on the left, the corrosion potential, and on the right, the measured Rc values on specimen CS2. Similarly, Figure 69 and Figure 70 show potential and Rc values measured on Specimen FS2 and Specimen FS3, respectively. These three specimens have been covered with wet sand for the duration of the high moisture exposure. The potential evolution on both follow a similar trend. The most recent potential values measured on Specimen CS2 were approx. -0.38 V. From day 200 to about day 700, the average potential value ranged between -0.38 and -0.42 V on both FS2 and FS3 specimens. Then, these two specimens were

brought to the lab and subjected to an accelerated chloride transport, followed by a modest galvanostatic pulse so as to accelerate the corrosion of the steel wire mesh. The last set of potential values ranged between -0.65 and -0.7 V. The Rc values ranged between 0.4 and 0.1 kΩ on specimen CS2. The Rc values measured on specimens FS2 and FS3 (prior to additional chloride transport) ranged between 0.8 to 0.2 kΩ (the latter) and 0.2 and 0.05 kΩ (the former). After the additional chloride transport and two weeks of applied current the Rc shifted to ~0.01 kΩ.

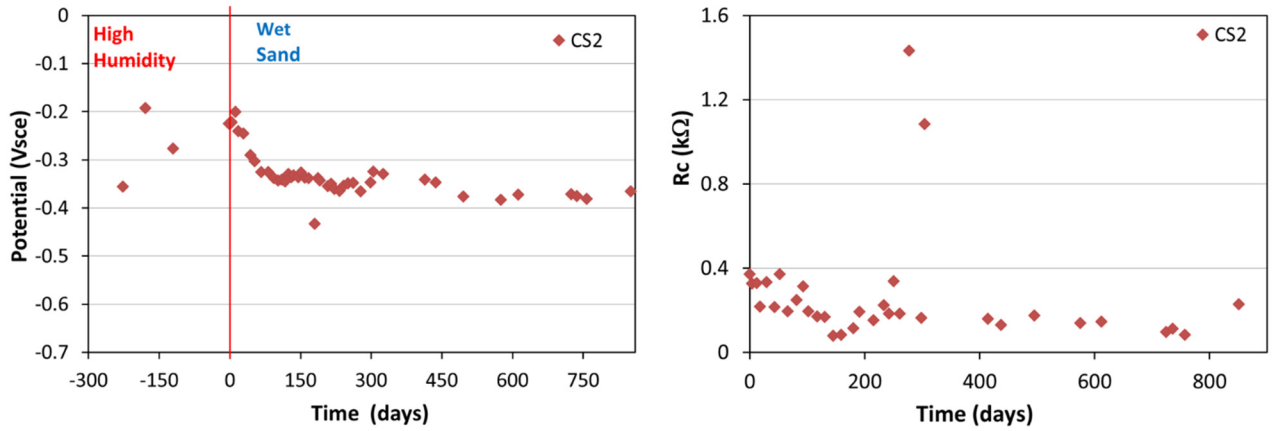

Figure 68 – Potential and Rc values for specimen CS2.

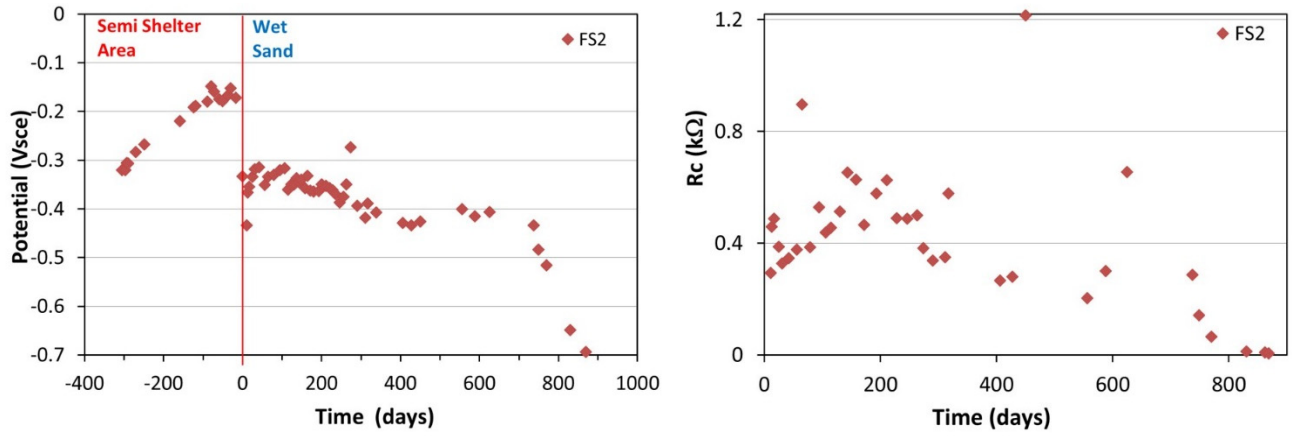

Figure 69 – Potential and Rc values vs. time for specimen FS2.

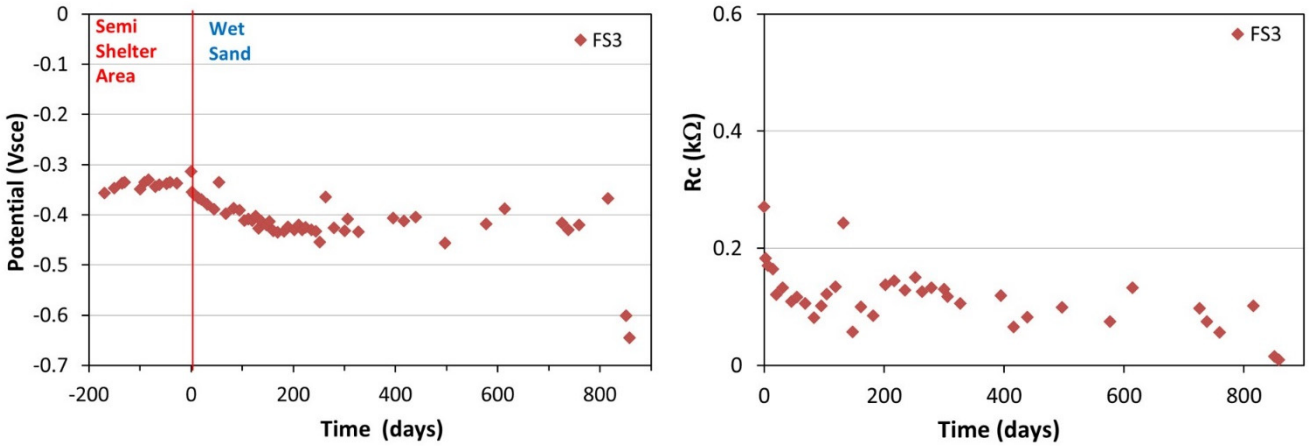

Figure 70 – Potential and Rc values for specimen FS3.

3.5.3.2 Immersed in Water and Later Covered with Sand

The Potential and Rc vs. time for specimens FI1 and CI2 are shown in Figure 71 and Figure 72, respectively. These specimens were immersed in water for approximately 400 days, removed from the water for about a week, and then moved to the exposure covered with saturated sand for close to 500 days. The reinforcement potential while the specimens were fully immersed was as negative as -0.6 V on specimen FI1 and -0.5 V on specimen CI2. While covered with wet sand, the potential drifted toward more positive values, with the shift being more pronounced on specimens CI2. The Rc values measured on both specimens were less than 0.2 kΩ while immersed in water. The Rc measured on FI1 remained the same over the next 300 days while covered with wet sand, and just recently increased, and with the last reading, approached 2 kΩ with a corresponding potential of -0.7 V (moisture was not kept as high for day 800 to day 950). Upon increasing the moisture content, the Rc shifted back to -0.6 kΩ, whereas for specimen CI2, the Rc increased when moved to the exposure covered with wet sand to values as large as 1 kΩ (day 700); however, the last two measurements were 0.5 kΩ.

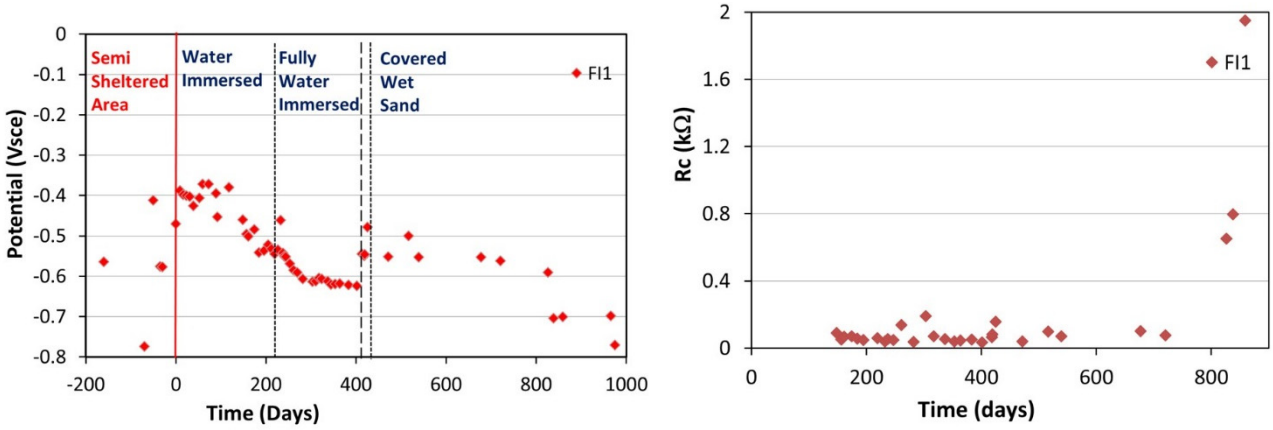

Figure 71 – Potential and Rc values for specimen FI1.

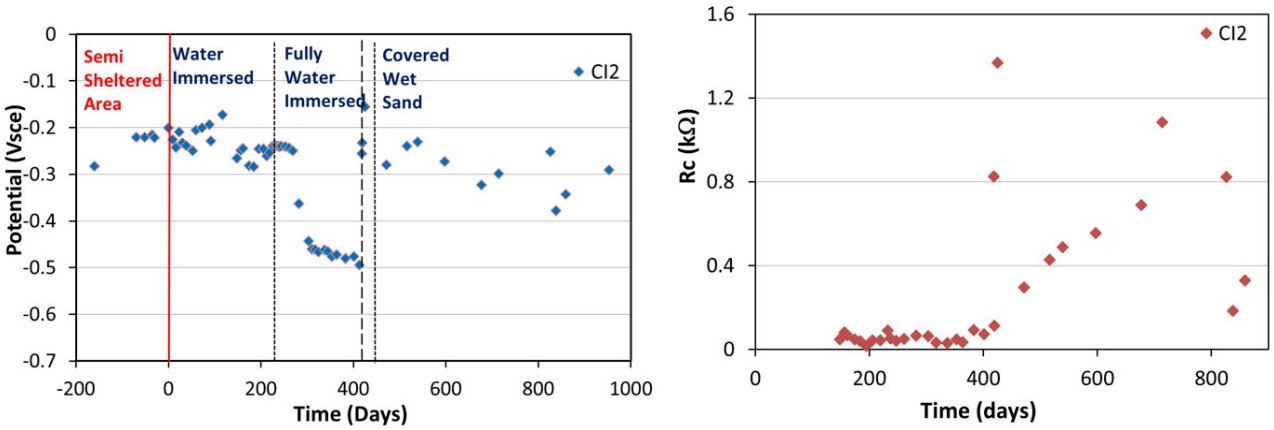

Figure 72 – Potential and Rc values for specimen CI2.

3.5.3.3 High Humidity

Figure 73 shows the potential evolution for the ring specimen that is being exposed indoors inside a high humidity chamber. The reinforcement potential has been around -0.3 Vsce since corrosion initiated (with a drift to more positive values for a short period of time). The Rc values ranged between 1.8 and 0.3 kΩ, with most values being less than 0.8 kΩ.

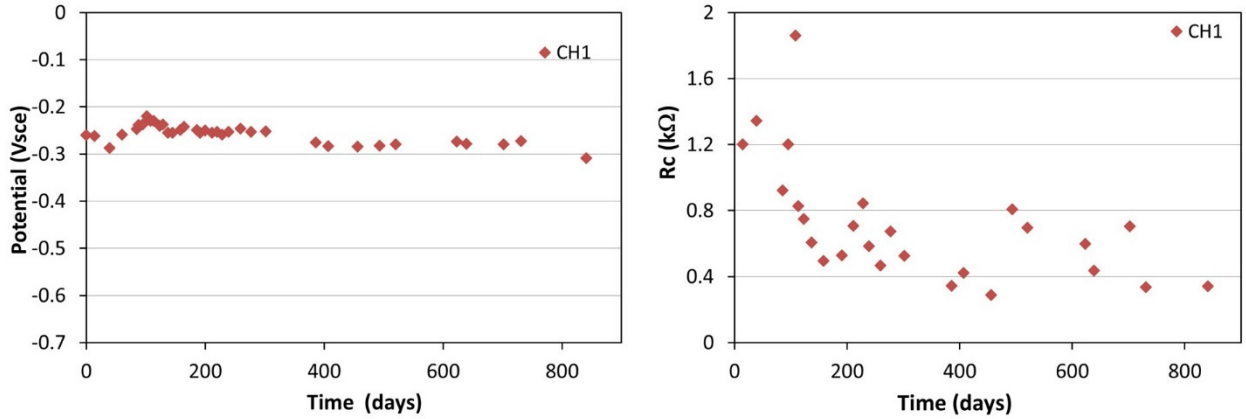

Figure 73 – Potential and Rc values for specimen CH1.

3.5.4 Potential, Rc, and Rs on Segmented Specimens Obtained from Terminated Ring Specimens

This section describes the electrochemical monitoring for the six C specimens named C40 to C45, and six F specimens named F40 to F45, that were obtained from ring specimens forensically analyzed after 400 days in high moisture. Specimens F40, F42, F43, C40, C41, C42 and C45 were subjected to galvanostatic pulse (500 μA) for about 100 days during the fall of 2014. The other specimens were not. Then, all of these specimens continued to be monitored while exposed in high moisture environment. The specimens were subjected to high moisture exposure and the solution reservoir was filled with 10,000 pmm of Cl^- ions.

Figure 74 shows steel potential, Rs and Rc vs. time for specimens of type C that were obtained from terminated ring samples. For example, the reinforcement potential for specimen C42 was significantly more positive (approx. -0.13 V) than that observed on specimen C44 (approx. -0.32 V). The steel potential value measured on specimen C44 suggests that the reinforcement might be corroding. The Rc values measured on specimen C44 tend to confirm this by the smaller Rc values observed for C44 reinforcement as compared to those measured on specimen C42. The Rc value is about 5 times larger on specimen C42 (2 kΩ) than on specimen C44 (0.4 kΩ). Specimen C43 was selected for forensic examination.

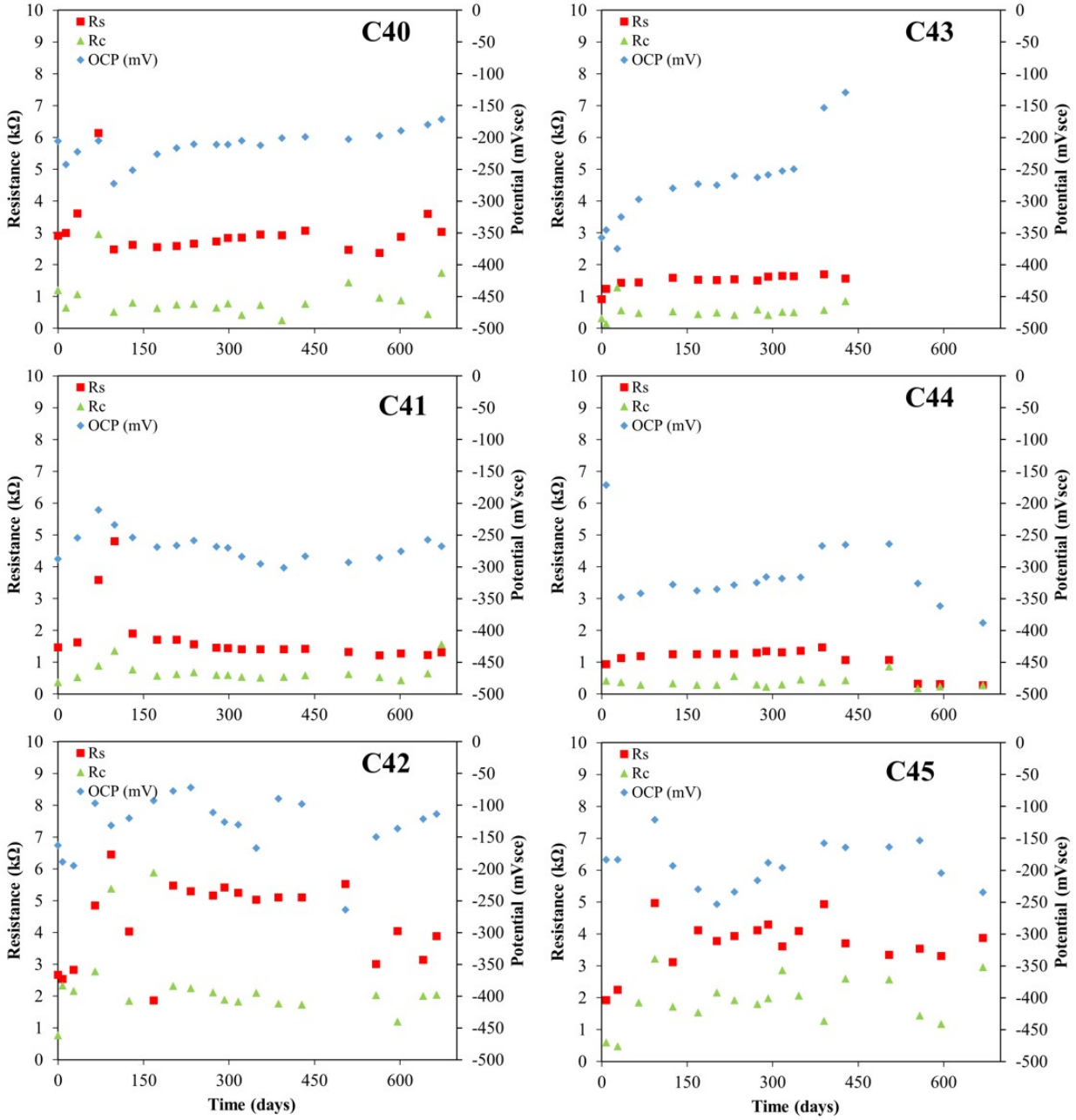

Figure 74 – Potential, Rs, and Rc values for specimens C40 and C45.

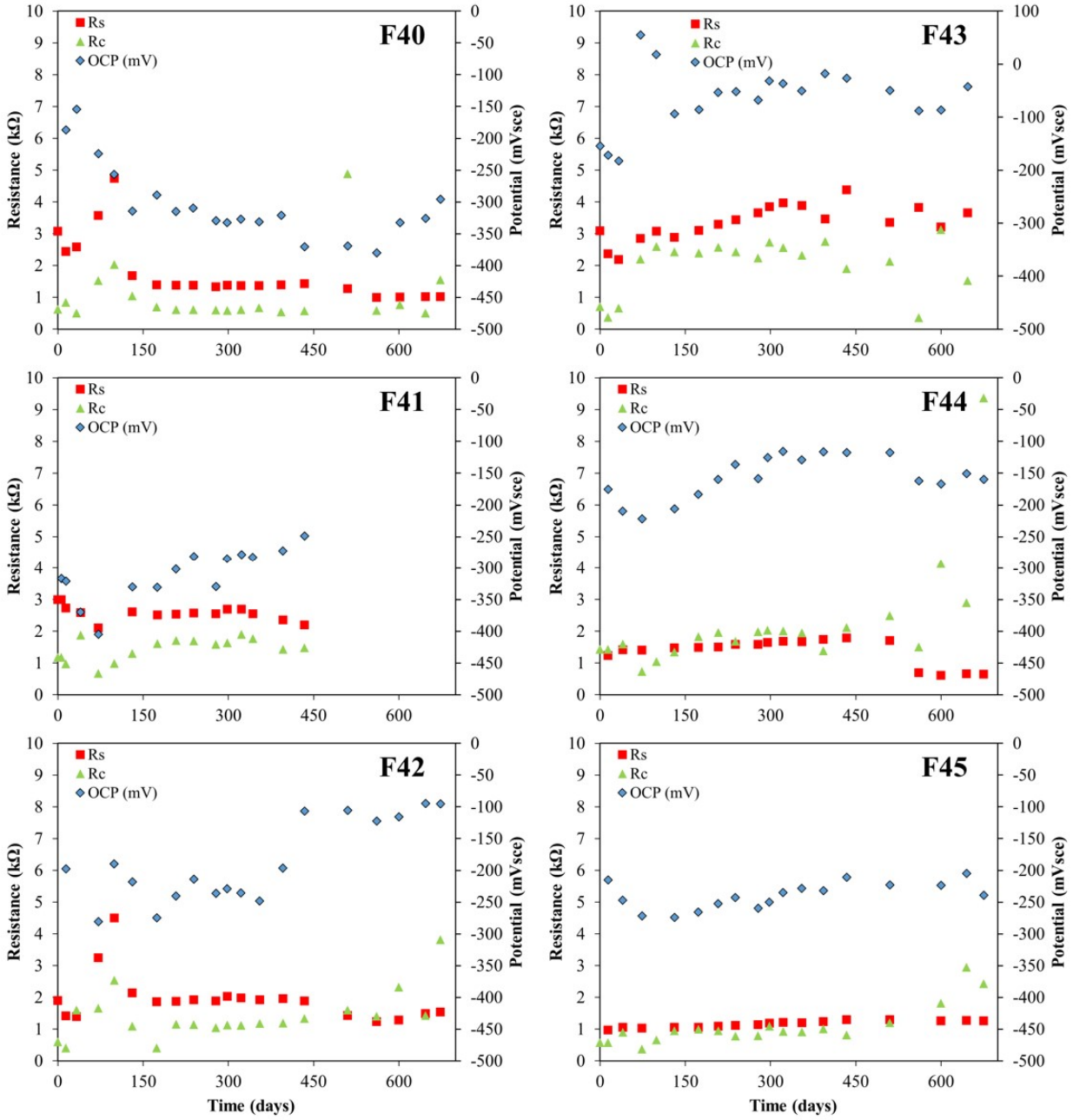

Figure 75 – Potential, Rs, and Rc values for specimens F40 and F45.

Figure 75 shows steel potential, Rs and Rc vs. time for specimens of type F. The reinforcement potential values for specimen F45 was somewhat more positive (currently -0.235 V) than that observed on specimen F40 (currently approx. -0.32 V). These potential values suggest that the reinforcement of both specimens might be corroding. The Rc values measured on specimen F45 and F40 are comparable currently: Rc is 0.8 and 0.6 kΩ, respectively. Specimen F41 was selected for forensic examination. The steel potential of specimen F43 (between 0 and -100 mVsce) was the most positive of the F type specimens and also showed the largest Rc values.

3.6 Calculated Mass Loss

Tables 13 and 14 show the calculated mass loss (using Rc values) for specimens exposed in the lab to the various high moisture environments. Table 13 contains the calculated masses for those specimens exposed in the vertical orientation and Table 14 shows the calculated masses for those specimens oriented horizontally. Specimens C21 and C24 (vertical covered with wet sand) had the largest calculated mass loss (11.24 g and 10.5 g, respectively) from those exposed vertically, whereas, specimens F2 and F1 had the largest calculated mass loss (14.5 g and 11.3 g, respectively) from those exposed horizontally. Specimens with a T next to the name indicate that the specimen was terminated. Table 15 contains the calculated mass loss on specimens for which corrosion of the steel was moderately accelerated for approximately 400 days; the values shown here were obtained using Rc after having the specimens disconnected. The largest calculated mass loss corresponded to specimen F7 (2.5 g), which has been forensically analyzed. Table 16 shows the calculated mass loss for the ring specimens. All ring specimens were forensically analyzed. Finally, Table 17 contains the mass loss calculated on lab specimens prepared after selected ring specimens were terminated during the summer of 2014. Specimens C43 and F41 were forensically analyzed. The largest masses calculated were 0.57 g and 1.34 g on specimens F40 and C44, respectively.

Table 13 – Calculated mass loss of exposed specimens on the vertical direction.

Specimen	Calculated Mass Loss (g)
Immersed in Water	
F10_T	5.94
F15_T	2.03
C18_T	7.53
C15_T	3.51
Covered Wet Sand	
F8_T	2.35
F9_T	2.55
F11_T	1.83
F13_T	2.51
C13_T	5.9
C16_T	3.12
C21_T	11.24
C24_T	10.5
C25	9.1
Partially Covered Wet Sand	
C12_T	1.43
C22_T	4.24
C23_T	6.75
High Humidity	
C17_T	2.76
C26_T	3.89

Table 14 – Calculated mass of exposed specimens in the horizontal orientation.

Specimen	Calculated Mass Loss (g)
Covered Wet Sand	
F1_T	11.33
F4_T	3.25
F5_T	1.11
C1_T	2.39
C2_T	3.94
C3_T	0.98
C11_T	0.7
Immersed in Water	
F12_T	1.85
F21_T	2.01
F22_T	1.87
C0_T	5.74
C5_T	0.97
C8_T	0.65
High Humidity	
F2_T	14.54
F6_T	2.92
C9_T	0.6
F3_T	1.52
C7_T	1.17
F0_T	1.99

Table 15 – Calculated mass of specimens subjected to accelerated corrosion.

ID	mass (g)	ID	mass (g)
F7_T	2.51	C4_T	0.69
F_17_T	1.75	C6_T	0.27
F19_T	0.90	C10	1.02
F23_T	0.18		
F20_T	1.10		
F18_T	1.25		
F16_T	1.55		

Table 16 – Calculated mass of ring specimens.

Sand	Calculated Mass Loss (grams)	Calculated Mass Loss (grams)	
CS1	**1.75**		Terminated Summer/14
CS2	**1.35**		
FS1	**0.87**		Terminated Summer/14
FS2	**3.40**	**6.00**	L Before and R After corr acc
FS3	**5.70**	**6.90**	L Before and R After corr acc
Immersed in Water			
CI1	**7.16**		Terminated Summer/14
CI2	**6.29**		Covered with sand 1 1/2 year
FI1	**8.02**		Covered with sand 1 1/2 year
FI2	**4.77**		Terminated Summer/14
High Humidity			
CH1	**1.45**		

Table 17 – Calculated mass of specimens 40s group

ID	Mass (g)	ID	Mass (g)
F40	0.57	C40	0.63
F41_T	0.20	C41	0.71
F42	0.37	C42	0.17
F43	0.31	C43_T	0.55
F44	0.25	C44	1.34
F45	0.43	C45	0.26

3.7 Discussion

The potential and apparent corrosion evolution results, observed during the propagation stage were influenced by a combination of changing reaction kinetics as the corrosion of the reinforcing steel progressed and also influenced by the different propagation environments (i.e., high humidity, covered with saturated sand, and immersed in water). The cathodic and anodic kinetics as well as the area in which these take place influence the rates of ongoing corrosion; hence, it could be that one or a combination of the following scenarios might have occurred over time.

3.7.1 Change in Chloride Concentration

Let's consider a case in which the cathode and anode areas are the same and that there was no change in the sizes of the anode area or the cathode area. Figure 76a shows an Evans[40] diagram with two anodic polarization curves that represent two different chloride concentrations at the anode for two different specimens[41]. Let us consider that the cathodic polarization curve farther to the right represents a situation with mix-control, but with higher O_2 concentration (e.g., lab humidity). The specimen with the lower chloride concentration at the anode would have the more positive mix potential and somewhat lower corrosion current density than another specimen with the higher chloride concentration at the steel surface. When the specimens are transferred to a high moisture environment (e.g., covered with wet sand or very high humidity), then the cathodic polarization curve in the middle might better represent the cathodic reaction. For both specimens, the new steel mix potential would be more negative, and the corrosion current density would be somewhat smaller.

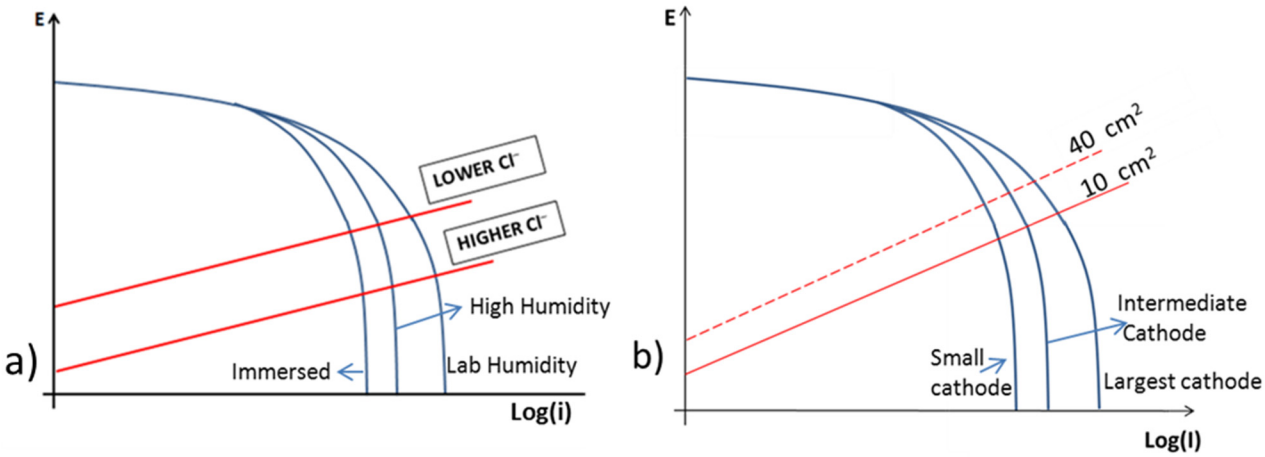

Figure 76 – Evans diagram: (a) change in Cl^- concentration and/or O_2, (b) change in areas.

Upon further O_2 reduction, the cathodic polarization curve on the left would represent full concrete saturation (e.g., covered with saturated sand) or immersed in water exposure. The mix potential would decrease to even more negative values, and the corrosion current density would be even smaller. The reduction in potential was observed in many cases upon exposure to high humidity or covered in saturated sand and even more negative potential values were observed when the specimen was immersed in water. However, the corrosion current density decay was not observed as per the Rc measured values. It is possible that because of the similarity in Rs and Rc magnitudes, there is some error in the calculated value; still, the activity appears to proceed at the same rate. The anode-to-cathode area ratios on most specimens tested are likely not the same (or don't remain the same with time) as it was assumed above. Moreover, on a given specimen, if the chloride concentration at the steel surface increases, then the polarization curve would shift from the low chloride anodic curve to the high chloride anodic curve, and the potential would shift toward more negative potential values. When this occurs, there is little or no change in the corrosion current density. Hussain[6] experiment used reinforcement segments embedded in high chloride concentration and when immersed in

water he observed a gradual potential increase, the values observed ranged from -.62 Vsce to -.4 up to a year. The observed range of potential values reported in here agrees with Hussain's even if the cathode to anode areas are different. The potential shift was even larger on some cases e.g., C8 (See Figure 46).

3.7.2 Change in Anode Area

Since the specimens during the propagation stage were exposed to high moisture conditions, the specimens are expected to eventually reach full saturation condition. This increase in moisture content likely reduce the concrete resistivity and hence allowed for a more favorable macrocell, which eventually might resulted in larger available cathode area which in turn would accelerate the corrosion and potentially increase the anode area. The diagram in Figure 76b shows an Evans diagram with an exaggerated increase in the anode area (not to scale), a four-fold increase in area would shift the anodic polarization curve from the solid red line to the dotted red line. For this scenario, the mix potential value would shift to a more positive potential value; provided that cathode area remains the same. This type of potential trend was reported by Hussain et al.[6], but not attributed to this explanation. Note that in this diagram (Figure 76b) the x-axis indicate current (not current density).

3.7.3 Change in Cathode Area

Assuming there is no change in anode area (Figure 76b). Due to the increase in moisture content in the specimens, the resistivity of the concrete would be lower and the anode would be able to interrogate a larger remote cathode. As indicated above the moisture content increase likely shifts the cathodic polarization curve to the left. However, better connectivity allows for a larger cathode which might compensate and still provide/match the required anodic current, resulting in very little change on the mix potential and measured corrosion current. Based on the experimental observations it is likely that this macro cell situation is taking place. Hence, the corrosion rates that are being observed. It is possible that upon additional exposure time the oxygen at the cathode might be consumed and not readily replenished, which would reduce the cathodic capacity (i.e., intermediate or smallest cathode shown in Figure 12b) and hence lower the corrosion rate. The high porosity of the concrete might explain why it is taking longer to reach this state compared to what others have found[7,10,11].

The specimens will continue to be monitored for some additional time. Cathodic polarization will be performed on selected specimens. Additionally, selected specimens will be terminated for forensic analysis to assess the anode area (corroding steel) as well as how much section has been lost, and how localized or uniform the corrosion is. If possible the concrete surrounding the reinforcement will be sectioned and observed in a stereo microscope to determine if the corrosion products are filling the pore structure.

Chapter 4 – Forensic Examinations: Lab Specimens

This chapter describes the forensic analysis performed on lab test specimens after corrosion propagation had taken place by the periods of time indicated in Table 3 and Table 4. The selected specimens were terminated at different times (From Spring 2014 to Summer 2016). The forensic examination documents the corrosion extent on the steel wire mesh. In the next section, the figures present pictures of the steel wire with some of the concrete removed, corrosion products penetration into the concrete and steel wire surface condition after concrete was removed.

Results revealed that on some specimens corrosion not only occurred on the top of the reinforcement, but on the sides and on the bottom too, but not uniformly (i.e., it was localized but spread). In some cases; corrosion took place not only on the steel wire under the reservoir, but also at locations several cm outside the solution reservoir. Forensically analyzed samples include most of the samples subjected to natural corrosion propagation under various high moisture environments, with several specimens analyzed during July 2016. Nine of the ten samples subjected to accelerated corrosion method. Specimens F7, F16, F17, F18, F19, F20, F23, C4 and C6 were selected for autopsy to visually inspect the condition of the steel reinforcement. The forensic analysis on specimens F16 and F17 was recently performed (July 2016).

Most of the steel wire meshes were then chemically clean as per ASTM G-01. The pictures after cleaning the reinforcement display the location and degree of corrosion of the steel reinforcement for selected terminated specimens. In most cases, the photos are of the steel surface directly below the solution reservoir instrumented unless otherwise stated.

4.1 Concrete Removal

Recall that on some specimens (F0, F1, F2, F3, C0, C1, C2 and C3) the solution was 15% NaCl while the accelerated chloride transport took place. This high chloride concentration in the solution likely translates on a higher chloride concentration at the steel surface when compared to the other specimens. During the corrosion propagation the solution was 10,000 ppm of chloride ions in the solution for all specimens.

4.1.1 Specimen F0

Figure 77 show pictures taken for Specimen F0 before removing the reservoir and for selected locations as the reinforcement was being removed. The pictures in the center show that a thin crack was present (before (top) and after applying a dye-penetrant (bottom picture)). The two pictures on the right show a portion of the reinforcement as the concrete was being removed; the corrosion spots appear to be localized in specimen F0. Figure 78 shows how much the corrosion penetrated into the concrete on specimens F0. The corrosion products penetrated close to 20 mm at various locations as can be observed from the picture. The corrosion sites

were 5 to 10 mm long and there were several of these spots (see picture shown below after cleaning).

Figure 77 – Forensic examination of specimen F0.

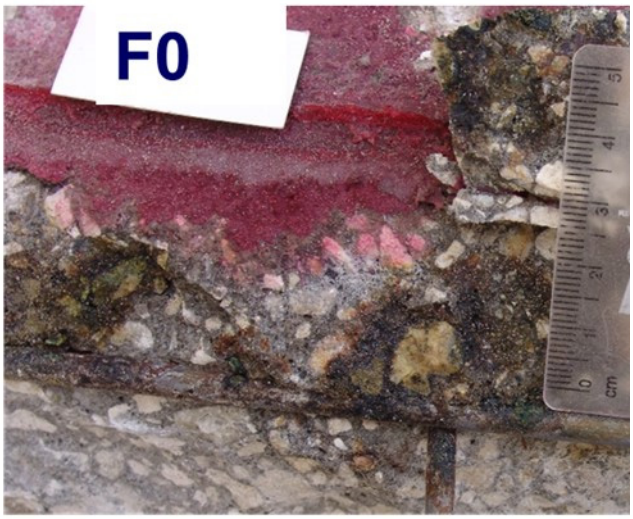

Figure 78 – Corrosion penetration into the concrete for specimen F0.

4.1.2 Specimen F1

The initial high chloride concentration in the reservoir during chloride migration might explain the significant extent of corrosion observed on the steel wire mesh exposed from F1 specimen, combined with the exposure history of this specimen (See Table 3). Figure 79 shows picture of the several steps followed to obtain the steel wire mesh. The images with exposed steel show significant amount of corrosion under the solution reservoir. The color of the corrosion products were dark green and penetrated the concrete several mm. Figure 80 was taken a few days later and by then the corrosion products have turned to dark brown rust in some areas.

Figure 79 – Removal of concrete on specimen F1.

Figure 80 – Section of steel wire with greater cross-section loss of specimen F1.

4.1.3 Specimen F2

Specimen F2 was exposed in a high humidity chamber for an extended period of time. Figure 81 shows the corrosion extent that took place at several locations of the steel wire mesh. On this specimen, significant corrosion took place on the steel underneath the solution reservoir. The corrosion products upon removing the concrete were black to dark green. The corrosion products penetrated close to 10 mm at multiple locations.

Figure 81 – Removal of concrete on specimen F2.

4.1.4 Specimen F3

Upon removing some of the concrete on specimen F3, the steel reinforcement's corrosion under the ponding at the reinforcement junction was a mix of red and green/black rust. Corrosion occurred in this region as can be seen in Figure 82. Figure 83 shows black/green rust observed outside of the ponding along of the transverse steel wires. The steel reinforcement of specimen F3 can be seen in Figure 84 displaying the locations where corrosion occurred. As seen in Figure 85, specimen F3 experienced mild corrosion at location 1 under the ponding at the reinforcement junction. Severe cross-section loss can be seen at location 2 along the side of the transverse steel wire (spiral). Corrosion did occur outside the ponding.

Figure 82 – Red and black/green rust observed upon opening specimen F3.

Figure 83 – Black/green rust observed outside the ponding along the transverse reinforcement for specimen F3.

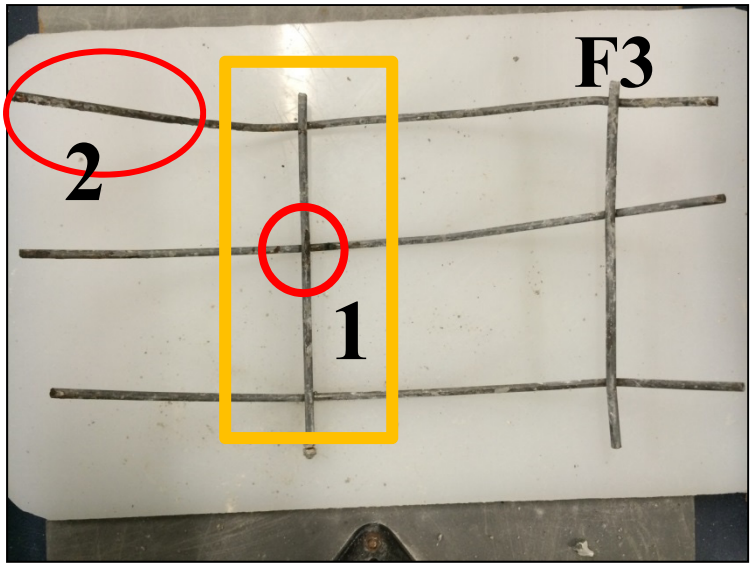

Figure 84 – Autopsy result of specimen F3 – full steel wire mesh.

Figure 85 – Autopsy result of specimen F3. Left: location 1. Right: location 2.

4.1.5 Specimen F11

Specimen F11 was oriented vertically and covered with wet sand. Modest corrosion was observed on the area under the solution reservoir as can be observed on Figure 86.

Figure 86 – Specimen F11 while concrete was being removed.

4.1.6 Specimen F12

Figure 87 shows pictures taken on Specimen F12. The picture on the left shows that there were several red corrosion spots on the concrete surface within the area occupied by the solution reservoir. Upon removing the concrete (see pictures on the right) a modest amount of corrosion was observed. Corrosion took place on the steel wire underneath the reservoir.

Figure 87 – Steel wire removed from specimen F12.

4.1.7 Specimen F21

As the concrete was being removed on specimen F21, it was observed (Figure 88) that corrosion took place both outside (left picture) and under (right picture) the ponded section. Two additional pictures are included in Figure 89 that show the whole steel wire mesh after removing the concrete and the section under the ponding that showed the most corrosion. The corrosion products were dark green and became red rust as time passed.

Figure 88 – Concrete removal on specimen F21.

Figure 89 – Steel wire removed from specimen F21.

4.1.8 Specimen F22

Specimen F22 was exposed horizontally while immersed in water. Figure 90 shows pictures of the steel wire mesh. The picture on the left shows the whole mesh, whereas the picture in the middle shows a close-up of the site with the most corrosion. The steel wire section showing corrosion was below the solution reservoir. On this case, corrosion took place also on the back-side of the steel wire (picture on the right in Figure 90).

Figure 90 – Steel wire removed from specimen F22.

4.1.9 Specimen F41

Specimen F41 was obtained from one of the ring specimens. Modest amount of corrosion was found at various locations outside of the solution reservoir. Figure 91 shows a picture on the left while the concrete was being removed and on the right after removing the concrete. Several of the rust spots were outside of the area below the solution reservoir, as can be observed on the transverse steel wires to the right of the longitudinal on the left.

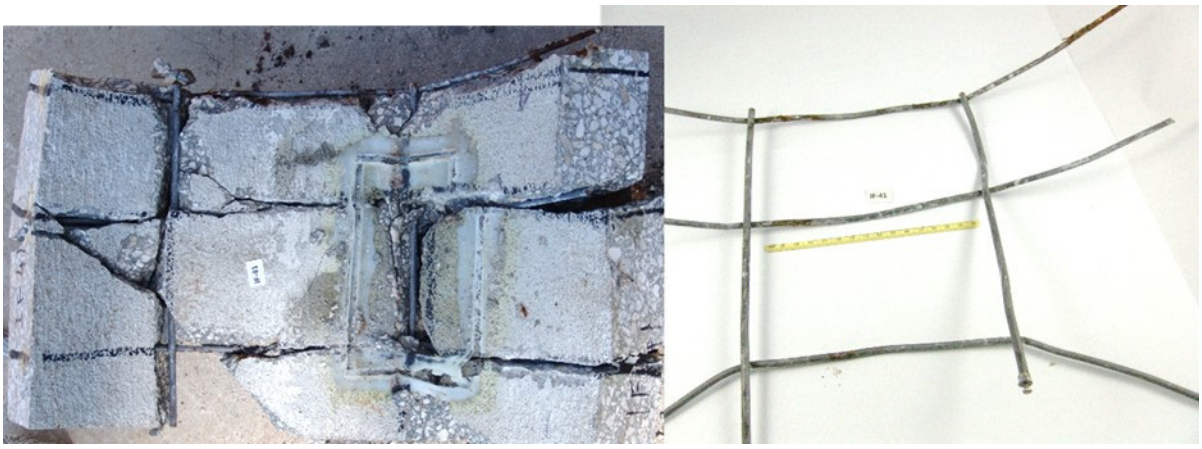

Figure 91 – Specimens F41 prior to and after concrete removal.

4.1.10 Specimen C0

Specimen C0 was exposed horizontally and immersed in water. Figure 92 shows pictures after the concrete had been removed. The picture on the left shows the steel mesh, with rust spot on the center longitudinal (below the reservoir). The pictures on the center and right are close-ups of the section that showed the most corrosion. A white layer (might be calcareous deposits) was found on most of the steel wire surface that was not corroding.

Figure 92 – Steel wire after removing concrete for specimen C0.

4.1.11 Specimen C1

Figures 93 and 94 show the pictures taken for specimen C1. The picture on the top left showed no corrosion spots (Figure 93). The picture on the right (Figure 93) shows that corrosion took place on the exposed steel and that the corrosion products were dark green. The corrosion products penetrated into the concrete between 2 and 3 mm. Figure 94 shows the whole steel

wire obtained after removing the concrete on specimen C1. It is evident that significant corrosion took place at two of the transverse (circumferential) steel wires.

Figure 93 – Specimen C1 while removing concrete.

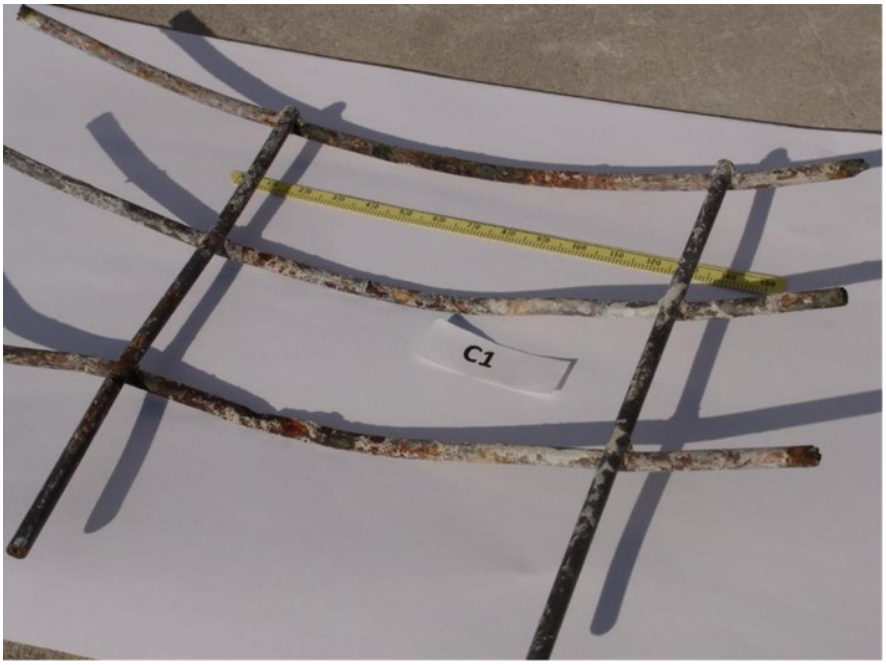

Figure 94 – Steel wire mesh removed from specimen C1.

4.1.12 Specimen C5

The corrosion extent observed at selected locations of the steel wire embedded on specimen C5 is shown in Figure 95. The center top picture shows corrosion products on the exposed steel and the concrete, a deep dark green (almost black) spot was found for this specimen. This specimen was exposed immersed in water. Figure 96 shows the surface condition upon removing all concrete, a spot with significant corrosion was outside the solution reservoir. Under the solution reservoir, the steel showed some red rust spots and appear to be superficial corrosion. The white products were more dispersed on this reinforcement.

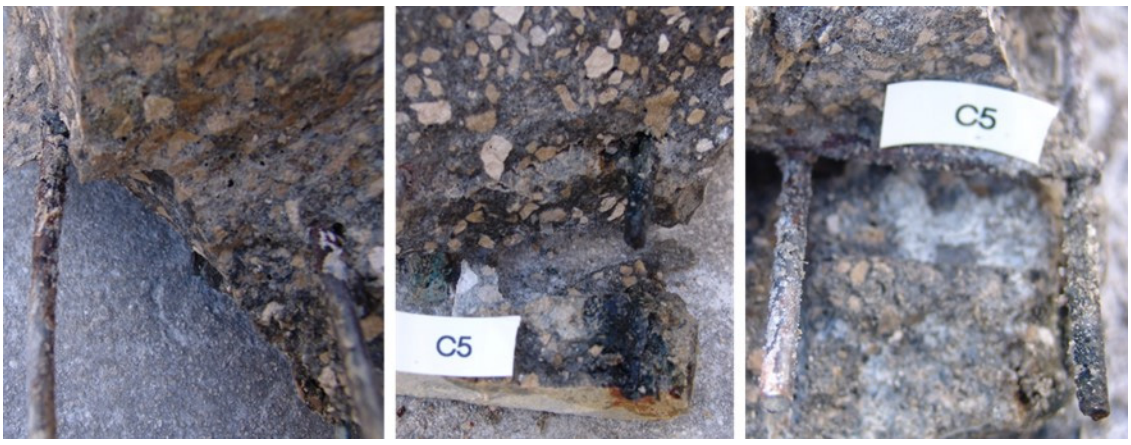

Figure 95 – Steel wire while concrete is removed on specimen C5.

Figure 96 – Steel wire after removing concrete for specimen C5.

4.1.13 Specimen C7

Before opening specimen C7, two dark black/green rust stains were observed on the bottom of the specimen. This can be seen in Figure 97. Upon opening the specimen, the steel reinforcement's corrosion spots observed were above where the black/green rust stains were located. The corroding area can be seen in Figure 98. Specimen C7's steel reinforcement can be seen in Figure 99 displaying the locations where corrosion occurred. Specimen C7 experienced mild to no corrosion. Under the ponding there was mild corrosion at the junction and along the longitudinal reinforcement shown at location 1 in Figure 100. A small amount of corrosion occurred outside the ponding.

Figure 97 – Dark black/green rust stains on the bottom of specimen C7.

Figure 98 – Corrosion observed under the ponding on specimen C7.

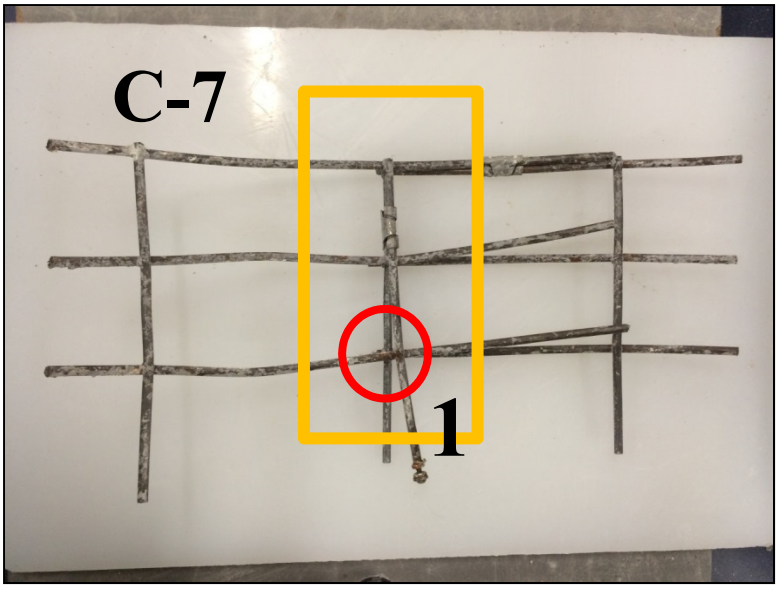

Figure 99 – Autopsy result for specimen C7 – whole steel wire mesh.

Figure 100 – Autopsy result for specimen C7 (location 1).

4.1.14 Specimen C8

Specimen C8 was exposed horizontally immersed in water. Figure 101 shows that a significant section of the steel wire below the solution reservoir was corroding. The corrosion products were dark green. The steel wire in this specimen had a white (mortar/cement) paste attached to the areas in which the steel wire was no corroding.

Figure 101 – Steel wire after removing concrete for specimen C8.

4.1.15 Specimens C12 and C22

Specimens C12 and C22 were vertically oriented and partially covered with wet sand (1/3rd) and exposed in high humidity. Figure 102 and Figure 103 show the corrosion extent on steel wires removed from Specimens C12 and C22, respectively. Modest corrosion was observed on the steel wire on both specimens. It is interesting to note that corrosion took place on the steel wire some distance above the solution reservoir.

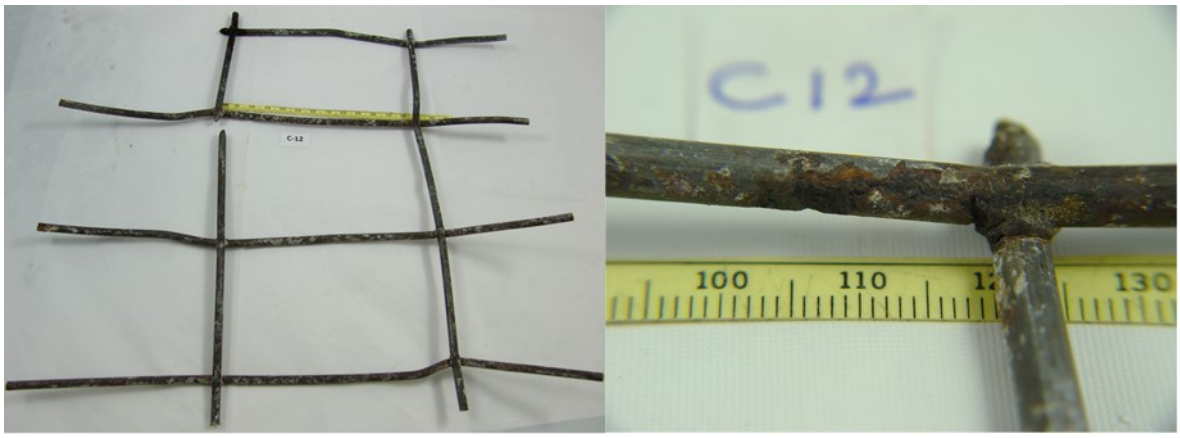

Figure 102 – Steel wire mesh for specimen C12.

Figure 103 – Steel wire areas showing the most corrosion (specimen C22).

4.1.16 Specimen C24

Specimen C24 was oriented vertically and covered with wet sand. A large spot (20 mm long) with modest corrosion was observed above the solution reservoir area (See Figure 104).

Figure 104 – Steel wire area showing significant corrosion from specimen C24.

4.1.17 Specimens C16

Specimen C16 was exposed while oriented vertically and covered with wet sand during the corrosion propagation stage. Figure 105 shows the extent of corrosion on the steel wire as the concrete was being removed. Figure 106 shows the steel wire after all concrete was removed and a close-up of the two sections with the most corrosion. More corrosion was observed on this specimen than what was observed on specimen C24.

Figure 105 – Corrosion extent on steel while removing concrete specimen C16.

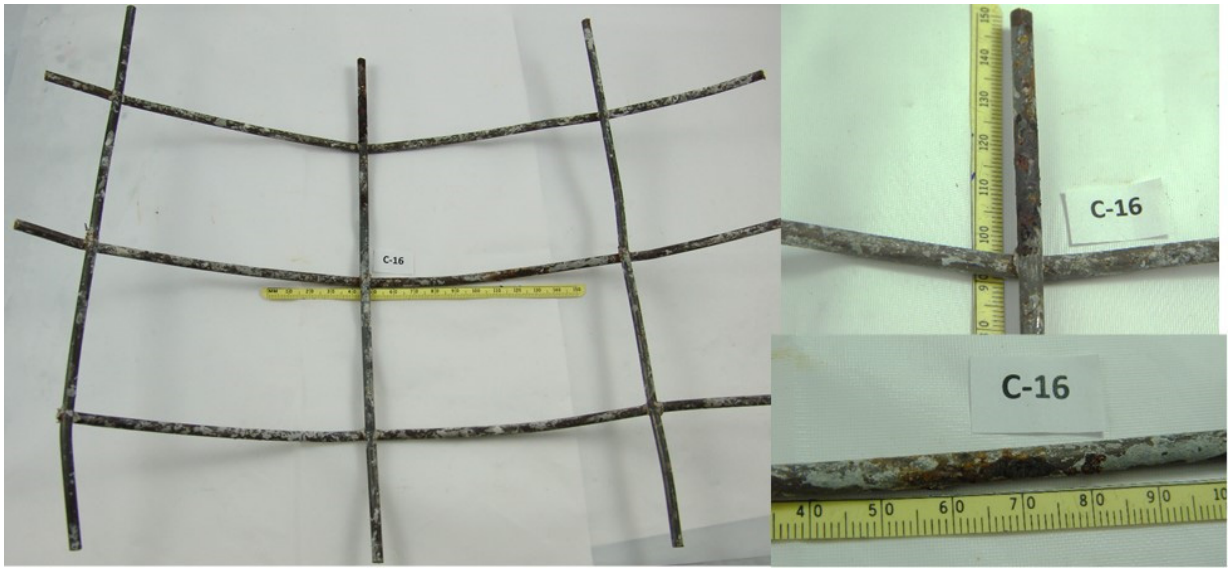

Figure 106 – Steel wire removed from specimen C16.

4.1.18 Specimen C43

Figure 107 shows a partially exposed steel wire for specimen C43. No corrosion was found under the solution reservoir on the steel wire mesh.

Figure 107 – Partially exposed steel wire on specimen C43.

4.1.19 Specimen F7

Before cracking the specimen open, two red/orange rust stains were seen located under the ponding and ~0.5 inch from the ponding. The rust stains can be seen in Figure 108. Upon breaking the specimen open, the steel wire's corrosion appeared greenish/black in color. The "green" or "black" color of the corrosion products can be seen in Figure 109 and Figure 110. The steel reinforcement of specimen F7 can be seen in Figure 111 displaying the locations where corrosion occurred the most severe. Specimen F7's applied current was increased to 125 µA before termination. As can be seen in Figure 112, location 1 experienced significant corrosion and occurred under the ponding at the reinforcement junction. Severe cross-section loss can be seen along the transverse reinforcement at location 2 in Figure 108. However, on F7 corrosion did occur outside the ponding as seen at location 3 (Figure 111).

Figure 108 – Rust stains observed near the ponding on specimen F7 before opening.

Figure 109 – (1) Black/green rust observed upon exposing steel on specimen F7.

Figure 110 – (2) Black/green rust observed upon cracking open specimen F7.

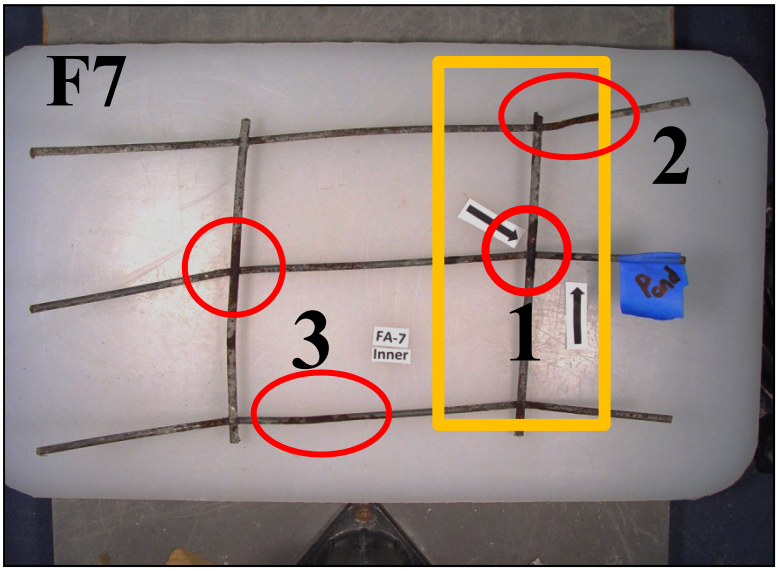

Figure 111 – Autopsy result of specimen F7 – whole steel wire mesh.

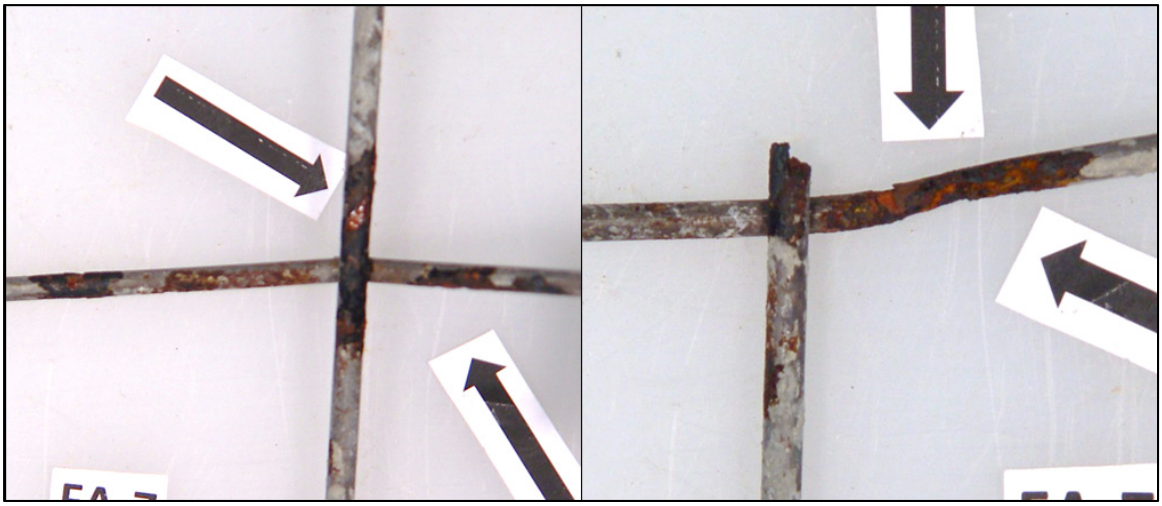

Figure 112 – Autopsy result of specimen F7. Left: location 1. Right: location 2.

4.1.20 Specimens F18

Specimen F18 was subjected first to accelerated chloride transport, at room temperature. Specimen F18 was then exposed to modest galvanic current to accelerate corrosion rate for approx. 365 days, then no additional current was applied and the specimen was exposed in high humidity for additional 300+ days. Figure 113 shows in the left picture that there was a rust-spot on the surface of the concrete inside the reservoir area, the picture on the right shows the extent of corrosion that took place. Some of the corrosion took place outside of the solution reservoir. The corrosion products on the steel under the solution reservoir were dark green/black.

Figure 113 – Surface condition and exposed steel wire from specimen F18.

4.1.21 Specimen F20

Similar to specimen F7, before cracking the specimen open a red/orange rust stain was seen located under the ponding in the lower left hand corner. The rust stain can be seen in Figure 114. Upon breaking the specimen open, the steel reinforcement's corrosion appeared greenish/black in color. The "green" or "black" rust can be seen in Figure 115 at the rust stain

location. The steel reinforcement of specimen F20 can be seen in Figure 116 displaying the location where corrosion occurred. Specimen F20's applied current was increased to 125 µA before termination and also the specimen was covered with saturated sand during latter part of the exposure period. As seen in Figure 117, location 1 experienced significant corrosion occurred under the ponding at the reinforcement junction. Upon exposure the corrosion products were blackish green suggesting that moisture was present. Mild corrosion can be seen along the transverse reinforcement at location 2 in Figure 117. Corrosion did not occur outside the ponding.

Figure 114 – Rust stain observed under the ponding on specimen F20 before opening.

Figure 115 – Black/green rust observed upon exposing steel on specimen F7.

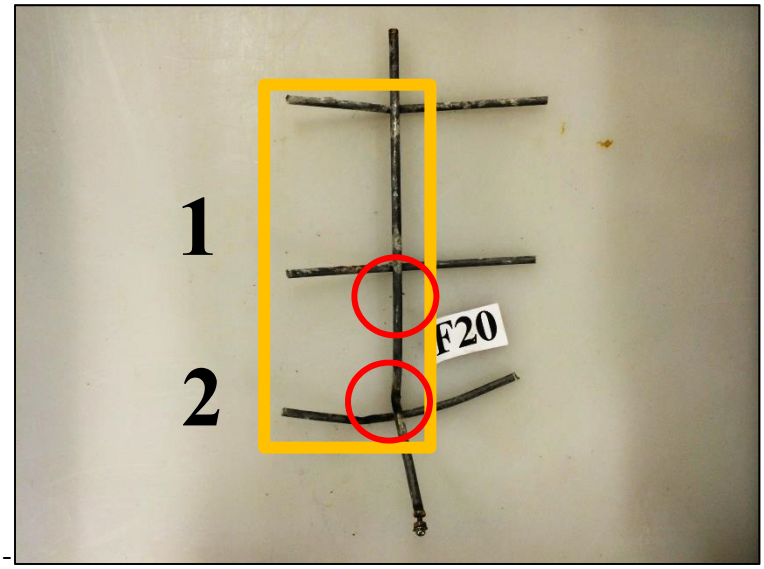

Figure 116 – Autopsy result of specimen F20.

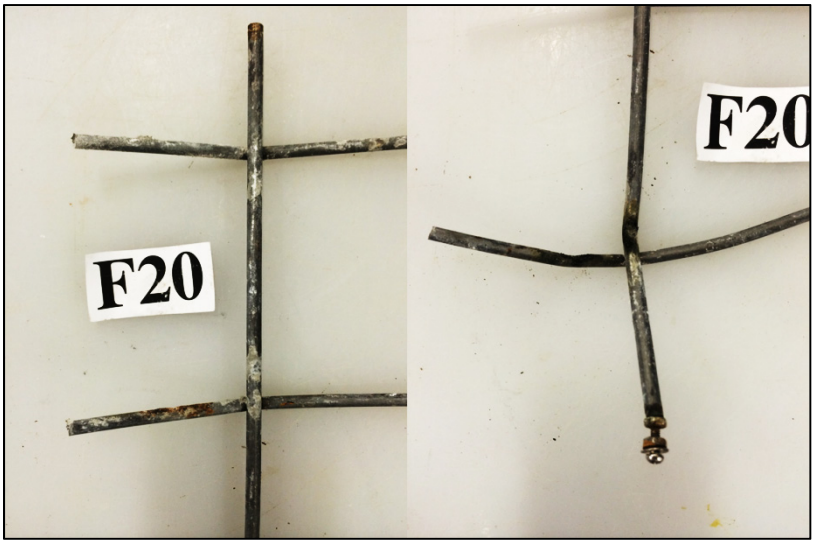

Figure 117 – Autopsy result of specimen F20. Left: location 1. Right: location 2.

4.1.22 Specimen F23

Upon breaking the specimen open, the steel reinforcement's corrosion products were red rust. It is likely that there was plenty of oxygen available at the steel's depth. This can be seen in Figure 118. The steel reinforcement of specimen F23 can be seen in Figure 119 displaying the locations where a small amount of corrosion occurred. In both location 1 and 2 a small amount of corrosion occurred at the steel junction and also extended 1" from the junction along the transverse steel which can be seen in Figure 120. A larger area of the steel reinforcement did not show corrosion which may be due to a smaller chloride concentration at the corroding sites. Corrosion did occur outside the ponding.

Figure 118 – Red rust observed upon explosion steel on specimen F23.

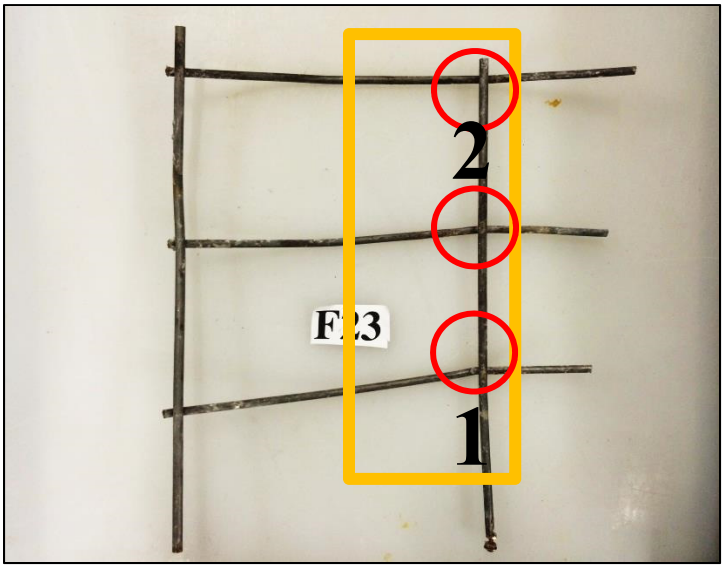

Figure 119 – Autopsy result of specimen F23.

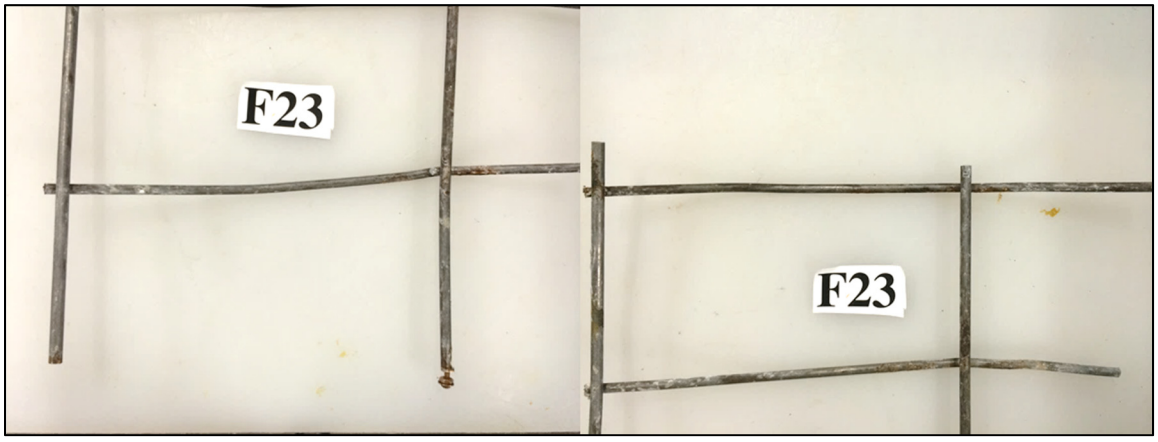

Figure 120 – Autopsy result of specimen F23. Left: location 1. Right: location 2.

4.1.23 Specimen C4

Before cracking the specimen open, the exposed ends of the steel reinforcement were observed to be corroding as seen in Figure 121. Upon breaking the specimen open, the steel reinforcement's corrosion observed was red in some areas and "black" (or " dark green) in other areas as seen in Figure 122. The steel reinforcement of specimen C4 can be seen in Figure 123 displaying the locations where corrosion occurred. Specimen C4's applied current was increased to 125 µA before termination and also the specimen was covered with saturated sand. As seen in Figure 124 corrosion occurred at the steel junction at locations 1 and 2, and also along the transverse and longitudinal wires between the junction. Upon exposure the corrosion products were blackish green suggesting that there was significant moisture at the steel depth. Corrosion did occur outside the ponding at location 3.

Figure 121 – Exposed steel reinforcement ends corroding on specimen C4.

Figure 122 – Red and black/green rust observed on specimen C4 after opening.

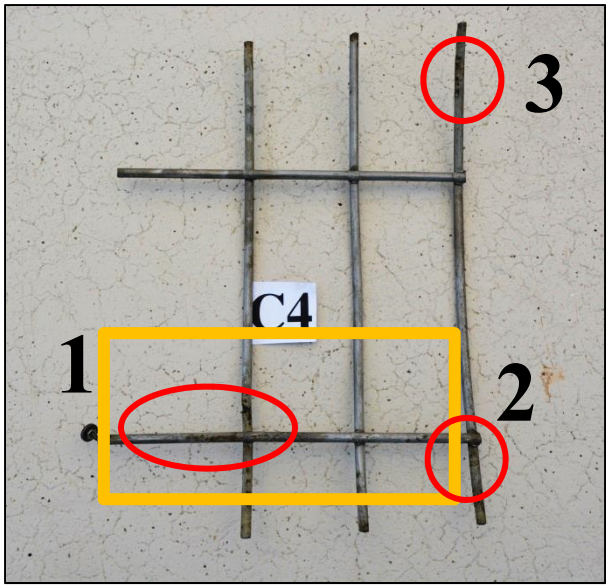

Figure 123 – Autopsy result of specimen C4.

Figure 124 – Autopsy result of specimen C4. Left: location 1. Right: location 2.

4.1.24 Specimen C6

Upon breaking the specimen open, the steel reinforcement's corrosion observed was red rust in some areas as seen in Figure 125. The corrosion products color was "black" (or "dark green") at other locations as seen in Figure 126. The steel reinforcement of specimen C6 can be seen in Figure 127 displaying the locations where corrosion occurred. Specimen C6's applied current was also increased to 125 µA before termination. As seen in Figure 128, location 1 experienced mild corrosion under the ponding at the reinforcement junction. Also, mild corrosion can be seen at the junction along the transverse steel shown in Figure 128. Corrosion did not occur outside the ponding. Specimen C6 experienced more corrosion than C4 which may be attributed to the higher current applied and the fact that specimen C4 was covered with saturated sand for the last 140 days before being terminated whereas specimen C6 was exposed in high humidity.

Figure 125 – Red rust observed under the ponding upon opening specimen C6.

Figure 126 – Black/green rust observed upon opening the end of specimen C6.

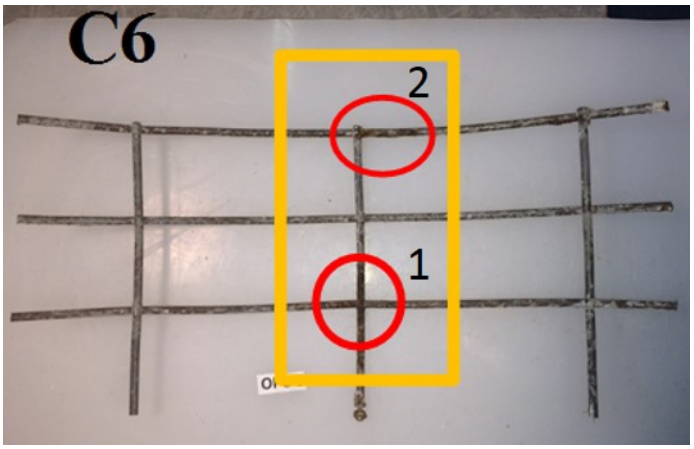

Figure 127 – Autopsy results of specimen C6 – whole steel wire mesh.

Figure 128 – Autopsy result for specimen C6. Left: location 1. Right: location 2.

4.2 Pictures of Specimens after Chemical Cleaning the Steel Wire Mesh

Selected steel wires were chemically cleaned as per ASTM G01[36]. The figures in this section present pictures of the steel wire after it has been cleaned for selected specimens. In some cases, the figure shows pictures before and after cleaning the steel wire.

4.2.1 Specimen F0

Figure 129 shows the portion of the reinforcement under the solution reservoir for specimen F0 after cleaning. From the pictures, it can be observed that corrosion took place at several spots, and significant cross-section loss is evident at several of these sites. Corrosion took place both on the longitudinal and circumferential directions. Corrosion also took place on the back side, but to a lesser extent. The bottom picture shows corrosion at both left and right intersections.

Figure 129 – Close-up of corroding sites for specimen F0 (along the ponding reinforcement), top and back side.

4.2.2 Specimen F1

Figure 130 shows the steel wire after cleaning for specimen F1. It is evident that corrosion took place at multiple spots and that the cross-section loss was significant (i.e., more than 1 mm)

Figure 130 – Close up of steel corroding sites after cleaning on specimen F1.

4.2.3 Specimen F2

Figure 131 shows three pictures after cleaning steel from specimen F2. The pictures show different locations where corrosion, the pictures on the left and right show the most significant cross-section loss. The picture on the right show a broken wire, the cross-section loss is

significant, but it is not clear if the separation took place during the concrete removal or it this had taken place previously.

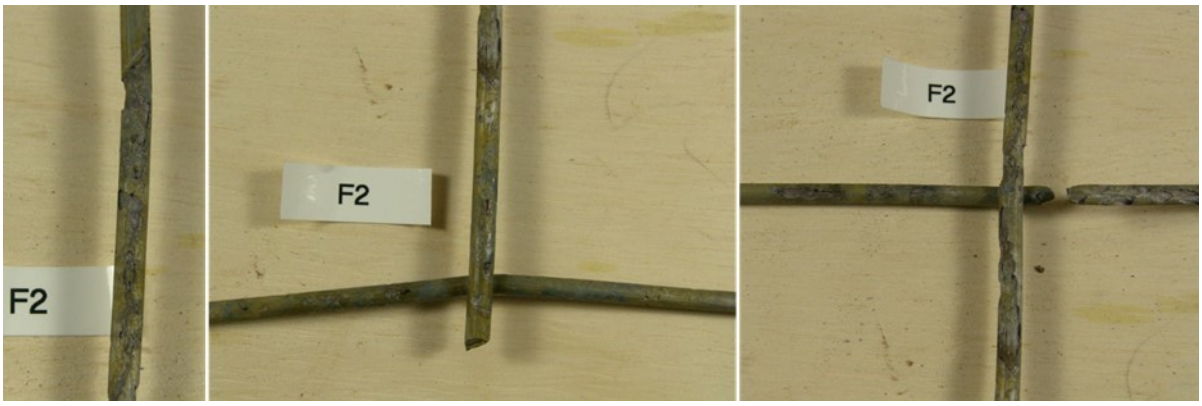

Figure 131 – Close-up of corroding sites for specimen F2.

4.2.4 Specimen F3

The steel reinforcement of specimen F3 can be seen in Figure 132 displaying the locations where corrosion occurred. Specimen F3 was not polarized. It was exposed in high humidity during the corrosion propagation stage. Specimen F3 experienced corrosion at two locations. One site was under the ponding at the reinforcement junction. Severe cross-section loss can be seen at one other location along the side of the transverse steel. Corrosion did occur outside the ponding. However, the corrosion observed did not spread from the reinforcement junction as compared to specimens subject to applied current during the propagation stage.

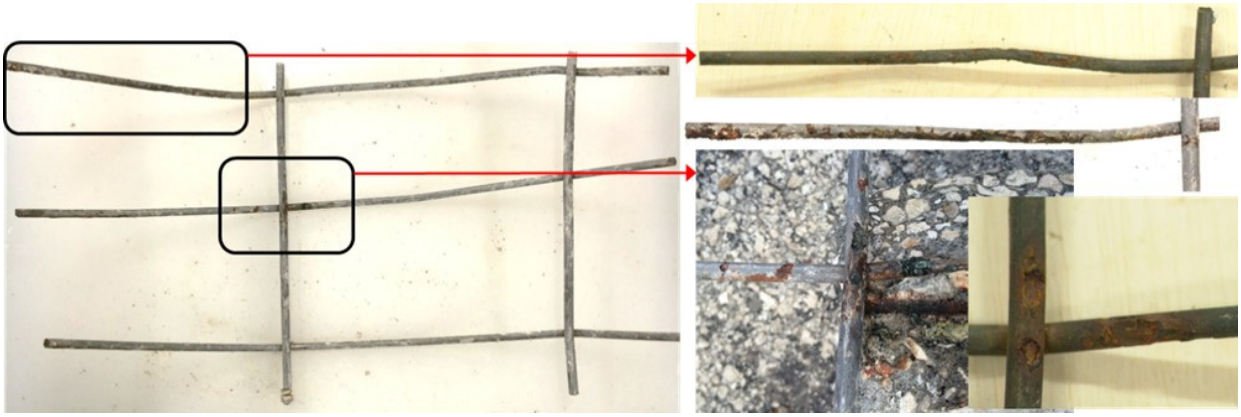

Figure 132 – Autopsy result of specimen F3. Left: after opening. Right: close-ups.

4.2.5 Specimen F4

Figure 133 shows the front and back of the section that presented the more corrosion. Corrosion took place on the top side of the steel, as well as on the side and on the back side of one of the spiral wires.

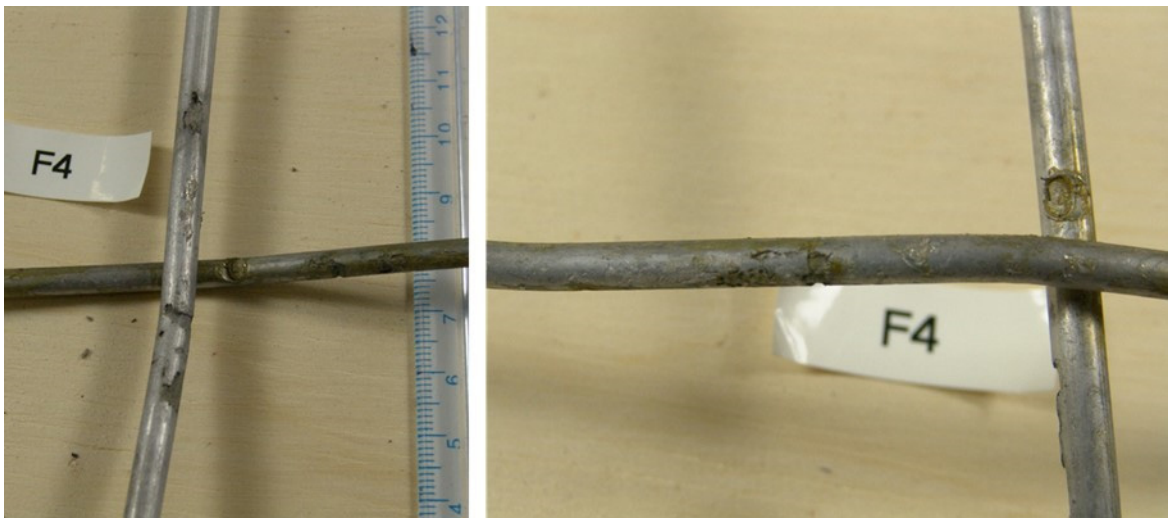

Figure 133 – Steel wire mesh after cleaning for specimen F4.

4.2.6 Specimen F6

Figure 134 shows pictures of the cleaned steel wire mesh for Specimen F6. The longitudinal wire show significant amount of corrosion for the portion of the longitudinal steel wire that was under the solution reservoir.

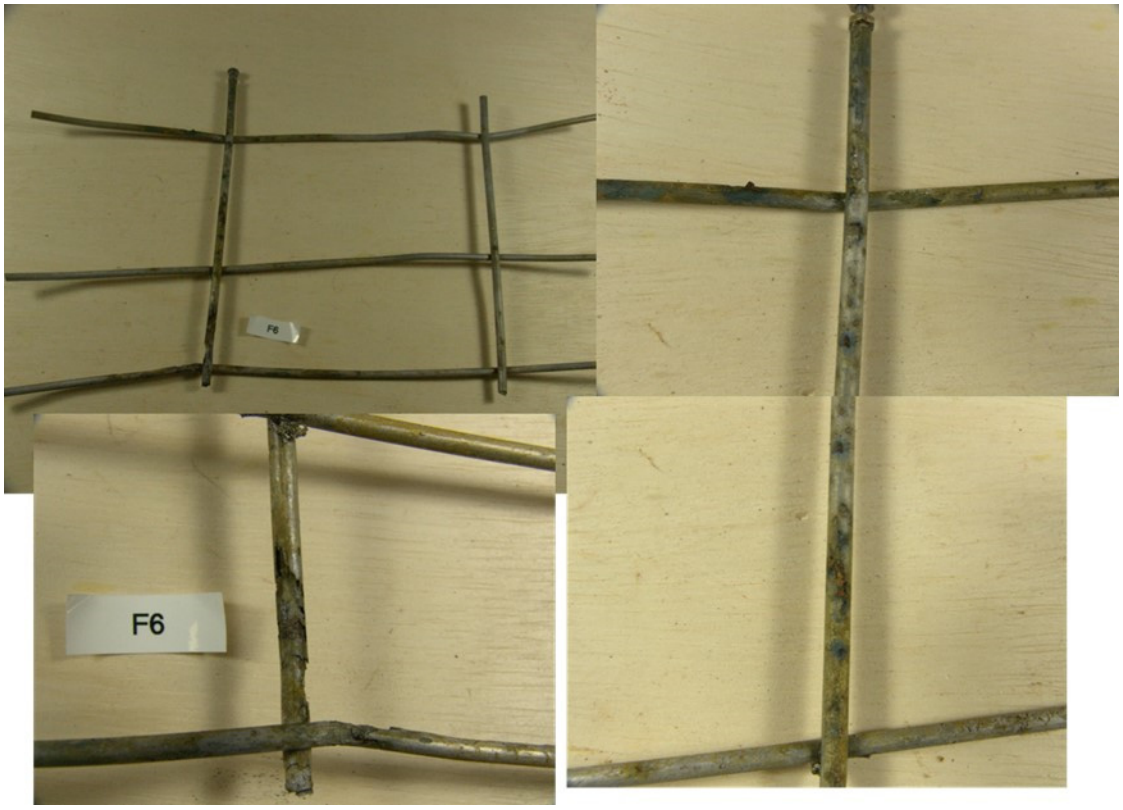

Figure 134 – Steel wire mesh for specimen F6 after cleaning.

4.2.7 Specimens F9, F12, and F21

Figure 135, Figure 136 and 137 show pictures of the cleaned steel wires for specimens F9, F12 and 21 respectively. Significantly less cross-section loss and corrosion extent was observed on these specimens.

Figure 135 – Steel wire mesh of specimen F9 after cleaning.

Figure 136 – Steel wire mesh specimen F12 after cleaning.

Figure 137 – Steel wire mesh specimen F21 after cleaning.

4.2.8 Specimen F22

Figure 138 shows the steel wire removed from specimen F22 after cleaning. The close-up picture in the center shows that there were two spots with significant cross-section loss (spiral) and a small corrosion spot ~2 mm diameter (longitudinal) that looked like a deep pit. The inset on the right show that at a location away from the reservoir: corrosion also took place (about 5 mm wide), but the cross-section loss was modest.

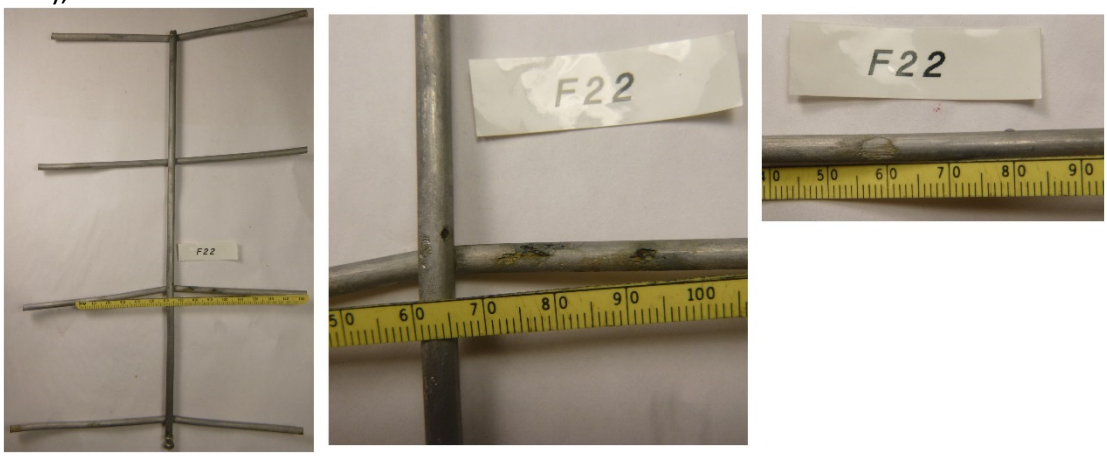

Figure 138 – Steel wire mesh specimen F22 after cleaning.

4.2.9 Specimen C0

Figure 139 shows on the left the wire mesh from Specimen C0 after chemical cleaning. The picture on the right shows a close up of the region that suffered significant cross-section loss. Several spots 10 mm long (or more) are easy to identify.

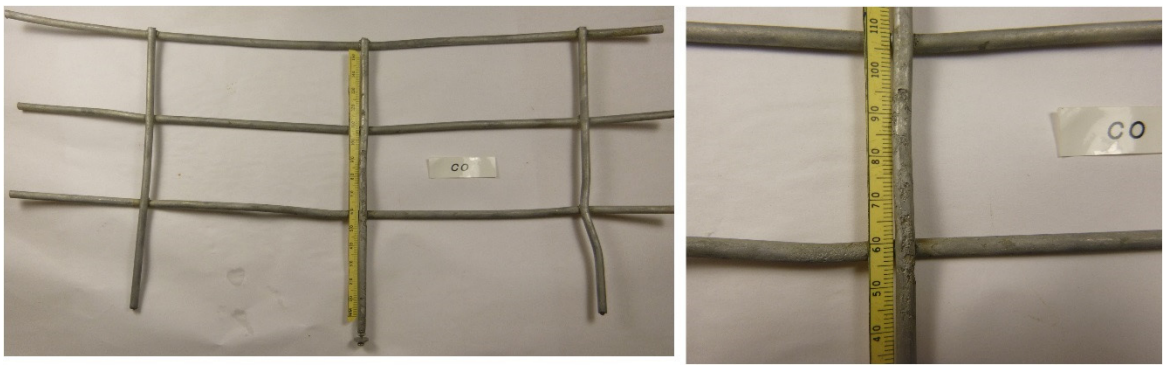

Figure 139 – Steel wire mesh specimen C0 after cleaning.

4.2.10 Specimen C2

Significant corrosion took place along one of the longitudinal steel wires on Specimen C2 as can be seen on the pictures on Figure 140. The picture on the left shows that corrosion took place also on one of the transverse steel wires a certain distance from where the multiple corrosion spots were present on the longitudinal steel wire. The corrosion spots are pit like shape of various sizes ranging from less than one mm to several mm in diameter.

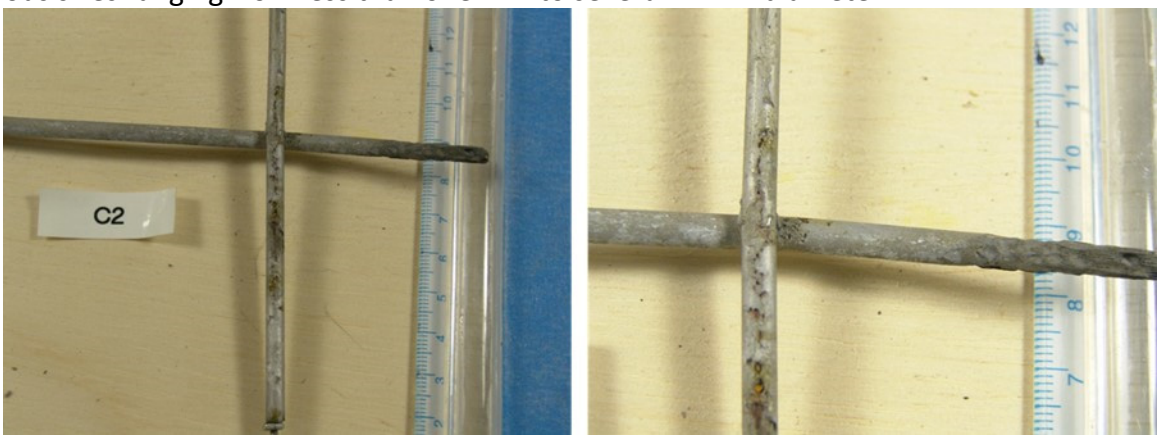

Figure 140 – Steel wire mesh specimen C2 after cleaning.

4.2.11 Specimen C7

Specimen C7's steel reinforcement can be seen in Figure 141 displaying the locations where corrosion occurred. Like specimen F3, specimen C7 was not polarized when placed in high humidity during the corrosion propagation stage. Specimen C7 experienced mild to no corrosion. Under the ponding there were two spots with corrosion at the junction and along the longitudinal reinforcement shown by the close-up pictures on the right. A small amount of corrosion occurred outside the ponding.

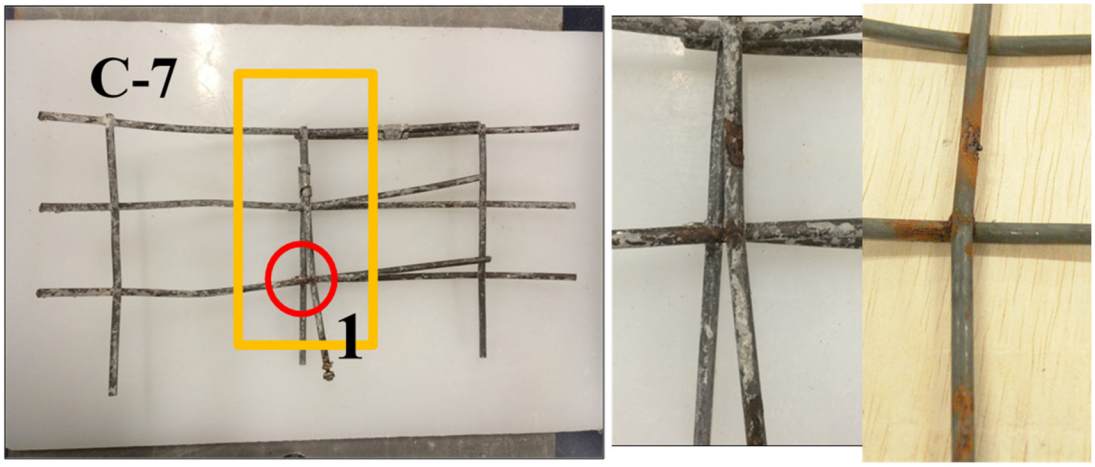

Figure 141 – Autopsy result for specimen C7 – Left: full wire mesh. Right: close-up.

4.2.12 Specimen C8

Figure 142 shows on the left the steel wire mesh from Specimen C8 after chemical cleaning. The picture on the right shows a close up of the region that suffered significant cross-section loss. The corroding region was below the solution reservoir. Several spots 10 mm long (or more) are easy to identify. Both, longitudinal and transverse wires showed corrosion, although corrosion was more pronounced on the longitudinal steel wire.

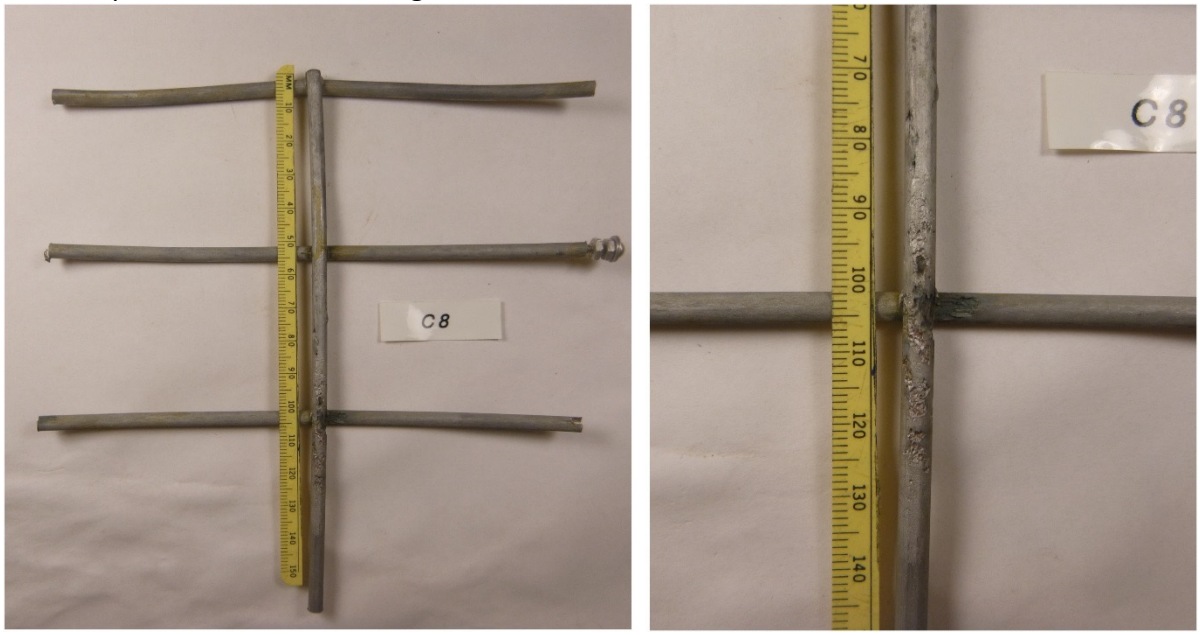

Figure 142 – Steel wire mesh after cleaning for specimen C8.

4.2.13 Specimen C9

Figure 143 shows on the left the whole steel mesh after cleaning and the pictures on the right show a couple of close ups of sites where corrosion was the most significant. One of the corrosion sites along the longitudinal was longer than 15 mm long and with a significant cross-

section loss. The smaller inset shows additional section of the longitudinal wire that goes below the larger inset. The cross-section can be observed both on the longitudinal and the transverse direction.

Figure 143 – Steel wire mesh specimen C9 after cleaning.

4.2.14 Specimen C16

Figure 144 shows a couple of locations where corrosion took place on the cleaned steel that was removed from Specimen C16. Some of the corrosion sites presented significant cross-section loss. The length of these spots ranged from one mm to six/seven mm.

Figure 144 – Close-up after cleaning steel wire of specimen C16.

4.2.15 Specimens C12 and Specimen C22

Figure 145 shows close-ups for the steel wire meshes removed from specimens C12 and C22. It is evident that the cross-section loss was significant on both cases. The location of the corrosion sites was above the solution reservoir. Both of these specimens were exposed in the vertical

direction. The steel wire for specimen C12 showed corrosion on both sides of the wire (the two pictures on the right show front and back surface).

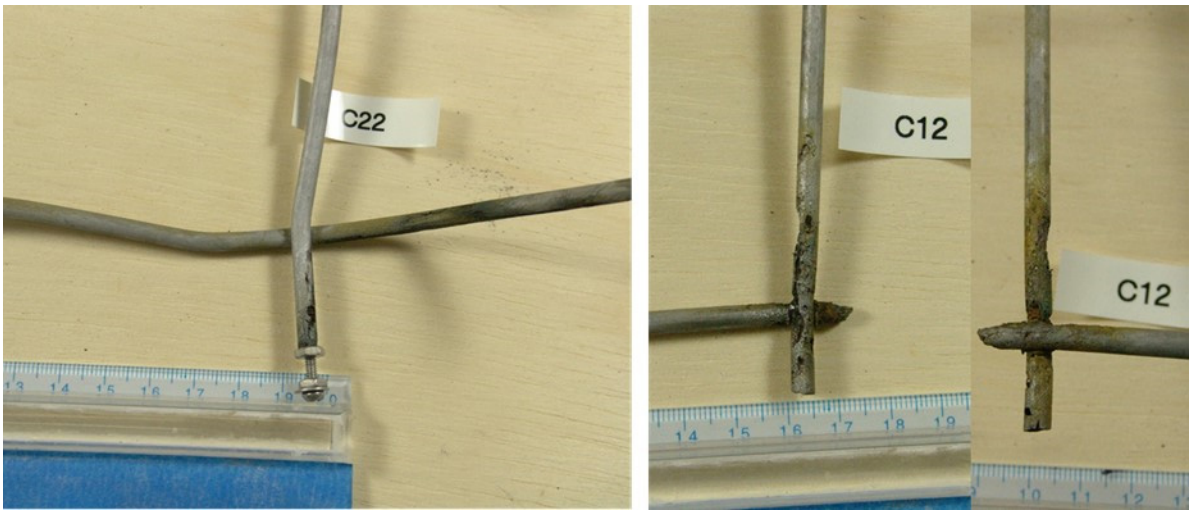

Figure 145 – Steel wires after cleaning for specimen C22 and specimen C12.

4.2.16 Specimen C24

Figure 146 shows on the left the whole steel mesh after cleaning and the picture on the right shows a close up of the region where corrosion was more significant. Both longitudinal and transverse steel wire closes to the connection post showed corrosion. This specimen was exposed vertically and it is likely that chlorides might have move up-wards by diffusion due to concentration differential. The oxygen likely reached this section of the steel easier compared to the rest of the longitudinal steel wire.

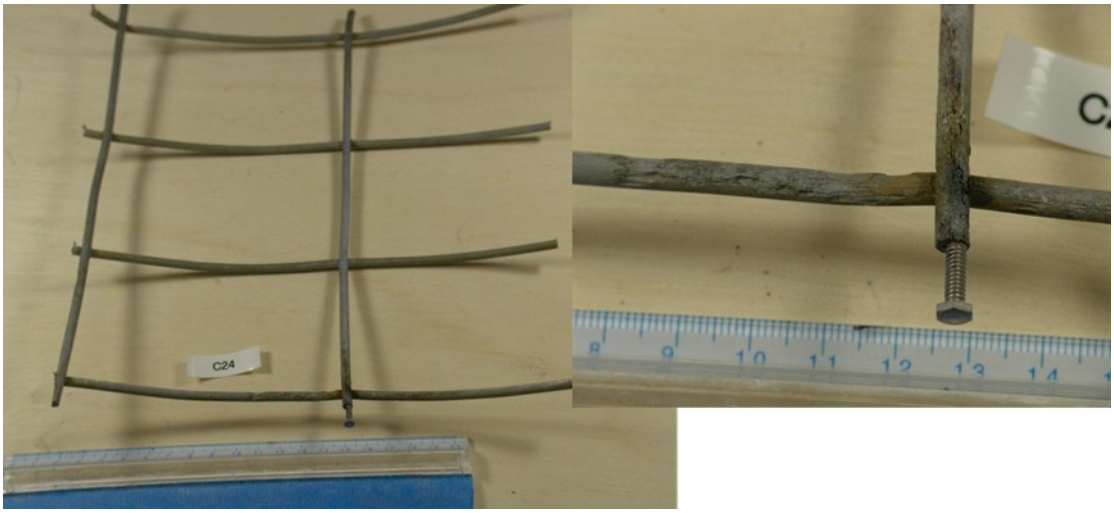

Figure 146 – Close-up after cleaning steel wire for specimen C24.

4.2.17 Specimen F7

The steel reinforcement of specimen F7 can be seen in Figure 147 displaying the locations where corrosion occurred the most severely. As can be seen in the Figure 147 picture on the right (after cleaning the reinforcement), the top site experienced significant corrosion and occurred under the ponding at the reinforcement junction. Severe cross-section loss can be seen at the two close-up sites shown.

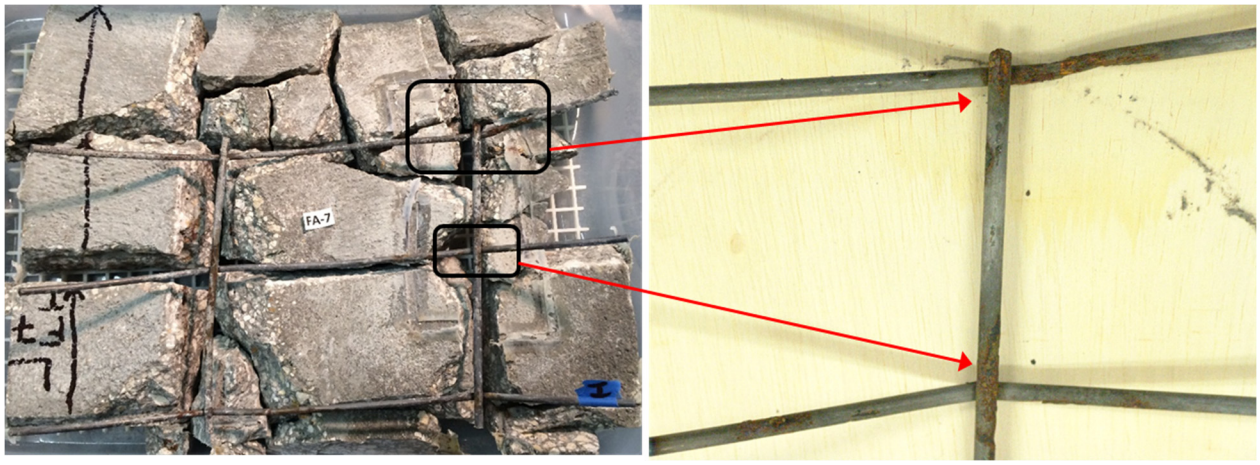

Figure 147 – Specimen F7: Left: shortly after opening. Right: locations under the ponding.

4.2.18 Specimen F20 and Specimen F19

The steel reinforcement of specimen F20 can be seen in Figure 148 displaying the location where corrosion occurred (pictures taken after cleaning). Specimen F20's applied current was increased to 125 µA before termination and also the specimen was covered with saturated sand. As seen in the Figure 148 picture on the right, the steel experienced significant corrosion occurred under the ponding at the reinforcement junction. Upon exposure the corrosion products were blackish green suggesting that there was very little oxygen at the steel depth (not shown). Corrosion did not occur outside the ponding. Figure 149 shows pictures of the reinforcement in Specimen F19. Corrosion occurred under the ponding, but the cross-section loss was not as significant.

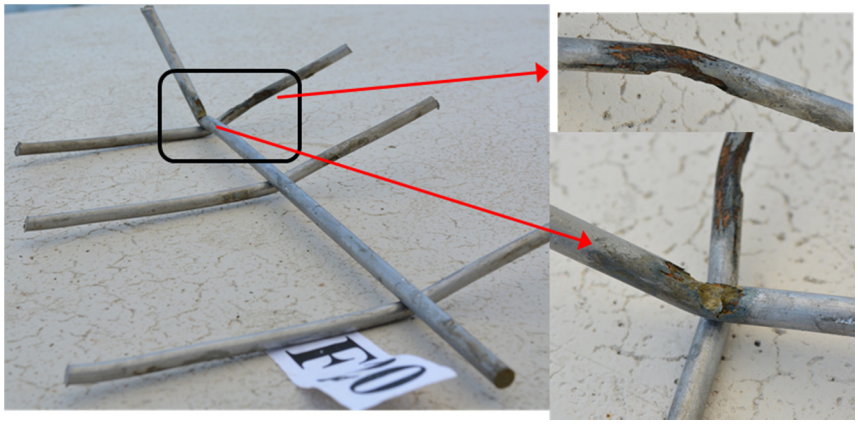

Figure 148 – Autopsy result of specimen F20. Left: all reinforcement 1. Right: corroding sites.

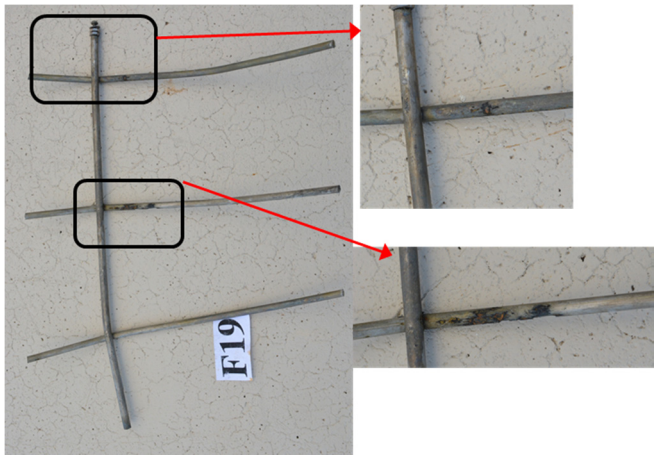

Figure 149 – Autopsy result of Specimen F19: Left: all reinforcement, Right: corroding sites.

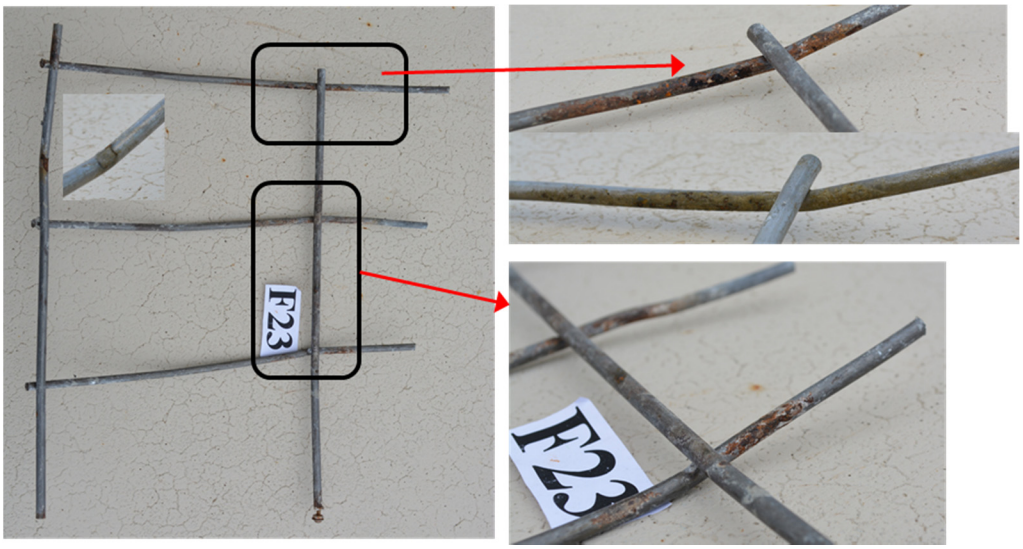

Figure 150 – Autopsy result of specimen F23. Left: all steel wire. Right: corroding sites.

4.2.19 Specimen F23

The steel reinforcement of specimen F23 can be seen in Figure 150 displaying the locations where a small amount of corrosion occurred. In both locations, a small amount of corrosion occurred at the steel junction and also extended ~1" from the junction along the transverse steel which can be seen in top two pictures on the right column of Figure 150. A larger area of the steel reinforcement did not show corrosion, which may be due to a lower chloride concentration at the corroding sites. Corrosion did occur outside the ponding (see close up on the inset within the picture on the left – small spot).

4.2.20 Specimen C4

The steel reinforcement of specimen C4 can be seen in Figure 151 displaying the locations where corrosion occurred. The picture on the left shows the reinforcement shortly after exposing the

steel. Specimen C4's applied current was increased to 125 µA before termination and the specimen was covered with saturated sand, as well. As seen in the Figure 151 picture on the right (after cleaning), corrosion occurred at the steel junction, and also along the transverse and longitudinal steel between the junctions. Upon exposure the corrosion products were blackish green suggesting that there was very little oxygen at the steel depth (Not shown in here). Corrosion did occur outside the ponding. See inset on picture on the left column.

Figure 151 – Autopsy result of specimen C4. Left: after opening. Right: close-up after cleaning.

4.2.21 Specimen C6

The steel reinforcement of specimen C6 can be seen in Figure 152 displaying the locations where corrosion occurred. Specimen C6's applied current was also increased to 125 µA before termination. As seen in the Figure 152 pictures on the right, the reinforcement experienced corrosion under the ponding at the reinforcement junctions. Also, mild corrosion can be seen at the middle junction along the transverse steel shown. Corrosion did not occur outside the ponding. Specimen C6 experienced more corrosion than C4 which may be attributed to the fact that specimen C4 was covered with saturated sand for the last 140 days before being terminated.

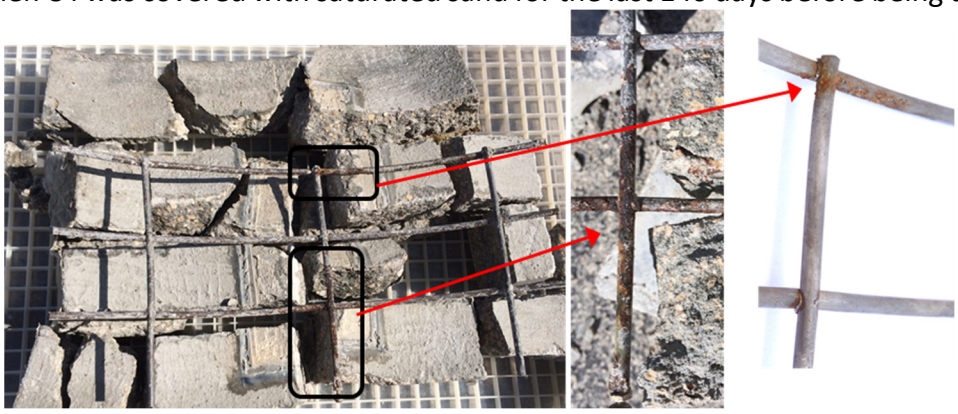

Figure 152 – Autopsy result of specimen C6. Left: after opening. Right: close-ups of corroding sites.

4.3 Calculated and Measured Mass Loss

As presented above, selected lab exposed specimens were forensically analyzed: i.e., the concrete was removed to expose the steel wire mesh. Pictures were taken while this took place. Additional pictures were taken of the whole steel wire mesh to assess its surface condition. The steel wire mesh of most specimens were then chemically clean to observe how much cross-section loss took place at the corroding sites, and the gravimetric change with respect to the initial mass was obtained. This mass is labeled here "measured mass loss". Table 18 and Table 19 show the calculated and measured mass loss for specimens that were subjected to forensic analysis and that were chemical cleaned to remove corrosion products. The column farthest to the right indicates when each specimen was forensically analyzed. Table 18 presents the results for specimens that were exposed in the horizontal direction. In many cases there is a significant difference between the calculated mass and measured mass loss. For example, the calculated mass loss calculated for Specimen F1 was 11.3 grams and the measured mass loss was 1.4 grams. In this case a significant amount of the corrosion products penetrated the concrete pore structure (see Figure 79 and Figure 80) and steel wire mesh after chemical cleaning showed significant cross-section loss at multiple sites (Figure 130).

On most specimens certain amount of the corrosion products moved into the concrete pore structure (e.g., F1), rather than accumulating on the reinforcement trace. In other cases, the corrosion was not significant and thus not much corrosion products were available to be transported into the concrete. For those cases the measured mass loss was small and usually less than the calculated mass loss (e.g., C3, F5, F8, F15), but in other cases both mass values were comparable (e.g., C7, C8, F0). In other cases, as for example the specimens that were immersed in water in the horizontal direction, the corrosion products moved into the pore structure and upon removing the concrete there was sometimes evidence of significant mass loss, but very little mass loss was recorded upon chemically cleaning the steel. For example the measured mass loss to calculated mass loss ratio (expressed in percentage) was 5.4% and 16% for Specimen F12 and Specimen F22 respectively.

There were cases (about 7) in which the measured mass loss was larger than the calculated mass. In most of these cases, some of the observed corrosion took place on sections away from the solution reservoir (e.g., Specimen C9 and Specimen F11).

There were several interesting observations. The idea that oxygen allows corrosion to proceed at a faster pace for conditions under high moisture are better exemplified by C specimens in the vertical direction (e.g., C13, C16, C24). Additional chlorides might have reached outside the solution reservoir due to gravity and concentration gradient, but also due to periodic filling of the solution reservoir that might allowed for some of the solution to spill on the areas surrounding/next to the reservoir.

Table 18 – Comparison of calculated mass and measured mass loss (horizontal specimens).

Specimen	Calculated Mass Loss (g)	Measured Mass Loss* (g)	Date
Covered Wet Sand			
F1_T	11.33	1.4	12/15/2014
F4_T	3.25	0.9	4/19/2016
F5_T	1.11	0.35	7/15/2016
C1_T	2.39	1.2	12/16/2014
C2_T	3.94	1.5	4/18/2016
C3_T	0.98	0.67	7/15/2016
C11	0.7	1.87	7/15/2016
Immersed in Water			
F12_T	1.85	0.1	7/8/2016
F21_T	2.01	0.5	2/23/2016
F22_T	1.87	0.3	7/8/2016
C0_T	5.74	0.64	7/8/2016
C5_T	0.97	1.8	2/23/2016
C8_T	0.65	0.53	7/8/2016
High Humidity			
F2_T	14.54	10.3	4/17/2016
F6_T	2.92	1	1/17/2016
C9_T	0.6	10	1/17/2016
F3_T	1.52	0.6	2/15/2014
C7_T	1.17	1.2	2/15/2014
F0_T	1.99	2	12/15/2014

The corrosion extent did vary somewhat with respect to the number of corroding sites and how deep the corrosion was. On horizontally exposed specimens, corrosion usually took place under the solution reservoir.

Table 19 – Comparison of calculated mass and measured mass loss (vertical specimens).

Specimen	Calculated Mass Loss (g)	Measured Mass Loss* (g)	Date Concrete
Immersed in Water			Removed
F10_T	5.94	1.19	7/11/2016
F15_T	2.03	0.61	7/11/2016
C18_T	7.53	2.8	7/11/2016
C15_T	3.51	2.24	7/11/2016
Covered Wet Sand			
F8_T	2.35	0.7	7/15/2016
F9_T	2.55	1	2/18/2016
F11_T	1.83	6.02	7/21/2015
F13_T	2.51	0.7	7/15/2016
C13_T	5.9	1.0	7/15/2016
C16_T	3.12	4.4	7/16/2015
C21_T	11.24	1.1	7/15/2016
C24_T	10.5	2.3	7/16/2015
C25	9.1		
Partially Covered Wet Sand			
C12_T	1.43	2.7	4/17/2016
C22_T	4.24	1.5	4/17/2016
C23_T	6.75	2.1	7/15/2016
High Humidity			
C17_T	2.76	1.3	7/15/2016
C26_T	3.89	3.2	7/15/2016

The calculated and measured mass loss values shown in Table 20 correspond to specimens that were subjected to galvanostatic pulse (so as to moderately accelerate corrosion). The calculated mass loss (no current) values are based on the measured Rc values from the LPR measurements 2-3 days after suspending the current application. Calculations were performed from measured Rc values and also the additional mass contributed by the applied current assuming 100% efficiency. Table 20 also includes a column with the measured mass loss after cleaning the reinforcement of each terminated sample, with respect to the mass of the reinforcement before cleaning.

Table 20 – Calculated and measured mass loss.

Specimen ID	Days After Corrosion Initiation	Calculated Mass Loss no current (g)	Calculated Mass Loss (due to applied current (g))	Calculated Mass Loss	Measured Mass Loss
		LPR			
F7	707	2.51	0.16	2.67	1.4
F16	1349	1.55	0.29	1.84	1.8
F17	1349	1.75	0.29	2.04	1.4
F18	1027	1.25	0.29	1.54	3.2
F19	642	0.9	0.25	1.15	0.3
F20	642	1.01	0.49	1.5	0.3
F23	544	0.18	0.25	0.43	0.1
C4	847	0.69	0.49	1.18	1.1
C6	604	0.27	0.14	0.41	1.4
C10	1184+	1.02	0.29	1.31	

The two columns farther to the right can be used to compare the gravimetric weight loss measurements to the calculated mass loss (Faraday's law) including the applied current for the specimens that were terminated. It can be observed that for the F specimens that were terminated earlier (F7, F19, F20 and F23) the gravimetric measured mass loss is 50% to 25% of the calculated mass from the integrated charge. For F16 and F17 the measured mass loss corresponds to 98% and 68.5% of the calculated mass loss, respectively. The steel mesh for specimen F18 was not cleaned right after removal and the measured mass loss was larger than the calculated mass loss. The smaller measured mass loss is explained by some of the corrosion products penetrating into the pore structure and not being available during the cleaning procedure (experimentally observed). The gravimetric mass loss for C specimens is ~1-3.5 times larger than the mass loss predicted from Faraday's law. For C specimens, an explanation for this observation could be that when measuring the polarization resistance using LPR tests, not all the steel corroding outside of the ponding is taken into account since the counter electrode only covers the area with the ponding. However, a factor of two on either direction has been reported previously[6,32] for cases in which corrosion is taking place with corrosion moderately accelerated.

On some specimens subjected to the galvanostatic pulse, corrosion also took place at locations outside of the ponding area. An explanation could be that as time passes during the propagation stage, some chlorides are transported toward the reinforcement outside the ponding via diffusion within the saturated concrete pore structure of the concrete; eventually reaching the concrete/steel interface at locations outside the reservoir. The chloride concentration is likely lower than under the solution reservoir, still for cases in which the steel is polarized to positive values (i.e., on steel potential values ranging from -100 to 400 mVsce

were observed when the current was being applied), pitting corrosion at these lower chloride levels could have then initiated. No cracks were observed, even though in some specimens a significant cross-section loss was observed. It is possible that a longer exposure period is required for cracks to occur (i.e., a larger cross-section loss). Additionally, the high moisture content in the concrete allowed some of the corrosion products to be transported and fill the pore structure, thus delaying the occurrence of cracks. The small diameter of the steel stirrup (5 to 6 mm) might also contribute to delaying the crack appearance. Wet/dry cycles might be needed for cracks to appear, the cycles would allow the hydroxide corrosion products to be converted to oxides that require a larger volume thus causing the tensile stress known to cause the cracks.

Chapter 5 – Field Visits

This chapter describes the field visits. At several of the sites visited, the reinforced concrete pipe had been removed as part of a construction project. The visits to these sites took place between summer/2013 and summer/2015. Additional sites were visited during spring/2016 and early summer/2016. The sites visited during 2016 were selected from locations that had been visited previously or sites in which the RC pipes are exposed to aggressive environments (discharge to seawater or intracoastal water). At these sites, the reinforced concrete pipes continue to be in service (an exception is removed RCPs found next to Hathaway Bridge (HWB) in Panama City). At most sites, potential profiles were measured along selected longitudinal steel wires.

For most sites where pipes had been removed, pieces of RCP were cut-off, cored or a piece collected from available small pipe pieces. These pipe sections were subjected to forensic analysis by removing the concrete and exposing the steel wire. The observations upon removing the concrete to expose the steel wires are described below.

This chapter also includes 3EB tests results performed on ring specimens and the corresponding forensic analysis.

5.1 Sites Where RCPs Have Been Removed

The pipes at these sites were generally in very good to good condition. In most instances, some damage did occur during pipe removal. Some visited sites were inland: Zolfo Springs, Tallahassee, Titusville (but pipes located at Apopka). Other sites were at a distance less than two/three miles from the seawater or intracoastal water: e.g., Miami Beach, Dania Beach (Dania Beach Boulevard), Hudson, and Panama City (next to HWB). A third group corresponds to sites where the RCPs discharge to the intracoastal water: Dania Beach (Marina), and Indian Rock. Potential profiles were measured along selected longitudinal steel wires on the removed RC pipes. Resistivity and surface moisture was measured at most of these sites. When possible soil or solution was also obtained for additional testing in the lab (resistivity and in some cases chlorides and/or sulfates).

Miami Beach (Alton Road): A small diameter (12 in) RCP pipe was removed and provided for characterization in the Lab. No soil or water was available. Potential profiles were measured. A piece of the pipe was cut and milled from both sides and chloride concentrations obtained at several depths.

Dania Beach Marina: The steel embedded in the reinforced concrete pipe was characterized for corrosion potential values (i.e., assess if corrosion was taking place) on two of the removed RCPs. Figure 153 shows a picture of two of the removed pipes. Marine growth can be observed on the inside of the pipe. One of the inset pics show the side of the pipe that was damaged upon removal and that some of the steel wires were corroding. Small pieces were brought into

the lab for forensic analysis. Soil surrounding the pipe was obtained. A piece of the pipe was milled from both surfaces (several layers) and total chlorides were measured using FDOT method. From this location, two of the removed RCP segments were taken by Rinker Materials. One of them was later tested at their site 3 edge bearing test (the results of that test are included in this chapter).

Figure 153 – Two of the pipes removed at Dania Beach Marina.

Zolfo Springs: Two type of pipes were removed at this site. An older type of pipe had two layers of reinforcement. A core and small RCP pieces were obtained during this visit and forensically analyzed at the lab. Soil sample was also collected from this site. The concrete cover on one of the pipes was 4 cm.

Indian Rock Beach (close to Largo, FL): Potential measurements were performed on two reinforced concrete pipes available at the site. Several segments from one of the two pipes were cut. The cut segments were brought back to the lab. Three of these pieces were forensically analyzed (i.e., concrete removed and the steel wire mesh exposed). Soil samples were also obtained.

Hollywood Florida: Unfortunately, the pipes removed at this location were no RCP, but rather non-reinforced concrete pipe. Soil samples and concrete pipe segments were obtained from this site.

Tallahassee: This site was visited early 2015. The local FDOT personnel coordinated with the sub-contractor and PI. The sub-contractor assisted during the visit with site measurements. Potential profiles, surface resistivity and moisture content were measured on selected pipes. A small piece of pipe was cut-off from one of the RCP that were characterized on-site. Soil sample was also obtained from this location.

Dania Beach Boulevard: Old RCP segments were found next to a state park in Dania Beach, a visual inspection took place and potential measurements were performed. It is not clear how

long have these pipes being removed from service. These pipe were found while driving by. The pipe is very similar to that characterized at Apopka (i.e., pre-world war II) see below. No soil was available.

Apopka: The RCP pieces were pre-world war II and they were removed from the Titusville airport. No soil was available. The potential of the reinforcing steel embedded in these pipes was measured to assess if corrosion was taking place. Resistivity and moisture measurements were also performed.

US19 and SR52 in Hudson, FL: – This visit took place during summer 2015, two stops were made at locations where pipes had been removed. Three pipes were characterized during this trip. Samples were taken from three pipes. At the site closest to the gulf the pipes were elliptical in shape. Potential, resistivity and moisture measurements were performed.

Panama City, FL. Next to the Hathaway Bridge (May 2016). This site was located close to the Hathaway Bridge. Several old RCP (two layers of reinforcement) had been removed due to new construction taking place. (Fly over) Potential profiles were measured along longitudinal steel wires on selected pipes.

5.2 Visited Sites with Pipe Not Removed

Several sites were visited at which the RCP continue to be in service. The following paragraphs describe these sites. No concrete samples were obtained from these sites.

5.2.1 Madeira Beach Area (April 2016). Two sites were visited.

SR-666 (SB) NW side of Tom Stuart Causeway. Culvert outflows into Boca Ciega. The culvert drains out of a seawall. No potentials were measured at this site. A section of the pipe had marine growth (shell/barnacles). Pictures were taken and solution obtained.
Madeira Beach End of 127th Ave. E side of Gulf Blvd. This pipe drains out of a seawall. The crown was found be below high tide. The pipe was in fair to good conditions with a crack now visible. Potential and resistivity values were measured on this pipe.

5.2.2 Dunedin (April 2016). Two sites were visited.

End of Tilden St. W side of Bayshore Blvd. Draining into tidal beach. Potentials and Resistivity measurements were performed at this site. Concrete now shows cracks.
End of San Jose St. – W side of Bayshore Blvd. Draining into tidal beach. During the visit the crown was below high tide (although previously reported as above high tide). The recent visit took place during king tides season. This pipe has now a polymeric liner. Potential and surface resistivity was measured.

5.2.3 Panama City Beach area (May 2016)

Several sites were visited along Front beach road. The culverts discharge to the Gulf of Mexico. Round reinforced concrete pipes were found at five/six of these sites. At three other locations, box culverts were found: one with no reinforcement, one reinforced single box and a double box. During day one of the visit, several of the sites were either fully covered with water (due to high king tides) or more than 90 percent covered with waves breaking that wetted the whole pipe, thus these sites were revisited on the second day. During the second day, reinforced concrete pipes at two of the sites re-visited were mostly covered with water. Potential profiles and resistivity values were measured on round RCP not fully covered with water.

5.3 Typical Measurements

At selected sites soils samples were collected, Table 21 shows the resistivity values measured both as received (exposed outdoor during dry season) and also upon adding tap water (column named wet). For selected cases the Sulfate content was measured, as well as the chloride content was measured for the soil of two sites. The resistivity of the wet soil was less than 200 ohm-cm at four of the sites (five values but two are from Indian Rock site).

Table 21 – Measurements performed on collected soils.

	resistivity in Ω-cm		Sulfate	Chlorides
Location	As received	Wet Soil*	(ppm)	(ppm)
Zolfo Springs	> 1×106	5800	8.9	29.6
Dania Beach	> 1×106	120	130.8	1820
Hollywood	640	180		
Indian Rock - Outside Visit 1	5600	160	34.9	
Indian Rock - Inside Visit 2	> 1×106	175	846	
Tallahassee	45000	11000		
Hudson (US19 and SR52)	> 1×106	6500		
Dunedin (Tilden Rd)	5460	198		

Solutions were obtained a ten of the sites visited during 2016. Table 22 shows the chloride concentration measured and the resistivity obtained (using a soil box). The chlorides were highest at Madeira Beach (127th Ave.) and Dunedin (Tilden St.) and with the lower resistivity. Interestingly, the sites at Panama city beach area had a wide range of values.

Table 22 – Chlorides and resistivity measured in solution (sites visited 2016).

	Site	Chlorides ppm	Resistivity ohm-cm
1	127 Ave. Madiera Beach	20436.9	23
2	Tilden St. Dunedin	19070.5	24
3	SR 666 Tom Stuart Causeway	15433.7	28
4	San Jose Park, Dunedin	11779.0	34
5	17942 Front Beach Rd PCB	434.4	690
6	Seagull villa #73 PCB	36.1	5170
7	16691 Front Beach Rd PCB	40.2	5100
8	12213 Front Beach Rd PCB	966.4	340
9	Surfside Christian Ret.	1941.1	180
10	#2 Site 5/9/16 Pineapple villas	3560.4	115

Chloride profiles were measured on concrete obtained from Miami Beach and Dania Beach Marina. On a couple of other places the chloride concentration was measured in one case close to the reinforcement, and for two samples at the concrete close to the exposed surface.

5.3.1 Miami Beach (Alton Road)

Figure 154 shows the 12 inch inside diameter pipe segment obtained during the site visit to Alton Road in Miami Beach. Figure 155 shows the potential profiles measured along each of the longitudinal steel wires. The potential values (measured against an Ag/AgCl electrode) measured along three of the longitudinal steel wires (L1, L7 and L8) suggest that corrosion was taking place. After additional exposure to the lab humidity the potential on all longitudinal steel wires shifted toward more positive values.

Figure 154 – Reinforced concrete pipe removed from Miami Beach (Alton Road).

Figure 156 shows the chloride concentrations measured from both sides on two concrete pieces that were milled. The chloride concentration at 1.25 cm from the surface ranged between 3 and 3.5 kg/m^3.

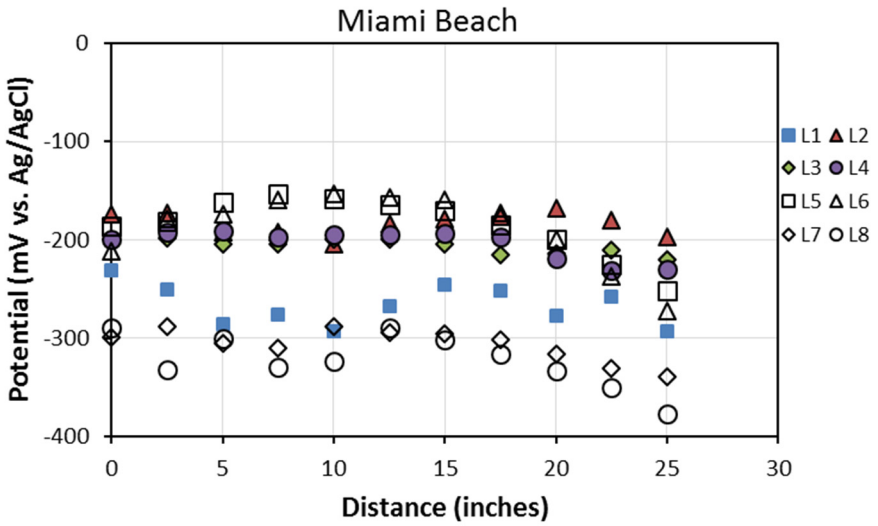

Figure 155 – Potential profile along longitudinal.

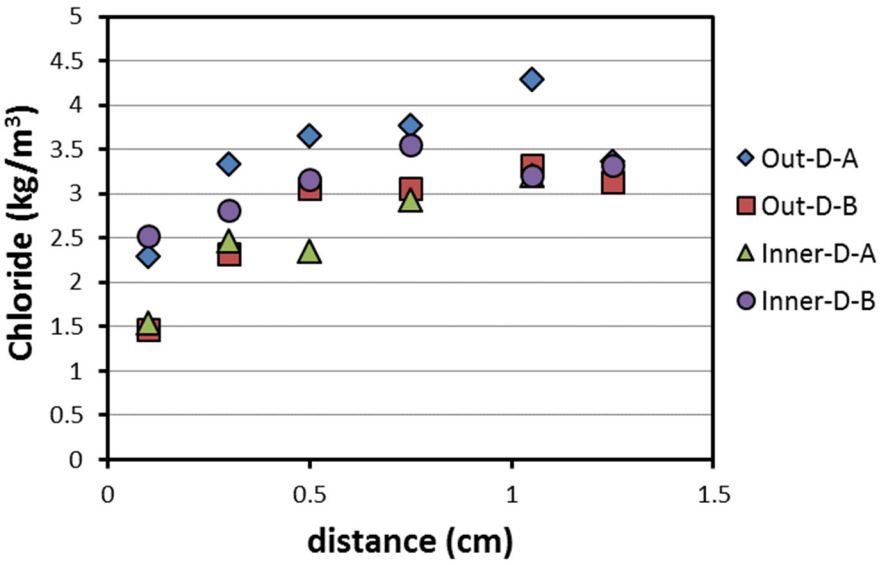

Figure 156 – Chloride profile for Miami Beach specimen.

5.3.2 Dania Beach, at Dania Beach Marina

The marina at Dania Beach was renovated during Fall 2013, two new buildings were added and all decks were replaced. As part of this new construction three RCP of 30 inch internal diameter were removed. The removed pipes were in direct contact with the intracoastal. Part of the pipe was subjected to wet/dry cycles from the tides. The potential profile was measured along selected longitudinal steel wires on two of the removed pipes. Two of the three pipes suffered some damage during removal and exposed several of the steel wire reinforcements. These

exposed steel wires were used to check continuity and as electrical connections. Figure 157 shows the potential profiles measured along the longitudinal reinforcements. Several small pieces were brought into the lab for forensic examination. Concrete was milled from the surface of both the inner and outer side of a pipe concrete piece. Chlorides were measured from the pulverized concrete. Figure 158 shows the chloride profiles obtained. At a depth of 1.4 cm the chloride concentration ranged between 6 and 7.5 kg/m^3.

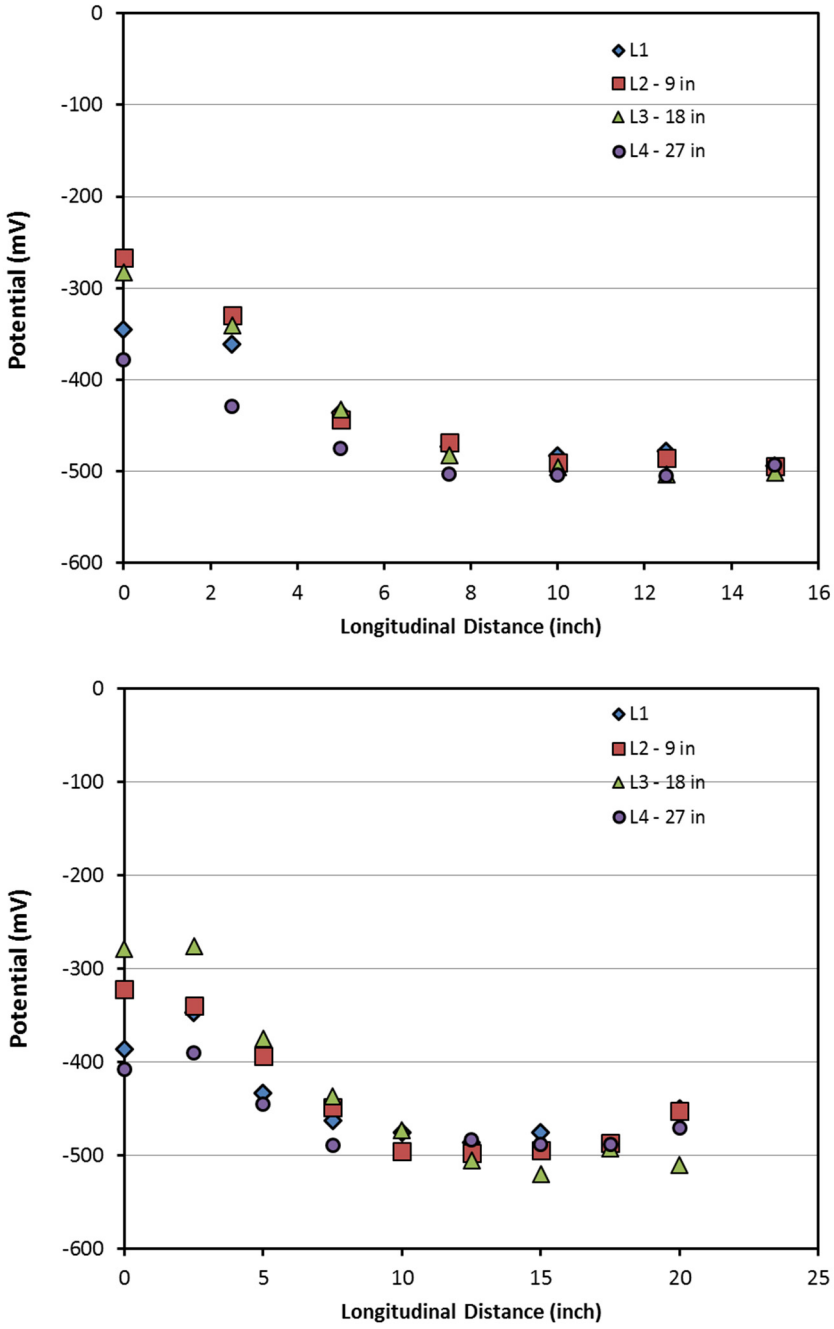

Figure 157 – Potential profiles measured along longitudinal wires (Dania Beach Marina).

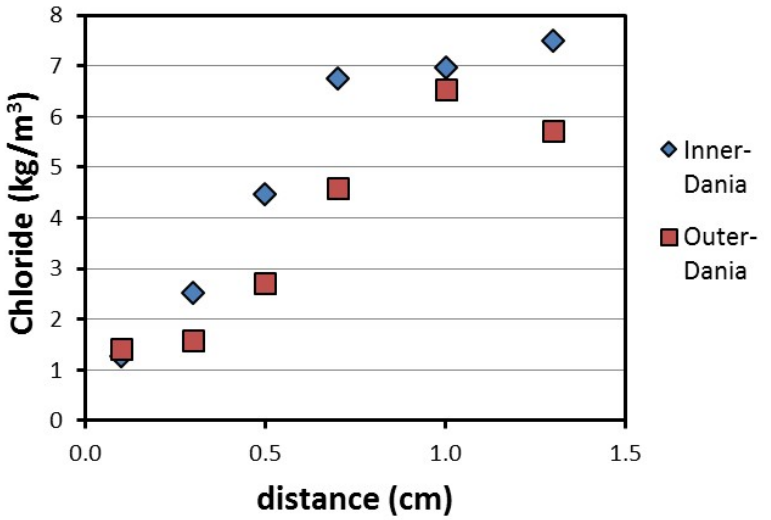

Figure 158 – Chloride profile from RCP at Dania Beach Marina.

5.3.3 Titusville Airport (pipes inspected at Apopka)

Three pre-world war II pipes had been removed from the Titusville Airport and transported to Rinker Materials' Apopka plant. These three RCPs were characterized during a field trip that took place December 2014. It rained the night of December 21 2014 (the night before the visit to the site), thus this might have affected the moisture content closest to the surface.

The pipes were labeled A, B and C. Pipe C had the smoother concrete surface (least aggregate exposed), followed by Specimen A and the one with the most aggregate exposed was Specimen B. The outside diameter of the pipe was 77 cm (30 inches), the pipe thickness was found to be between 7.2 and 7.4 cm. The concrete cover measured from the inner-side averaged 2 cm.

Moisture meter readings: On the areas with aggregate exposed the moisture meter did not have a good contact, and the values measured on the relative scale of the meter ranged between 2 and 4. On the smoother areas the values were between 8 and 10. The maximum reading on the reference scale is 20.

Readings with the surface resistivity were performed with a 3.8 cm (1.5 inches) spacing between electrode probes. The average apparent resistivity value measured was 55.8 and the minimum apparent resistivity value measured was 42 kΩ-cm. It is likely that the measured values are affected to some extent by the concrete moisture content, the reinforcement and the finite thickness of the concrete. This high values are typical indicator of a concrete that is quite dry and prepared with low water to cement ratio. Typical saturated concrete bulk resistivity for low water to cement concrete ranges between 10 and 15 kΩ- cm.

The potentials of the reinforcing steel were measured vs. a saturated calomel values, and all measured values were made along several of the longitudinal reinforcements. The potential values measured ranged between -30 mVsce and -130mVsce. The average values for specimen

A was -85 mVsce, B was -103 mVsce, and C was -63 mVsce. The plots on Figure 159 display the potential profiles measured on each pipe. All measured values suggest that either there is no on-going corrosion or that there is a very low probability that corrosion is taking place.

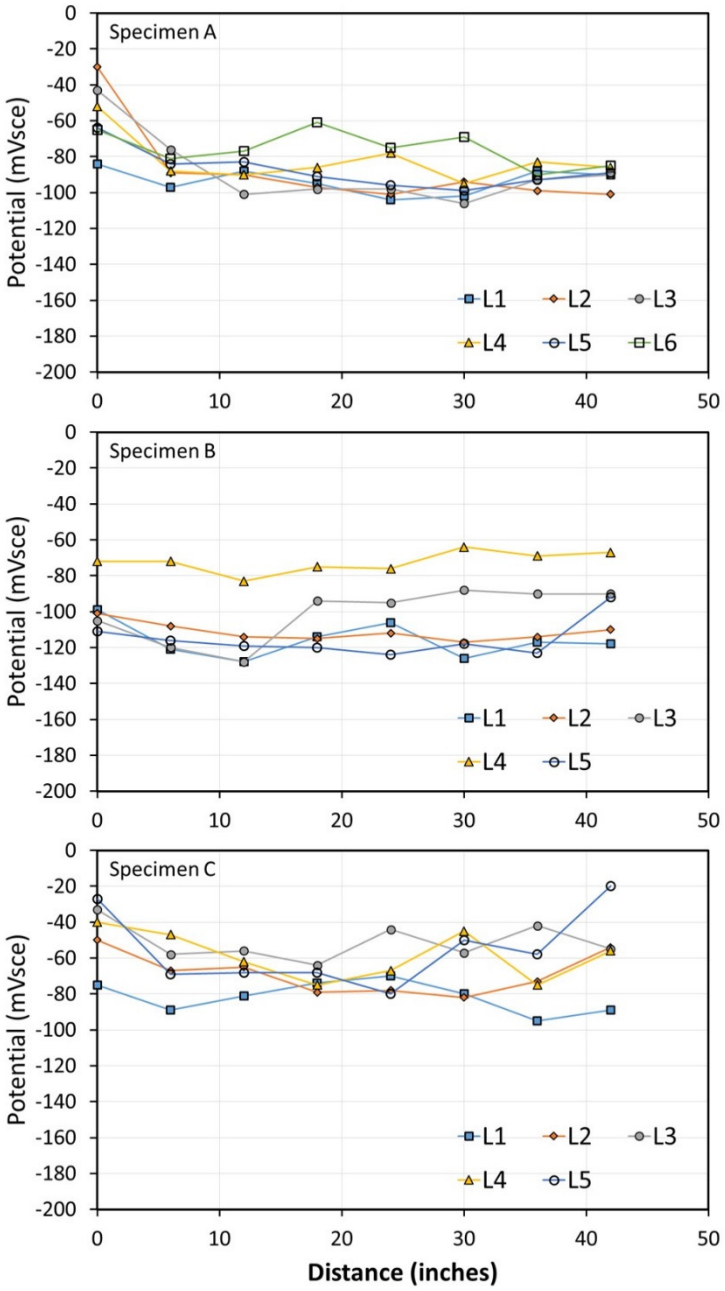

Figure 159 – Potential profiles measured on pipes taken from the Titusville Airport.

5.3.4 Indian Rock Beach, FL

Figure 160 show plots of the potential values measured along selected longitudinal reinforcements on the RCPs at Indian Rock Beach (Largo FL). The reference electrode used during this visit was an Ag/AgCl reference electrode. Based on the measured values two

longitudinal reinforcements (L7 and L8) appear to be active on sample A; whereas on Sample B four longitudinal reinforcements appear to be active (Along L3, L4 and L5 on the left side and L2 on the right side) based on the steel potential. Several concrete pieces were cut-off from the latter pipe (Sample B).

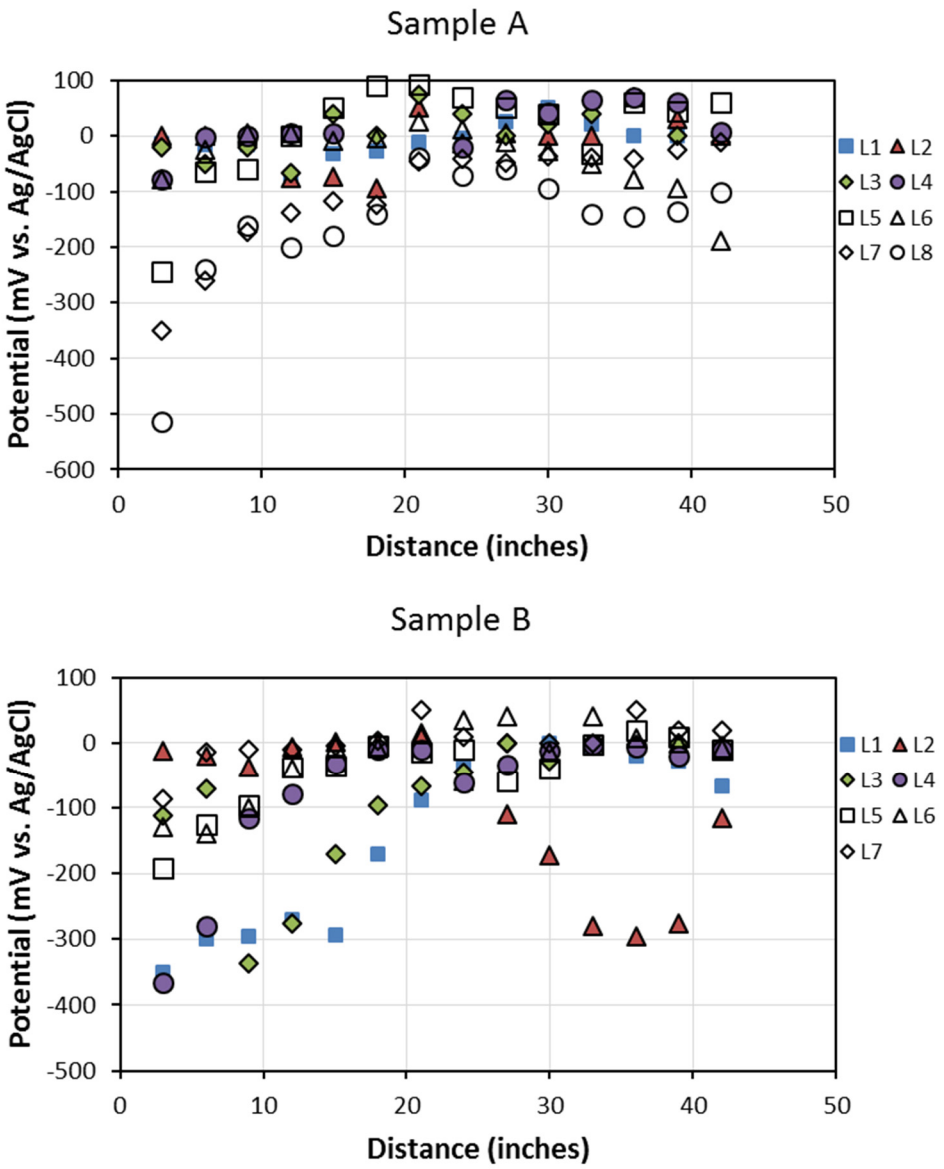

Figure 160 – Potential maps along the longitudinal reinforcements on samples at Indian Rock Beach.

5.3.5 Tallahassee

The steel potential values were measured along several longitudinal strands on three different pipes during the visit to the Tallahassee site. The steel potentials were measured against a copper sulfate electrode (CSE). Figure 3 below shows plots of the potential profiles measured

along the selected steel strands. Only pipe 2 appear to have a few active spots. A segment was cut off from pipe 2 for forensic analysis in the laboratory.

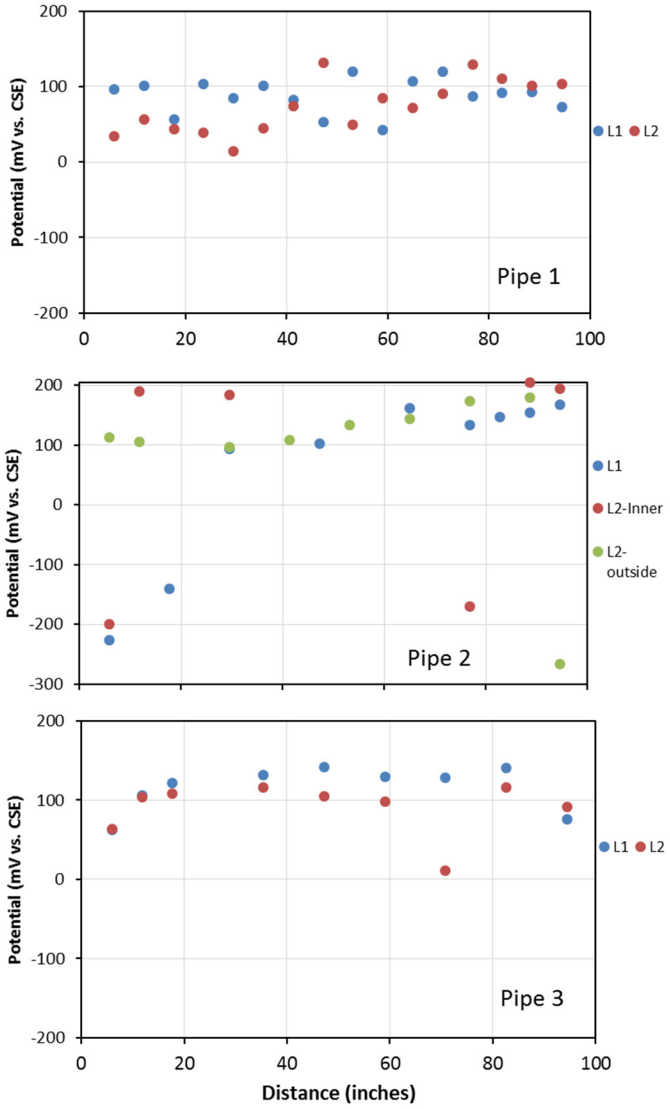

Figure 161 – Potential values along the longitudinal reinforcements on RCP (Tallahassee).

5.3.6 US19- SR52 (Hudson, FL)

This section describes the reinforcement potential values measured along selected longitudinal wires on pipes found during the visit to Hudson, FL. The potential values shown are vs. CSE in mV. Figure 162 shows a plot with the values measured on one of the elliptical RCPs named elliptical #1. The reinforcement potential values measured on the outside surface were 100 to 150 mV more negative than those measured inside the pipe. The visit took place in July during the rainy season, which might in part explain the potential difference. Figure 163 shows the potential values measured on a pipe labelled elliptical #2, and Figure 164 shows the potential values measured along the longitudinal on a round RCP pipe found a few miles from the two

elliptical pipes measured. Most potential values measured were more positive than -150 mVcse, which suggest that the reinforcing wire was likely not corroding. Segments were obtained from three pipes and brought to FAU SeaTech for forensic analysis.

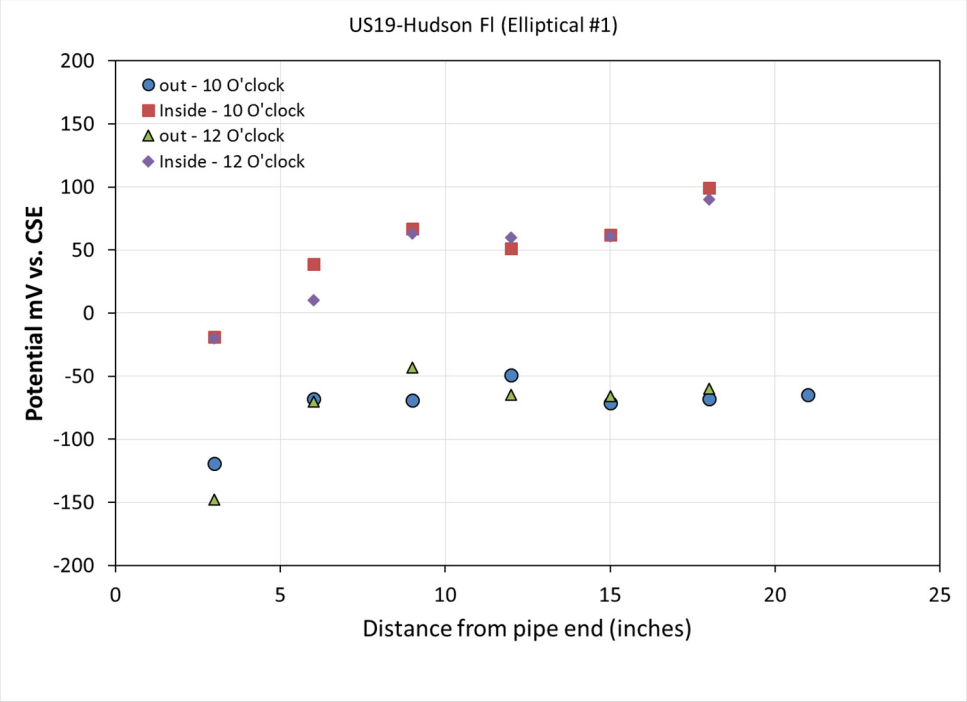

Figure 162 – Reinforcement potential along longitudinal wires (Elliptical 1).

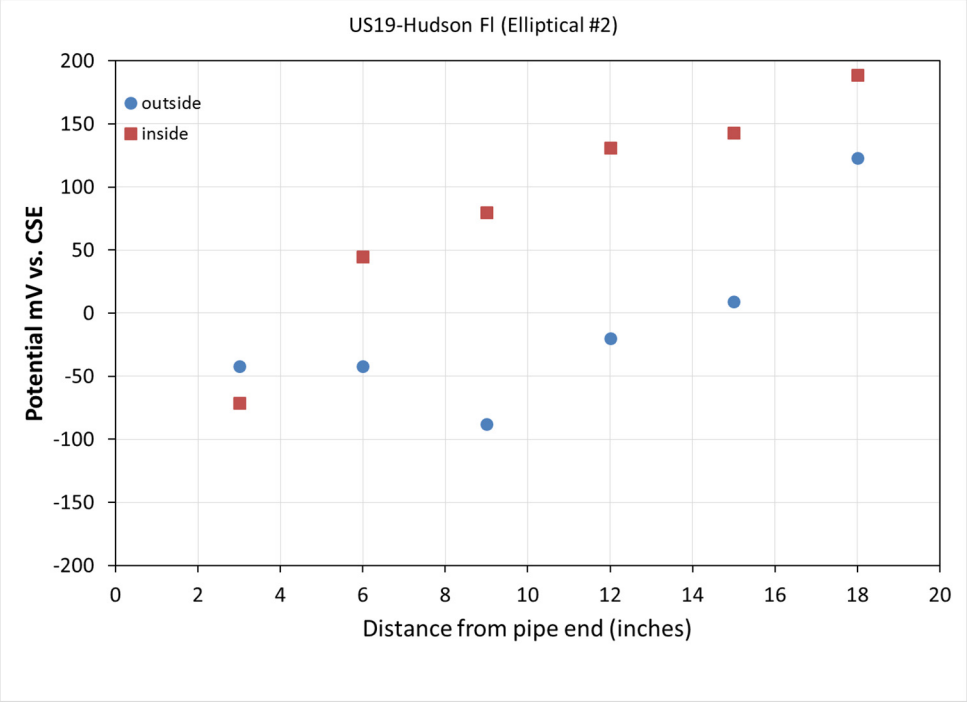

Figure 163 – Reinforcing wire potential along the top longitudinal wire (Elliptical 2).

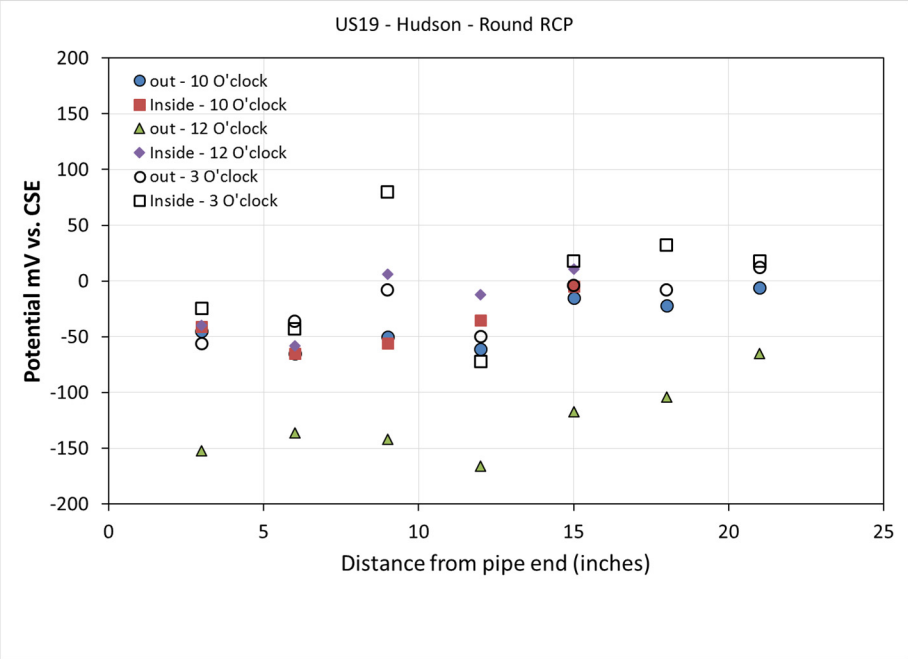

Figure 164 – Reinforcing wire potential along three longitudinal wires, on a round RCP.

5.3.7 Panama City

A good number of RCPs were found just before reaching the Hathaway Bridge (from land side). Two of the several pipes already removed were selected to characterize the steel potential along selected longitudinal reinforcements. The pipe inside diameter was 4 ft wide. These pipes have two wire meshes (inner and outer), similar to those found at Zolfo Springs. The potential series marked as in correspond to values measured on inner longitudinal reinforcements and out refers to values measured along a longitudinal reinforcement wire of the outer mesh. Figure 165 and Figure 165 show the potential profiles measured on two different pipes. The magnitude of the potential values suggest that corrosion is not taking place. A CSE reference electrode was used.

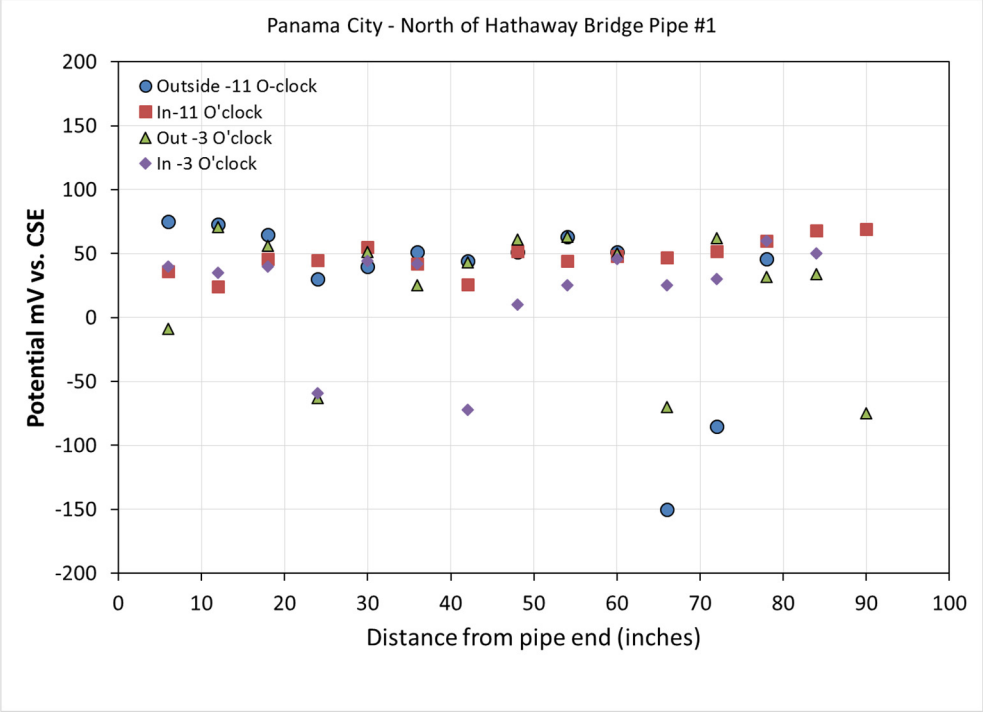

Figure 165 – Potential values along longitudinal wires on pipe #1 north of Hathaway Bridge.

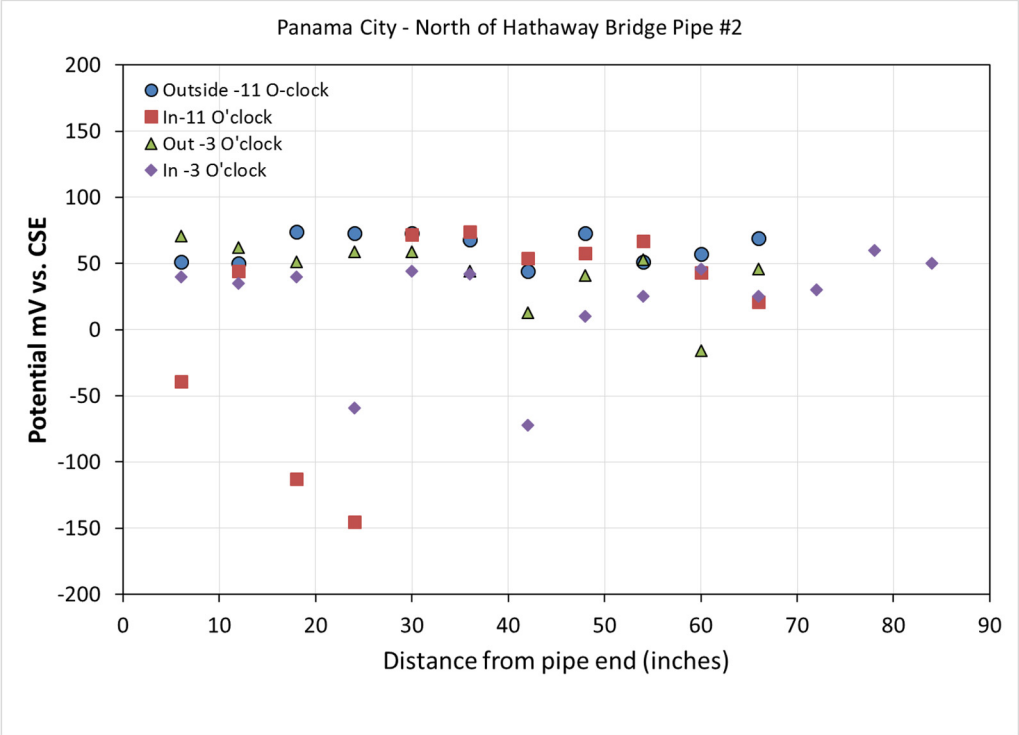

Figure 166 – Potential values along longitudinal wires on pipe #2 north of Hathaway Bridge.

5.4 Measurements on Pipes That Continue to Be in Service.

5.4.1 Madeira Beach

Madeira Beach sites were visited September 1999 (The pipes were then 39 yr for the one located at SR666 and 28 years old for the one at 127th Ave). By May 2016 these RDPs were 56 years and 45 years old respectively.

The two pipes located along SR666 were visually inspected, but no potential measurements were made as no portion of the pipe outer surface was exposed outside of the seawall. Potential measurements were performed on pipe located on 127th Ave that discharge to the intra-coastal. Figure 167 shows on the left picture one of the pipes at SR666 and on the right pictures of the pipe at 127th Ave. Marine growth was observed on the pipes at both sites. Upon inspecting the pipe along SR666, the inside of the pipe showed a crack and a rust stain was observed (see picture inset on the left). The pipe on 127th Ave had been cored during the visit in 1999, the top view of the pipe shows also a crack that extended more than 10 cm. Drilling was necessary to make an electrical connection (see inset in Figure 167).

Figure 167 – Pictures of pipes found in Madeira Beach, FL (Left – SR-666, right –127th Ave).

Reinforcement potential values along three longitudinal wires were measured for the RCP on 127th Ave, Figure 168 shows the measured potential values. The magnitude of the potential values suggest that corrosion is taking place, and possibly under mass transport (as at some locations the potential was more negative than -0.6 Vcse). The water level was quite high due to seasonal high king tide and covered a good portion of the pipe. Thus, oxygen concentration might be low at the reinforcement depth for the portion of the pipe where the concrete is highly moist. A crack was observed on this pipe along one of the longitudinal steel wires (above water). This pipe was previously visited in 1999 and was reported to be in good condition. A core was obtained during the previous visit that was not filled (see pictures). Other than the visible crack the pipe appears to be in good condition.

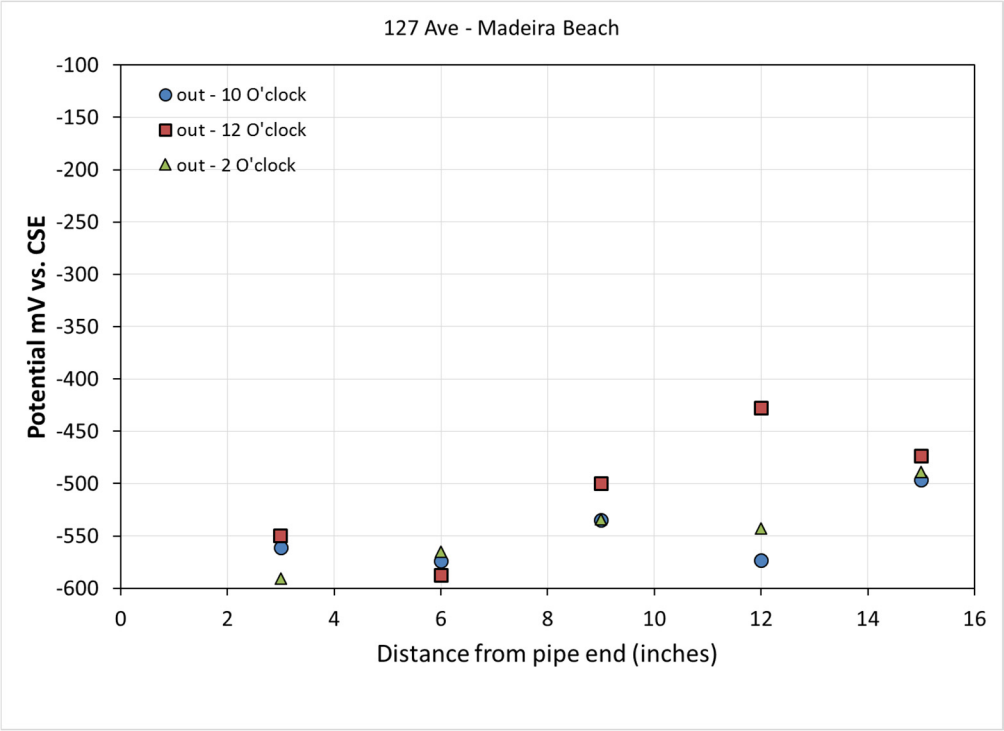

Figure 168 – Potential values along longitudinal wires measured on pipe at 127th Ave. Madeira Beach, FL.

5.4.2 Dunedin

The sites visited in Dunedin were previously visited on February 2000. The pipe at the End of Tilden was 42 yr old and the RCP at the end of San Jose St was 43 yr). These sites were revisited in May 2016. The pipes at Dunedin are now 58 yr (End of Tilden St.) and 59 yr (End of San Jose St.)

One pipe is located on St. Jose Park (end of San Jose St.) and during day one was fully covered with water due to high tide. During day 2, reinforcement potential measurements were performed. This pipe had the most amount of damage during the previous visit. A liner has now been installed on this pipe, and the average resistivity measured from the outer surface was 29 kΩ-cm. An electrical connection was made to the reinforcing steel. See Figure 169. The measured steel potential values (shown in Figure 170) suggest that the reinforcing wire mesh continues to corrode.

Figure 171 shows the pipe condition for the RCP located at Tilden St. Some of pictures show red rust stains inside of the pipe, and one of the inset pictures show that there is a crack several cm long. Figure 172 shows the potential values measured along the longitudinal wires on the pipe located at Tilden St. The measured values suggest that the reinforcing steel mesh is likely undergoing corrosion. No portion of this pipe was immersed during the visit. The resistivity measured on the inside of the pipe range between 1 kΩ-cm and 6 kΩ-cm.

Figure 169 – RCP located at San Jose Park (Dunedin, FL).

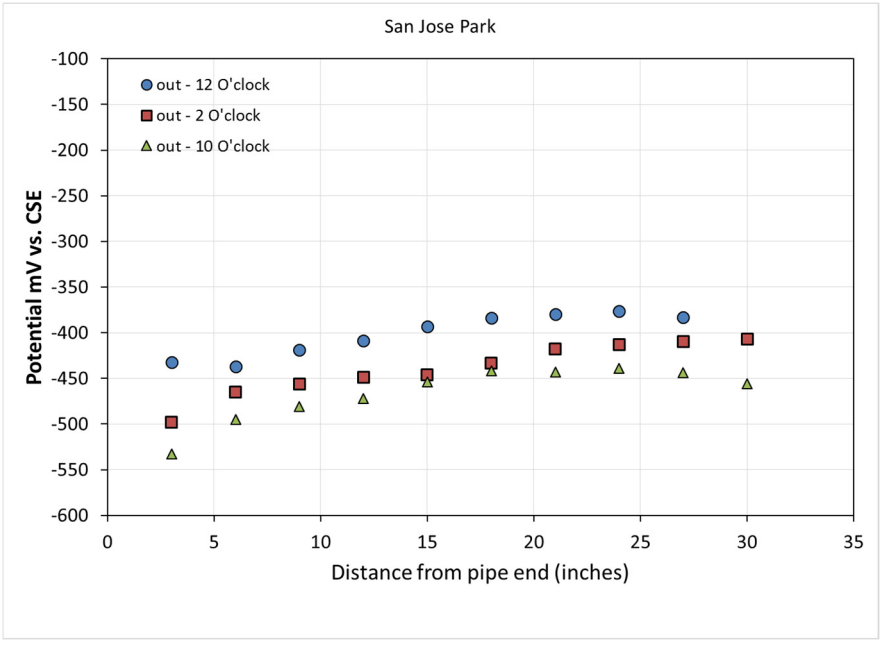

Figure 170 – Potential values along longitudinal wires at St. Jose Park pipe (Dunedin FL).

Figure 171 –RCP found at Tilden Street (Dunedin, FL).

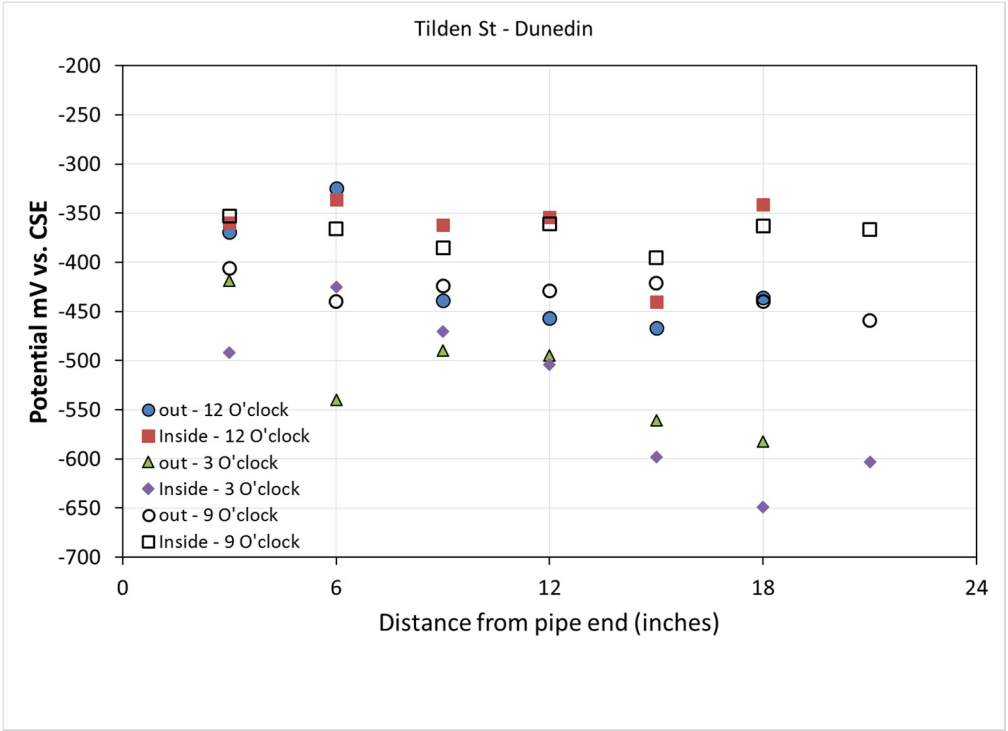

Figure 172 – Potential values along longitudinal wires at Tilden St. pipe (Dunedin, FL).

5.4.3 Panama City Beach Area

5.4.3.1 Sugar Sands Site

A 24” diameter pipe discharging into the Gulf of Mexico was found at this site. Figure 173 shows a couple of pics of the RCP found at this location. Reinforcement potential values were measured along two longitudinal wires. The resistivity measure on the top side of the pipe was 14 kΩ-cm. One of the spiral wires closest to the surface was exposed and at some location had lost significant section and was now 2 mm. This exposed wire was used to do the electrical connection. The reinforcement potential values range between -450 and -550 mVcse. Figure 174 shows the potential profile. The potential values suggest that corrosion is on-going.

Figure 173 – RCP found at location close to Sugar Sands Inn.

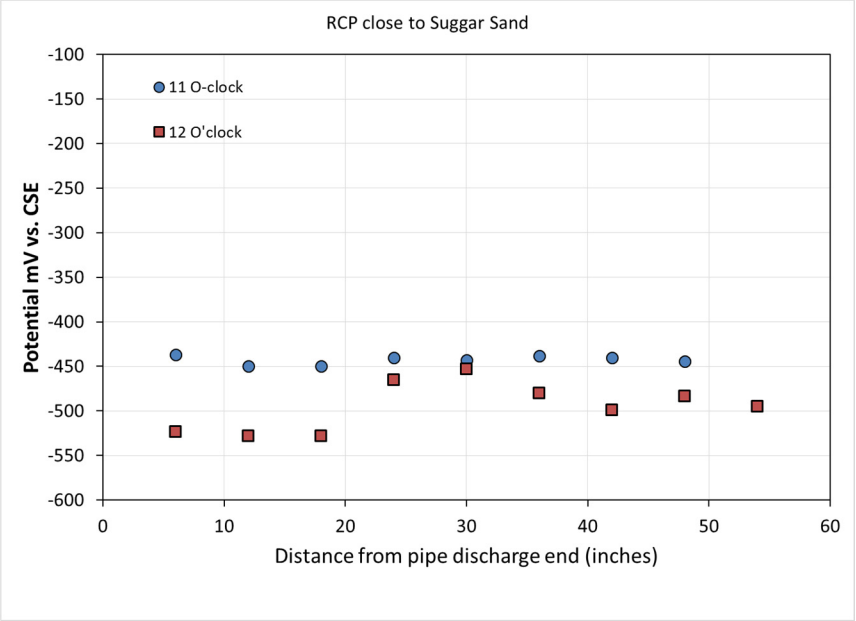

Figure 174 – Potential values measured along longitudinal wires on RCP at Sugar Sand site.

5.4.3.2 PCB 17942 Front Beach Road Site

A 36” diameter pipe was found at this site. A liner is installed on the inside of this pipe. The concrete cover was 1.5” from the inside and 2.5” cover measured from the outside. Figure 175 show the potential profiles measured along selected longitudinal wire reinforcements. The potential values were more negative than -400 mVcse, suggesting that corrosion of the steel is taking place. The lower resistivity measured on this pipe was 12.6 kΩ-cm and the largest measured value was 40 kΩ-cm.

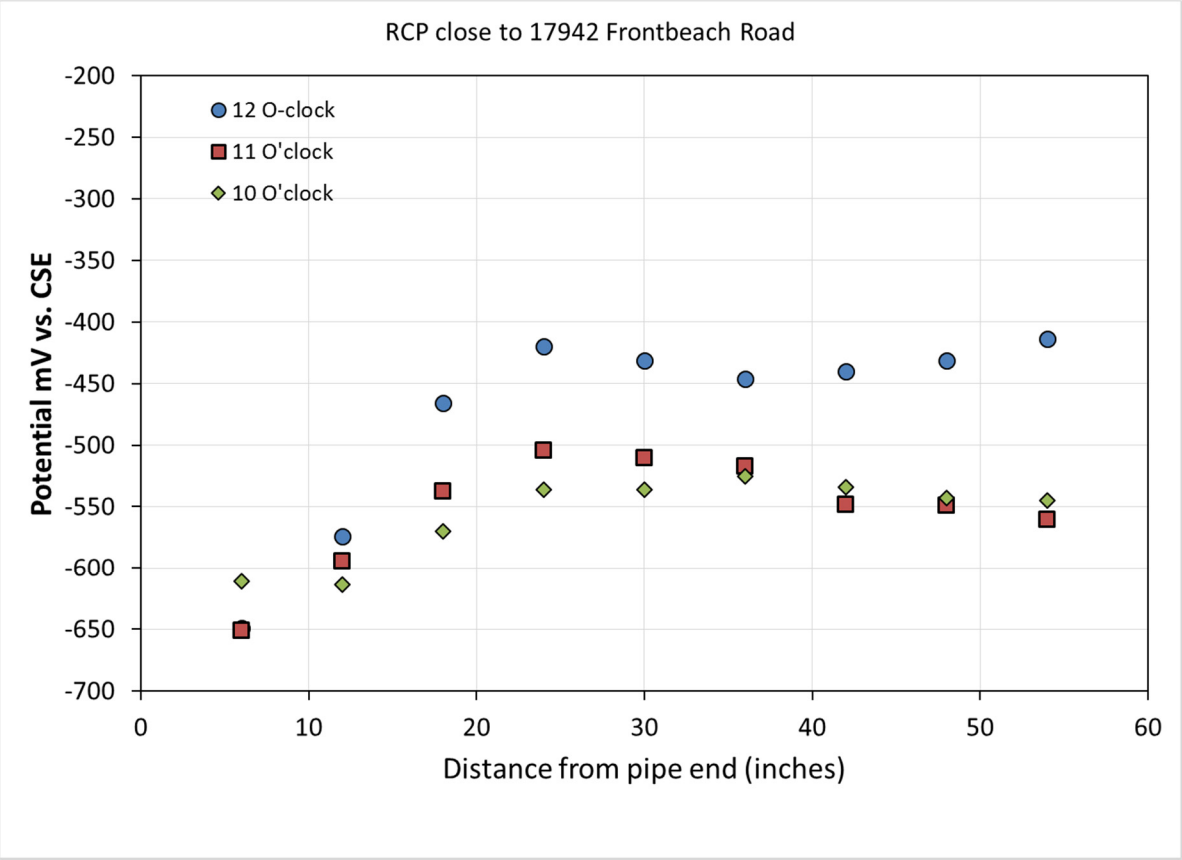

Figure 175 – Potential values measured along longitudinal wires on RCP close to 17942 Front beach Road Site.

A 3-ft diameter RCP was found close to Public Beach entrance #73, but during both visits the water level cover the whole pipe. No exposed steel was observed, no liner is installed on this pipe. The concrete resistivity ranged between 9.4 and 14.5 kΩ-cm. No potential measurements were made at this site.

5.4.3.3 16691 Front Beach Road Site

The RCP found at this site was 4 feet in diameter. This RCP has a dual wire cage. The cover from the inside to the inner cage was two inches and the concrete cover from the outside surface to the outer cage is one inch. The potential profile corresponds to values measured along a couple of the outer longitudinal wires. A concrete resistivity of 2.5 kΩ-cm was measured at a few location and was the lowest measured value. At a different location the concrete resistivity was 30 kΩ-cm. Figure 176 shows that all potential values measured were more negative than -350 mVcse, suggesting that the steel wire mesh is undergoing corrosion.

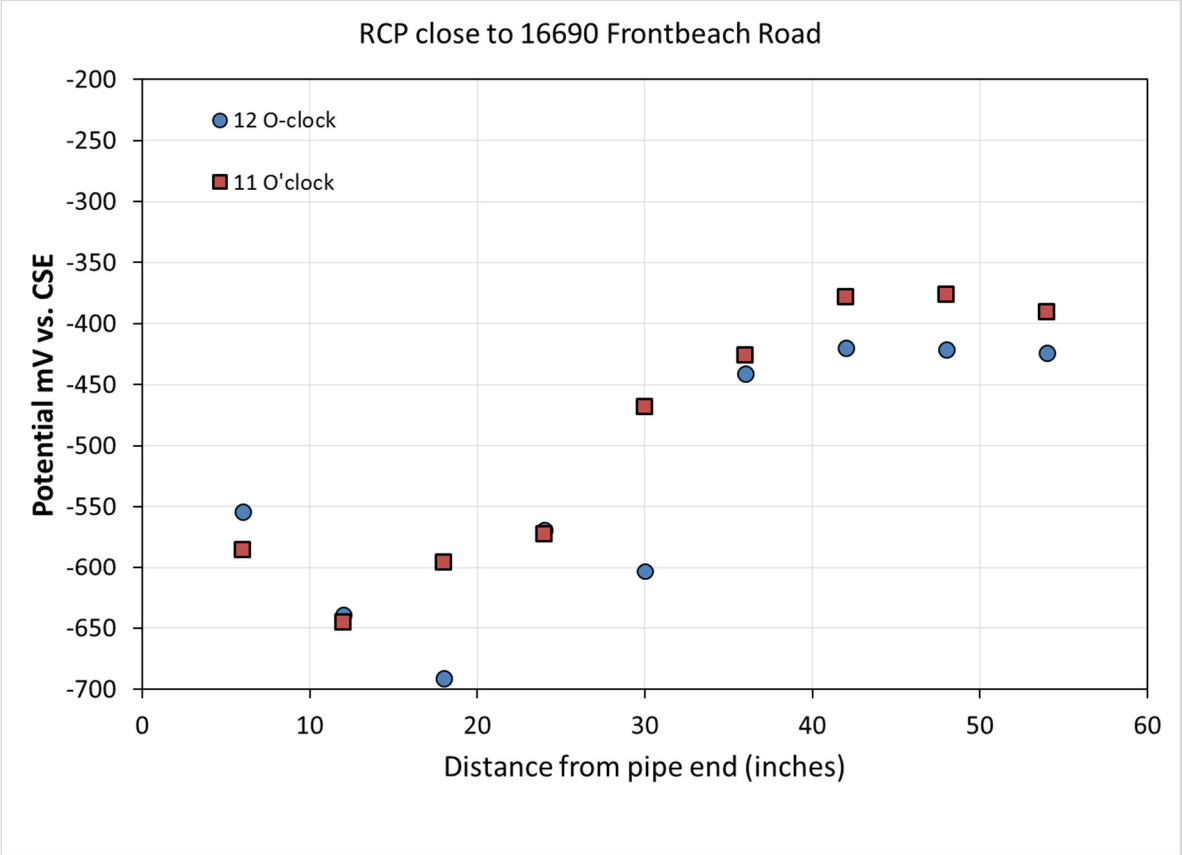

Figure 176 – Potential values measured along longitudinal wires on RCP close to 16690 Front Beach Road Site.

Three other sites were visited that had round RCP. At two sites (14531 Front Beach Rd and 14415 Front Beach Rd) the pipes were completely covered with water during both visits. The pipe at site close to 14415 Front Beach Road is newer than the pipes at all other visited pipes, it appears that was recently extended to discharge closer to the water. A square structure surrounds the round pipe. The third site at 11211 Front Beach Rd and was fully covered water during day one, and due to work being perform close by and a strong smell found during the second visit. It was decided to only perform resistivity measurements, the resistivity values ranged between 22 and 34.9 kΩ-cm.

5.5 Forensic Examination

5.5.1 Dania Beach Marina

During Fall/2013 the Dania Beach Marina underwent a major upgrade (a new building and added dockage), as result of this several 30" internal diameter pipe segments were removed. One of the pipes removed during construction to enlarge the marina was given to Rinker. The pipe has been in place for about 31 years at Whiskey Creek (Dania Beach Marina). On February 26, 2015 – A 6.6-ft. piece of 30-inch RCP was 3EB load tested (See pictures in Figure 177). A one-ft. by two-ft. cut-out was made prior to testing to examine the cross-section. Mild corrosion products were visible on some steel. Circumferential steel appeared to be 0.24 inch diameter at three-inch spacing, resulting in 0.18 sq.in./ft., which is the min. amount of steel area of a ASTM C76 Class III B-Wall 30-inch RCP. For this length, the design load is 22,300 lb. and the ultimate load is 33,000 lb. This pipe, after 31 years in inter-coastal water and missing a one by two feet section was loaded to 36,000 lb before a hairline crack was observed. The pipe developed a 0.01-inch wide crack at 42,000 lb, and the pipe eventually yielded at 51,600 lb. Intracoastal water level was above the pipe crown, according to the dock-master for most of the year.

Figure 177 – Pipe tested for 3EB.

During Fall/2013, two small RCP pieces were obtained from the removed pipes. The concrete was removed and the reinforcing steel exposed. Figure 178 and Figure 179 show the reinforcement surface condition. Figure 2 shows that the reinforcing wire had undergone significant corrosion. Figure 3 shows that the steel wire had only a couple of superficial rust spots.

Figure 178 – Reinforcement exposed from a small segment obtained from Dania Beach Marina site.

Figure 179 – Reinforcement exposed from a small segment obtained from Dania Beach Marina site.

5.5.2 Indian Rock (Close to Largo Florida)

Three RCPs were extracted during Fall/2013 at this site and replaced with new RCPs. Two of the removed pipes were available during the field visit that took place December/13, and one pipe was selected for cutting to obtain samples. Several sample pieces were obtained. The cut pieces were not forensic examined right away. A piece was forensically examined during Spring/2014 and two additional segments forensically examined during April 2015. This section includes pictures of the forensic examination for the latter.

Segments terminated during April 2015 are shown in Figure 180, Figure 181 and Figure 182. Figure 180 and Figure 181 shows that the reinforcement corroded completely on some areas and on other areas a significant cross-section had taken place. Figure 182 shows that the steel reinforcement had corroded significantly along one of the longitudinal wires, but not on the rest of the steel mesh.

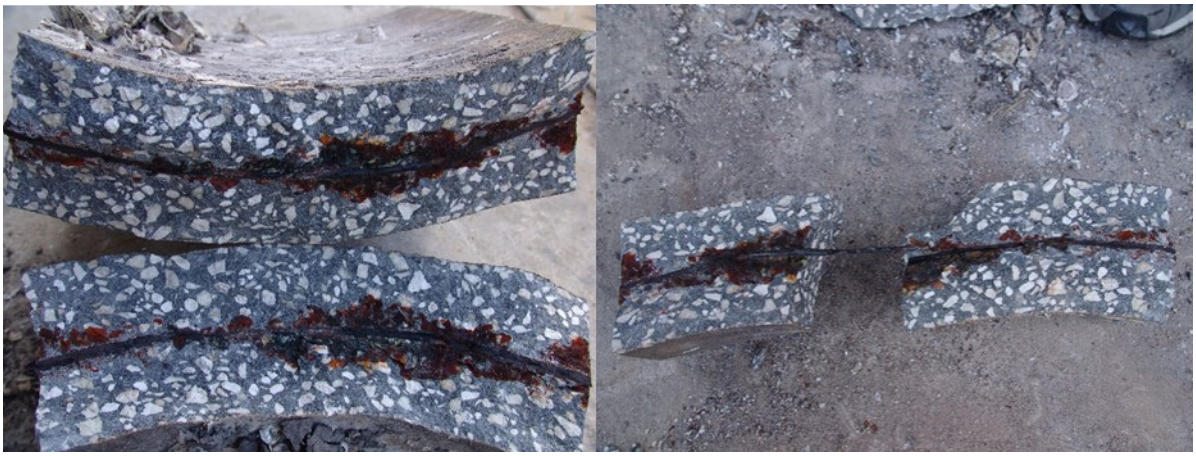

Figure 180 – After breaking the segment in two pieces. Significant cross-section loss observed on wire.

Figure 181 – Section with no solid steel wire

Figure 182 – Steel wire mesh removed from a different concrete segment from the same pipe

5.5.3 Alton Road – Small Diameter Pipe

A small pipe (12 inches internal diameter) segment was obtained from a Miami Beach project during summer 2013. Most of the pipe removed at the site was not RCP. The pipe was stored (exposed to lab humidity and room temperature) after removal from the site at the marine materials lab for more than a year. The segment had a portion of the mesh exposed to the lab environment. A piece of the RCP was cut-off. The steel wire was exposed for a portion of the mesh covered with concrete (i.e., the concrete was removed). Figure 183 shows the surface condition after removing the concrete. It is evident that corrosion took place, but no significant cross-section was observed.

Figure 183 – Removed concrete revealed that only surface rust was observed.

5.5.4 Apopka (Titusville Airport RCP)

Pre-World War II RCP 24-inch diameter pipes were removed during the re-construction of the Space Coast Regional Airport Taxiway B, Titusville, Florida, during 2013. Selected pipes were moved to Rinker concrete pipe plant in Apopka. The pipes were 4-ft. long, with mortar joints. It is estimated that the pipe segments are ~75 years young. Potential measurements were performed on these pipes during a site visit that took place December 2014. Rinker provided the picture shown below after a cut was made on one of these pipes. No signs of corrosion are observed from the cross-sections shown on Figure 184.

Figure 184 – Cross-section shortly after wet cut. No signs of corrosion are visible.

5.5.5 Tallahassee

A small piece of pipe was cut-off from a RCP extracted at this site. The segment cut was selected from an area where potential measurements were taken and a steel potential drop was observed. Upon removing the concrete it was found that corrosion had started and propagated locally. It is not clear why corrosion initiated at this section of the pipe. Figure 185 shows in the bottom row two pictures displaying the corrosion extent after cleaning the reinforcement. Significant cross-section was observed at several sites.

Figure 185 – Corrosion extent observed on the wire mesh from segment obtained at Tallahassee site.

5.5.6 US19 SR52

Several pipes were extracted and available for inspection at this site. The visit took place during Summer/2015. In general all pipes looked in good condition (except some damage that might have occurred during pipe extraction). Segments were cut from three pipes. This section shows the steel wire surface condition after removing the concrete for several concrete pipe pieces obtained from the US19 SR52 site. Figure 186 shows that corrosion initiated at several regions/spots but that no significant section loss was observed.

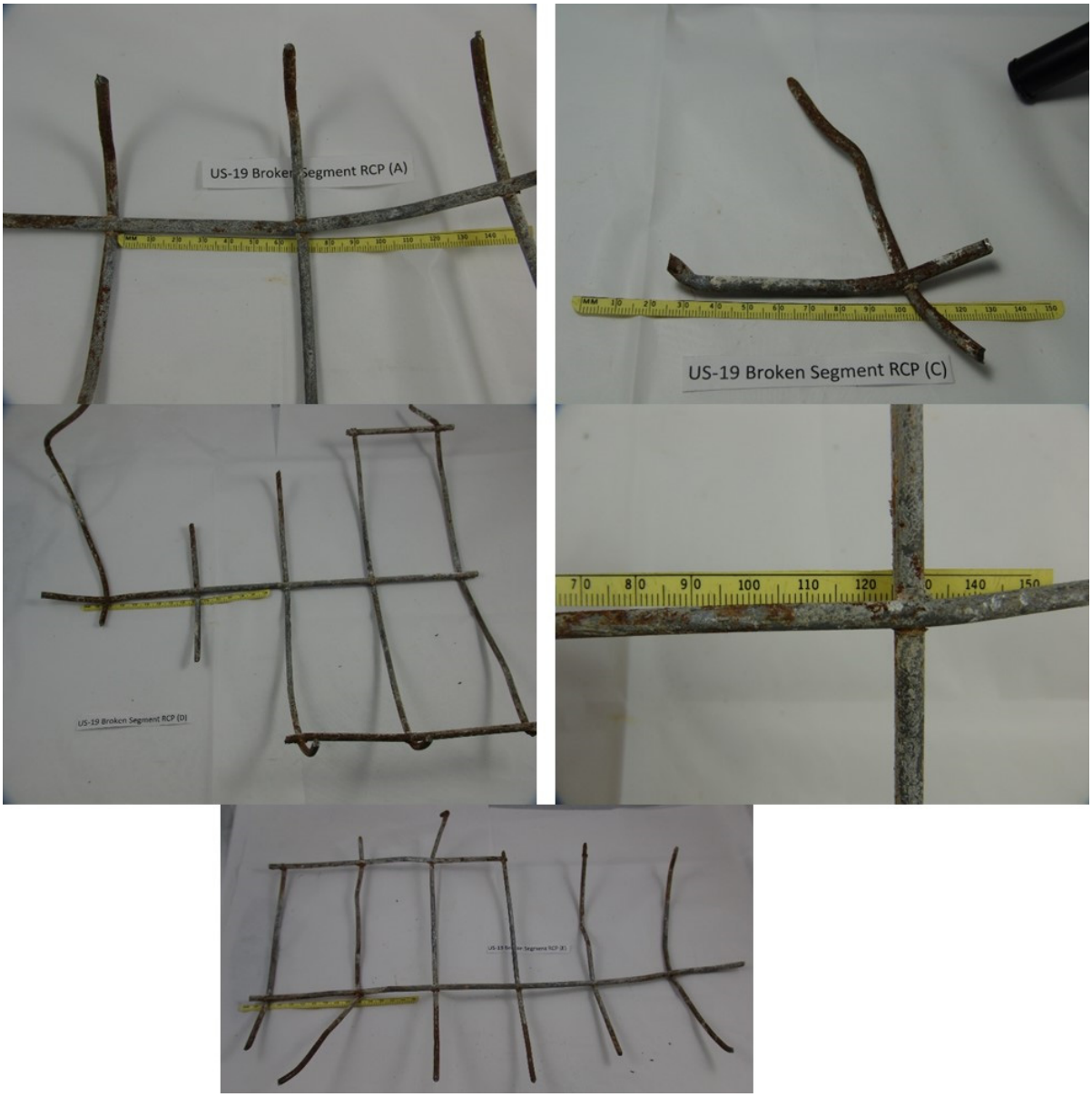

Figure 186 – Wire mesh after removing concrete on several segments.

5.6 3EB Testing on Ring Specimens

Recall that corrosion had initiated on the ring specimens. The ring specimens were exposed to high moisture environments for over 700 days during the corrosion propagation. The results chapter described the electrochemical monitoring that took place during this time. The ring specimens for which corrosion had initiated are subdivided in two groups: C and F. C specimens contain only OPC, these pipe segments have a larger concrete cover and more steel.
In one of the C specimens (CHH) corrosion was not accelerated, whereas on the other two C ring specimens (CS2 and CI2) additional chloride transport took place and corrosion was moderately accelerated. A small amount of corrosion is believed to improve the bond with concrete and this is what might have happened on specimen CS2 and specimen CI2. F specimens contain FA, smaller cover and smaller amount of steel. Corrosion was not accelerated on one of the F specimens (FI1), but additional chloride transport took place and a galvanostatic pulse took place for 3 week, so as to accelerate the corrosion on a larger steel area on specimen FS2 and specimen FS3). Rust stains reached the surface of the pipe at various locations (see pictures below), and also it was confirmed after removing the concrete to expose the steel wire.

During Fall/2015, six ring samples (approximately one foot wide, see Table 23) were taken from SeaTech to Rinker's facility at Apopka for 3EB modified testing, the manufacturer added three specimens from RCP recently produced. The manufacturer's ring specimens: R_A, R_B and R_C were of similar length and not exposed to chlorides. Table 23 shows the results of the test normalized per specimen length and diameter. All samples exceeded the D-load and the yield ultimate load indicated by the standard (when normalized per unit length and diameter). It is interesting to note that the yield ultimate load of all F specimens had the smallest percent over the minimum required value. This observation might be indicative that these ring specimens have lost some of its properties, particularly when compared to yield ultimate load observed on the R_ specimens that were not pre-corroded (top three values). Except for CHH, the other two C specimens had a yield ult-load comparable to the R_ specimens. The additional chloride transport on CS2 and CI2 allowed corrosion to initiate at additional regions, but no significant cross-section loss (see section below) was observed. This might allowed for an improved bond between steel wire and concrete.

Table 23 – Results of 3EB load tests on ring specimens.

Date of Test	Manufacturer	Rinker/ FAU ID	Dimensions (Inches)			D-Load (Lbs/Ft/Ft)		% Over Minimum	Yield Ult-Load (Lbs/Ft/Ft)		% Over Minimum
			Diam.	Wall	Length	Specified	Observed		Specified	Observed	
10/22/2015	Rinker	R_A	18	B	12	1350	**2367**	**75.3%**	2000	**3647**	**82.3%**
10/22/2015	Rinker	R_B	18	B	12	1350	**2613**	**93.6%**	2000	**3307**	**65.3%**
11/3/2015	Rinker	R_C	18	B	11.5	1350	**2240**	**65.9%**	2000	**3450**	**72.5%**
11/3/2015	DelZotto	CHH	18	C	10	1350	**2968**	**119.9%**	2000	**3048**	**52.4%**
11/3/2015	DelZotto	CS2	18	C	10	1350	**3040**	**125.2%**	2000	**3704**	**85.2%**
11/3/2015	DelZotto	CI2	18	C	10	1350	**3448**	**155.4%**	2000	**3576**	**78.8%**
11/3/2015	Rinker	FI1	18	B	9.75	1350	**2855**	**111.5%**	2000	**2453**	**22.7%**
11/3/2015	Rinker	FS3	18	B	10	1350	**2400**	**77.8%**	2000	**2792**	**39.6%**
11/3/2015	Rinker	FS2	18	B	10	1350	**2392**	**77.2%**	2000	**2408**	**20.4%**

NOTE: B and C under wall column indicates that C specimens had a thicker wall.

3EB tests results show (Table 23) that all C and F specimens surpassed the designed D-load and yield ultimate load even with corrosion initiated and propagated for close to two years (On four of the specimens, corrosion initiated at a larger area as additional chlorides reached the steel wire mesh). A couple of interesting observations can be said about the D-loads and ultimate yield loads (normalized by sample length and diameter) measured on ring specimens of type C and F. For specimens type C, the specimen subjected to high humidity all the time had the smaller increase when comparing the measured D-load and ultimate yield load. The yield ultimate load on specimen CHH was smaller than that observed on the CI2 and CS2 specimens. Although corrosion initiated on a larger steel area on CI2 and CS2 specimens, the corrosion propagation was modest and this likely improved the bond between the surrounding concrete and the corroding steel wire. For F specimens, the percent over minimum ultimate yield load ranged between 20 to 40 percent. The cross-section loss in one of the specimens was significant, and might have reached a point where the performance was comparable to that measured on the specimen with only a small area corroding. The third specimen FS2, had corrosion taking place on a large surface area of the steel, and similar to what was mention for CI2 and CS2, the bonding improved between the corroding steel and the concrete. For specimens not corroding, the ultimate yield load % over minimum ranged between 65 and 82%. Thus it appears that some reduction in performance due to corrosion (assuming similar early behavior) took place on F specimens.

After 3EB load testing, selected sections of the ring specimens were brought back to FAU-SeaTech for forensic analysis. The pages that follow contain figures with pics that were taken while performing 3EB load tests, pictures were taken while removing the concrete (for selected cases) and finally pictures that show the steel wire mesh after removing all the concrete.

5.6.1 Non-corroded Segment

Figure 187 shows a specimen that was about 14 inches long and that was not pre-corroded. The picture was taken shortly after the RCP specimen had been loaded and developed a crack. The concrete was not removed for this specimen.

Figure 187 – Rinker's specimen tested in November 2014.

5.6.2 C Group Specimens

5.6.2.1 Specimen CHH.

Corrosion was initiated via the migration method on this specimens and was stored in high humidity all the time (for about 2.5 years). Figure 12 shows on the left a picture of this specimen prior the 3EB loading test.

Figure 188 – CHH specimen prior to 3EB load test and on the right after starting to remove the concrete.

Figure 188 shows on the right a picture of the corrosion extent that took place close to the solution reservoir, shortly after the 3EB load test was performed and after removing some of the concrete covering the steel wire. The picture on the top left corner of Figure 189 shows that a section of the steel wire corroded away. The picture on the top right shows that at areas away of the solution reservoir there was no corrosion or a very modest amount. The picture on the bottom shows the steel wire after removing the concrete for the segment brought back to the lab.

Figure 189 – Pictures were taken after removing and while removing the concrete.

5.6.2.2 CI2 Specimen

Corrosion initiated after a few months of applying a galvanostatic hold on this specimen, and then it was immersed for over a year in tap water, then covered with sand for one year. A month before the 3EB load test, corrosion was accelerated by immersing about half of the specimen in sodium chloride and applying an electric field to drive additional chlorides into the concrete. Based on the pictures shown in Figure 190 and Figure 191 corrosion did initiate outside of the solution reservoir, but a moderate cross-section loss was observed. (It is possible that a section with more corrosion than that shown in here was not brought back to the lab)

Figure 190 – Steel wire mesh after removing concrete on two pieces from CI2 specimen.

Figure 191 – Close-ups of sites showing corrosion for steel wire from CI2 specimen.

5.6.2.3 Specimen CS2

This specimen was covered with sand once corrosion initiated. It was covered with sand for close to two years of corrosion propagation. The specimen was later brought in to the lab and electro-migration applied, so as to initiate corrosion at other sites besides the area under the solution reservoir. Figure 192 and Figure 193 show that on the selected segment brought back to the lab for forensic analysis; three longitudinal wires were not corroding and one longitudinal wire was corroding. On Figure 193, it can be observed that a portion of the circumferential wires showed signs of corrosion close to the corroding longitudinal wire. A modest cross-section loss took place.

Figure 192 – Steel wire mesh after removing concrete on a segment for CS2 specimen.

Figure 193 – Close-ups pics for sites showing corrosion of the steel wire from CS2 specimen.

5.6.3 F Group Specimens

5.6.3.1 Specimen FI1

Specimen FI1 was first exposed for 400 days immersed in water and then exposed outdoors covered with sand. Two segments were selected for forensic analysis from this ring specimen. Figure 194 shows that some corrosion took place on two of the longitudinal wires. Figure 195 shows a small spot where corrosion took place on the second steel wire mesh.

Figure 194 – Steel wire while removing the concrete on segment 1 of FI1 specimen.

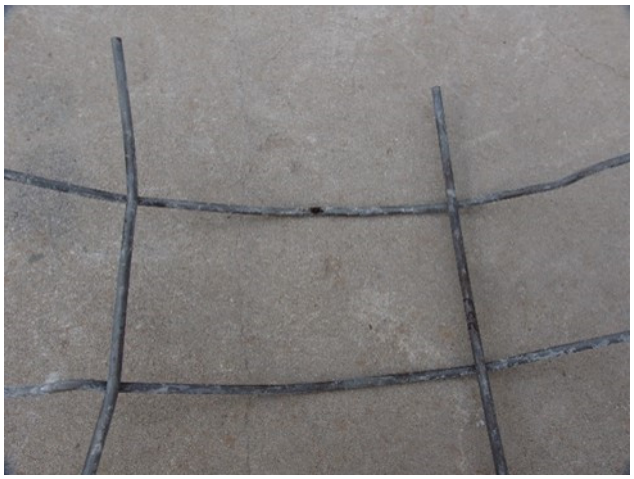

Figure 195 – Steel wire after removing concrete on segment 2 of FI1 specimen.

5.6.3.2 Specimen FS3

Corrosion initiated under the reservoir after a few weeks on Specimen FS3. This specimen was subsequently covered with wet sand for about two years, during this time corrosion likely continued. Specimen FS3 and specimen FS2 were selected for exposure to additional chlorides via electromigration (via an electric field), followed by applying a constant small current directly to the steel wire mesh to accelerate corrosion. Figure 196 shows specimens FS3 upon completing the 3EB load test. Figure 197 shows the corrosion extent on a segment selected to expose the wire mesh. A moderate amount of corrosion took place on a portion of steel reinforcement.

Figure 196 – Specimen FS3 after 3EB load test. Note the various rust spots.

Figure 197 – Steel wire upon removing the concrete on a segment (Specimen FS3).

5.6.3.3 Specimen FS2

Figure 198 shows that corrosion products bleed/reached a significant surface area on Specimen FS2. After the 3EB load test part of the concrete was removed to assess the steel wire condition. Figure 199 shows dark green corrosion products at the reinforcement and concrete reinforcement trace upon removing the concrete, and some areas showing red rust. Figure 200 show significant penetration into the concrete of the corrosion products that did not cause cracks. Figure 201 and Figure 202 showed that red (dark or light) color was observed upon removing all the concrete and allowing for a few days to pass.

Figure 198 – Specimen FS2 prior to 3EB load test. Note the various rust spots.

Figure 199 – Partial concrete removal after 3EB test (FS2).

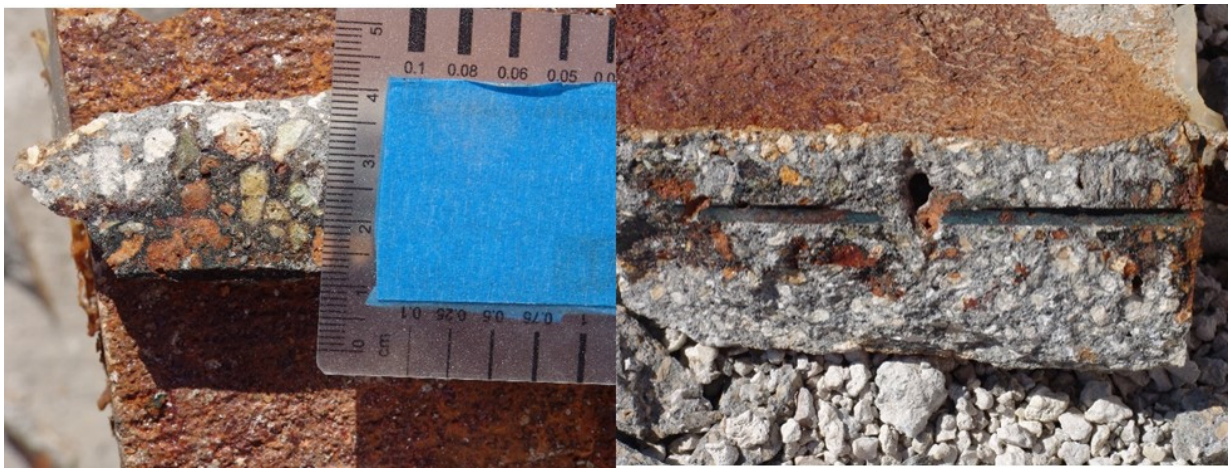

Figure 200 – Penetration into the concrete from the corrosion products (FS2).

Figure 201 – Partial and full concrete removal exposing steel wire mesh (FS2).

Figure 202 – Close-ups of selected sites where significant cross-section took place (FS2).

Figure 199 to 202 show certain similarity with what was observed on a couple of the forensically analyzed sections obtained from the Indian Rock site (Figure 180 to 182). The corrosion was not as severe/advanced on specimen FS2 when compared to the steel removed from the segment shown in Figures 180 to 182 (Indian Rock pipe), which was not longer there at some locations.

Chapter 6 – Conclusions

o The time to allow the initiation of corrosion varied from a couple of days to several months. The time range was not just as a function of the applied method, but also the type of concrete (i.e., resistivity, diffusivity, porosity) and concrete cover.

o Although specimens from type F RCP contained Fly ash showed lower porosity and D_{nssm}. The higher resistivity and smaller concrete cover allowed the reinforcing steel to initiate corrosion in a shorter period of time than specimens from type C RCP.

o All three approaches used to accelerated chloride transport allow to shorten the time to corrosion initiation.

o Specimens exposed to 95% R.H. - 98% R.H. did not experience a reduction in corrosion rate even after a prolonged exposure (1000 days), i.e., no significant mass transport (no O_2 depletion) effects were observed. This is possibly due to high concrete porosity and/or due the size of the corroding area. A significant potential drop (shift to more negative values) during the exposure to high humidity was observed on specimens (approximately 300 mV) that had a potential upon corrosion initiation from -200 mVsce - to -350 mVsce.

o There was no decrease in corrosion rate observed on specimens (both type F and C) that were covered with saturated sand. The potential drifted to more negative potentials during these exposures.

o The specimens which were immersed in water with small cover thickness shows a significant shift in potential (-538 mVsce to-633 mVsce) at a faster rate (for specimens of both types F and C). However, no change (reduction) in corrosion rate was observed.

o The potential and apparent corrosion evolution results, observed during the accelerated corrosion test were influenced by a combination of changing reaction kinetics as the corrosion of the reinforcing steel progressed and were also influenced by the different propagation environments (i.e., high humidity, covered with saturated sand).

o Corrosion was usually observed on lab specimen under the reservoir area at the intersection between the longitudinal and transverse reinforcement. Except for one case, no cracks were observed on the lab specimens that were forensically analyzed.

o Significant cross-section loss was observed on several specimens for both types of lab specimens.

o The research results presented above confirm that under certain circumstances corrosion propagation can take to the extent that there is no longer reinforcement without generating the typical corrosion cracks. This appears to take place for situations in which the concrete is kept under high moisture conditions. This was found on lab observations (e.g., Specimen F1 and Specimen F2), ring specimens (FS2 and FS3). It was later confirmed via forensic examination of samples obtained from the field (Indian Rock site).

o However, if the concrete is exposed to wet/dry cycles, cracks could develop which could accelerate corrosion and could allow water infiltration or exfiltration. Such situation was confirmed via field observations for pipes that continue to be in service. Some of these pipes are 40+ years in service exposed at Madeira Beach and Dunedin. Similar observations were seen at a couple of sites visited in Panama City Beach area. Thus duration of exposure and wet/dry appear to be important parameter that lead to cracks after corrosion has propagated for several years.

o For the pipe diameter tested, both the D-load and Yield ultimate load exceeded the minimums by at least 20% (in the case of the ring specimens F-type), and in some cases exceed it by >80%. The corrosion extent on the tested pipes ranged from localized to spread but the cross-section loss was moderate except on two F ring specimens that were subjected to additional chloride transport.

o Tests performed in this study confirms the high porosity and concrete cover distribution of dry cast steel reinforced concrete pipes and the roll that this porosity plays in the transport of chlorides and other contaminants. Under these conditions, the time to corrosion initiation could be compromised (less than predicted by the FDOT actual model) even under natural exposure (i.e., not accelerated chloride transport).

o However, because of apparent over design, corrosion of the reinforcement on dry cast pipes may be present and the pipes can still maintain the physical requirements of the D-load testing of ASTM C76. This would give an added assurance that the service live based on corrosion initiation can be achieved.

References

1. D. W. Cerlanek, R. G. Powers, "Drainage Service Life – Performance and estimate," State of Florida Department of Transportation, Report No. 93-4A, 1993.
2. A.A. Sagüés, et al., "Corrosion Resistance and Service Life of Drainage Culverts," Florida Department of Transportation, Final Report WPI0510756, 2001.
3. R. A. Reis, "Development of Proposed Improvements to Caltrans' Method for Estimating the Corrosion Service Life of Precast Concrete Culverts," State of California Department of Transportation, 2006.
4. C.A. Baker, "Durability of Concrete Pipe in a Marine Environment," Concrete Pipe Association of Australasia, 2000.
5. E. R. Busba, A. A. Sagüés, G. Mullins, "Reinforced Concrete Pipe Cracks –Accepted Criteria," Florida Department of Transportation, Final Report BDK84 977-06, 2011.
6. A. Torres-Acosta, A.A. Sagüés, Concrete Cracking by Localized Steel Corrosion – Geometric Effects, *ACI Materials Journal* vol. 101 p 501, 2004.
7. W. López and J.A. González. Influence of the degree of pore saturation on the resistivity of concrete and the corrosion rate of steel reinforcement. *Cement and Concrete Research* vol. 23, no. 2, pp. 368-376, 1993.
8. J.A. Gonzalez, W. Lopez and P. Rodríguez, Effect of Moisture Availability on Corrosion Kinetics of Steel Embedded in Concrete, *Corrosion* vol. 49, no. 12, pp. 1004-1010, 1993.
9. A. Molina, C. Andrade, C. Alonso, J.A. Gonzalez, "Factores Controlantes de la velocidad de Corrosion de las Armaduras Embebidas en Morteros de Cemento," *Rev. Tec. Ing.*, Univ. Zulia, Vol 8, pp. 9-15, 1985.
10. F. Pruckner and O.E. Gjorv, "Electrical Resistivity for Evaluation of Concrete Corrosivity," in 3rd Int Conf on Concrete Under Severe Conditions, N. Banthia, K. Sakai, and O.E. Gjorv Eds, The University of British Columbia, Vancouver, Canada, 2001.
11. L. Bertolini, and R.B. Polder, "Concrete resistivity and reinforcement corrosion rate as a function of temperature and humidity of the environment," TNO Report 97-BT-R0574, 1997.
12. F. Hunkeler, "Corrosion in reinforced concrete: processes and mechanisms," Chapter 1 in Corrosion in reinforced concrete structures, Hans Böhni Ed., Boca Raton, FL, CRC Press, 2005.
13. L. Coppola, R. Fratesi, S. Monosi, P. Zaffaroni, and M. Collepardi, "Corrosion of Reinforcing Steel in Concrete Structures Submerged in Seawater," in ACI SP-163, 1996, pp. 127-150.
14. O.E. Gjorv, O. Vennesland, AHS El-Busaidy, "Diffusion of dissolved oxygen through concrete," Corrosion/1976, Paper No. 17, Houston, Texas, NACE, 1976.
15. M. Raupach, "Investigation on the influence of oxygen on corrosion of steel in concrete – Part 1,"*Materials and Structures* vol. 29, no. 3, pp. 174-184, 1996.
16. M. Raupach, "Investigation on the influence of oxygen on corrosion of steel in concrete – Part 2," *Materials and Structures* vol. 29, no. 4, pp. 226-232, 1996.
17. H. Arup, "The mechanisms of the protection of steel by concrete," in Corrosion of Reinforcement in Concrete Construction, A.P. Crane, Ed. Chichester, England, Ellis Horwood, 1983.

18. C.E. Locke, “Corrosion of Steel in Portland Cement Concrete: Fundamental Studies,” in Corrosion effect of Stray Currents and the Techniques for Evaluating Corrosion of Rebars in Concrete, ASTM SPT906, V. Chaker, Ed., ASTM, Philadelphia, 1986, pp.5-14.
19. R.R. Hussain and T. Ishida, “Influence of connectivity of concrete pores and associated diffusion of oxygen on corrosion of steel under high humidity,” *Construction and Building Materials*, vol. 24, no. 6, pp. 1014-1019, 2010.
20. R.R. Hussain, T. Ishida, and M. Wasim, “Oxygen Transport and Corrosion of Steel in Concrete under Varying Concrete Cover, w/c, and Moisture,” *ACI Materials Journal*, vol. 109, no. 1, pp. 3-10, 2012.
21. D. Trejo, R.G. Pillai, “Accelerated Chloride Threshold testing: Part I – ASTM A 615 and A 706 Reinforcement”, *ACI Materials Journal*, vol. 100, no. 6, pp. 519-527, 2003.
22. D. Trejo, R.G. Pillai, “Accelerated Chloride Threshold testing: Part II – Corrosion-Resistant reinforcement”, *ACI Materials Journal*, vol. 101, no. 1, pp. 57-64, 2004.
23. C. Castellote, C. Andrade, “Assessment of the behavior of concrete in the initiation period of chloride induced corrosion of rebars,” in Concrete Repair, Rehabilitation and Retrofitting II, Alexander et al eds, London, UK, Taylor & Francis Group, , 2009.
24. C. Castellote, C. Andrade, C. Alonso, “Accelerated simultaneous determination of the chloride threshold and of the non-stationary diffusion coefficient values,” *Corrosion Science*, vol. 44, no. 11, pp.2409-2424, 2002.
25. NT Build 492, “Chloride migration coefficient from non-steady-state migration experiment,” Espoo, Finland, Proj. 1388-98, 1999.
26. G.K. Glass and N.R. Buenfeld, “The Presentation of The Chloride Threshold Levels for Corrosion of Steel in Concrete,” *Corrosion Science,* vol. 39, no. 5, p.1001-1013, 1997.
27. U. Angst, B. Elsener, C.K. Larsen, and Ø. Vennesland, “Critical chloride content in reinforced concrete – A review, “, *Cement and Concrete Research*, vol. 39, p.1122-1138, 2009.
28. U. Angst, B. Elsener, C.K. Larsen, and Ø. Vennesland, “Chloride induced reinforcement corrosion: Electrochemical monitoring of initiation stage and chloride threshold values”, *Corrosion Science*, vol. 53, p 1451-1464, 2011.
29. F. Presuel-Moreno, R. G. Powers, W. H. Hartt, "Corrosion Resistant Alloys for Reinforced Concrete," Final Report BD229, Florida Department of Transportation, Florida Atlantic University, 2008.
30. C. Alonso, C., Andrade and J. Rodriguez, “Factors Controlling Cracking of Concrete Affected by Reinforcement Corrosion”, *Materials and Structures*, vol. 31, pp. 435 – 441, 1998.
31. T. Vidal, A. Castel, and R. Francois, “Analyzing crack width to predict corrosion in reinforced concrete”. *Cement and Concrete Research,* vol. 34, pp. 165–174, 2004.
32. E. Busba and A.A. Sagüés, “Critical Localized Corrosion Penetration of Steel Reinforcement for Concrete Cover Cracking”, CORROSION/2013, paper no. C2013-0002747 (Houston, TX: NACE, 2013)
33. ASTM C76 Standard Specification for Reinforced Concrete Culvert, Storm Drain, and Sewer Pipe (West Conshohocken, PA: ASTM).
34. ASTM C642 (latest revision), ”Standard test method for density, absorption, and voids in hardened concrete,” (West Conshohocken, PA: ASTM).

35. ASTM G1 – 03 “Standard Practice for Preparing, Cleaning, and Evaluating Corrosion Test Specimens”, American Society for Testing and Materials, ,” (West Conshohocken, PA: ASTM).
36. F. Presuel-Moreno, et al., “Diffusion vs. Concentration of Chloride Ions in Concrete”, Final Report BDK79-977-03, Florida Atlantic University, 2014.
37. F. Presuel-Moreno, et al., “Analysis and estimation of service life of corrosion prevention materials using diffusion, resistivity and accelerated curing for new bridge structures,” Final Report BDK79-977-02 (Volume 1); Florida Atlantic University, 2013.
38. B. Weber, “Accelerated Corrosion of Steel In Dry-Cast Reinforced Concrete Pipes After Initiation”, M.S. thesis, Ocean and Mechanical Engineering Dept., Florida Atlantic University, Boca Raton, 2014.
39. B. Seo, “Initiation and Propagation of Corrosion in Dry-Cast Reinforced Concrete Ring Specimens”, M.S. thesis, Ocean and Mechanical Engineering Dept., Florida Atlantic University, Boca Raton, 2014.
40. M.G. Fontana and , “Modern Theory - Principles” Chapter 9 in “Corrosion Engineering”, 3rd edition, McGraw-Hill, 1986, pp. 445-480.
41. P. Schiessl, “Corrosion of Steel in Concrete” Report of the TC60-CSC RILEM, Chapman and Hall, London, 1988
42. H. Balasubramanian, “Initiation and Propagation Of Corrosion In Dry-Cast Reinforced Concrete Pipe”, M.S. thesis, Dept. Ocean and Mechanical Engineering, Florida Atlantic University, Boca Raton, 2013.
43. F. Presuel-Moreno, H. Balasubramanian, Y.-Y. Wu, “Corrosion of reinforced concrete pipes: an accelerated approach”, CORROSION/2013, paper no. C2013-2551 (Houston, TX: NACE 2013) (Proceedings published on-line and on CD).
44. F. Presuel-Moreno, H. Balasubramanian, Y.-Y. Wu, “Corrosion propagation of dry-cast reinforced concrete pipes exposed to simulated field environments”, paper C2014-4371 CORROSION/2014, (San Antonio, TX 2014) (Proceedings published on-line and on CD)
45. F. Presuel-Moreno, B. Webber, “Corrosion Propagation under Modest Accelerated State”, paper C2015-5837, CORROSION/2015 (Dallas, TX 2015) (Proceedings published on-line and on CD)
46. M. C. Rocha-Filho. M. U.- Macdonald, and M. D. D. Macdonald, "Theoretical Assessment of AC Impedance Spectroscopy for Detecting Corrosion of Rebar in Reinforced Concrete," *Corrosion*, vol. 44, no. 1, pp. 2-7, 1988.